Spring 5-5-2012

Immunoglobulin Gamma Subclasses and Corresponding Fc Receptors in Rhesus Macaques: Genetic Characterization and Engineering of Recombinant Molecules

Doan C. Nguyen
College of Arts and Sciences

IMMUNOGLOBULIN GAMMA SUBCLASSES AND CORRESPONDING FC RECEPTORS IN RHESUS MACAQUES: GENETIC CHARACTERIZATION AND ENGINEERING OF RECOMBINANT MOLECULES

by

DOAN CONG NGUYEN

Under the Direction of Roberta Attanasio

ABSTRACT

Rhesus macaques represent a valuable model in biomedical research and in development of vaccines and therapeutics. Due to the lack of reagents, the general properties of IgG and corresponding cellular receptors (FcγR) in this species are poorly characterized. We engineered recombinant IgGs containing each of the four rhesus macaque heavy constant region (CH) subclasses. To define FcγRs that mediate IgGs, we identified and characterized three FcγR classes, and generated recombinant cDNA constructs. cDNA IgH constructs were created by fusing – by sequence overlap extension PCRs – a gene segment encoding the murine variable heavy domain specific for the hapten NIP, an established specificity system for assessing antibody effector functions, with rhesus macaque CH fragments. The complete IgH constructs were transfected into J558L cells, a murine IgH-lost myeloma cell line expressing anti-NIP light chain. Secretion of engineered IgGs was determined by ELISAs using NIP-BSA and anti-

monkey IgG-specific antibodies. Molecular cloning methods were applied to identify and clone FcγR genes, and recombinant FcγR cDNA constructs were created by the recombinant DNA method. Four engineered IgH cDNA constructs were successfully created. Recombinant IgGs, in the intact Ig form and retaining the original anti-NIP specificity, were successfully produced. Compared to those in humans, FcγRs in rhesus macaques share high homology, yet also feature a relatively high level of intra-species polymorphism and possess different N-linked glycosylation patterns. FcγR constructs and expression vectors were successfully generated. The chimeric recombinant IgGs are powerful tools for defining IgG functional properties and studying CH structure/function relationship. These molecules can also be used as immunogens for generation of antibodies capable of unequivocally detecting individual IgG subclasses. The findings on FcγRs validate rhesus macaques as a model for studying antibody responses, and underscore the need to take into account of the genetic heterogeneity. The FcγR constructs and vectors serve as a tool for further studies of IgG/FcγR interactions.

We also reported here our findings from a separate study that the main female hormone, 17β-estradiol, is capable of restoring antibody responses to an influenza vaccine in a postmenopausal mouse model, suggesting that immunogenicity and efficacy of influenza vaccines should be evaluated in postmenopausal women.

INDEX WORDS: Rhesus macaque, Antibody, Immunoglobulin, IgG, IgG1, IgG2, IgG3, IgG4, Fc receptor, FcγR, CD64, CD32, CD16, Allele, Polymorphism, Effector functions, Recombinant DNA method, Therapeutic antibodies, Estrogen, 17β-Estradiol, Influenza vaccine

IMMUNOGLOBULIN GAMMA SUBCLASSES AND CORRESPONDING FC RECEPTORS IN RHESUS MACAQUES: GENETIC CHARACTERIZATION AND ENGINEERING OF RECOMBINANT MOLECULES

by

DOAN CONG NGUYEN

A Dissertation Submitted in Partial Fulfillment of the Requirements for the Degree of

Doctor of Philosophy

in the College of Arts and Sciences

Georgia State University

2012

IMMUNOGLOBULIN GAMMA SUBCLASSES AND CORRESPONDING FC RECEPTORS IN RHESUS MACAQUES: GENETIC CHARACTERIZATION AND ENGINEERING OF RECOMBINANT MOLECULES

by

DOAN CONG NGUYEN

Committee Chair: Roberta Attanasio

Committee: Julia Hilliard

John Houghton

Franco Scinicariello

Electronic Version Approved:

Office of Graduate Studies

College of Arts and Sciences

Georgia State University

May 2012

DEDICATION

To my Mother – For her Love

To my Father – For his Trust

To Ha, Hoa, and Duong – In their Love I Trust

ACKNOWLEDGMENTS

I thank Dr. Roberta Attanasio for providing me with the opportunity to do my graduate studies in her laboratory and for her mentorship and patience throughout this process. I am indebted to Dr. Franco Scinicariello for his guidance and encouragement, without which this work would certainly not be completed. I am grateful to my other dissertation committee members, Drs. Julia Hilliard and John Houghton, for their direction and support. I express my gratitude to my past and present laboratory members, Kenneth Rogers, Feda Masseoud, Anton Chesnokov, Jason Chiu, and Jing Wang, for their assistance and friendship. I have great appreciation of the helps and discussion from my colleagues, both inside and outside of school, Debby Walthall, Ping Jiang, Matthew Davis, Dr. Michael Hart, Dr. Jacqueline Katz, Dr. Prakash Sambhara, Dr. Lu Xiuhua, and Dr. Taronna Maines. I am appreciative to LaTesha Warren for her assistance and to the Molecular Basis of Diseases fellowship program for financial support.

Finally, I thank my families for being with me – always.

TABLE OF CONTENTS

ACKNOWLEDGMENTS ..... **v**

LIST OF TABLES ..... **xii**

LIST OF FIGURES ..... **xiii**

LIST OF ABBREVIATIONS ..... **ixx**

CHAPTER 1 INTRODUCTION AND STUDY OBJECTIVES **1**

1.1. Rhesus macaques as a biomedical research model for human diseases **1**

1.1.1. Rhesus macaques are widely modeled for human diseases and are considered the best animal model for HIV/AIDS-related studies ***1***

1.1.2. The rhesus macaque model: Incomplete characterizations of Ig/FcR immune system components and mechanisms ***3***

1.1.3. The need for comprehensive characterization of rhesus macaque Ig/FcR immune system components and mechanisms ***6***

1.2. Antibody molecules: Overview, structural and functional features, genetic basis, classification, and IgG class and subclasses **7**

1.2.1. Antibody molecules: Overview ***7***

1.2.2. Structural features and Ig L and H domains ***8***

1.2.3. Functional features and Ig V and C regions ***15***

1.2.4. Functional features and the role of the hinge and glycosylation ***20***

1.2.5. Gene organization, DNA rearrangement, and production of Ig ***22***

1.2.6. Ig classification: Ig L and H chain classes (isotypes) ***24***

1.2.7. IgG: General functional activities and subclass classification ***24***

1.2.8. IgG subclasses: Distinct characteristic patterns of effector functions ***29***

1.3. Ig and IgG Fc receptors: Overview, classification, structural and functional features, and allelic polymorphism 31

1.3.1. Ig Fc receptors (FcRs) and IgG Fc receptors (FcγRs): Overview 31

1.3.2. FcγRs: Classification, structural features, and effector cell distribution patterns.. 37

1.3.3. FcγRs: Functional activities, IgG isotype-binding affinity, and signal transduction of activating and inhibitory FcγRs 41

1.3.4. Intra-species (inter-individual) allelic polymorphism (allotypic variation) of FcγRs 44

1.4. Monoclonal antibodies, molecularly-engineered (recombinant) IgG and FcγR molecules, and recombinant DNA method 45

1.4.1. Monoclonal antibodies (mAbs) as basic research and diagnostic tools as well as prophylactic and therapeutic agents..... 46

1.4.2. The hybridoma technique: The traditional method for production of mAbs 47

1.4.3. The recombinant DNA method for production of mAbs and molecularly-engineered IgGs and FcγRs: Overview 48

1.4.4. The recombinant DNA method for production of mAbs and molecularly-engineered IgGs and FcγRs: Advantages and limitations..... 50

1.4.5. Creation of recombinant Ig gene constructs: Sequence overlap extension polymerase chain reaction (SOE-PCR) 52

1.4.6. Mammalian expression systems for production of recombinant IgGs and FcγRs.. 58

1.5. Structural and functional features of rhesus macaque IgG and FcγRs: Current status of knowledge 59

1.5.1. Presence of four IgG subclass genes, each with similar length and organization as that of humans 59

1.5.2. A single exon encoding the IgG3 hinge region and key amino acid differences of IgGs compared to human counterpart 60

1.5.3. Intra-species IgG H chain genes: Relatively high level of heterogeneity (polymorphism) and variability of disease susceptibility 62

1.5.4. Rhesus macaque FcγR biology system and related pathogen-clearance mechanisms are largely uncharacterized 64

1.6. Study objectives and specific aims 67

CHAPTER 2 ENGINEERING OF CHIMERIC MOUSE-RHESUS MACAQUE IGG1, IGG2, IGG3, AND IGG4 SUBCLASS RECOMBINANT ANTIBODIES RECOGNIZING THE HAPTEN 5-IODO-4-HYDROXY-3-NITROPHENACETYL 70

2.1. Summary 70

2.2. Materials and Methods 71

2.2.1. Construction of NIP-specific murine VH–rhesus macaque IgG CH (rhIGHG) cDNA hybrids (NIP-rhIGHG): DNA sources, SOE-PCR, and primer design 71

2.2.2. Construction of the NIP-rhIGHG cDNA hybrids: Optimization of SOE-PCRs and amplification strategies 78

2.2.3. Cloning and sequence analysis of the NIP-rhIGHG cDNA constructs 82

2.2.4. pLNOH2 and P2561/2/3 expression vector systems and the murine IgH-defective myeloma J558L cell line 91

2.2.5. Generation of expression vectors for NIP-rhIGHG chimeric constructs 105

2.2.6. Production of transient and stable J558L transfectoma cell lines expressing recombinant NIP-rhIGHG chimeras *109*

2.2.7. Detection of Igλ and complete (assembled) recombinant NIP-rhIGHG chimeric antibodies *111*

2.3. Results **112**

2.3.1. Four NIP-rhIGHG cDNA hybrid constructs were successfully generated by SOE-PCRs and were properly incorporated into pCR2.1-TOPO cloning vector *112*

2.3.2. Four NIP-rhIGHG cDNA hybrid constructs were successfully engineered into pLNOH2, pcDNA3.1(+), and P2561/2/3 expression vectors *119*

2.3.3. Four chimeric NIP-rhIGHG IgH chains with NIP-specificity of the original murine VH were successfully expressed by J558L cells *124*

2.3.4. Four NIP-rhIGHG intact IgG subclass Abs that retained binding specificity of the original V regions were successfully produced by J558L cells *124*

2.4. Discussion **141**

CHAPTER 3 RHESUS MACAQUE IGG FC RECEPTORS: CHARACTERIZATION AND ALLELIC POLYMORPHISMS OF ENCODING GENES AND GENERATION OF RECOMBINANT cDNA EXPRESSION VECTORS **150**

3.1. Summary **150**

3.2. Materials and methods **151**

3.2.1. Blood samples, total RNA isolation, reverse transcription, and cDNA synthesis of FcγR genes *151*

3.2.2. Design of primers *156*

3.2.3. Cloning and sequencing of amplified FcγR cDNAs *157*

3.2.4. Construction of rhesus macaque FcγR cloning vector *159*

3.2.5. Construction of rhesus macaque FcγR expression plasmid systems using pcDNA3.1(+) (HindIII/BamHI), as well as pcDNA3.1(+) (Not/Xho) and P2561/2/3 (Not/Xho) vectors *159*

3.2.6. Sequence analysis *162*

3.3. Results **165**

3.3.1. Rhesus macaque FcγRI (CD64) and FcγRII (CD32) cDNA clones exhibit the typical mRNA primary structure of their human counterpart *168*

3.3.2. The rhesus macaque CD64 and CD32 extracellular C-like, ligand-binding portion shares high homology with that of human CD64 and, to a lesser degree, CD32, respectively *172*

3.3.3. A relatively high level of intra-species polymorphism is present in macaque FcγR sequences *176*

3.3.4. Susscessful generation of recombinant FcγR gene cDNA constructs as well as their cloning and expression vectors *185*

3.4. Discussion **192**

CHAPTER 4 17β-ESTRADIOL RESTORES ANTIBODY RESPONSES TO AN INFLUENZA VACCINE IN A POSTMENOPAUSAL MOUSE MODEL **199**

4.1. Summary **199**

4.2. Introduction **200**

4.3. Materials and methods **201**

4.3.1. Mice, bilateral ovariectomy, and estrogen deliver *201*

4.3.2. Immunization *201*

4.3.3. Evaluation of specific serum antibody response *202*

4.3.4. Data analysis *204*

4.4. Results **205**

4.5. Discussion **209**

CHAPTER V CONCLUSIONS AND FUTURE DIRECTIONS **218**

CHAPTER VI REFERENCES **226**

LIST OF TABLES

Table 2.1. Primers used for generation of rhesus macaque IgG gene fragments and recombinant constructs by PCR and SOE-PCR amplifications..... 79

Table 2.2. Deduced amino acid sequences of the hinge of IgH CH1, CH2, and CH3 domains of four IgG isotypes (IgG1, IgG2, IgG3, and IgG4) from human (*Homsap*) and rhesus macaque (*Macmul*)[a]..... 123

Table 3.1. Primers used for amplification of rhesus macaque FcγR[a] cDNAs..... 158

Table 3.2. Primers used for generation of rhesus macaque FcγR recombinant DNA constructs by SOE-PCR amplifications. 160

Table 3.3. Correspondence between sequence positions and IMGT unique numbering for potential N-linked glycosylation sites in rhesus macaque FcγRs[a]. 174

Table 3.4. Location and type of allelic polymorphism present in rhesus macaque FcγRs[a]. 175

Table 4.1. Neutralizing antibody titers in ovariectomized (OVEX) mice, OVEX mice subjected to 17β-estradiol (E2) replacement (OVEX + E2) and Intact mice. 211

LIST OF FIGURES

Fig. 1.1. Schematic representation showing two-dimentional general structure of a conventional antibody, or immunoglobulin (Ig), molecule. This representation displays both amino acid (A) and nucleotide level (B), showing the structure and arrangement of Ig heavy and light chains, the relative positioning of inter-chain disulfide bonds, the paired domains and the classical Ab fragments, as well as illustrating germ-line genetic organization of separate gene segments (exons) encoding for Ig heavy-chain constant domains (not drawn to scale)..... 10

Fig. 1.2. Functional features of Ig V and C regions and Ig domain structure/function properties. 18

Fig. 1.3. Human IgG: most common in serum, classified into four subclasses, possessing slight structural yet significant functional differences..... 27

Fig. 1.4. Mechanisms of action of FcRs: Binding of FcRs with Ig-opsonized particles triggers the cell signal transduction events and initiates various cell-killing immune effector functions, resulting in cellular activation or inhibition of other immune-competent cells..... 33

Fig. 1.5. Activating and inhibitory FcRs and the regulatory functions of immune complexes.... 36

Fig. 1.6. Activating and inhibitory IgG FcRs: Structure, function, binding affinity, and cellular expression profiles. 40

Fig. 1.7. Among the advantages of engineering Abs: Strategies for enhancing the potency and activity of antitumor antibodies. 54

Fig. 1.8. Diagrammatic overview of the sequence overlap extension polymerase chain reaction (SOE-PCR) procedure to assemble a chimeric/mixed gene fragment. The procedure is also called by various other names, such as overlap extension PCR, splice overlap extension PCR, overlap PCR, overlapping PCR, two-step PCR, two-step overlap extension PCR, or three-part PCR..... 57

Fig. 2.1. Flowchart representation summarizing the major steps involved in construction, production, and detection of NIP-rhIGHG chimeras using recombinant DNA technology (genetic engineering). 73

Fig. 2.2. Schematic representation illustrating the separate exons that encode for individual heavy-chain constant domains of an Ig molecule, as well as diagrammatic representation depicting organization of a complete IgG3 heavy chain gene fragment with name and location of a pair of primers at the CH2-CH3 boundary, shown as an example for overlap primer sequences. 77

Fig. 2.3. Flowchart diagrams outlining different experimental strategies for generation of recombinant NIP-rhIGHG cDNA constructs by SOE-PCRs (not drawn to scale). 87

Fig. 2.4. Ligation of PCR products into pCR2.1 TOPO TA cloning vector. 89

Fig. 2.5. Schematic representation of the PCR- and SOE-PCR-amplified *IGHG* fragments that make up of the four recombinant NIP-rhIGHG (Igγ) cDNA constructs. 94

Fig. 2.6. Schematic representation of the structure of a representative recombinant NIP-rhIGHG cDNA construct (shown is the NIP-rhIGH3 cDNA construct) and simplification of the architecture of the expression plasmid vector pLNOH2, highlighting regions of functional significance and relevant features (not drawn to scale). 96

Fig. 2.7. Schematic representation of generation of recombinant expression plasmid vector pLNOH2-IgH (not drawn to scale). 100

Fig. 2.8. Simplification of the architecture of the expression plasmid vector P2561/2/3, highlighting regions of functional and relevant features (not drawn to scale). 102

Fig. 2.9. Schematic representation of generation of recombinant expression plasmid vectors pcDNA3.1-IgH and P2561/2/3-IgH (not drawn to scale). 107

Fig. 2.10. Gel electrophoresis separation of DNA products resulting from SOE-PCR annealing and amplification or digestion of clones of recombinant gene constructs of NIP-rhIGHG1 (A), NIP-rhIGHG2 (B), NIP-rhIGHG3 (C), and NIP-rhIGHG4 (D) that were ligated into cloning and expression vectors. 114

Fig. 2.11. Gel electrophoresis separation of DNA fragments resulting from digestions of clones of recombinant gene constructs of NIP-rhIGHG1, NIP-rhIGHG2, NIP-rhIGHG3, and NIP-rhIGHG4 that were ligated into cloning and expression vectors. 118

Fig. 2.12. Alignment of deduced amino acid sequences of IgH CH1, CH2, and CH3 domains of four IgG isotypes (IgG1, IgG2, IgG3, and IgG4) from human (*Homsap*) and rhesus macaques (*Macmul*). 121

Fig. 2.13. Two-dimentional representation, or IMGT Colliers de Perles, of rhesus macaque (*Macmul*) CH domain sequences of each of the four IGHG subclass molecules. 131

Fig. 2.14. Prediction of potential N-glcosylation sites for CH3 domains of human (above) and rhesus macaque (below) IgG4 sequences, conducted by the use of the online tool NetNGlyc 1.0 Server (http://www.cbs.dtu.dk/services/NetNGlyc/), which is based on identifying Asn-Xaa-Ser/Thr consensus sequences (Julenius et al., 2005). 133

Fig. 2.15. Expression by J558L cells of NIP-specific mouse Igλ associated with secreted recombinant IgHs as detected by sandwich ELISA for its binding to purified anti-mouse IgL λ Abs produced in goat (NIP anti-λ ELISA). 135

Fig. 2.16. Production of recombinant NIP-rhIGHG IgH chains of different IgG subclasses as determined by sandwich ELISA for their binding to an affinity purified anti-monkey IgG produced in goat (monkey-specific anti-gamma ELISA). 138

Fig. 2.17. Production of complete recombinant NIP-rhIGHG Abs of different IgG subclasses as determined by capture (indirect) ELISA for their binding to NIP-BSA (NIP coupled to BSA) antigen (NIP-specific anti-gamma ELISA). 140

Fig. 2.18. Different yields in production of recombinant NIP-rhIGHG Abs of different IgG subclasses as determined by ELISA for their binding to NIP-BSA antigen [(A); NIP-specific anti-gamma ELISA] or to an affinity purified anti-monkey IgG produced in goat [(B); monkey-specific anti-gamma ELISA]. 143

Fig. 3.1. Flowchart representation illustrating major steps involved in identifying and cloning rhesus macaque FcγR genes, as well as in generation of recombinant FcγR cloning and expression plasmid vectors. 153

Fig. 3.2. Schematic representation of FcγRIIIa genomic and cDNA structure and of gene fragments encoding the extra cellular domains of FcγRI and FcγRII molecules, as well as strategy for creating recombinant cDNA fragments. 155

Fig. 3.3. Schematic representation of major steps in generation of recombinant expression plasmid vector pcDNA3.1-FcγR-Hind/Bam (not drawn to scale). 161

Fig. 3.4. Schematic representation of major steps involved in generation of the recombinant expression plasmid vectors pcDNA3.1-FcγR-NotI/XhoI and P2561/2/3-FcγR (not drawn to scale). 164

Fig. 3.5. Nucleotide and deduced amino acid sequences of rhesus macaque Fcγ receptor I (FcγRI, CD64) (GenBank accession number: HQ423396). 167

Fig. 3.6. Nucleotide and deduced amino acid sequences of rhesus macaque Fcγ receptor II (FcγRII, CD32) (GenBank accession number: HQ423393). 171

Fig. 3.7. IMGT Colliers de Perles of rhesus macaque CD32 (FcγRII) C like [D1] (I), and [D2] (II) as well as CD64 (FcγRI) C-like [D1] (III), [D2] (IV) and [D3] (V) domains (on one layer; obtained with the IMGT/Collier-de-Perles tool in the IMGT/DomainGapAlign) (Ehrenmann et al., 2010). 179

Fig. 3.8. A phylogenetic tree indicating the amino acid sequence similarity among independent allelic variants of macaque FcγR molecules identified in this study. 180

Fig. 3.9. Alignment of the deduced amino acid sequences of rhesus macaque CD64 (FcγRI) (GenBank accession numbers: HQ423394-HQ423396) (obtained by cloning and sequencing whole blood cDNAs) with a human CD64a representative (shown as “Human”; GenBank accession number: AK291451.1). 182

Fig. 3.10. Alignment of the deduced amino acid sequences of rhesus macaque CD32 (FcγRII) (GenBank accession numbers: HQ423389-HQ423393) obtained by cloning and sequencing whole blood cDNAs with a human CD32a representative (shown as “Human”; GenBank accession number: BC020823.1). 184

Fig. 3.11. Schematic representation illustrating the extracellular domain 1 ([D1], or EC1) putative secondary structure of a representative sequence from each of three rhesus macaque FcγR classes in alignment with those in humans: no variation at known human functional positions is found in the animal molecules. 187

Fig. 3.12. Schematic representation illustrating the extracellular domain 2 ([D2], or EC2) putative secondary structure of a representative sequence from each of three rhesus macaque FcγR classes in alignment with those in humans: no variation at known human functional positions is found in the animal molecules. 189

Fig. 3.13. Gel electrophoresis separation of DNA products resulting from PCR and SOE-PCR annealing and amplification or digestion of clones of recombinant gene constructs of FcγRI (A), FcγRII (B), and FcγRIII (C), as well as gel electrophoresis separation of DNA fragments resulting from digestions of clones of recombinant FcγR gene constructs in pCR2.1 TOPO TA cloning vector cut by *EcoRI* (D), in pCR2.1 TOPO TA cloning vector cut by *NotI* and *XhoI* (E), and in P2561/2/3 expression vector cut by *NotI* and *XhoI* (F)..... 191

Fig. 4.1. Grouping of animals. Numbers denote individual animal numbering (for label purpose). 203

Fig. 4.2. Immunization and blood collection timeline..... 203

Fig. 4.3. Specific protective antibodies were induced and restored in the presence of 17β-estradiol (E2) through six months after the boosting immunization..... 207

Fig. 4.4. Effect of 17β-estradiol (E2) on influenza-specific antibody production as measured by Single Radial Hemolysis (SRH) assay..... 210

Fig. 5.1. Future studies and directions.……221

LIST OF ABBREVIATIONS

AA (aa)	Amino acid
Ab	Antibody
ABTS	2-2'-azino-di-(3-ethylbenzthiazoline sulfonic acid)
ADCC	Antibody dependent cell cytotoxicity
ADCP	Ab-dependent cellular phagocytosis
AIDS	Acquired immunodeficiency syndrome
APC	Antigen presentation cells
BCR	B cell receptor
BSA	Bovine serum albumin
C	Constant
CD	Cluster of differentiation
CD16	Immunoglobulin G Fc receptor III
CD32	Immunoglobulin G Fc receptor II
CD64	Immunoglobulin G Fc receptor I
CDC	Complement-dependent cytotoxicity
cDNA	Complementary Deoxyribonucleic Acid
CH (C_H)	Constant region/domain of heavy chain (Heavy chain constant domain)
CH1 (C_H1)	First constant domain of heavy chain
CH2 (C_H2)	Second constant domain of heavy chain
CH3 (C_H3)	Third constant domain of heavy chain
CK	Constant region/domain of kappa chain

CL (C_L)	Constant region/domain of the light chain (Light chain constant domain)
CLL	Constant region/domain of lambda (λ) chain
CMV	Cytomegalovirus
CTL	Cytotoxin T lymphocyte
Cys (CYS)	Cysteine
CYT	Cytoplasmic
D	Ectodomain (extracellular domain)
D1	Ectodomain (extracellular domain) 1
D2	Ectodomain (extracellular domain) 2
D3	Ectodomain (extracellular domain) 3
DMEM	Dulbecco's modified Eagle medium
DNA	Deoxyribonucleic acid
dNTP	Deoxynucleoside 5'- triphosphate
E2	17β-Estradiol
EC	Extracellular domain
E. coli	Escherichia coli
ELISA	Enzyme linked immunosorbent assay
Fab (F_{ab})	Antigen binding fragment
FBS	Fetal bovine serum
Fc (F_c)	Fragment crystallizable or Fragment of the CH2/CH3 of both heavy chains
FcR	Immunoglobulin Fc receptor
FcRn	Neonatal Fc receptor
FcαR	Immunoglobulin A Fc receptor

FcγR	Immunoglobulin G Fc receptor
FcγRI	High affinity IgG Fc receptor I
FcγRII	Low affinity IgG Fc receptor II
FcγRIII	Low affinity IgG Fc receptor III
FITC	Fluorescein isothiocyanate
GPI	Glycosyl phosphatidyl inositol
H	Heavy
H_2O	Water
H_2O_2	Hydrogen peroxide
HA	Hemagglutination
HAMA	Human anti-mouse antibody
Hg	Hinge (of Ig molecule)
HI	Hemagglutination inhibition
HIV	Human immunodeficiency virus
Homsap	*Homo sapiens*
HRP	Horseradish peroxidase
IC	Ig(Ab)-antigen complex
Ig	Immunoglobulin
IgA	Immunoglobulin A
IgD	Immunoglobulin D
IgE	Immunoglobulin E
IgG	Immunoglobulin G
IgH	Immunoglobulin heavy chain

IGHC	Immunoglobulin heavy constant region gene
IGHG	Immunoglobulin heavy constant gamma (IgG) gene
IGHV	Immunoglobulin heavy variable region gene
IgL	Immunoglobulin light chain
IgM	Immunoglobulin M
IgSF	Immunoglobulin superfamily
i.m.	Intramuscular(ly)
IMDM	Iscove's modified Dulbecco's medium
IMGT	ImMunoGeneTics (the international information system for IgSF)
ITAM	Immunoreceptor tyrosine activation motif
ITIM	Immunoreceptor tyrosine inhibition motif
L	Light
LTR	Long terminal repeat
MAb (mAb)	Monoclonal antibody
MAC	Membrane attack complex
Macmul	*Macaca mulata*
MFI	Mean fluorescence intensity
MHC	Major histocompatibility complex
MN	Micro-neutralization
mRNA	Messenger Ribonucleic Acid
NHP	Nonhuman primate
NIP	5-iodo-4-hydroxy-3-nitrophenacetyl
NIP-BSA	5-iodo-4-hydroxy-3-nitrophenacetyl–bovine serum albumin

NK	Natural killer
OD	Optical density
OPD	O-phenylenediamine
OVEX	Ovariectomized
PBMC	Peripheral blood mononuclear cells
PBS	Phosphate buffered saline
PCR	Polymerase chain reaction
PE	Phycoerythrin
PMN	Polymorphonuclear (leukocytes)
Pro	Proline
rAb	Recombinant antibody
RDE	Receptor-destroying enzyme
RE	Restriction endonuclease (enzyme)
Rh (rh)	Rhesus macaque
RNA	Ribonucleic acid
RSS	Recombination signal sequence
RT-PCR	Reverse transcriptase-polymerase chain reaction
SHIV	Simian human immunodeficiency virus
SIV	Simian immunodeficiency virus
SLE	Systemic lupus erythematosus
SOE	Sequence overlap extension
SOE-PCR	Sequence overlap extension polymerase chain reaction
SRH	Single-radial hemolysis

TCR (TR)	T cell receptor
TH	T helper
TM	Transmembrane
V	Variable
VH (V_H)	Variable region/domain of heavy chain (Heavy chain variable domain)
VK	Variable region/domain of kappa chain
VL (V_L)	Variable region/domain of light chain (Light chain variable domain)
VLL	Variable region/domain of lambda (λ) chain
WHO	World Health Organization

CHAPTER 1

INTRODUCTION AND STUDY OBJECTIVES

1.1. Rhesus macaques as a biomedical research model for human diseases

1.1.1. Rhesus macaques are widely modeled for human diseases and are considered the best animal model for HIV/AIDS-related studies

The macaque model has been in the past century used for over 70 human infectious diseases (Gardner and Luciw, 2008). From pandemics and notable global infections, such as acquired immunodeficiency syndrome (AIDS), influenza, hepatitis, and tuberculosis, to a variety of infections typically seen in pediatrics or in tropics, as well as diseases caused by newly emergent infectious or other viral, bacterial, fungal, or parasitic pathogens, including potential bioterrorism diseases, and oncogenic and chronic degenerative neurologic disorders, have been studied in these animals. Other non-infectious diseases, such as Parkinson's and Alzheimer's diseases and age-related disorders (Herodin et al., 2005; Carlsson et al., 2004), have also been modeled in this versatile model.

Studies using animal models, including those with macaques, are crucial part for understanding human disease mechanisms so as to improve diagnostics, to rationally design vaccines, and to develop therapies. Use of the macaque model has proved to be an invaluable resource for understanding pathogenesis of human diseases. This model has also represented essential tools in vaccinology and passive immunization studies, such as for assessing the safety and efficiency of new vaccines, including these properties of different adjuvants being used to boost vaccine-induced immune responses (Sibal and Samson, 2001). Furthermore, macaques have served as models for evaluation of efficacy of novel therapeutic applications, the

mechanisms of action and pharmacokinetics of therapeutic antibodies, as well as strategies to prevent allograph rejection in transplantation research.

The macaque species most commonly used as human disease models is rhesus macaques (*Macaca mulatta)*. Rhesus macaque animals are extensively available and are closely related anatomically, physiologically, and phylogenetically to humans (Shedlock et al., 2009; Gardner and Luciw, 2008). As a nonhuman primate (NHP) model, rhesus macaques are further valued by their capacity of being naturally infected (and expressing disease symptoms) with NHP etiologies similar to those causing related diseases that are difficult to study in humans (Gardner and Luciw, 2008). In particular, rhesus macaques experimentally infected with simian immunodeficiency virus (SIV) [considered the viral substitute of the AIDS-causing human immunodeficiency virus (HIV), which does not replicate in most animal species (Lackner and Veazey, 2007)], were shown to recapitulate human HIV infection immunologically, virologically, and pathologically, as well as to develop AIDS-like disease (Shedlock et al., 2009; Thomas, 2009). Rhesus macaque species, to date, is considered the most suitable model for studying HIV pathogenesis as well as for testing potential therapies and developing vaccines against HIV/AIDS (Shedlock et al., 2009; Nath et al., 2000). Indeed, this species has played a key role in characterizing HIV viral immunobiology and in correlating the host innate and adaptive immune responses with *in vivo* protection induced by HIV/AIDS vaccine candidates (Shedlock et al., 2009; Gardner and Luciw, 2008). The recent availability of the rhesus macaque genome sequence (Gibbs et al., 2007) and microarray chips of macaque-specific genes has certainly increased the potential use of rhesus macaques in biomedical research.

1.1.2. The rhesus macaque model: Incomplete characterizations of Ig/FcR immune system components and mechanisms

When using the rhesus macaque model, particularly for evaluation of vaccines and antibody (Ab)-based therapeutic applications, much of the attention has been focused on assessing the host immune responses. In such responses, the two main molecular players are Ab [also known as immunoglobulin (Ig)], and their cellular Fc receptor (FcR). These molecules together carry out the various so-called cell-killing effector functions that aim to destroy and "clear" pathogens. Indeed, Ab responses, particularly those of neutralizing Abs, correlate with *in vivo* protection and represent the major protective components against SIV and HIV infections (Schmitz et al., 2003). Many therapeutic agents directed at Igs or FcRs are under development for treatment of various human diseases, including cancer and autoimmune disorders. Nevertheless, apart from the general similarity of the overall biology of infection between SIV-infected rhesus macaques and HIV-infected humans, as well as the evolutionary relatedness between these two species, the Ig/FcR immune system components and mechanisms of rhesus macaque model relevant to studies of human diseases are not completely characterized. In the absence of known human disease mechanisms, the design and interpretation of experimental data generated from the rhesus macaque model are based on the similarity of the disease pathogenesis and manifestation between these two species (Shedlock et al., 2009). It is the scientific assumption that crucial immune molecules in rhesus macaques could be highly conserved with those of humans, both structurally and genetically, and that their interactions could generally mimic those in humans. However, this premise has not been fully evaluated.

Early studies show that rhesus macaque Igs share a high degree of homology with their human counterpart (Calvas et al., 1999). This finding suggests that these molecules would be less

immunogenic (at least compared to murine counterpart) in humans, and consequently, might induce a low level of the so-called human anti-mouse antibody (HAMA) response (Laffly and Sodoyer, 2005). Indeed, rhesus macaque monoclonal Abs (mAbs) have been proposed as an alternative to humanized rodent mAbs, which causes a high HAMA response when used for therapeutic purposes (Ehrlich et al., 1988; van Meurs and Jonker, 1986). On the other hand, anti-human Ab reagents in many cases poorly or rarely cross-react with rhesus macaque effector cells, suggestive of less conserved antigenic determinants (epitopes) between the corresponding molecules of the two species. Some immune cell surface molecules between the two species, while structurally similar, are even sufficiently distinct antigenically to invoke an immune response. For instance, rhesus macaques elaborate specific humoral immune responses against the human CD4 cell surface molecule (Lodgberg et al., 1994; Newman et al., 1992). Indeed, it had been suggested that rhesus macaques had the potential to be employed for production of specific Abs recognizing antigens and receptors on the surface of human immune cells (Lodgberg et al., 1994). Subsequently, several "primatized" mAbs containing variable regions from a macaque species (although it was not rhesus, but cynomolgus macaque) and an IgG human constant region have been developed. Among these mAbs are anti-CD4 [Keliximab; for rheumatoid arthritis (Newman et al., 2001; Reddy et al., 2000)], anti-CD23 [for allergies (Nakamura et al., 2000)], and anti-CD80 [Galiximab; for autoimmune and inflammatory diseases, like psoriasis (Gottlieb et al., 2004; Schopf 2001)].

Like with Abs, studies of murine Ig Fc cell surface receptors (FcRs) have traditionally provided important insights for better understanding human FcR biology. However, the human FcR system is complicated and extensively different from that of mice. Humans possess several FcRs with which no homologues are found in mice, such as FcγIIa, FcγRIIc, FcγIIIb, and FcαR

(Pleass and Woof, 2001). As FcR biology varies greatly among species, insights from a more "human" FcR model system – such as those from an NHP species instead of mice – would be more practically translatable into human FcRs. As discussed above, owning to their close anatomical, physiological, and phylogenetical relatedness to humans (Gardner and Luciw, 2008), rhesus macaque species is already used extensively for immunological research. Rhesus macaque FcR biology research, however, is largely unexplored (Rogers et al., 2008, 2006, and 2004). Indeed, several FcγRs found in mice, including FcRs for IgA and IgM, have not even been fully characterized in NHP species (Rogers et al., 2004).

Therefore, the various Ig and FcR systems and related pathogen-clearance mechanisms are still largely unexplored in the rhesus macaque model. In particular, little is presently known about the structure of Ig and FcR molecules in rhesus macaques, and the extent of similarity to their human counterpart is not completely defined. No current information about the functional properties and structure-function relationships that characterize rhesus macaque IgG molecules, as well as interaction of IgG subclasses and corresponding FcγR classes, is available. It is not known at what extent the various components of the rhesus macaque immune system mimic corresponding components of the human immune system upon antigen exposure, particularly that directing against HIV and SIV. Also, the relative level of IgG subclasses present in rhesus macaque serum is not known. As many therapeutic Abs – either approved or in trials or development – are of IgG Ab class, comprehensive understanding of interaction between IgG subclasses and corresponding FcγRs would enable the rational design and production of novel therapeutic Abs, as well as prognosis for treatment success.

1.1.3. The need for comprehensive characterization of rhesus macaque Ig/FcR immune system components and mechanisms

Owing to almost 25 million years of evolution (Shedlock et al., 2009), human and rhesus macaque species might possess important structural and thus, functional, differences related to their Ig and FcR components that have not been completely characterized. The incomplete characterization has limited the scope of biomedical research performed with this model. Importantly, these differences might mislead data interpretation and translation to human diseases. Indeed, recent studies suggest that the safety and performance of drugs or vaccines observed in NHP animals, particularly rhesus macaques, are not necessarily similar to or translatable into humans. For instance, while the CD28 super-agonist Ab TGN1412 had showed no adverse effects in macaques, it caused, with 500 times less in dose and within an hour of administration, life-threatening conditions in healthy human volunteers in a 2006 clinical study (Attarwala, 2010). More recently, a leading HIV vaccine candidate that demonstrated apparent protection in rhesus macaques appeared to fail to protect humans (Thomas, 2009). Molecularly, recent studies revealed that there are more active immune genes in rhesus macaques than in humans (Gibbs et al., 2007). Several key differences that exist between rhesus macaques and humans related to their major histocompatibility complex (MHC), as well as Ig and FcR molecules, both structually and functionally, have also been recently revealed (Rogers et al., 2008; Gibbs et al., 2007; Rogers et al., 2006; Scinicariello et al., 2006; Daza-Vamenta et al., 2004; Scinicariello et al., 2004).

Collectively, these findings suggest that interspecies differences between rhesus macaques and humans regarding immune gene expression and immune responses might contribute – by means that are currently not fully understood – to pathogenesis and progression

of infection (Shedlock et al., 2009). Failure to recognize these differences may lead to erroneous expectations or confounding interpretation of data generated by using this model for evaluation of vaccines or therapeutic Abs.

1.2. Antibody molecules: Overview, structural and functional features, genetic basis, classification, and IgG class and subclasses

1.2.1. Antibody molecules: Overview

Antibodies (Abs), or Igs, are host glycoproteins naturally produced in vertebrates in response to invading foreign particles or organisms (antigens), or to, in abnormal or pathological circumstances, other agents in the body. Igs are the antigen-specific and multifunctional adaptor molecules expressed by B lymphocytes as either membrane-bound or secreted products. Membrane-bound Igs, also known as B cell receptors, act as cell-surface receptors for specific antigens, which mediate cell signaling and cell activation (like activation of phagocytes, natural killer cells, or the complement cascade). Secreted Igs, which are synthesized by antigen-specifically proliferated and terminally differentiated B cell clones (Parham, 2000), circulate in the blood. These circulating Igs serve as the soluble effector molecules, which are capable of individually and specifically binding and neutralizing pathogens/toxins at a distance, or marking them for elimination through activating mechanisms that effect their destruction and clearance (effector functions). Igs, therefore, play a critical role in the protection and defense of a host organism against pathogens and malignancies.

Every individual Ig recognizes and binds to just one single antigen, which could be protein and/or carbohydrate particles present on microorganisms and viruses, or could be distinctive molecules expressed on the surfaces of tumor cells. Because of this exquisitely-

specific and high-affinity binding characteristics, Igs are ideal molecular tools for basic research and diagnostics. Igs have been widely used, both *in vitro* and *in vivo*, for detecting, localizing, and purifying both known and unknown molecular targets. As will be discussed further, Igs have also greatly been increasingly used as therapeutic agents over the last several decades. Indeed, Igs are among the most powerful immune-therapeutic agents currently available, and neutralizing Igs are the most sought-after molecules of actions induced from vaccinating against a variety of infectious pathogens.

Igs belong to the eponymous Ig "superfamily" (IgSF) that constitute the humoral branch of the immune system in most vertebrates, including fishes, amphibians, reptiles, birds, and mammals (Clark, 1997). IgSF molecular members adopt a tertiary globular structural motif known as IgSF domain, or Ig domain, that result from independent folding of their polypeptide chains, as their basic building block (Schroeder and Cavacini, 2010). In an Ig molecule, the variable domains localize at the amino termini and confer the antigenic specificity, whereas the constant domains reside within the carboxyl terminus and define the different effector functions. The recognition of this domain structure/function property of Igs has facilitated the manipulation of the Ig genes and thus, their recombinant protein products of predefined specificity and/or desired species (Clark, 1997). Indeed, generation and production of chimeric recombinant molecules used for therapeutic purposes or for basic research studies, including those of the structural basis of Ig functions, have been great success.

1.2.2. Structural features and Ig L and H domains

All Igs, independent of their antigenic specificity, generally have a common structure that has been conserved through evolution. It is a Y-shaped symmetrical structure composed of four

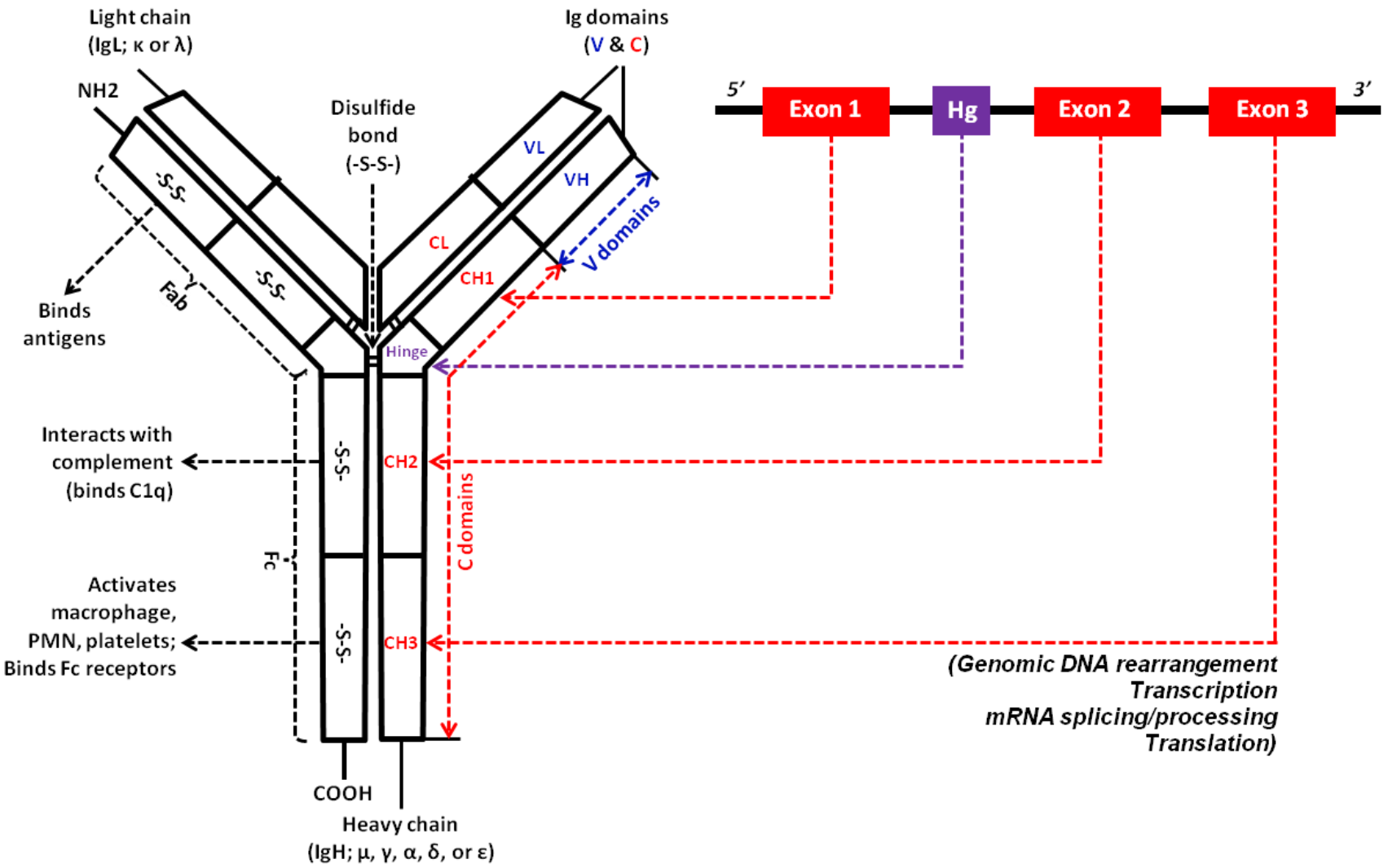
Light chain
(IgL; κ or λ)
Ig domains
(V & C)
NH2
Disulfide
bond
(-S-S-)
VL
VH
V domains
CL
CH1
-S-S-
-S-S-
Fab
Binds
antigens
Hinge
Interacts with
complement
(binds C1q)
-S-S-
CH2
C domains
Fc
Activates
macrophage,
PMN, platelets;
Binds Fc receptors
-S-S-
CH3
COOH
Heavy chain
(IgH; μ, γ, α, δ, or ε)
5′
Exon 1
Hg
Exon 2
Exon 3
3′
(Genomic DNA rearrangement
Transcription
mRNA splicing/processing
Translation)
The four-polypeptide chain structure of Ig
Germline DNA heavy constant (IGHC) genes
(A)
(B)

Fig. 1.1. Schematic representation showing two-dimentional general structure of a conventional antibody, or immunoglobulin (Ig), molecule. This representation displays both amino acid (A) and nucleotide level (B), showing the structure and arrangement of Ig heavy and light chains, the relative positioning of inter-chain disulfide bonds, the paired domains and the classical Ab fragments, as well as illustrating germ-line genetic organization of separate gene segments (exons) encoding for Ig heavy-chain constant domains (not drawn to scale). (A) This diagram depicts the four-chain structure of an Ig molecule, a dimeric protein composed of two identical light (L) chains (IgL) and two identical heavy (H) chains (IgH), each consisting of a variable (V) region and a constant (C) region. Individual IgL and IgH chains are folded into domains (also known as Ig folds), which are discrete and compactly folded protein regions. Ig domains have similar structures and, by themselves or through interactions with other domains, form functional units of the Ig molecule. Each IgL comprises two domains, a variable (VL) and a constant (CL), and each IgH comprises four (or five) domains, a V domain (VH) and three followed C domains (CH1, CH2, and CH3). Each Ig domain, V or C, comprises about 110 amino acid residues and an intra-chain disulfide bond (-S-S-) between two cysteine residues, forming a loop of about 60 amino acids. Individual IgL and IgH chains are held together by inter-chain disulfide bonds and form a flexible Y shape of the molecule. The VH region, which is adjacent to the CH1 region, is located at the amino terminus (NH2), and the CH3 (some have a CH4) region is positioned at the carboxy terminus (COOH), which is at the 3’ end of the IgH [which can be either membrane-bound, mIg (or B-cell receptors, BCRs) or secreted, sIg]. The CH1 domain contributes to the stability of V regions and to the diversity of Igs. In between the CH1 and CH2 domains is the hinge portion, which contributes in the flexibility of the molecule. Based on the similarity level of amino acid sequences, two major IgL types, namely κ and λ (encoded at different genetic loci

and referred as Igκ and Igλ, respectively), and five major IgH classes isotypes), namely μ, γ, α, δ, and ε (referred as Igμ, Igγ, Igα, Igδ, and Igε, respectively), are classified. IgHs in IgG, IgA, and IgD classes contain four Ig domains and a hinge region, whereas those in the IgM and IgE contain an additional Ig domain that replaces the hinge region. The five IgH isotypes also vary in function, serum concentration, and serum stability. IgL type is not a determinant of the Ig class (isotype) nor known to be associated with specific effector functions of the molecule. Each IgH class Ig molecule has only one type of IgL. Ig chains can also be associated with carbohydrate moieties (Ig CH2 has conserved glycosylation sites). Igs and BCRs are for antigen recognition and destruction and also illustrated in this diagram are the regions that participate in antigen recognition/binding (Fab; two identical sites constituted by the V regions and capable of binding essentially any macromolecule, including proteins, carbohydrates, lipids, and nucleic acids, with most binding proteins or carbohydrates), and the regions that mediate different effector functions (Fc; constituted by the CH2 and CH3 domains of dimerized IgH chains and capable of recruiting cells/molecules of effector functioning for destruction of antigens and pathogens), which include interacting with complement (binding C1q), activating macrophage, polymorphonuclear leukocytes (PMN), platelets, and binding Fc receptors, as indicated. Igs themselves are also antigens. The hydrophobic leader sequence of both H and L chain is removed immediately after synthesis and is not present in the mature Ig molecule. (B) This diagram depicts germ-line (non-rearranged) organization of human IgH chain gene segments (exons). Shown is for an Igγ3 (to be used as an example), which consists of three exons (represented by red-filled, enlarged boxes; numbered as indicated) encoding the corresponding C domains, and one exon (Hg; represented by the purple-filled, enlarged box) encoding the hinge region. Due to sequence repetition, human Igγ3 can have two to four hinge exons. Straight black lines indicate introns. Long and colorful

arrows indicate the correspondence between the DNA exon segments and the different domains of the IgH polypeptide that is encoded. Ig gene components are widely scattered through different chromosomes (chromosomes 2 and 22 for Igκ and Igλ, respectively, and chromosome 14 for IgHs) and to assemble an intact Ig molecule, they are first rearranged/spliced at the DNA level (i.e. not RNA splicing), as illustrated. Ig genetic organization, which contains individual exons that encode for different functional domains of the protein products in which binding specificity resides within V domains while subclass effector functions reside within C domains makes it possible for generation of recombination Igs combining different binding specificity and effector functions.

polypeptide subunits – two identical heavy (H) and two identical light (L) chains. These four polypeptide chains are held and stabilized together by covalent disulfide bonds between the H and L chains and between the two H chains, as well as by non-covalent intra- and inter-chain binding forces (such as salt linkages, hydrogen bonds, and hydrophobic bonds). Each of these chains comprises of two distinct regions – a variable (V) region, which is found at the amino terminal portion and has the greatest amino acid sequence variation among Ig molecules of different specificity, and a constant (C) region, which is found at the carboxyl terminal portion and, in contrast to the V region, is of relatively constant (i.e. more conserved) sequence. Fig. 1.1 shows the structure and arrangement of H and L chains and the relative positioning of inter-chain disulfide bonds.

Being IgSF protein members, Igs utilize a globular, fairly constant motif structure known as Ig domain (also called IgSF domain or Ig fold) as their basic building block (Fig. 1.1). Each Ig domain is a specific tertiary homologous structural polypeptide unit consisting of from 110 to 130 amino acids and weighting approximately 12-13 kD. Regardless of amino acid differences among Ig molecules of different classes, subclasses, or specificity, each Ig L and H chains independently fold into homologous domains, where each contains of two sandwiched β-pleated sheets linked together and stabilized by an intra-chain disulfide bond between the two conserved cysteine residues and by hydrophobic interactions between the sheets (Schroeder and Cavacini, 2010; Williams and Barclay, 1988; Amzel and Poljak, 1979). Each L chain consists of one V (VL) and one C (CL) domain, whereas each H chain contains one V (VH) and three to four C (CH) domains (CH1-CH4), depending on the Ig class (as will be discussed below). In general, Ig CH domains are defined as CH1-CH2-CH3 (IgG, IgA, and IgD), or with an additional domain (CH4) (for IgM and IgE) (Schroeder and Cavacini, 2010). The two L chains and the two H

chains weight ~25 kD and ~50-55 kD, respectively. The classical folding pattern of Ig molecules remains intact in all of regions and fragments (Attanasio et al., 1994).

The entire L chains, VH, and CH1 domains together constitute two identical fragments that recognize and bind antigens, known as Fab (Fragment – antigen binding), represented by the arms of the symmetrical Y shape (Fig. 1.1). The rest of the Ig molecule [i.e. the remaining CH domains (i.e. CH2 and CH3; also CH4 in IgM and IgE)] form a fragment that specify effector functions, termed Fc (Fragment – crytallizable), represented by the tail (the stem) of the Y shape. The V domains of both chains, which provide the structural basis of antigenic specificity, unsurprisingly, localize to the Fab. As described previously, the CH1 domains localize to the Fab, whereas the remaining CH domains (CH2-CH3 or CH2-CH3-CH4) constitute the Fc (Schroeder and Cavacini, 2010). Fig. 1.1 also illustrates the paired domains and the classical Ab fragments.

In addition to the relatively "constant", or highly conserved, CH domains, the C region of the IgH chains also contains between its CH1 and CH2 domains a nonglobular helical, extended "spacer" region of 12-15 amino acids [an exception exists with human IgG3 hinge: it contains up to 62 amino acids, dependent upon the number of repetitive sequences (Lefranc and Lefranc, 2001)] that has the highest Ig class/subclass sequence variability, both intra-species and inter-species. The region also varies in length between different Ig classes within a species. This flexible region is called the hinge, and is characterized by evolutionary instability (Scinicariello et al., 2004; Attanasio et al., 2002; Sumiyama et al., 2002; Scinicariello and Attanasio, 2001). The hinge is rich in Cys and Pro residues and can be structurally split, based on crystallographic data and the intermolecular interactions, into three discrete segments: the upper, the core (the middle), and the lower hinges (Burton and Woof, 1992; Oi et al., 1984). The upper hinge is

towards the amino terminal segment and exhibits the least homology of all sections, followed by the core. The hinge can also be exposed to enzymatic or chemical cleavage, a characteristics that has facilitated early studies of Ig structure/function relationships. For instance, papain cuts an IgG molecule into two Fab and one single Fc, whereas pepsin digests it into one single dimeric $F(ab)_2$ and one single Fc (Schroeder and Cavacini, 2010).

1.2.3. Functional features and Ig V and C regions

Ig molecules serve many and varied functions through binding antigens and targeting them to other components of the immune system (Fig. 1.2). On the basis of Ig forms of existence, these functions can be separated into two purposes: those of circulating soluble effector molecules, which recognize antigens at a distance and neutralize them, and those of cellular receptors for antigen, which trigger cell activation and signaling (Schroeder and Cavacini, 2010). On the structural basis, Igs can be subdivided into two distinct functional units: the paired V domains (i.e. Fab, a combined property of VH and VL domains) that bind antigens and confer antigenic specificity, and the Ig CH domains (i.e. Fc) that mediate effector functions and define Ig isotypes (Schroeder and Cavacini, 2010). Igs, therefore, eliminate pathogens and toxins by both cellular and non-cellular mechanisms through specific binding to them with their V domains, followed by activating cell-killing effector mechanisms via their C domains. Because of the domain structure of Ig molecules, for many purposes, the antigen-binding properties of the whole Ab and the Fab are usually considered equal (Burton, 1991).

The key Ig Fab-mediated functional activity of Ig molecules is to neutralize, or directly inactivate, toxins and infectious pathogens, particularly viruses (Fig. 1.2). For *in vivo* anti-virus protection, directly neutralizing virion infectivity is considered the most important activity of Igs

(Burton, 2002). Mechanistically, these functional activities are carried out by blocking of pathogenic functional sites through enzymic or receptor binding activity: thank to their relatively large molecular size (similar to the size of a typical virus envelope spike), Igs block virus entry into host target cells through binding to free virus particles and occupying virion sites necessary for attachment or fusion to the cells (cell receptors) (Parren and Burton, 2001). In this case, Igs, or more specifically, neutralizing Abs, can act alone, without cellular effector immune mechanisms, to protect vertebrates from viral pathogens. As described above, a single, intact Ig molecule contains two identical Fab fragments (antigen binding sites), the so-called "bivalency". A single Ig molecule, therefore, although capable of recognizing only one type of antigen, can bind and neutralize two antigens simultaneously. Furthermore, this bivalency characteristics allows Igs to bind antigens possessing repeating antigenic determinants or aggregated antigens with higher avidity (Clark 1997; Janeway et al., 1996). Due to the domain structure of Ab, the antigen-binding properties of Fab are typically considered those of entire Ab.

The Ig Fc regions typically act through the interactions between their various Ig Fc receptors (FcRs) and the Ab-antigen complexes (or immune complexes; ICs), which induce diverse and potent immune responses that are critical for healthy immunity (Fig. 1.2). Following the formation of ICs, the Fc regions can activate different cell-killing immune effector mechanisms that effect the destruction and clearance of antigens and pathogens through their binding to FcRs, which are expressed on various immune cells, or through recruiting other immune mediators, such as complement (Schroeder and Cavacini, 2010). In normal immune systems, three major mechanisms for the destruction and clearance of the antibody-coated (also known as opsonized) antigens – all result in lysis of the pathogens by lytic enzymes – are known:

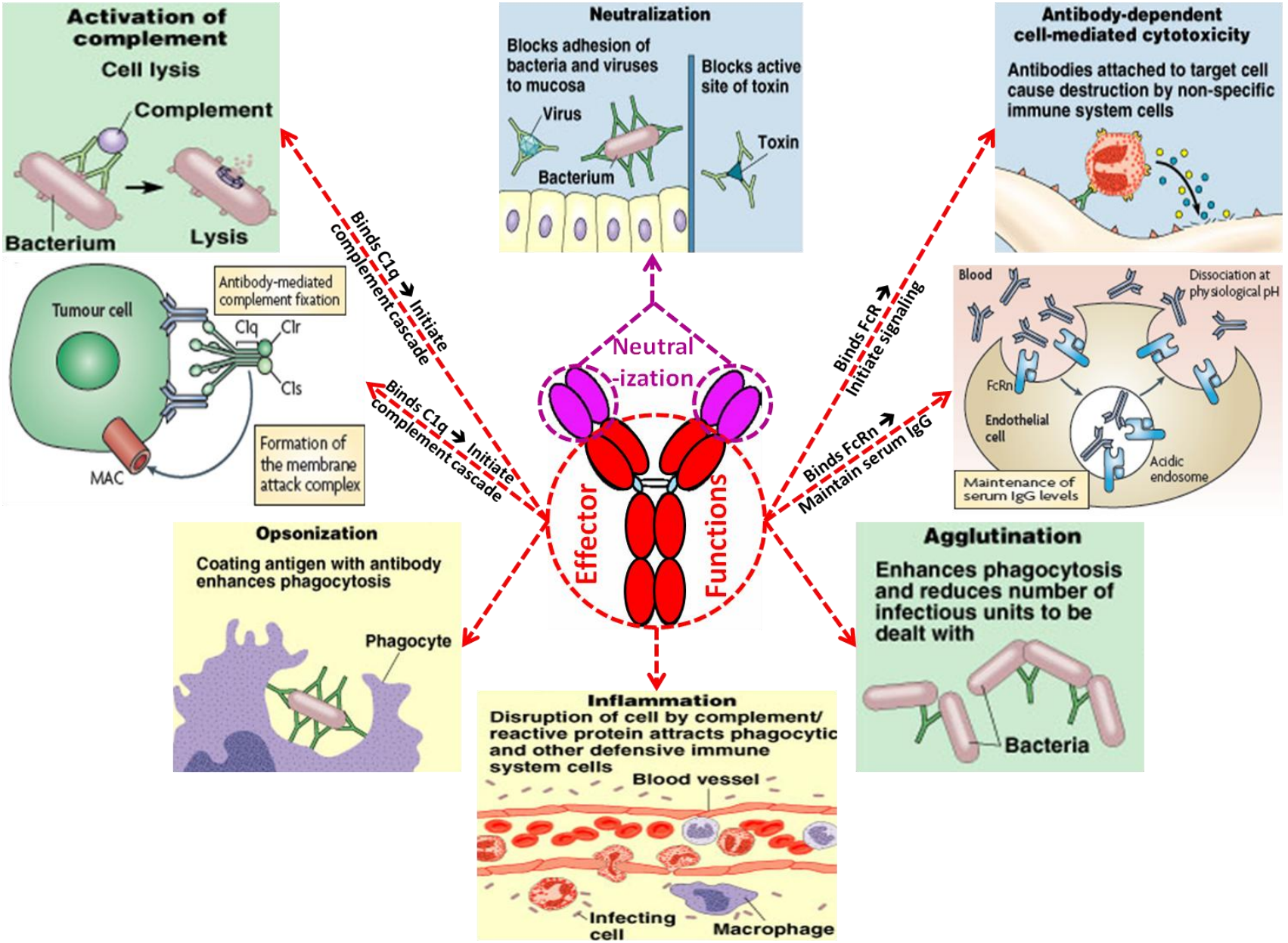
Activation of complement
Cell lysis
Complement
Bacterium
Lysis
Neutralization
Blocks adhesion of bacteria and viruses to mucosa
Blocks active site of toxin
Virus
Bacterium
Toxin
Antibody-dependent cell-mediated cytotoxicity
Antibodies attached to target cell cause destruction by non-specific immune system cells
Tumour cell
Antibody-mediated complement fixation
Clq
Clr
Cls
MAC
Formation of the membrane attack complex
Binds C1q → Initiate complement cascade
Binds C1q → Initiate complement cascade
Neutral-ization
Effector Functions
Binds FcR → Initiate signaling
Binds FcRn → Maintain serum IgG
Blood
Dissociation at physiological pH
FcRn
Endothelial cell
Acidic endosome
Maintenance of serum IgG levels
Opsonization
Coating antigen with antibody enhances phagocytosis
Phagocyte
Agglutination
Enhances phagocytosis and reduces number of infectious units to be dealt with
Bacteria
Inflammation
Disruption of cell by complement/ reactive protein attracts phagocytic and other defensive immune system cells
Blood vessel
Infecting cell
Macrophage

Fig. 1.2. Functional features of Ig V and C regions and Ig domain structure/function properties. See texts for details. Figure is modified from Weiner et al., 2010, Casadevall et al., 2004, and the internet.

1) Antibody-dependent cell cytotoxicity (ADCC), in which the ICs activate effector cells [through the Fc-FcR (specifically, FcγRIIIa) binding], such as natural killer cells or monocytes; 2) Complement-dependent cytotoxicity (CDC; through C1q binding), in which the complement pathway is recruited and the complement cascade is activated; and 3) Fc-mediated phagocytosis, or Ab-dependent cellular phagocytosis (ADCP), in which phagocytic cells (i.e. macrophages neutrophils, and dendritic cells) are activated [through the Fc-FcR (FcγRII/I) binding] (Fig. 1.2). Other Ig functional activities and responses that assist in directing appropriate immune responses include opsonizing, inducing respiratory burst, releasing inflammatory mediators (inflammation), antigen presentation, degranulation of cytotoxic cells, mast cell degranulation, as well as other antigen-independent functions, such as crossing the placenta [placental transport; through binding to the neonatal FcR (FcRn)], maintaining half-life (through binding to FcRn), multimerizing, regulating lymphocyte proliferation and differentiation, including B cell activation, secreting cytokines and chemokines, and being secreted on mucosal surfaces (Schroeder and Cavacini, 2010; Smith and Clatworthy, 2010; Weiner et al., 2010; Jefferis et al., 1998; Burton and Woof, 1992). Therefore, through the binding of ICs to specific FcRs, the Ig Fc regions can provide humoral immunity with a cell-based effector functional system (Smith and Clatworthy, 2010).

In addition to being capable of inducing Ab-dependent killing of target cells, the Fc regions can also affect V domain binding affinity and specificity (Torres and Casadevall, 2008) and suppress humoral immunity (Smith and Clatworthy, 2010) (will be discussed in more details later). Also, in abnormal immune circumstances, such as autoimmunity or allergies, the IC-FcR interactions might cause adverse consequences, like development of tissue injury, or might even

be involved in pathogenesis of immunological disorders and diseases, including rheumatoid arthritis and systemic lupus erythematosus (SLE) (Takai 2005; Hogarth 2002).

1.2.4. Functional features and the role of the hinge and glycosylation

As discussed previously, the Ig hinge region contains several conserved Cys residues and can be divided into three sections. The core hinge is rich in Cys (and Pro) residues that form the IgH inter-chain disulfide bonds and is thus relatively inflexible (i.e. rigid). The upper and the lower hinges can mediate Ig segmental (Fab-Fc) and rotational (Fab-Fab) flexibility by directly allowing the two Fab portions of the Y-shaped molecule to "open" or "close" (for two Fab arms as a whole), and rotate (for each individual Fab arm) – relative to the Fc position (Clark, 1997). The ability of Fab arms to be differently positioned improves Ig access and accommodation, and thus allows differently spaced and/or distinctly oriented antigens or antigen determinants to be bivalently recognized by the two binding sites (Clark, 1997; Kim et al., 1994; Burton and Woof, 1992).

In addition to playing a role in intermolecular covalent assembly and flexibility (the core hinge), the hinge also plays a crucial role in IC formation (the upper hinge), may be required for FcR binding and complement activation (the lower hinge) (Coloma et al., 1997; Roux et al., 1997), as well as may affect signal transduction (Clark, 1997; Rudich et al., 1988). The flexibility of Fc portion, relative to Fab fragments, can influence interactions of Igs with coresponding FcRs or other molecules. As a consequence, the extended human IgG3 hinge is believed to have better flexibility, and thus be more effective in antigen binding and in triggering effector mechanisms (Burton and Woof, 1992). The hinge of IgG subclasses will be described further in the following sections. Distinct structures of the hinge in different species might,

therefore, alter molecular flexibility, neutralizing ability, reactivity with and binding affinity to FcRs, the capability to activate the complement cascade, susceptibility to proteolytic enzymes, or other Ig functional properties of Igs (Torres and Casadevall, 2008; Thommesen et al., 2000; Michealsen et al., 1990, Tan et al., 1990).

As mentioned above, Igs are glycoproteins in their nature. While IgL chains are aglycosylated, IgH chains (in particular, Fc portions) are integrally attached covalently with oligosaccharide groups (i.e. carbohydrate moieties), usually at CH2 domain (Sutton and Phillips, 1983). The extent of glycosylation varies, dependent upon Ig isotype (Arnold et al., 2007). Carbohydrates are important for proper Ig folding and for stabilizing IgG-FcγR binding (Schroeder and Cavacini, 2010; Lund et al., 1995). Fc-associated glycans are also capable of affecting Ab functions, including mediating complement activation and influencing FcR binding (Schroeder and Cavacini, 2010; Miletic and Frank, 1995). Changes in glycosylation of IgH chains can, therefore, result in alteration of Ig functions, including effector functions (particularly complement activation) (Schroeder and Cavacini, 2010). Indeed, more effective therapies might be obtained from differential or modified glycosylation patterns engineered in passive immunotherapy or *in vivo* treatment (Collin et al., 2008; Smith et al., 2004).

Collectively, Abs are extremely versatile molecules, structurally and functionally. The globular domain structure of Ab molecules is facilitative of genetic engineering (as will be discussed later). Changes in the Fc may influence the end result of Ab-antigen interactions, including the affinity and/or kinetics of the Fab-mediated antigen recognition and binding (Schroeder and Cavacini, 2010; Torres and Casadevall, 2008).

1.2.5. Gene organization, DNA rearrangement, and production of Ig

Higher vertebrates feature with a humoral immune system that is uniquely characterized by its ability to generate a vast diversity of Abs to respond to virtually unlimited array of antigens or pathogens sharing little or no similarity. This unique characteristics relies largely on the Ig gene organization and DNA rearrangement mechanisms. In humans, IgH and IgL chains are encoded by separate multi-gene families located on three different chromosomes (Schroeder and Cavacini, 2010; Tonegawa, 1983). Specifically, IgL κ and λ families are located on chromosomes 2 and 22, respectively, whereas IgH family is located on chromosome 14 (Lefranc and Lefranc, 2001). Each multi-gene family contains different, independent gene segments that encode individual V and C domains of each Ig H or L chain. In particular, IgL κ and λ families consist of V, J (for joining), and C gene segments, whereas IgH family contains V, D (for diversity), J, and C gene segments. Each V gene segment generally contains its own promoter, a leader exon, an intervening intron, an exon encoding V domain, and a recombination signal sequence (RSS) (Schroeder and Cavacini, 2010). The IgH C gene (*IGHC*) segments consist of nine functional and two pseudo (Ψ), non-functional, C genes. Each Ig isotype is encoded by a separate CH gene region, namely μ, δ, γ, α, or ε, which correspond to the five IgH isotypes. These CH region gene segments are aligned in the same transcriptional orientation on chromosome 14, in the IgH locus, downstream of V region genes (*IGHV*) (Bengten et al., 2000). Generally, each CH gene region consists of three main exons, each individually encoding CH1, CH2, and CH3 IgH domains, and of one or more additional exons encoding the hinge (Schroeder and Cavacini, 2010; Bengten et al., 2000).

Ig V and C domains are produced through two independent DNA rearrangement and recombination events. VL and VH domains are expressed by the so-called rearranged VJ and

rearranged VDJ gene segments, respectively. These VJ and VDJ rearranged gene segments result from a number of gene rearrangement events that occur in B cells during their early development in the bone marrow – in the absence of antigens. They are expressed in association with the Ig μ chain (to produce IgM) and following antigen exposure, can undergo somatic hypermutation that allow maturation and increase of affinity for the antigens. Ig CL and CH domains are expressed by the C gene segments in the L and H multi-gene families, respectively. Different CH domains (i.e. γ, α, or ε) can be produced in response to antigenic stimulation (such as by immunization or infection) and cytokine regulation by activated B cells in their late development – in the spleen or lymph nodes. They can then be subjected to the so-called class switch recombination event (i.e. from IgM to IgG, IgA, or IgE), a process in which effector functions may be altered but antigen-binding specificity remains unchanged (Schroeder and Cavacini, 2010). Not only the antigen and the signaling pathways, but also the local microenvironment may have influence on which Ig isotype is to be chosen during class switch (Schroeder and Cavacini, 2010).

Therefore, a vast Ig repertoire with a great number (~10^{16}) of structurally distinct molecules (that is, against virtually any antigenic structure) can be generated through a number of molecular mechanisms that alter the DNA of individual B cells. These mechanisms include genetic organization by individual gene segments, somatic variation and random combinatorial rearrangement of these segments, as well as combinatorial association between different L and H chains – and all processes are without the presence of antigens (or further diversification by hypermutation) (Schroeder and Cavacini, 2010). Thus, although an individual Ig molecule can only bind a limited set of ligands, as discussed previously, Igs as a population can bind to an almost unlimited array of antigens or chemical structures.

1.2.6. Ig classification: Ig L and H chain classes (isotypes)

Humans Igs are categorized into five major classes (or isotypes), IgM, IgG, IgA, IgD, and IgE, which are defined by and correspond to the five main classes of their low-variability CH regions, designated μ, γ, α, δ, and ε, respectively (Clark, 1997). IgL high-variability regions can be grouped into two types, κ and λ. In a complete Ig molecule, each class (or isotype) of the five H chains (i.e. μ, γ, α, δ, or ε) is associated to either – but not both – a κ or a λ chain. In some species, these classes are further split into subclasses, which suggest their recent evolution (i.e. recent gene duplication events) (Clark, 1997; Bruggemann, 1988). The ratio of Igs with κ or λ chains represented in human serum is about 60:40, whereas it is 95:5 in mouse serum. The numbers of Ig classes also vary among species.

It is the CH regions that distinguish the five different Ig classes and define their specific effector mechanisms (Clark, 1997). In addition to exhibiting distinct characteristic patterns of functional effector activities, classes also differ in some other properties, including size and subclass response to antigen (Schroeder and Cavacini, 2010). Amino acid substitution or polymorphism in Ig CH regions may also affect effector functions of Abs.

1.2.7. IgG: General functional activities and subclass classification

Human IgG represents the most abundant Ig class found in the body, including in serum [constituting ~80% of the total serum Igs (Clark, 1997)], extracellular fluid, and lymph nodes (Fig. 1.3). IgG exists as monomers and has the longest Ig serum half-life and is also most extensively studied. This Ig class also represents the most frequently used Ig isotype in cancer immunotherapy. IgG can be used as a model for considering many key Ig functional features,

including binding antigen through V domains and, at the same time, interacting with conserved effector systems through C domains.

IgG may contribute directly to an immune response, such as neutralizing toxins, viruses, and other infectious pathogens. Patients diagnosed with low levels of IgG (hypogamma-globulinaemia) exhibit increased susceptibility to infections (Smith and Clatworthy, 2010). IgG is capable of carrying out all the Ig cell-killing effector functions necessary for removal of pathogens. Such functional activities include ADCC, CDC, ADCP, opsonization, as well as sensitization and activation of other (than natural killer cells and macrophages) immune effector cells, such as neutrophils, basophils, and mast cells, as discussed previously (Fig. 1.3). IgG that coats antigens can bind FcRs through its Fc and trigger signaling through immunoreceptor tyrosine-based activation motifs (ITAMs) or immunoreceptor tyrosine-based inhibitory motifs (ITIMs). In addition to these antigen-dependent functions, this Ig class can also bind neonatal Fc receptors (FcRn) on endothelial cells to maintain serum IgG levels or to define Ab half-life. The binding to tumor cells of two or more IgG molecules can lead to subsequent recruitment and binding of complement component 1q (C1q) to IgG Fc, which can then initiate the complement cascade, resulting in tumor cell lysis by the membrane attack complex (MAC) (Weiner et al., 2010). Regardless of subclasses (see below), IgG is also able to be transferred from the maternal plasma to the fetus through the placenta to provide fetal immunity (trans-placental transport) (Parham, 2000; Clark, 1997), as well as to participate in the secondary immune responses (Schroeder and Cavacini, 2010).

Based on structural, antigenic, and functional differences in CH region, human IgG is split into four subclasses, IgG1, IgG2, IgG3, and IgG4, designated γ1, γ2, γ3, and γ4, respectively (Schroeder and Cavacini, 2010) (Fig. 1.3). This numbering of IgG subclasses is referred to the

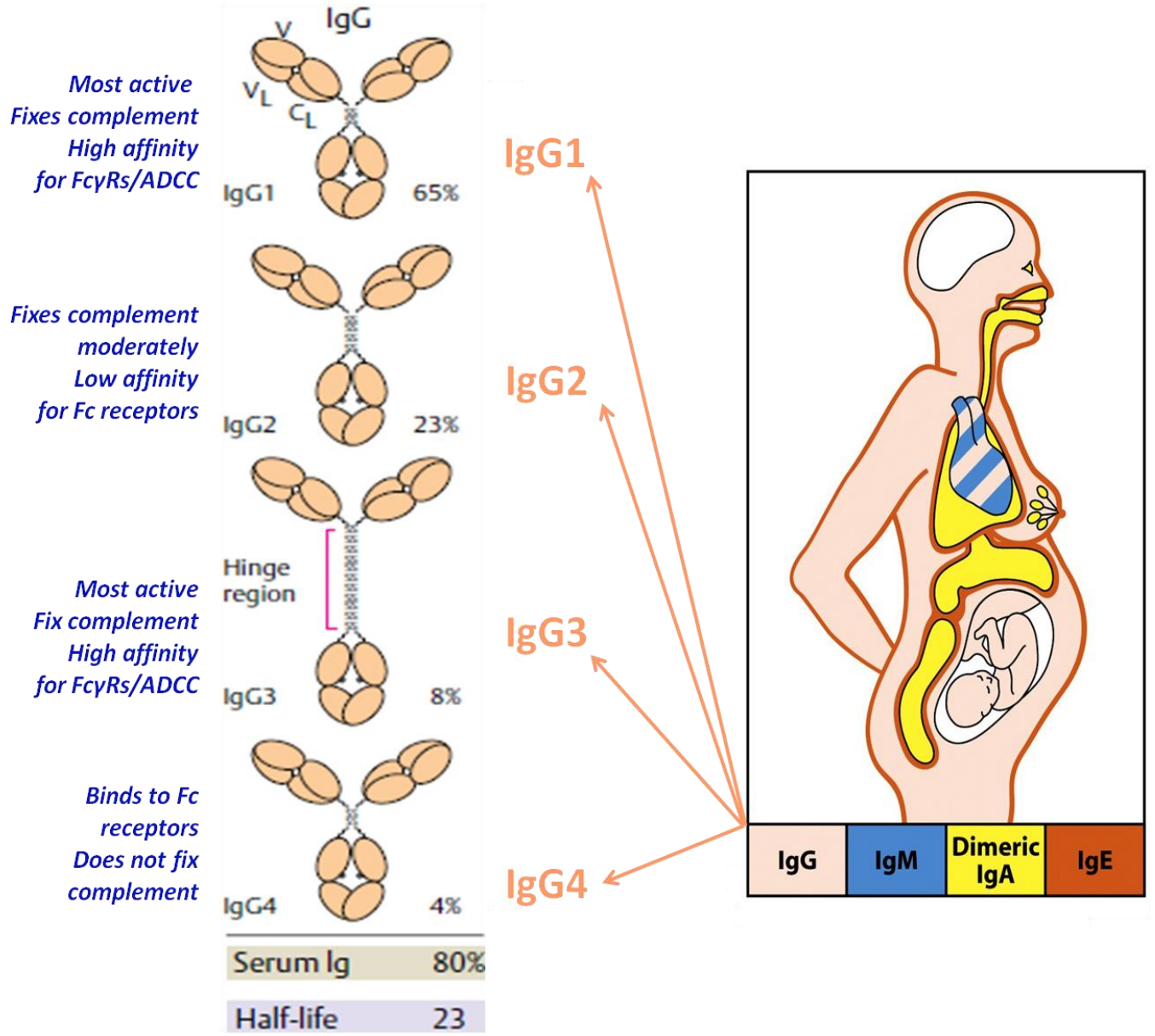
IgG
V
V_L
C_L
Most active
Fixes complement
High affinity
for FcγRs/ADCC
IgG1 65%
Fixes complement
moderately
Low affinity
for Fc receptors
IgG2 23%
Hinge region
Most active
Fix complement
High affinity
for FcγRs/ADCC
IgG3 8%
Binds to Fc
receptors
Does not fix
complement
IgG4 4%
Serum Ig 80%
Half-life 23
IgG1
IgG2
IgG3
IgG4
IgG
IgM
Dimeric IgA
IgE

Fig. 1.3. Human IgG: most common in serum, classified into four subclasses, possessing slight structural yet significant functional differences. See texts for details. Figure is modified from Murphy et al., Immunobiology, 7th Edition, Garland Publishing, 2008, and Burmester and Pezzutto, Color Atlas of Immunology, Georg Thieme Verlag, 2003.

decreasing order (i.e. IgG1, IgG2, IgG3, and then IgG4) of their serum concentration level (Schroeder and Cavacini, 2010). The production of IgG subclasses may be influenced by various factors, including properties of antigens (i.e. structure and quantity, route of administration, and duration of stimulation) and characteristics of individual host (such as age and the genetic background) (Bachmann and Zinkernagel, 1996). Like with the class definition, the identity of subclass of an individual IgG is determined by variations in its CH regions. Indeed, due to recent gene duplication events (as described above), the four human IgG subclasses share high homology in CH domain sequences (>90%; Clark, 1997). By contrast, the hinge, which is unique to each subclass and most diverse among subclasses by amino acid composition and structure, exhibits the greatest sequence variations among IgG subclasses within an individual species (~56-60% identity among subclasses, compared to >90% homology shared by CH domains). Therefore, the hinge can be used to rapidly differentiate the four subclasses (Papadea et al., 1989) (the four subclasses, indeed, also differ in the number and arrangement of their interchain disulfide bonds). Consequently, as will be described later, while the high identity within IgG subclasses has facilitated studies of the key Ab functional residues, the heterogeneity of the hinge can obscure investigating amino acids crucial for Ab intermolecular interactions (Clark, 1997; Roux et al., 1997).

As previously discussed, glycosylation pattern varies among Ig classes and subclasses. Although glycosylation variation is also observed among IgG molecules (Schroeder and Cavacini, 2010), the N-linked glycosylation site located at Asn297 on each CH2 domain is highly conserved throughout IgG evolution. In addition, not only forming extensive contacts with amino acid residues within CH2 domains and subjected to posttranslational modifications, but also the N-glycan at Asn297 is involved in IgG-FcγR recognition and binding. These

findings suggest that this N-linked carbohydrate moiety plays an important role in Ig domain stabilization and may even be capable of optimizing IgG *in vivo* effector functions (Schroeder and Cavacini, 2010; Burton and Woof, 1992).

The CH region genes of the four IgG subclasses (*IGHG*) are designated as *IGHG1*, *IGHG2*, *IGHG3*, and *IGHG4*, according to the IMGT nomenclature (Lefranc and Lefranc, 2001). Each of the four *IGHG* genes consists of four individual exons, namely CH1, the hinge, CH2, and CH3, each individually encoding the corresponding CH domain (i.e. CH1, the hinge, CH2, and CH3 domains, respectively). An exception exists in human IgG3, where its hinge, due to sequence repeats, is encoded by two to five exons (Lefranc and Lefranc, 2001; Burton and Woof, 1992), as previously discussed. The IgG lower hinge, which is defined based on the intermolecular interactions, is, nevertheless, encoded by partial CH1 (C-terminus) exon and partial CH2 exon (Burton and Woof, 1992).

1.2.8. IgG subclasses: Distinct characteristic patterns of effector functions

While the four IgG subclasses exhibit light differences in sequence and structure, they express significant differences in function. Each subclass is characteristic of its own patterns and properties of functional activities, including in clearance mechanisms of opsonized antigens that are carried out upon antigen exposure, and at level of expression in response to specific antigenic stimulation (Schroeder and Cavacini, 2010). Generally, IgG1 and IgG3 are the most efficient activators, followed by IgG2 which is moderately potent, whereas IgG4 is only marginally active or inactive (Morrison et al., 1994). In particular, IgG1 and IgG3 are most effective with ADCC and CDC, whereas IgG2 is only moderately efficient in and IgG4 is incapable of carrying out CDC. Also, within the secondary immune response, while IgG1 and IgG3 are predominantly

produced against protein antigens, IgG2 and IgG4 are generally induced by polysaccharide antigens (Schroeder and Cavacini, 2010).

The four IgG subclasses also differ in their binding capability and affinity to the three major IgG FcR (FcγR) classes: IgG1 and IgG3 are capable of binding and have the highest affinity for all three FcγR classes, IgG2 fails to bind FcγRI and FcγRIII, whereas IgG4 can bind FcγRII and FcγRIII but only with low affinity (Schroeder and Cavacini, 2010) (Fig. 1.3).

Binding of IgG subclasses can further be influenced by other factors, such as their hinge structural diversity and flexibility, as well as the attached carbohydrates (glycans). Typically, ligand IgG molecules bind coressponding FcγRs in the lower hinge through an extensive contact surface. This area contains overlapping but not identical residues from the two IgH (Fc) chains, thus the binding is asymmetrical. Also, the length and flexibility extent of IgG subclass hinge regions are as from the greatest to the least as IgG3, IgG1, IgG4, and IgG2 (Clark, 1997; Roux et al., 1997; Brekke et al., 1995). Early studies have recognized a correlation between effector function efficiency (including complement activation) and flexibility patterns of IgG subclasses (Clark, 1997; Burton and Woof, 1992). More recent data suggest that IgG subclasses differ in their efficiency of neutralizing viruses and toxins, and that the hinge structure may influence the *in vitro* neutralizing activity of Abs (Cavacini et al., 2003; Liu et al., 2003; Scharf et al., 2001; Cavacini, 1995). In these studies, IgG3 appeared be more efficient than IgG1 at neutralizing virus antigens (Schroeder and Cavacini, 2010). IgG3 is also highly susceptible to proteolytic endonuclease cleavage (Clark, 1997). As previously discussed, the advantage of IgG3 in virus neutralizing capability may lie in its unique, extended hinge structure, which can increase the segmental flexibility and improve the accessibility of the molecules onto the antigens, thus enhance effector functions (Cavacini et al., 2003; Scharf et al., 2001). These

findings imply the possibility of designing Ab molecules with improved functions through manipulating their hinge region.

Taken as a whole, specific IgG subclass responses, amino acid residues involved in specific FcγR binding and effector functions, and interactions with different antigenic stimulations, can therefore all be associated with healthy immune responses (and, similarly, individual disease processes). Understanding these specific responses and properties, particularly different types of clearance mechanisms, will improve efficiency in the control and prevention of diseases and infections, as well as in development of vaccines and therapeutic Abs (Schroeder and Cavacini, 2010).

1.3. Ig and IgG Fc receptors: Overview, classification, structural and functional features, and allelic polymorphism

1.3.1. Ig Fc receptors (FcRs) and IgG Fc receptors (FcγRs): Overview

To carry out their cell-killing effector functions, Igs, upon binding specific antigens with their paired V domains and forming the Ab-antigen immune complexes (ICs), interact with different innate immune effector cells through binding to their cell-surface receptors with their C domains. Fc receptors (FcRs), as they are termed, are transmembrane glycoproteins that specifically recognize and bind the multifunctional Fc portion of Igs. FcRs bind to Igs that are attached to pathogens (antigens) or infected cells, or that are bound to tumor cells (i.e. Ig-opsonized particles, or ICs). This binding triggers the cell signal transduction events and initiates various immune cell-killing effector functions (such as ADCC, CDC, and ADCP, as previously described), resulting in cellular activation or inhibition of other immune-competent (phagocytic or cytotoxic) cells (Ravetch and Bolland, 2001). Ultimately, activated phagocytic or cytotoxic

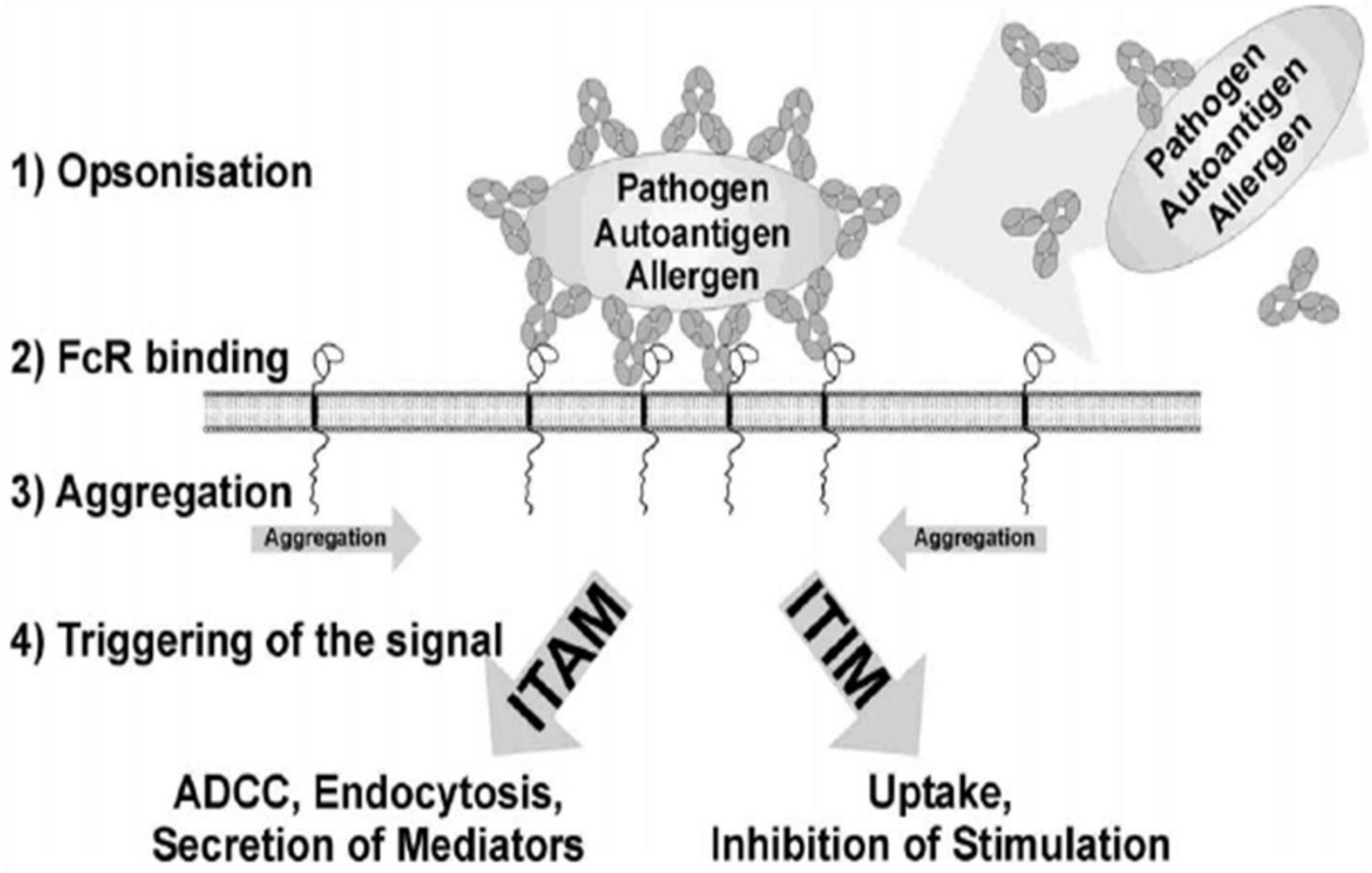
1) Opsonisation
2) FcR binding
3) Aggregation
4) Triggering of the signal
Pathogen
Autoantigen
Allergen
Pathogen
Autoantigen
Allergen
Aggregation
Aggregation
ITAM
ITIM
ADCC, Endocytosis,
Secretion of Mediators
Uptake,
Inhibition of Stimulation

Fig. 1.4. Mechanisms of action of FcRs: Binding of FcRs with Ig-opsonized particles triggers the cell signal transduction events and initiates various cell-killing immune effector functions, resulting in cellular activation or inhibition of other immune-competent cells. See texts for details. Figure is reproduced from Sondermann and Oosthuizen, 2002.

cells destroy and remove invading pathogens or infected cells, and promote tumor cell lysis (Ravetch and Bolland, 2001) (Fig. 1.4). FcRs, therefore, form a bridge between the humoral and cell-based immunity and couple the potency of cellular effector activities with the specificity of Ig binding responses.

In addition to fulfilling such protective effector functions, FcR-mediated immunity also plays an important role in the regulation of normal, healthy immune responses, including modulation of Ig production by B cells (Fig. 1.5). It is also involved in a variety of diverse disease groups, including autoimmune disorders (in particular, systemic lupus erythematosus), allergies, infectious diseases, as well as in inflammatory diseases, hypersensitivity, and cancer. Because of their involvement in diseases and capability to act as activators or inhibitors (i.e. regulators) of the immune system, FcRs have been considered excellent targets for therapies. Indeed, particular FcγR allelic variations that are associated with disease susceptibility and/or severity, or that can influence the outcome of Ig-based treatments, have been documented (van Sorge et al., 2003; Cartron et al., 2002). FcR-derived immunotherapies, particularly the technology for enhancement of therapeutic monoclonal Ig potency through optimizing the Ig-FcR interactions, have risen as a promising approach for the treatment in numerous clinical situations, including those named above (Sondermann and Oosthuizen, 2002).

FcRs, as a population, are expressed on the surface of many immune cells, virtually all immunologically active and competent cells (called effector cells), or in other words, of almost every cells of the immune system (Smith and Clatworthy, 2010; Sondermann and Oosthuizen, 2002) (Fig. 1.5). Due to several reasons, including encoding gene organization, multiple transcripts (isoforms), and polymorphic forms, as discussed below, the cellular expression of FcγR classes is complex. In humans, FcRs are classified based on the class of Igs that they

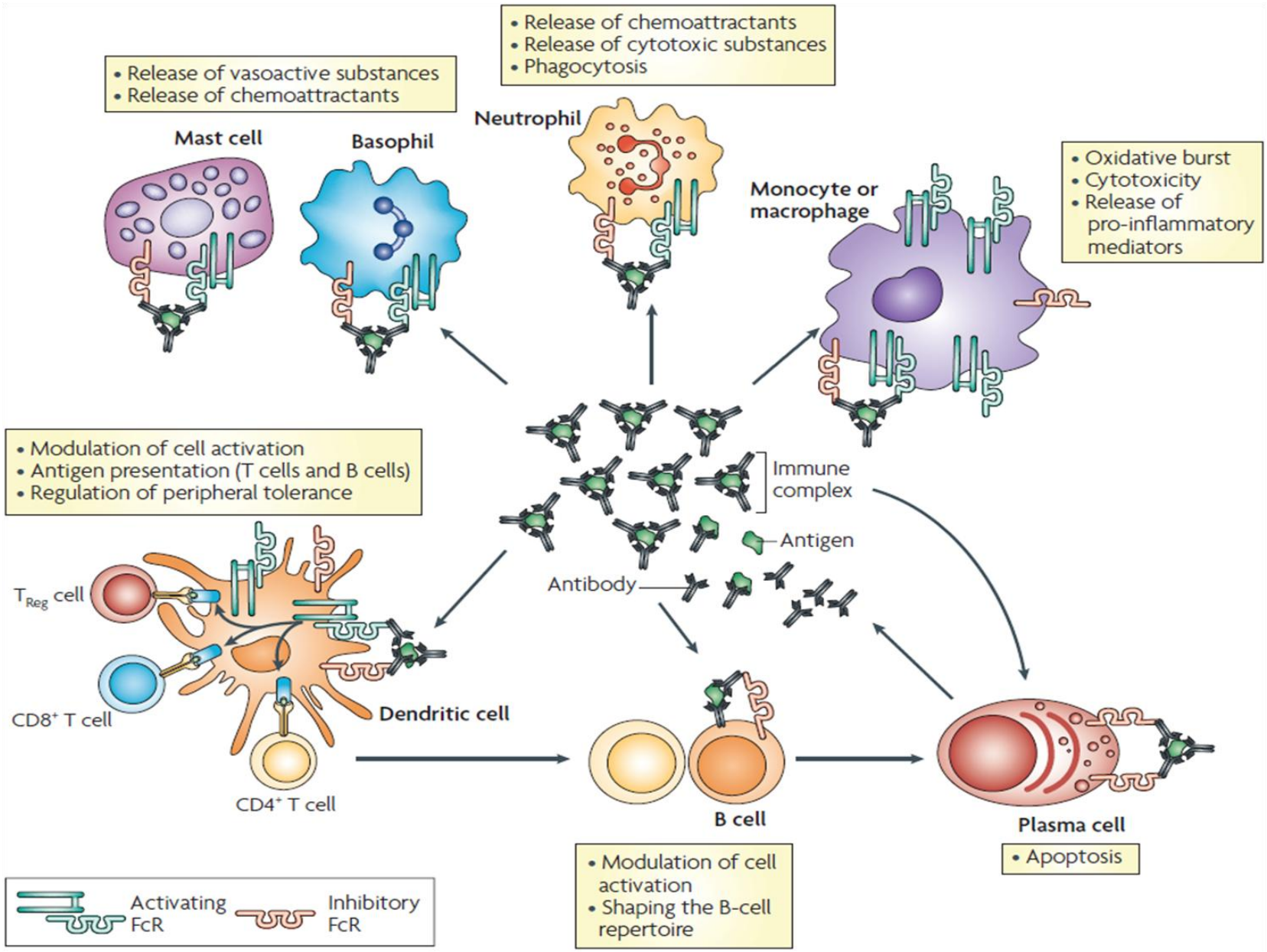
• Release of vasoactive substances
• Release of chemoattractants
Mast cell
Basophil
• Release of chemoattractants
• Release of cytotoxic substances
• Phagocytosis
Neutrophil
Monocyte or macrophage
• Oxidative burst
• Cytotoxicity
• Release of pro-inflammatory mediators
• Modulation of cell activation
• Antigen presentation (T cells and B cells)
• Regulation of peripheral tolerance
Immune complex
Antigen
Antibody
T_{Reg} cell
$CD8^+$ T cell
Dendritic cell
$CD4^+$ T cell
B cell
Plasma cell
• Modulation of cell activation
• Shaping the B-cell repertoire
• Apoptosis
Activating FcR
Inhibitory FcR

Fig. 1.5. Activating and inhibitory FcRs and the regulatory functions of immune complexes. See texts for details. Figure is reproduced from Nimmerjahn and Ravetch, 2008.

recognize. FcRs for IgG, the most common serum and extracellular fluid Ig, are termed FcγRs. FcγRs play an important role in promotion and regulation of the immune and inflammatory responses to Ab-antigen immune complexes (Smith and Clatworthy, 2010). FcγRs have also been most extensively studied among FcRs, and will be the only focus to be discussed hereafter. The neonatal Fc receptor (FcRn), an IgG Fc receptor that mediates the transcytosis of maternal IgG to the neonate and regulates serum IgG level (i.e. half-life) (Schroeder and Cavacini, 2010), is neither included from consideration in this dissertation.

1.3.2. FcγRs: Classification, structural features, and effector cell distribution patterns

Human FcγRs are classified, based on sequence and molecular structure, into three classes with eight members, FcγRI (CD64; consisting of three members a, b, and c), FcγRII (CD32; consisting of three members a, b, and c), and FcγRIII (CD16; consisting of two members a, and b) (Jefferis and Lund, 2002; Clark, 1997) (Fig. 1.6). Not only these classes exhibit considerable genetic, structural, and functional diversity, but also they differ significantly in binding affinity (due to ditinct molecular structure) and specificity for ligands (i.e. IgG subclasses) (Smith and Clatworthy, 2010). These molecules also have unique cell type distribution patterns (cell-specific distribution) and effector functions (Smith and Clatworthy, 2010; Jefferis and Lund, 2002; Ravetch and Kinet, 1991).

Structurally, all FcγRs represent typical type I transmembrane glycoproteins and are members of the Ig superfamily (IgSF), which comprised of a unique ligand (IgG)-binding α-chain consisting of Ig C-like extracellular domains (ectodomains) (D), followed by a short cytoplasmic tail (CYT) that links the receptor to the cellular plasma membrane (transmembrane; TM), and a signaling chain (Daeron, 1997) (Fig. 1.6). In general, FcγR classes either have CYT

domains that are capable of delivering signal transduction or associate with signaling co-receptor complexes (Ravetch, 1994). However, an exception exists in CD16b: it is attached by glycophosphatidylinositol (GPI) tail instead of the TM/CYT (i.e. lacking a transmembrane domain and being GPI-linked to the outer membrane) (Clark, 1997; Ravetch, 1994). CD32 and CD16 contain two conserved ectodomains, N-terminal (membrane-distal) D1 and C-terminal (membrane-proximal) D2, whereas CD64 has a third ectodomain, D3 (Ravetch and Bolland, 2001). These receptors are also composed of a signal/leader (L) peptide that allows their transport to the cell surface.

All FcγR classes are encoded by a gene family located on chromosome 1. These genes share common overall intron-exon genetic organization consisting of five or six exons: two encoding leader (L) peptide, two or three encoding D ectodomains, and one encoding the TM/CYT tail (van de Winkel and Capel, 1993). Individually, each of these three FcγR classes is encoded by a cluster of closely related genes: the three human CD64 or CD32 isoforms are encoded by three closely related genes, FcγRIa, FcγRIb, and FcγRIc, or FcγRIIa, FcγRIIb, and FcγRIIc, respectively; similarly, the two human CD16 isoforms are encoded by two separate highly homologous genes, FcγRIIIa and FcγRIIIb (Clark, 1997).

FcγRs also differ in their cellular expression profiles, as discussed above (Fig. 1.6). In general, CD64 and CD32a are produced by both myeloid and granulocyte cells, whereas CD16a or CD16b is expressed by myeloid cells or granulocyte cells, respectively (Smith and Clatworthy, 2010). In particular, CD64 and CD32a are constitutively expressed, to varying degrees, on innate immune cells capable of fulfilling multiple effector functions, including phagocytosis and ADCC, which include macrophages, monocytes, neutrophils (granulocytes), and dendritic cells (Schroeder and Cavacini, 2010; Nimmerjahn et al., 2008; Clark, 1997).

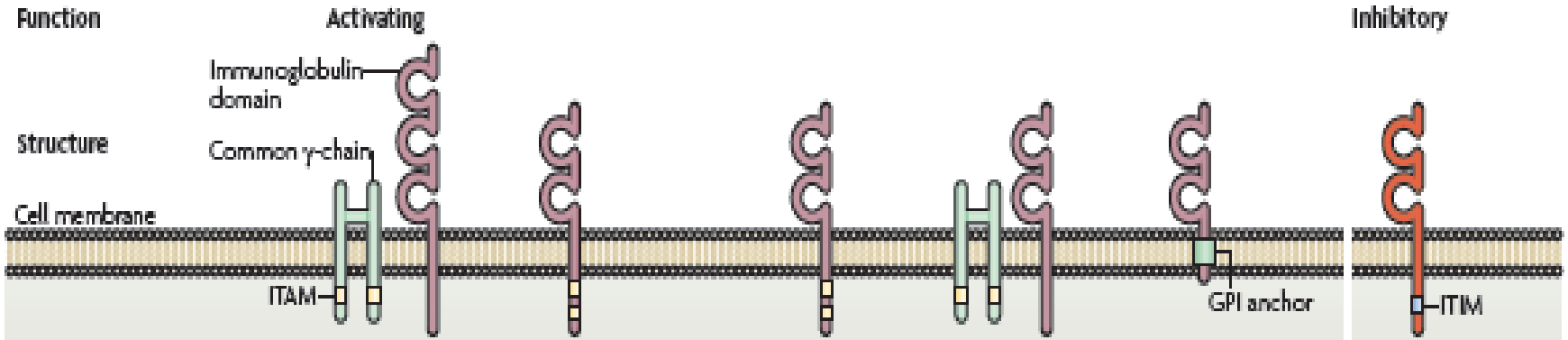

Name		FcγRI	FcγRIIA	FcγRIIC	FcγRIIIA	FcγRIIIB	FcγRIIB
Expression	Lymphoid	Not expressed	Not expressed	NK cell	NK cell	Not expressed	B cell and plasma cell
	Myeloid	Monocyte, DC and macrophage	Monocyte, DC, platelet and macrophage	Not expressed	Monocyte, DC and macrophage	Not expressed	Monocyte, DC and macrophage
	Granulocyte	Neutrophil and eosinophil	Neutrophil	Not expressed	Not expressed	Neutrophil, mast cell and eosinophil	Neutrophil, basophil and mast cell
IgG binding affinity		IgG1>>>IgG2, IgG3 and IgG4	IgG1 and IgG3>> IgG2>IgG4	IgG1>IgG3>> IgG4>IgG2	IgG1>>IgG2 and IgG3 >IgG4	IgG1 and IgG3>> IgG2 and IgG4	IgG1>IgG3>> IgG4>IgG2

Fig. 1.6. Activating and inhibitory IgG FcRs: Structure, function, binding affinity, and cellular expression profiles. See texts for details. Figure is reproduced from Smith and Clatworthy, 2010.

CD32b is mainly expressed on B-cells. Indeed, CD32b is the only FcγR expressed by B cells (Smith and Clatworthy, 2010), and is also found on other immune effector cells, including macrophages, dendritic cells, activated neutrophils, mast cells, and basophils (Smith and Clatworthy, 2010; Nimmerjahn et al., 2008). CD16a is nearly exclusively expressed on natural killer (NK) cells (which is also the only FcγR expressed on these cells), which are the principal cell type carrying out ADCC. However, CD16a is also found on other effector cells such as macrophages, monocytes, neutrophils, and dendritic cells, while CD16b, which has only been described in humans, is exclusively present on neutrophils (Clark, 1997). Of immune effector populations, NK cells, macrophages, neutrophils, and dendritic cells are most potent.

1.3.3. FcγRs: Functional activities, IgG isotype-binding affinity, and signal transduction of activating and inhibitory FcγRs

Binding of ICs to FcγRs can induce potent and diverse immune responses. In healthy immunity systems, the binding to activating FcγRs (see below for the concept) mediates pathogen clearance – directly by various effector functional activities of Ab-dependent killing of target cells, as well as indirectly through other antigen-dependent and antigen-independent mechanisms, such as the release of cytokines and other inflammatory mediators (Smith and Clatworthy, 2010; Nimmerjahn et al., 2008) (Fig. 1.5). The binding to inhibitory FcγRs, on the other hand, can suppress humoral immunity (Smith and Clatworthy, 2010). FcγRs also mediate neutralization of pathogen- or toxin-bound IgG complexes (Perez et al., 2009; Verma et al., 2009). In abnormal immunity status, such as in autoimmunity, however, the binding to FcγRs (especially FcγRIIa) might induce robust inflammatory responses with adverse consequences in diseases or disorders like rheumatoid arthritis and SLE (Takai, 2005; Hogarth, 2002), as

previously disccussed. Moreover, CD16-mediated ADCC responses are important for killing tumor cells and thus, for the efficacy of therapeutic Abs in treating cancers (such as in follicular lymphoma and Waldenstrom's macroglobulinemia patients).

As discussed previously, FcγRs differ in binding affinity to different IgG subclasses (Fig. 1.6). In general, they have the highest affinity for IgG1, then IgG3 and IgG4, whereas mostly they do not bind IgG2 (Schroeder and Cavacini, 2010; Smith and Clatworthy, 2010). Furthermore, upon ligand binding, they also exhibit differences in the signaling pathway (which is associated with the initiation, amplification, and termination of both innate and adaptive immune responses). In particular, an activating signal is transmitted upon IgG binding of CD64, CD32a, or CD16a, an inhibitory signal is associated with binding of CD32b, whereas no signal is delivered when IgG binds CD16b (Schroeder and Cavacini, 2010; Smith and Clatworthy, 2010; Weiner et al., 2010). The five activating FcγRs, CD64, CD32a, CD32c, CD16a, and CD16b, are thus referred as activating (or stimulatory) FcγRs, whereas CD32b is the only FcγR that has an inhibitory function (referred as inhibitory FcγR) **(**Smith and Clatworthy, 2010). These opposite FcγR functional activities must be appropriately coordinated to ensure healthy effector immune responses. The exclusively B cell-expressed CD32b, thus, as the only inhibitory FcγR capable of negatively modulating cell activation state previously initiated by an activating FcγR through ICs formed upon antigen exposure, plays a unique role in these responses **(**Smith and Clatworthy, 2010).

Among the three FcγR classes, CD64 exhibits high IgG binding affinity, whereas the other two are capable of only medium- to low-affinity binding (Fig. 1.6). Consequently, CD64 is the only FcγR able to bind monomeric IgG with high affinity and functions during early immune responses. In contrast, for efficient binding, CD32 and CD16 (CD16a) require the formation of

ICs or IgG aggregates (i.e. IgG polymeric forms) surrounding multivalent antigens during late immune responses (Schroeder and Cavacini, 2010; Nimmerjahn et al., 2008). Thus, CD64 is referred as the high-affinity FcγR, whereas CD32 (i.e. CD32a and CD32c) and CD16 (i.e. CD16a and CD16b) are referred as low-affinity FcγRs **(**Smith and Clatworthy, 2010).

Different FcγR classes may also differ in their N-glycosylation patterns, which play an important role in the molecule folding, structure, degradation, and cell-cell adhesion (van Sorge et al. 2003). N-glycosylation is also capable of influencing ligand binding and leukocyte expression patterns of FcγRs (including the case of CD16 on ligand binding and cellular expression) (Rogers et al., 2006; van Sorge et al. 2003).

FcγRs transduce activating or inhibitory signals through intrinsic immunoreceptor tyrosine-based activation motifs (ITAMs) or inhibitory motifs (ITIMs), respectively (Smith and Clatworthy, 2010) (Fig. 1.4 and 1.6). The ITAMs are present in either the CYT tail/domains (for CD32a and CD32c) or the associated FcR common accessory γ-chain (for CD64 and CD16a), whereas the ITIMs are present in CYT tail/domain (for CD32b) (Smith and Clatworthy, 2010) (thus, each CD32 molecule possesses an ITAM or an ITIM of its own and has no additional signaling chains). Mechanistically, cross-linking by Ab-antigen/pathogen ICs of activating or inhibitory FcγRs results in the ITAM or ITIM phosphorylation, respectively (Smith and Clatworthy, 2010). Such phosphorylation of ITAMs or ITIMs leads to signal transduction and cell activation (i.e. the activating signaling cascade) or to inhibition of the activating signaling cascade, respectively (Smith and Clatworthy, 2010). In addition, several FcRs expressed on a single type of leukocytes may cooperate to modulate many cellular functional effects of IC binding and cellular effector functions (Daëron, 1997). For instance, when on human neutrophils CD16b is cross-linked to CD32a through a divalent antigen, the neutrophil cells can be

synergistically activated (Green et al. 1997). Similarly, cross-linking on human B cells of CD32b with B cell receptor (BCR) may result in an increase of the "threshold" (i.e. the ratio of binding of an IgG subclass to activating FcγRs and inhibitory CD32b; also known as A/I ratio) for B cell activation and a decrease of Ab production by these B cells (Smith and Clatworthy, 2010). Also, CD16b, the GPI-linked receptor that has no CYT domain and does not contain the associated FcR common γ-chain (Smith and Clatworthy, 2010), is also believed to modulate cellular neutrophil responses to pathogens/antigens through interactions with other neutrophil FcRs.

The final outcome (end result) of IC-FcR interactions is, therefore, complex and hard to predict – it is dependent upon the functional activities of the bound FcγR, the effector functions of a particular IgG subclass, the FcγR-expressing effector cell type, and applicable contributory (inhibitory or stimulatory) signals (Schroeder and Cavacini, 2010; Weiner et al., 2010).

1.3.4. Intra-species (inter-individual) allelic polymorphism (allotypic variation) of FcγRs

Adding to the complexity of distinct expression pattern, recognition, and activation profiles of FcγRs, each class of these receptors contains multiple isoforms and furthermore, a number of those isoforms exist as allelic dimorphisms (biallelic polymorphisms) (Takai, 2005; Jefferis and Lund, 2002). Correlation between allelic polymorphism and function has been demonstrated. Furthermore, a number of naturally-occurring single variations have established their functional and even clinical significance. In particular, R131 (CD32a) ([D2] R80, IMGT unique numbering), F158 (CD16a) ([D2] F108, IMGT unique numbering), and NA2 (CD16b) have been shown to exhibit higher affinity and functional activity compared to their corresponding alleles (H131, V158, and NA1, respectively) (Binstadt et al., 2003; van de Winkel and Capel, 1993). As a result, these allelic FcγR variants have the ability to affect susceptibility

and/or severity of certain autoimmune disorders, especially systemic lupus erythematosus, as well as inflammatory and infectious diseases (Takai, 2005; Binstadt et al., 2003; van Sorge et al., 2003). Moreover, these variations have been shown to influence the outcome of monoclonal antibody treatment (Cartron et al., 2002). For instance, CD16 polymorphisms have been recently shown to be associated with the therapeutic success in treatment of Waldenstrom's macroglobulinemia by the rituximab mAb. These polymorphisms, therefore, can serve as high-risk factors or genetic markers for certain diseases or IgG-based immunotherapies (van Sorge et al., 2003). Characterization of these allelic polymorphisms and their relations with two-dimensional and three dimensional structures are, thus, important for the understanding of their physiological effects. In this context, the IMGT Collier de Perles graphical two-dimensional representations may provide useful information for relating structure to potential function (Bertrand et al., 2004).

Thus, even a single amino acid substitution in FcγRs could result in significant differences in functional properties and ultimately, might establish clinical relevance. Consequently, on one hand, it might in a distant future be possible for a particular FcγR allelic isoform to be selectively regulated – and on specific cell types – for individualized immunotherapies (Jefferis and Lund, 2002). On the other hand, the efficiency of future or potential FcγR-directed immunotherapies might vary from individual patient to one another.

1.4. Monoclonal antibodies, molecularly-engineered (recombinant) IgG and FcγR molecules, and recombinant DNA method

1.4.1. Monoclonal antibodies (mAbs) as basic research and diagnostic tools as well as prophylactic and therapeutic agents

The capability of Abs to bind with exquisite discrimination and high affinity to virtually all possible arrays of diverse antigens and chemical structures has placed them to a special position in both biological sciences and practical medicine (Clark, 1997). Nowadays, recombinant mAbs represent important biomedical and pharmaceutical products. These molecules are utilized not only as valuable tools in basic research and diagnostic areas, but also as powerful agents in prophylaxis and therapeutics. More than two dozen therapeutic mAbs have to date been approved for use in the clinic, and hundreds (~350) more mAbs are in development or trials (Reichert, 2012; An, 2010).

MAbs, owning to their desirable safety profiles and high efficiency, have proved to improve human health, fight diseases, and even save lives. MAbs have been widely used in basic research and diagnostic tests such as Western blot, ELISA, immune dot blot, immune-histochemistry, immune-fluorescence, and flow cytometry, to name a few. Passive immunotherapy with mAbs, which initially introduced mAbs into practical medicine, still retains a powerful prophylactic and therapeutic strategy. It is routinely used for the control of hepatitis B, rabies, and cytomegalovirus infections (Sawyer, 2000). It also has the potential use for efficient control and treatment of other infectious diseases, such as the lethal influenza H5N1virus infection (Simmons et al., 2007). MAb treatment of infections caused by bacteria resistant to antibiotics may provide a lifesaving strategy (Keller and Stiehm, 2000). Not only being utilized in infectious diseases and antiviral prophylaxis, but also mAb-based strategies for treatment have been applied for a wide variety of other diseases and disorders, ranging from cancer and malignancies to rheumatoid arthritis, inflammatory diseases, as well as from

autoimmune disorders, to cardiovascular, asthma, poisoning, and organ transplantation (transplant rejection) (Laffly and Sodoyer, 2005; Brekke and Thommesen, 2003; Park and Smolen, 2001; Schulze- Koops and Lipsky, 2000; Zeitlin et al., 2000).

MAbs, including those produced from recombinant DNA molecules (i.e. recombinant mAbs), are produced by a single cell clone and are all structurally and functionally identical (An, 2010). Due to the availability of the murine hybridoma technology in the early time (see below), most therapeutic mAbs currently used in humans are of murine origin (An, 2010). Over the last three decades, advances in recombinant Ab technology that promotes production of genetically engineered mAbs has greatly driven the use of Abs, both as basic research and diagnostic tools as well as prophylactic and therapeutic agents.

1.4.2. The hybridoma technique: The traditional method for production of mAbs

Traditionally, mAbs are produced *in vitro* by immortalizing antibody-producing cells created through fusing myeloma (tumor) cells with the spleen cells from a mouse immunized with the wanted antigen. This method, termed hybridoma technique, was developed nearly four decades ago (Kohler and Milstein, 1975). It has been proven to be the most reproducible method for generating murine mAbs.

The method, however, has a number of limitations. Not only murine mAbs produced by this method consist of only fixed (unchangeable) CH class and subclass regions, have short serum half-life, and lack the capability to activate sufficient effector functions (including Ab-dependent killing of target cells, ADCC and CDC), but also the created hybridoma clones may be genetically unstable (Nielsen et al., 2006). In addition, the technique itself is time-consuming and laborious. More importantly, murine mAbs have poor pharmacokinetics in humans. When

used as therapeutic agents, murine mAbs are recognized by the human immune system as allogeneic proteins, resulting in a rapid removal of them from the blood, as well as in systemic inflammatory effects and human anti-mouse antibody (HAMA) immune responses (Steinitz, 2009; Laffly and Sodoyer, 2005).

The problems associated with murine mAbs produced by the hybridoma method have recently been overcome largely, owning to the advent of the recombinant DNA technology (i.e. the genetic engineering technique). This advanced technology allows reducing HAMA immunogenicity responses by making or modifying mAbs so as they are less "murine" or more "human", such as chimerizing murine/human mAbs, humanizing murine mAbs, or completely human mAbs (An, 2010; Kipriyanov and Le Gall, 2004).

1.4.3. The recombinant DNA method for production of mAbs and molecularly-engineered IgGs and FcγRs: Overview

Recombinant DNA method, or recombinant DNA technology, is a molecular technique for engineering recombinant proteins. The technique is widely used in biological and biomedical sciences, biopharmaceutical and biotechnology, as well as medicine. It takes advantage of the fact that production of proteins can be accomplished using cloned DNA sequences or recombinant DNA molecules to create plasmid constructs capable of growing and being expressed by cell culture (i.e. expressing recombinant genes). Thus, in this method, a recombinant DNA fragment (or gene segment) is first created by several molecular cloning steps, and is subsequently inserted into a cloning vector, which is then transformed into and multiplicated in competent cells (bacteria; such as E. coli competent cells). Prior to transfection, the recombinant DNA constructs must be directionally inserted into an expression plasmid vector

containing genetic sequences necessary for expression, including promoter, translational initiation signal, and transcriptional terminator. Upon transfection into the host organism, the recombinant foreign DNA molecule that is contained within the recombinant DNA plasmid construct may be transcribed and translated by the host cell translational apparatus. Finally, colonies producing the recombinant protein product were detected and isolated. These procedures, thus, utilize a number of molecular techniques, including cloning vector, restriction endonuclease digestion, DNA ligation (with DNA ligase), and selection of clones with desired DNA inserts by appropriate antibiotics-supplemented culture medium.

The recombinant DNA technology for production of recombinant antibodies (rAbs) (also called recombinant Ab technique) is a fully *in vitro* method for creating highly-specific and high-affinity mAbs. As discussed previously, it is the globular domain structure and genetic organization of Abs, in which specificity-determined Fab is formed by V domains while different effector functions Fc is constituted by C domains, that have greatly facilitated the manipulation of Ig genes for Ab genetic engineering. In particular, the Ig domain structure enables exchange and replacement of domains specializing in antigen-binding activities (Fab or partial Fab), or those responsible for cell-killing effector functions (Fc) among Abs (Kipriyanov and Le Gall, 2004). In this method, recombinant Abs are created in a way that V region is made of a particular species and C region is of another species. For instance, mouse V domains can be merged with (or fused to) human C domains to yield partially-mouse, partially-human ("humanized") mAbs.

Among available mouse V gene segment sequences that have enabled rapid production of recombinant Abs, murine V gene sequence specifically directed against the hapten 5-iodo-4-hydroxy-3-nitrophenyl acetyl (NIP) has been established as a specificity system that has facilitated studies of Ab effector functions. Traditionally used as a haptenic determinant, NIP

may be further radiolabeled and used as salts or derivatives. Additionally, production of NIP-specific recombinant Abs is relativey straightforward. Various Ab variants possessing anti-NIP specificity have been produced and used to assess the Fc-related structural basis of Ig effector functions (Loset et al., 2004; Furebring et al., 2002; Redpath et al., 1998; Clark, 1997). A variety of pre-designed expression vectors enabling rapid construction and driving expression of complete and fragmental recombinant Ab molecules, such as pLNOH2 (Norderhaug et al., 1997), have been also established.

1.4.4. The recombinant DNA method for production of mAbs and molecularly-engineered IgGs and FcγRs: Advantages and limitations

Recombinant Ab technique offer many advantages over the conventional hybridoma Ab production method. In the recombinant Ab method, mAbs can be produced in *in vitro* by cloning entire Ig V region gene repertoire, and no immunization nor experimentation with animals are needed (thus less time would be required). Indeed, the hybridoma cell lines are sometimes genetically unstable and in such cases, immortalization of unique Abs by cloning corresponding genes would be greatly useful. For many applications, only partial Ab molecules (i.e. Ab fragments, instead of whole Ab molecules) are needed. Here the recombinant Ab method has proved advantageous with its ability to genetically engineer Abs in bacterial expression systems, which is rapid and straightforward.

More importantly, given the availability of enormous Ab gene sequences and a variety of advanced molecular biology techniques, isolation and cloning of Ig genes can be rapidly carried out. These sequences can be readily amenable to genetic manipulation and fusion. Genetic manipulations, chemical modifications, or other intervening methods of the properties of

expressed mAb – owing to V and/or C regions – can greatly enable the design of novel Abs with predetermined effector functions or other desired functional activities (Fig. 1.7). Such manipulations can be done through a variety of genetic engineering methods and using various different strategies, such as "inserting" or "swapping-out" Ab portions, introducing mutations, and adding markers, cytotoxic agents, cytokines, or other labeling or functional conjugates, among other approaches (Carter, 2001; Clark, 1997). These modifications have enabled creation or alteration of recombinant Abs with additional desired antigen binding specificity, enhanced binding affinity, optimized or additional natural effector functions, or removal of unwanted functional activities (such as placenta transfer or complement activation) for particular applications (Carter, 2001; Clark, 1997). For instance, IgG Abs that are capable of binding FcRs but not complement – or vice versus (i.e. those with only complement activation potential) – can be designed. Engineering of recombinant Abs can also be further improved by manipulating amino acid composition (sequences) within individual Ig domains to obtain particular Abs for studying the structure basis and functional properties (such as binding, folding, stability, catalysis, and effector functions) (Clark, 1997).

Advances in the recombinant Ab techniques have allowed production of Abs to virtually any antigen, and facilitated generation of Abs never been made *in vivo*. Nevertheless, despite the large diversity of potential applications ascribed to recombinant Abs, the method lacks of an appropriate strategy for determining and selecting the desired high affinity Ab products that would be effective *in vivo*.

1.4.5. Creation of recombinant Ig gene constructs: Sequence overlap extension polymerase chain reaction (SOE-PCR)

As discussed above, the recombinant Ab techniques rely on the rapid cloning of isolated Ig gene segments before these genes can be cloned into cells that can grow and express recombinant Ab products. Cloning of Ig Ab genes can be done by either isolating these genesfrom the relevant genetic materials of a hybridoma cell line, or by synthesizing them using polymerase chain reaction (PCR) amplification with degenerate primers on a pool of Ab-producing cells obtained from an immunized animal or immunized human donor(s). The PCR method has indeed allowed amplification of the entire Ig genes (or some of their components). Subsequently, these genes can be introduced into a variety of cells for production of recombinant Abs. At present, the PCR method is commonly used to amplify genes encoding Abs with desired specificity. It can even be utilized to produce the entire Ab gene repertoire of immunized or non-immunized animals for cloning purposes.

Recombinant Ig gene constructs can be created from individual Ig gene segments by a method for splicing two pieces of DNA segments, known as sequence overlap extension PCR (SOE-PCR) (Yolov and Shabarova, 1990; Yon and Fried, 1989; Ho et al., 1989). This technique is a powerful tool for fusing two short DNA fragments whose total length is not greater than 3-4 kb at a time (Kuwayama 2002; Pont-Kingdon, 1997), which is ideal for creating Ig gene constructs. Fig. 1.8 illustrates the principle of SOE-PCR to assemble a gene construct from two DNA fragments. Two pairs of primers, the flanking and the internal pairs, are used. The overlap (homologous or complementary) sequence is incorporated in the two internal primers, which serve two functions: priming and overlapping, by their priming and overlap regions, respectively. In particular, the 5’ end sequence of the internal reverse primer (to be used for amplifying the

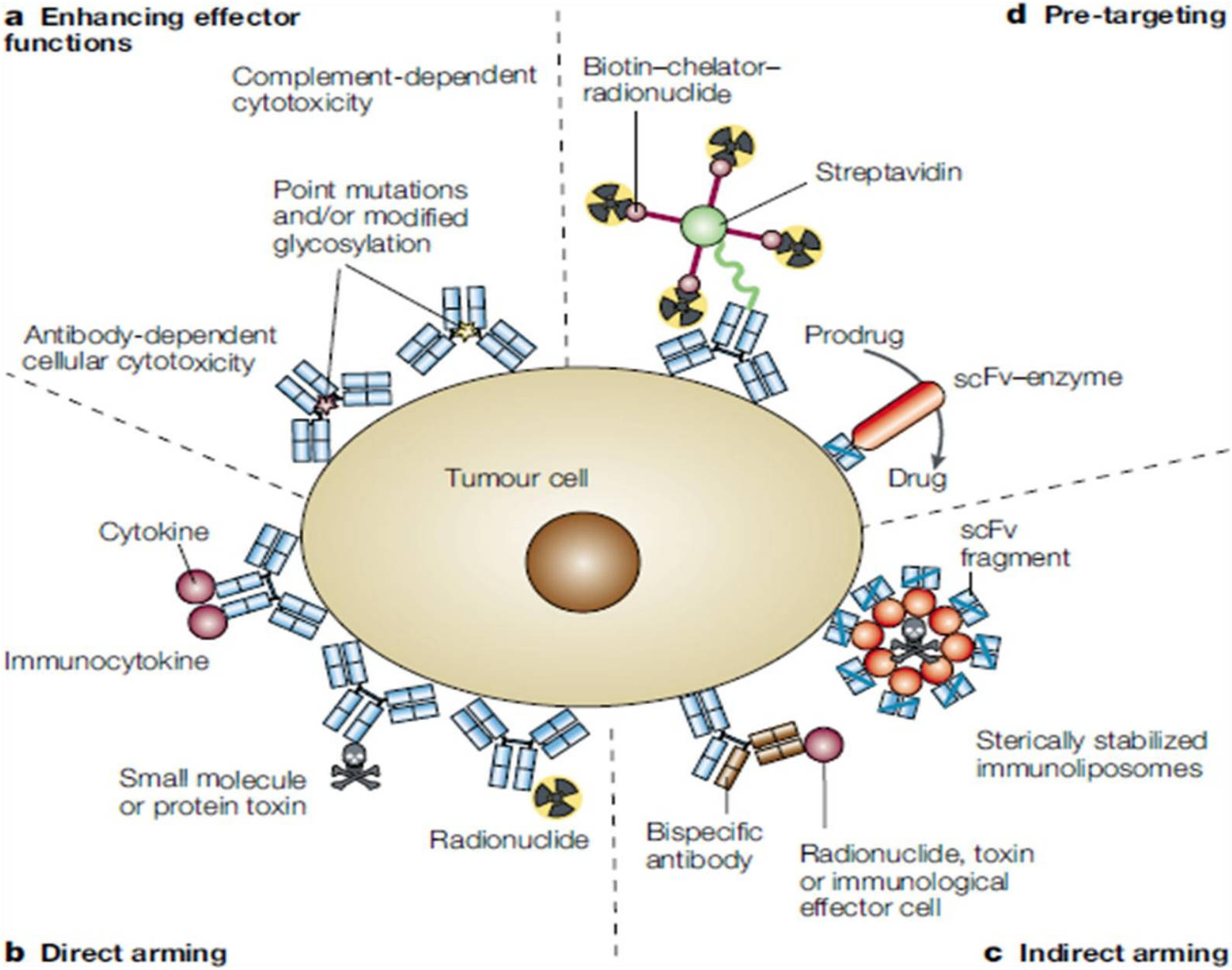
a Enhancing effector functions
Complement-dependent cytotoxicity
Point mutations and/or modified glycosylation
Antibody-dependent cellular cytotoxicity
Cytokine
Immunocytokine
Small molecule or protein toxin
Radionuclide
b Direct arming
d Pre-targeting
Biotin–chelator–radionuclide
Streptavidin
Prodrug
scFv–enzyme
Drug
Tumour cell
scFv fragment
Sterically stabilized immunoliposomes
Bispecific antibody
Radionuclide, toxin or immunological effector cell
c Indirect arming

Fig. 1.7. Among the advantages of engineering Abs: Strategies for enhancing the potency and activity of antitumor antibodies. See text for details. Figure is reproduced from Carter, 2001.

first PCR fragment) is complementary to a short sequence of the second PCR fragment – and thus, to the 5’ end sequence of the internal forward primer (to be used for amplifying the second PCR fragment).

The theoretical stages of SOE-PCR amplification are also summaried in Fig. 1.8. Firstly, two overlapping fragments are amplified in separate PCRs using the forward flanking and reverse internal primer pair – as well as the forward internal and reverse flanking primer pair – on the target sequence. In some cases, these two resultant PCR product fragments anneal to each other through their complementary sequences. Since these two DNA template fragments were introduced at their adjacent end an overlapping sequence, each of these overlap strands can act as a giant “primer” on the other to extend its 3’ end by DNA polymerase. These reactions result in the fused DNA species created in the mixture of early SOE-PCR products. The intact mixed DNA strands are finally generated when the overlap is extended and co-ordinately amplified with the outside forward and reverse flanking primer pair (i.e. hybridizing and amplifying the 3’ end of the upper strand of forward fragment and the 5’ end of the lower strand of the reverse fragment). In all reactions, a PCR cycle comprises steps of denaturation, annealing, and extension of the primed 3’ ends. Although SOE-PCR fusion offers greater speed and flexibility for construction of recombinant DNA molecules than traditional RE and ligase cloning, it is, however, expected to introduce errors, as any other PCR reactions.

Several sequential runs of SOE-PCR, with each run combining two DNA pieces at a time, can assemble more than two short segments and generate a final constructs with the desired length. Modifications of reaction parameters and/or conditions, such as designing longer chimeric primers, optimizing molar ratios and DNA concentrations, adjusting annealing temperature, and running with no primers for several first PCR cycles and using nested primers,

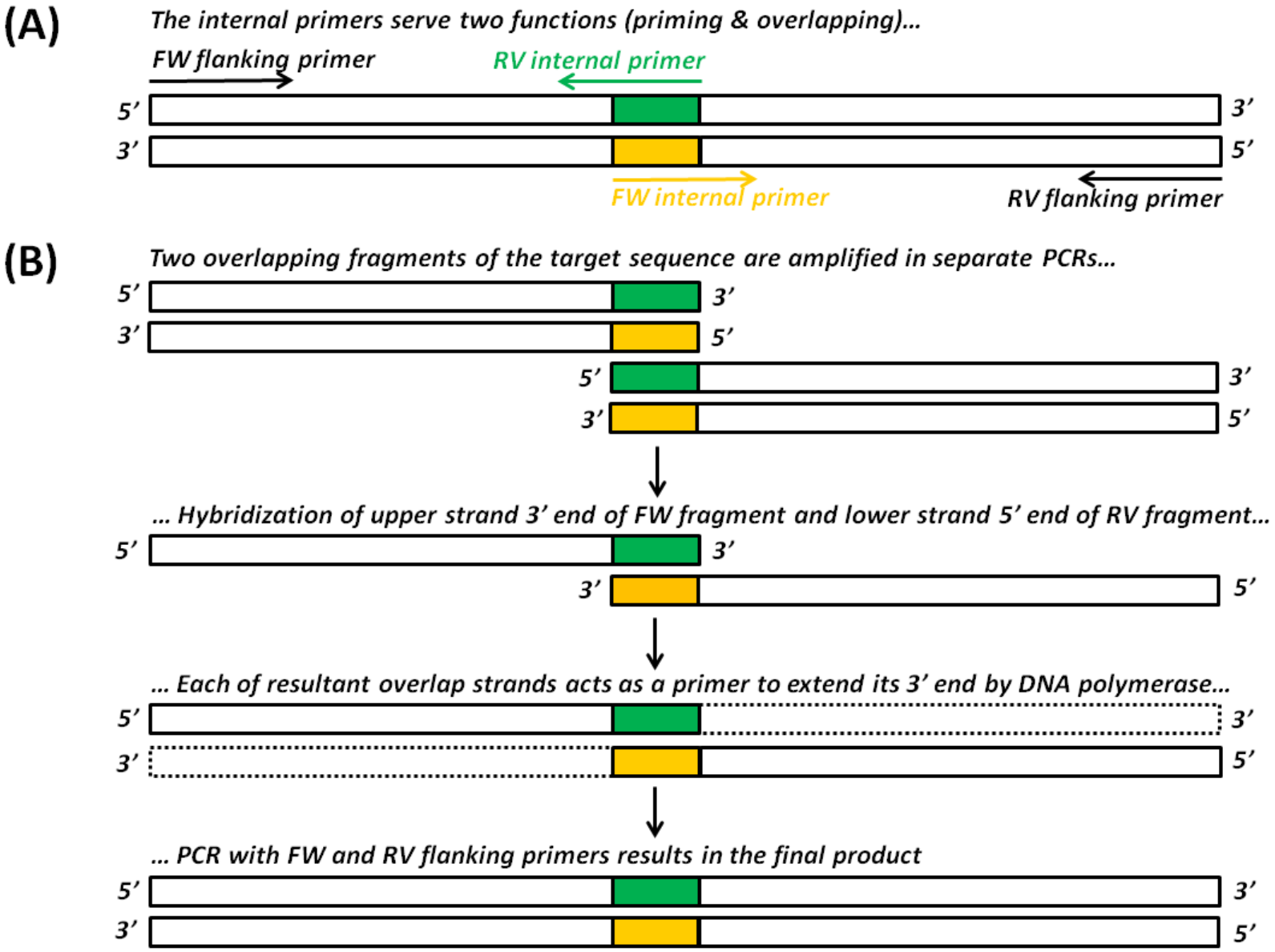
(A)
The internal primers serve two functions (priming & overlapping)…
FW flanking primer
RV internal primer
5′
3′
3′
5′
FW internal primer
RV flanking primer
(B)
Two overlapping fragments of the target sequence are amplified in separate PCRs…
… Hybridization of upper strand 3′ end of FW fragment and lower strand 5′ end of RV fragment…
… Each of resultant overlap strands acts as a primer to extend its 3′ end by DNA polymerase…
… PCR with FW and RV flanking primers results in the final product

Fig. 1.8. Diagrammatic overview of the sequence overlap extension polymerase chain reaction (SOE-PCR) procedure to assemble a chimeric/mixed gene fragment. The procedure is also called by various other names, such as overlap extension PCR, splice overlap extension PCR, overlap PCR, overlapping PCR, two-step PCR, two-step overlap extension PCR, or three-part PCR. (A) Individual strands of a DNA fragment displaying their 5' and 3' ends are illustrated as enlarged boxes. Two pairs of primers are used: FW flanking primer/RV internal primer and FW internal primer/RV flanking primer. The overlap (homologous or complementary) sequence is incorporated in the FW and RV internal primer. Primer direction is indicated as arrows. The two internal primers serve two functions, priming and overlapping, by their priming and overlap regions, respectively. Complementary ends are shown by different colors boxes (i.e. small green-filled and yellow-filled boxes). (B) Theoretical stages of formation of a SOE-PCR chimeric product. See text for details. Overlapping ends of identical sequences of fragments are indicated with the same color filled; complementary ends are shown by different colors boxes (i.e. small green-filled and yellow-filled boxes). A PCR cycle comprises steps of denaturation, annealing, and extension of primed 3' ends.

might be needed during the procedures in order to improve the success of reamplification and generate the best products, as well as to minimize non-specific bands (as will be discussed in more details later).

1.4.6. Mammalian expression systems for production of recombinant IgGs and FcγRs

Molecular engineering of Abs or Ab fragments enables manipulation and production of Igs in various eukaryotic and prokaryotic cell types, including bacteria, yeast, plant cells, insect cells, and mammalian cells (Kipriyanov and Le Gall, 2004). However, to be fully functional, recombinant Ig products that are expressed must be correctly folded, wholly assembled, and post-translationally modified. In particular, to form intact molecules, the two IgH chains must be disulfide bound (and to be able to carry out effector functions), CH2 domains must be correctly glycosylated, and CH3 domains must be paired (Kipriyanov and Le Gall, 2004; Brekke and Thommesen, 2003). Glycosylation is also crucial for efficacy of Abs and protein drugs targeted as human therapeutic agents. Expression systems possessing the mechanisms necessary for these processes and events have been seen in various mammalian cell lines, including nonsecreting myeloma, hybridoma, and nonlymphoid cells (Kipriyanov and Le Gall, 2004). Like with Igs, a mammalian cell line system (rather than prokaryotic cell types) should also be considered for expressing recombinant FcRs, as FcRs also contain conserved disulfide bridge (some FcR members also consist of unpaired Cys residues) in each of their IgSF domain.

Dependent upon the quantity of the recombinant Ab products needed, transient or stable expression of Abs in mammalian expression systems can be performed. In contrast to transient production which is rapid, stable expression of Abs is time consuming. The reason is that stable production is based on the stable integration of recombinant Ig genes into the host cell

chromosomes, which is a largely random event. To facilitate successfully transfected cell clones to be isolated from a heterogeneous population, the interested gene is integrated together with a selection marker during engineering of the recombinant constructs. Among common types of selection marker genes are those encoding resistance to antibiotics (such as neomycin gene, which encodes resistance to G418) and enzyme analogs [such as dihydrofolate reductase (DHFR) gene, which encodes methotrexate resistance].

Several mammalian expression cell lines capable of highly producing Ig molecules have been developed. The murine IgL lambda (λ)-producing, IgH-defective, myeloma (i.e. cells that produce Abs) J558L cell line is one of such cellular systems (details will be described later) (Howard et al., 2002; Oi et al., 1983). Intact, glycosylated Abs that are fully functional and capable of antigen-binding, have been successfully expressed and secreted by J558L cells transfected with vectors expressing IgH chains and carrying the G418 selectable marker (Howard et al., 2002; Fell et al., 1989; Oi et al., 1983).

1.5. Structural and functional features of rhesus macaque IgG and FcγRs: Current status of knowledge

1.5.1. Presence of four IgG subclass genes, each with similar length and organization as that of humans

Like humans, rhesus macaques express five Ig classes. Early studies had identified both in serum and in genomic DNA in healthy rhesus macaques only three IgG subclasses, IgGl, IgG2, and IgG3 (Calvas et al., 1999; Shearer et al., 1999). Later data obtained from genomic DNA analysis, however, show that this primate species possess four *IGHG* genes, based on their sequence similarity with the four corresponding human genes *IGHG1*, *IGHG2*, *IGHG3,* and

IGHG4 (Scinicariello et al., 2004). These genes are expressed at least at the mRNA level, including the lately-identified *IGHG4*, whose protein product (i.e. IgG4) may be present at almost undetectable levels in rhesus macaque serum (Scinicariello et al., 2004). The early serological failure of identifying the rhesus macaque IgG4 homologue of humans might also indicate the possibility that differences between human and rhesus macaque IgG4 had circumvented its detection and identification.

The intron-exon genomic organization of the four *IGHG* genes is similar between rhesus macaques and humans. Each of the four rhesus macaques *IGHG* genes is composed of four exons, individually encoding CH1, the hinge, CH2, and CH3 domains, and three introns, which take place in-between the exons. Each rhesus macaque CH domains contains a similar number of amino acids as that found in their human counterparts, which is 98, 109-110, and 107, in CH1, CH2, and CH3 domains, respectively. The length of the introns is also similar to that of the corresponding human introns (~390, ~120, and ~100 nucleotides for the intron located between CH1-the hinge, the hinge-CH2, and CH2-CH3 exons, respectively) (Scinicariello et al., 2004).

1.5.2. A single exon encoding the IgG3 hinge region and key amino acid differences of IgGs compared to human counterpart

IgG V region genes between rhesus macaques and humans are highly homologous and their IgG C region genes are generally homologous. Indeed, rhesus macaque IgG1, IgG2, IgG3, and IgG4 CH domains exhibit 89.9%, 88.0%, 92.9% and 91.4% amino acid identity to their human counterpart (Scinicariello et al., 2004). The deduced amino acid sequence of each of four rhesus macaque IgG subclasses differs from that of their human counterpart – generally for a few amino acids (Scinicariello et al., 2004) – yet they share most amino acid residues known to be

functionally conserved. Perhaps the most striking difference between rhesus macaque and human IgG subclass genes is at the IgG3 hinge. Rhesus macaque IgG3 contains only one hinge exon (Scinicariello et al., 2004), whereas, as previously described, the human IgG3 hinge most often consists of four exons (can be two to five exons; with repetitive sequences and separated by short introns) (Lefranc and Lefranc, 2001). In addition, it is deficient in Cys residues, which is important for Ig stability through formation of disulfide bonds.

Some other key amino acid differences in IgGs of rhesus macaques and their human counterparts have also been revealed. The upper hinge region of macaques contains several Pro residues [known to be involved in stabilization or maintaince of the IgG tertiary structure and might influence the hinge flexibility (Thommesen et al., 2000, Greenwood et al., 1993)] that are not present in the human counterpart. Chinese rhesus macaque IgG4 also possesses Ala instead of Pro at position 13 of the hinge. Also, rhesus macaque IgG4 has Pro at position 101 of CH2 domain, where in human IgG4 it is Ser. Moreover, in humans, unlike IgG4, other IgG subclasses capable of activating complement contain Pro at position 101. The inefficiency in complement activation of human IgG4 is thought to be associated with lack of Pro at the position 101 (Xu et al., 1994). The presence of Cys-to-Ser substitution at position 10 in rhesus macaque IgG4 CH1 domain as compared to humans might affect the formation of interchain disulfide bridges involved in this Cys residue (Scinicariello et al., 2004). Interestingly, a Ser exists at this position in IgG1 in both species.

Although characterized by evolutionary instability, as discussed previously, the structural distinctions of the IgG hinges in rhesus macaques as compared to human counterparts might lead to alterations in the formation of disulfide bridges and functional properties of IgG molecules, including molecular flexibility (Thommesen et al., 2000; Roux et al., 1997), neutralizing ability,

binding affinity to FcRs, capability of complement activation (Burton and Woof, 1992; Michealsen et al., 1990, Tan et al., 1990), and susceptibility to proteolytic enzymes. The single-hinge IgG3 in rhesus macaques (and other macaque species) might exhibit unique properties and/or carry out different effector functions when compared to human IgG3.

1.5.3. Intra-species IgG H chain genes: Relatively high level of heterogeneity (polymorphism) and variability of disease susceptibility

As previously mentioned, rhesus macaques are characterized by a high level of polymorphism of MHC genes (Shedlock et al., 2009). Like several other NHP species, rhesus macaques also feature a relatively high degree of intraspecies CH gene heterogeneity (allelic polymorphism) for IgGs, particularly IgG2 and IgG4, as compared to humans (Scinicariello et al., 2004; Scinicariello et al., 2001). Although IgG (i.e. *IGHG*) polymorphism level is less extensive than that of IgA in this animal species (Sumiyama et al., 2002; Scinicariello et al., 2001), many IgG substitutions are located in CH2 domains, the place that is responsible for most IgG effector functions and properties (Radaev and Sun, 2002).

In addition to species-specific differences from humans, individual rhesus macaque animals originated from different geographical areas also show considerable variation in immune conding genes and disease susceptibility. Examples of such variations include those observed with *IGHG2* and *IGHG4* genes of Chinese- versus Indian-originated macaques (Scinicariello et al., 2001). These geographically different rhesus macaque animals also vary in their susceptibility to infectious diseases, especially SIV infection: when inoculated with the same infectious challenge virua stock, some animals progressed disease – and at different extents – while others remained relatively unaffected (Reimann et al., 2005; Ling et al., 2002; Marthas et

al., 2001; Joag et al., 1994). Some rhesus macaque individual animals may thus be better than others to be used as a research model.

The extensive polymorphism in IgG CH genes might be involved in the presence of structurally, and thereby functionally, variable IgG molecules in different rhesus macaque animals. This relatively high level of allelic polymorphism might also reflect an alternative strategy developed by rhesus macaques to clear invading pathogens, however. Also, polymorphisms might explain the poor (cross)reactivity or inactivity of anti-human reagents to different rhesus macaque IgG subclasses. Moreover, these Ig allelic forms, with different functional properties, might contribute to different susceptibility, progression, or severity to infections. These differences should be taken into account when designing experimental strategies and protocols with various model systems – as well as to select appropriate animals for studying pathogenesis of human infectious diseases, immunization, and vaccine strategies.

Theoretically, substitutions in rhesus macaques of individual amino acid residues known in humans to be functionally important may lead to changes in Ig effector functions (such as ADCC, CDC, ADCP, or IgG half-life), as well as in Ig structure-function relationships. However, polymorphisms that occur co-locally in both IgG Fc ligand and their native FcγR molecules within their binding areas would, under natural evolutionary selection, have the potential to optimize functional activity and increase the binding fitness of both interacting players (Kim et al., 2001). Furthermore, because of the extensive contact surface and multiple residues interacting with receptors, the interactions between IgG (ligand) subclasses and different FcγRs and are complex. In addition, interaction of the homodimeric Fc fragment with its receptors is asymmetrical (i.e. overlapping but not identical residues in both Fc fragments may take part in binding). Therefore, in order to adequately assess the binding properties and the

ability to mediate effector functions of IgG molecules in rhesus macaques or other NHP animals, not only heterogeneity (polymorphism) of ligand IgGs themselves need to be considered, but also structure of corresponding FcγRs in those species must also be taken into account.

1.5.4. Rhesus macaque FcγR biology system and related pathogen-clearance mechanisms are largely uncharacterized

Although the information available on rhesus macaque Ab molecules and corresponding receptors is steadily increasing (Rogers et al., 2008, 2006a, and 2004; Scinicariello et al., 2004; Scinicariello and Attanasio, 2001; Calvas et al., 1999), basic characterization is still lacking for the majority of Fc receptors. Indeed, research on NHP FcR biology is still in its nascent stage. Rhesus macaque FcRs have only been described recently and are limited to few classes (Rogers et al., 2008, 2006b, and 2004). Within FcγRs in this species, only gene sequences for FcγRIII (CD16) have to date been identified (Rogers et al., 2008; Miller et al., 2007; Rogers et al., 2006b and 2004), whereas the genes encoding CD32 and CD64-"like" sequences have been only computationally predicted. Rhesus macaque CD16 gene shows 91.7% identity to human CD16a (Rogers et al., 2006b). Although CD16 molecules in NHP species (including rhesus macaques) and humans share an extensive similarity in sequence and genetic organization – with nearly complete conservation of residues known to be critical for IgG binding – they have been found to be different in some key aspects. In particular, while human CD16 consists of two isoforms encoded by two separate genes, only a single CD16 gene homologue, which encodes a protein with over 90% homology to human CD16, was identified in rhesus macaques and other NHP animals (Rogers et al., 2006b). CD16 cell-type expression patterns on the leukocyte population differ not only between humans and NHP scpecies, but also among different NHP species

(Warncke et al., 2012; Rogers et al., 2006). Also, in contrast to corresponding human FcγR, recombinant NHP CD16 exhibits different binding specificity to different NHP and human IgG subclasses (Rogers et al., 2006). Difference in functional properties of different cynomolgus IgG subclasses has also been recently characterized (Warncke et al., 2012; Jacobsen et al., 2011).

The findings about a high degree of inter-individual genetic heterogeneity of NHP IgSF molecules such as IgG and CD16 [as well as IgA and IgD (Rogers et al., 2006a)] characterized to date raise the question whether such diversity might also be reflected in other IgSF members, including other classes of FcγR, in these species. Although CD16 is known to be polymorphic in humans and its inter-individual allelic variants have recently been reported in rhesus macaques (Miller et al., 2007), we do not know at what extent these molecules are heterogeneous. More importantly, CD16 allelic variants appear to influence the host responses to mAb treatment (Miller et al., 2007). As discussed previously, CD16 also plays an important role in destruction of HIV-infected NK cells and malignancies via ADCC mechanism. The fact that the neutrophil expression profile of CD16 differs among several macaque species usually used in evaluation of therapeutic Abs based on IgG-FcγR interactions (Rogers et al., 2006), should be considered in experimental design and data interpretation.

As mentioned previously, even a single amino acid change in FcγR amino acid sequences might result in the possibility of significantly altering ligand binding affinity of a particular FcγR (Rogers et al., 2006a; Scinicariello et al., 2004; Scinicariello et al., 2001). Particular FcγR allelic variations might also be associated with disease susceptibility and/or severity, or can even influence the outcome of Ig-based treatments (van Sorge et al., 2003; Cartron et al., 2002). Thus, specific sequence alleles or variations indentified in individual animals might be assessed for their potentially altered binding affinity or specificity – or even clinical relevance as needed. In

addition, discrepancy should be considered when using NHP models in the evaluation of Ig-based or, in the near future, FcγR-derived, immunotherapies. These observations highlight the need to further characterize FcγRs in rhesus macaques.

Taken together, on one hand, rhesus macaque IgGs and associated FcγR systems characterized to date are conserved and extensively homologous compared to those in humans. This similarity suggests that immune responses and mechanisms of protection modeled from this species can be translated into humans. On the other hand, rhesus macaque IgGs are highly polymorphic and have several key differences from their human counterparts. This distinction suggests that efffector functional activities of IgG subclasses, including their interactions with corresponding FcγRs, between these two species may not be directly equal or simply similar. The presence of allelic forms of rhesus macaque IgG CH region and FcγR genes might result in production of IgGs and FcγR molecules exhibiting different functional properties, thus potentially contributing to individual immune responsiveness profiles. These differences should be clarified in order to correctly interpret and evaluate experimental results generated using the rhesus macaque model. Additionally, as discussed previously, amino acid changes in FcγRs might have the potential to influence the possible effects caused by IgG substitutions (due to relatively high polymorphism of *IGHG* genes), leading to the unique properties and functions of their IgGs in rhesus macaques. Comprehensive characterization of FcγR structures is, thus, necessary in order to adequately assess the binding properties and the ability to mediate effector functions of their IgG ligands. The first steps towards definition of all such functional activities and properties in rhesus macaques would, therefore, be the creation of their genetically engineered IgG subclasses.

1.6. Study objectives and specific aims

Taken together, rhesus macaques are used widely in immune-related research and vaccine studies, yet their immune system components and mechanisms are largely uncharacterized. Although extensively similar as compared to humans, IgGs and corresponding FcγRs in this species possess several key structural and functional differences that must be considered when interpreting experimental data and evaluating therapeutic strategies. To validate and improve the use of a rhesus macaque model for human diseases, comprehensive characterization of the elements responsible for the humoral immune responses and the mechanisms for elimination of invading pathogens is imperative. Previous work in our laboratory has successfully identified the IgG CH region genes in rhesus macaques. The presence of several allelic forms of IgG CH genes (and some other IgSF members identified to date) might result in production of Ab molecules exhibiting different functional properties. However, the effector functions and clearance mechanisms associated with rhesus macaque IgG CH regions are presently undefined. Information on IgG responses, including the preferential usage of certain IgG subclasses during various immune responses to pathogens or vaccination, is also currently unavailable. In addition, the structure-function relationship of molecules encoded by recently identified IgG CH region genes are uncharacterized.

These gaps of knowledge are mainly due to lack of specific reference reagents (Abs) capable of specifically recognizing and unequivocally differentiating rhesus macaque IgG subclass molecules. Such Abs represent a valuable tool to further characterize IgG immune responses and vaccine efficacy in this species. Also, although rhesus macaque CD16 genes have recently been described, other important FcγR classes, including CD64 and CD32, have not been

defined. The needs for complete characterization of various IgG and FcγR genes and for generation of their recombinant molecules are, therefore, widely recognized.

The present study was designed to fill some of these gaps. Specifically, the goal of this study is to define and further characterize the two major components of the humoral immune system, IgG and FcγR molecules, in rhesus macaques, focusing on the following aims:

1. To generate recombinant Abs for each of the four rhesus macaque IgG1, IgG2, IgG3, and IgG4 subclasses – to be utilized for defining IgG functional properties and immune response patterns in this species as well as for generation of reference Abs.
2. To identify and characterize FcγR genes and protein products existing within rhesus macaques, including identifying CD64 and CD32 genes, defining intraspecies variations of CD64, CD32, and CD16 genes, as well as determining their genetic polymorphisms and similarity with their human counterpart.
3. To generation of recombinant cDNA cloning and expression vectors for rhesus macaques CD64 and CD32 – to be utilized for expression of protein products for studying IgG/FcγR interactions and functional activities.

Accomplishment of these specific aims will add into the long-term goals of providing a well-defined rhesus macaque model for understanding IgG-mediated protective and pathogenetic mechanisms, as well as for evaluating efficacy of novel immune intervention strategies.

Apart from the findings about IgGs and FcγRs in rhesus macaques, we also reported in this study our data demonstrating that the main female hormone substance, 17β-estradiol, is

capable of restoring Ab responses to an influenza vaccine in a postmenopausal mouse model. These findings suggest that immunogenicity and efficacy of influenza vaccines should be evaluated in postmenopausal women, which belong to an age group that is highly susceptible to influenza infection and its most serious complications.

CHAPTER 2

ENGINEERING OF CHIMERIC MOUSE-RHESUS MACAQUE IGG1, IGG2, IGG3, AND IGG4 SUBCLASS RECOMBINANT ANTIBODIES RECOGNIZING THE HAPTEN 5-IODO-4-HYDROXY-3-NITROPHENACETYL

2.1. Summary

Four IgG subclass homologues, corresponding to the four human IgG subclass genes, were discovered and characterized in rhesus macaques, an important non-human primate research model for human diseases. The functional properties that distinguish these IgG subclasses, however, is largely unexplored. The obvious reason for such unavailability of information is lack of specific reagents. To fill this gap, we engineered all four chimeric mouse-rhesus macaque IgG1, IgG2, IgG3, and IgG4 subclass recombinant antibodies (Ab) specifically recognizing the hapten 5-iodo-4-hydroxy-3-nitrophenacetyl (NIP), an established specificity system for studying IgG effector functional properties. We first created recombinant IgG heavy chain (IgH) cDNA gene fragments encoding each rhesus macaque IgG class using sequence overlap extension (SOE)-PCRs, where murine VH anti-NIP and Chinese rhesus macaque CH region genes were PCR-amplified and joined together as single fragments. The resultant fragments were then cloned into specialized expression vectors. The IgH expression vectors were subsequently transfected into the murine IgH-loss-variant myeloma cell line, J558L, which synthesizes and secrets an IgL λ but does not produce murine intact Ig molecules. G418-selected cells were tested for IgG production and binding by ELISA with NIP coupled to BSA-coated microtiter plates and goat anti-monkey purified IgGs. Horseradish peroxidase (HRP)-conjugated anti-mouse IgL λ or HRP-conjugated goat anti-monkey IgG-specific was used as the detection

Ab. We successfully produced recombinant rhesus macaque IgG chimeras of the four subclasses, which would represent both the foundations and the tools for further studies on IgG effector functions and Ab structure-function relationship in the rhesus macaque model.

2.2. Materials and Methods

Fig. 2.1. represents the steps involved in the construction, production, and detection of the NIP-rhIGHG chimeras/chimeric molecules using recombinant DNA technology, which include the following precedures.

2.2.1. Construction of NIP-specific murine VH–rhesus macaque IgG CH (rhIGHG) cDNA hybrids (NIP-rhIGHG): DNA sources, SOE-PCR, and primer design

NIP-rhIGHG cDNA hybrids, including NIP-rhIGHG1, NIP-rhIGHG2, NIP-rhIGHG3, and NIP-rhIGHG4 IgG subclass gene cassettes, were constructed by sequential sequence overlap extension PCRs (SOE-PCRs). Firstly, separate PCRs were used to amplify cDNAs encoding NIP-specific mouse variable heavy (VH) and rhesus macaque (rh) constant heavy (CH) IgG gene segments (exons) of each of the four subclasses (referred to as rh*IGHG1*, rh*IGHG2*, rh*IGHGH3*, and *rhIGHG4*, according to the IMGT nomenclature). cDNA encoding VH, which has specificity for 4-hydroxy-3-iodo-5-nitrophenylacetic acid (NIP; a hapten that can be used for studying specific effector immune responses), was cloned from pLNOH2 “RNA-Chinese” vector (see below), which was available in our laboratory plasmid repository (Rogers et al., 2008), using primer set FVH5FW and FVH3G4R (Table 2.1). The resultant VH PCR product contains a *BsmI* restriction endonuclease (RE) recognition site at the 5’ end, and a 42-bp sequence at the 3’ end that is homologous to the 5’ end of rhCH1 IgG gene segment.

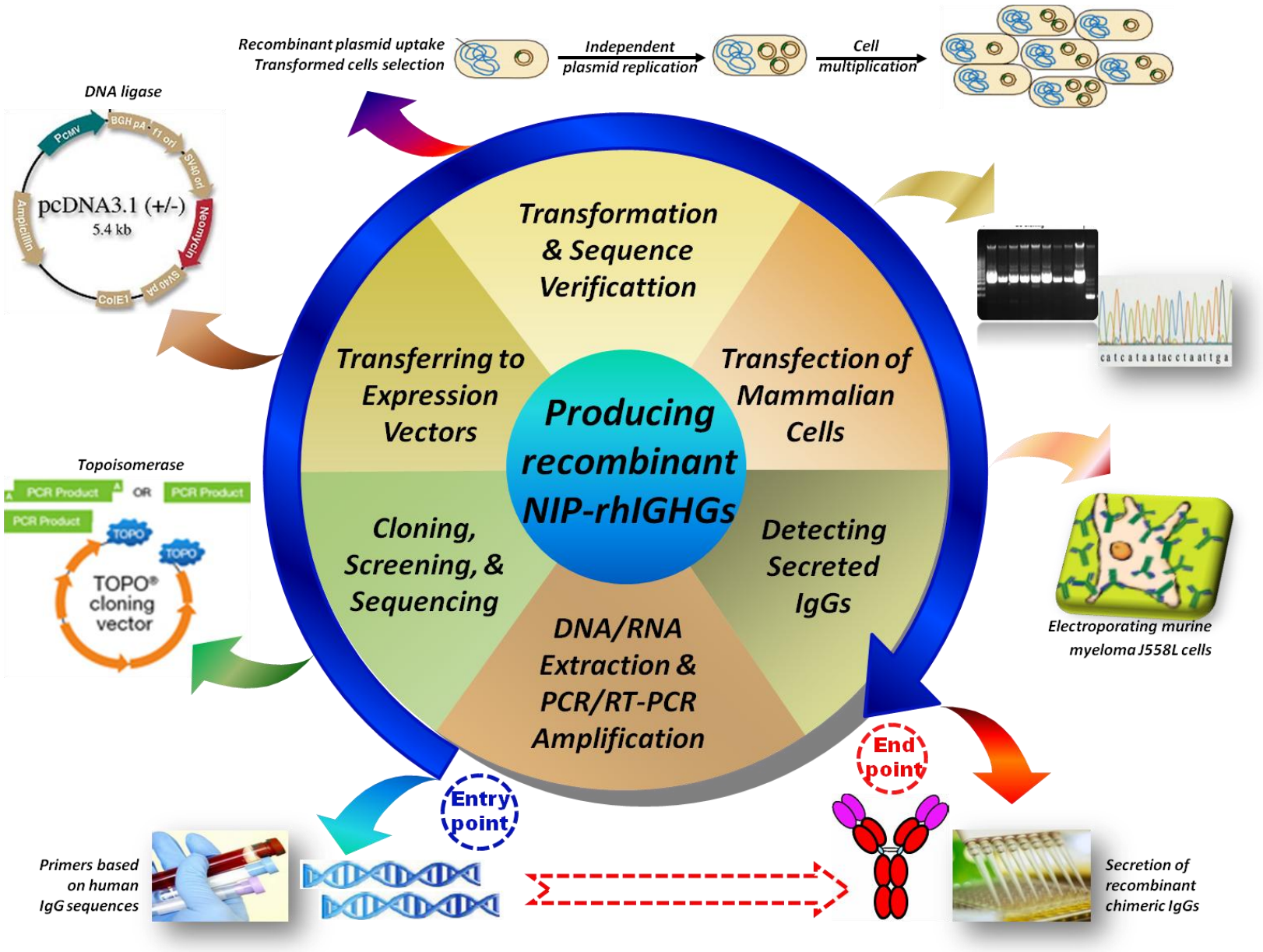
Recombinant plasmid uptake
Transformed cells selection
Independent
plasmid replication
Cell
multiplication
DNA ligase
pcDNA3.1 (+/-)
5.4 kb
Transformation
& Sequence
Verificattion
Transferring to
Expression
Vectors
Transfection of
Mammalian
Cells
Producing
recombinant
NIP-rhIGHGs
Cloning,
Screening, &
Sequencing
Detecting
Secreted
IgGs
DNA/RNA
Extraction &
PCR/RT-PCR
Amplification
Topoisomerase
PCR Product
OR
PCR Product
PCR Product
TOPO
TOPO
TOPO®
cloning
vector
Electroporating murine
myeloma J558L cells
Entry
point
End
point
Primers based
on human
IgG sequences
Secretion of
recombinant
chimeric IgGs

Fig. 2.1. Flowchart representation summarizing the major steps involved in construction, production, and detection of NIP-rhIGHG chimeras using recombinant DNA technology (genetic engineering). Individual DNA gene fragments were first isolated and amplified from the rhesus macaque Ab-producing cells by PCR/RT-PCR using primers that were designed based on known conserved regions of the publicly available rhesus macaque and corresponding human IgG sequences. These fragments were then used as DNA templates in SOE-PCRs to generate in *in vitro* the complete cDNAs, which contain a mouse VH in combination with rhesus macaque CH sequences. The resulting chimeric cDNA gene constructs were cloned into pCR2.1 TOPO TA cloning vector containing a selectable marker sequence. Selection for transformed clones that picked up the constructs and replicated in competent bacterium cells was made by culturing the cells in medium containing X-gals and ampicillin. The constructs were then amplified from the cloning vector by PCR using the primers that incorporated appropriate restriction sites which were used to transfer the desired constructs into an expression vector, where it fit exactly between the two defined restriction sites. To make a large quantity of the constructs, the resulting recombinant expression vector was transformed back into competent bacterium cells so that they were multiplicated by these cells following their division and replication. An appropriate amount of recombinant DNAs were then transfected into the appropriate recipient cell lines (murine myeloma J558L cells), where the cellular machinery directed the cells to synthesize, assemble, and secret protein products. Stable transfectants synthesizing the genes of interest are subsequently identified. The resulting chimeric IgGs now contained NIP-specific V domains derived from mice that was fused to rhesus macaque C domains. The secreted recombinant IgGs were detected from supernatants of cell cultures by ELISAs. Mammalian cell lines (not bacteria or yeast) must be used as the four chains of the molecules have to assemble correctly, as well as

the glycosylation and the large number of disulfide bonds have to be made correctly. Some figure pieces are reproduced from the internet.

Next, cDNAs encoding each of *IGHG* gene segments, rhCH1, rhCH2, and rhCH3, of each of the four subclass molecules of rhesus macaques were isolated and PCR-amplified from the appropriate plasmid vectors that contain *IGHG* genes identified in the genomic DNAs isolated from a Chinese rhesus macaque [available in our laboratory plasmid repository (Scinicariello et al., 2004)]. The primer sets used in these PCRs were designed so that short homologous or complementary nucleotide sequences were introduced at the joint of any two adjacent gene segments (Fig. 2.2). For example, for IgG2 molecule, the resultant rhCH1 PCR product contains a 30-bp sequence on the 3' end that is homologous to the 5' end of the resultant rhCH2 PCR product. Similarly, the resultant rhCH2 PCR product has a 43-bp and 30-bp sequence on the 5' end that is homologous to the 3' end of the resultant rhCH3 PCR product in IgG2 and IgG3 molecules, respectively (Table 2.1). The resultant rhCH3 PCR product further contains a *BamHI* or a *XhoI* RE recognition site at the 3' end.

Unlike in humans where IgG3 has three hinge segments due to sequence repetition (Roux et al., 1997), one hinge segment is identified in this IgG subclass of rhesus macaques (Scinicariello et al., 2004). To ascertain this feature in generation of rhesus macaque IgG3, a primer pair specific for the hinge, namely G3CHF (forward direction) and G3CHR (reverse direction), was designed. These IgG3 hinge primers, G3CHF and G3CHR, shares a 33-bp and 36-bp identical sequence with the forward primer for the IgG3 gene segment rhCH2 (i.e. G3C2F) and the reverse primer for the IgG3 gene segment rhCH1 (i.e. G3C1R), respectively (Table 2.1). For other IgG subclasses, primer sets specific for the hinge were embedded in the reverse primer for the rhCH1 gene segment and the forward primer for the rhCH2 gene segment.

All primers were designed to flank known conserved regions of human and NHP IgG gene sequences, and were subsequently optimized (such as increasing the length of overlaps in

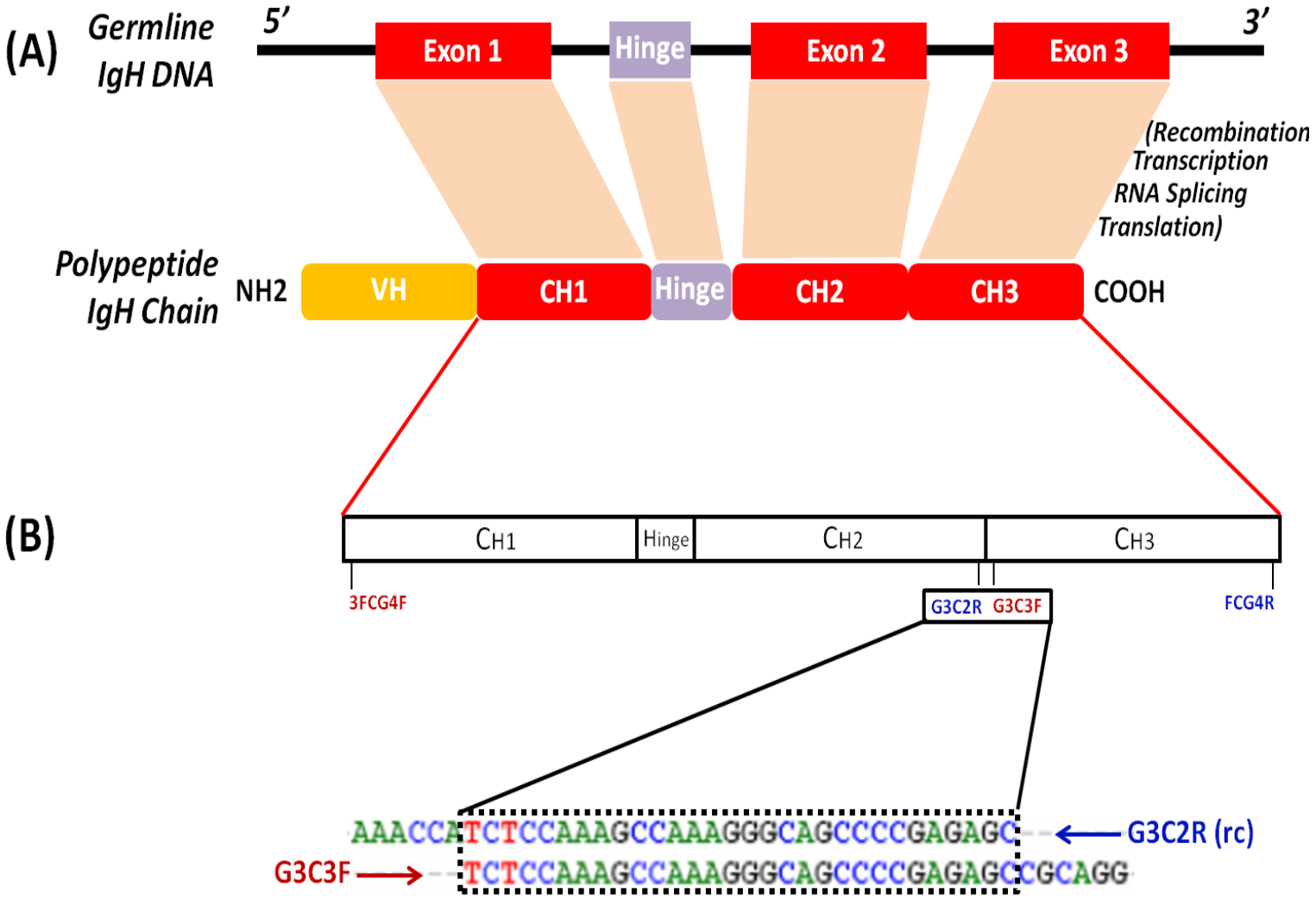
(A)
Germline
IgH DNA
5'
3'
Exon 1
Hinge
Exon 2
Exon 3
(Recombination
Transcription
RNA Splicing
Translation)
Polypeptide
IgH Chain
NH2
VH
CH1
Hinge
CH2
CH3
COOH
(B)
CH1
Hinge
CH2
CH3
3FCG4F
G3C2R
G3C3F
FCG4R
AAACCATCTCCAAAGCCAAAGGGCAGCCCCGAGAGC
G3C2R (rc)
G3C3F
TCTCCAAAGCCAAAGGGCAGCCCCGAGAGCCGCAGG

Fig. 2.2. Schematic representation illustrating the separate exons that encode for individual heavy-chain constant domains of an Ig molecule, as well as diagrammatic representation depicting organization of a complete IgG3 heavy chain gene fragment with name and location of a pair of primers at the CH2-CH3 boundary, shown as an example for overlap primer sequences. (A) Separate exons encoding individual heavy-chain constant domains of an Ig protein molecule (not drawn to scale). Shown is the organization of IgG3 H chain genes with CH1, hinge (Hg), CH2, and CH3 exons, represented in the 5' to 3' orientation. Purple and red boxes indicate exons and straight black lines indicate introns. Lightly purple shaded areas indicate the correspondence between the DNA segments and the different domains of the Ig polypeptide chain that they encode. The intron-exon organization of the *IGHG* genes was inferred from the human and rhesus macaque sequences publicly available. (B) Organization of a complete IgG3 heavy chain gene fragment and name and location of a pair of primers at the CH2-CH3 boundary, shown as an example for overlap primer sequences. The Ig intron-exon genetic segmental organization facilitates the design of primers for amplification of mRNA without interfering the DNA. Primers should flank the spliced regions where two exons are fused and contain the homologous annealing sequences that are seen in mRNA but not in the DNA. Individual IgG exons encoding corresponding CH domains is demonstrated by enlarged boxes. The necessary splice sites found at intron boundaries and the sequences of the introns were removed. Name and relative location (indicated by vertical bars) of primers used to amplify the appropriate fragments are illustrated. The red arrow indicates the direction of the forward primer and the green arrows indicates that of the reverse primer. The primer sequences shown in the dot-line box are the overlap sequence of these two middle (internal) primers. Alignment of these primer sequences were performed using BioEdit sofware. Code: rc, reverse complementary.

internal primers to reduce the background of non-specific products) following analysis of PCR and sequencing reactions. All primers were synthesized by Sigma–Aldrich Co. (St. Louis, MO). All primers have specificity to the corresponding 5’ and 3’ ends of all rhesus macaque domain coding regions and, as indicated above, were incorporated with RE recognition sites located outside V and C gene coding regions to allow subsequent cloning (see below). To all primers, ambiguous bases were introduced to make them compatible with the primer sets previously published. The final sequences of the primers are shown in Table 2.1.

2.2.2. Construction of the NIP-rhIGHG cDNA hybrids: Optimization of SOE-PCRs and amplification strategies

cDNA encoding the heavy chain rhCH fragment of each of the four rhesus macaque IgG subclasses was PCR-annealed together by SOE-PCRs using the resultant rhCH1, rhCH2, and rhCH3 cDNA gene segments as DNA templates, and by different strategies that were optimized and dependent upon each subclass (Fig. 2.3). By separate SOE-PCRs using appropriate primer pairs on the four gene segment PCR products, VH, rhCH1, rhCH2, and rhCH3, as DNA templates, immediate ligation fragments, including [VH+rhCH1], [rhCH1+rhCH2], and [rhCD2+rhCH3], were generated. These immediate fragments, together with the rhCH1, rhCH2, and rhCH3 segments, were subsequently used as DNA templates in additional SOE-PCRs to create rhIGHG fragments ([rhCH1+rhCH2+rhCH3]) using primers 3FCG4F and FCG4R. The final whole chimeric IgG fusion fragments, [VH+rhCH1+rhCH2+rhCH3] (NIP-rhIGHG), were constructed by annealing the VH gene segment with the rhIGHG fragment – or the [VH+rhCH1] fragment with the [rhCH2+rhCH3] fragment – by SOE-PCRs using primers FVH5FW and FCG4R. The size in base pairs (bp) of the whole chimeric recombinant constructs NIP-rhIGHG1,

Table 2.1. Primers used for generation of rhesus macaque IgG gene fragments and recombinant constructs by PCR and SOE-PCR amplifications.

Primer name[a]	Sequence (5'-3' direction)[b]	Specificity (region of genes; species)[c]	Sequence characteristics
FVH5FW	GGTG**TGCATTC**CCAGGTCCAATTGCAGCAGCCT	5'; murine anti-NIP VH	Containing *BsmI* site (5'-TGCATTC-3') Contained in full (33-bp sequence) in IgNotI
FCG4R	AGT**GGATCC**ATTACTAGTAGCAGGTGCCGTCCACCTCCGCCATGA***TCTGCGTGTAGTGGTTGTGCAG***A	3'; rhesus macaque IgG CH3	Containing *BamHI* site (5'-GGATCC-3') 22-bp homologous to IGC2
IGC2	***TCTGCGTGTAGTGGTTGTGCAG***	3'; rhesus macaque IgG CH3	Contained in part (65-bp sequence) in IgXhoI 22-bp homologous to FCG4R Contained in full (22-bp) in IgXhoI
FVH3G4R	***GACCGATGGGCCCTTGGTGGAGGCTGAAGAGACTGTGAGAGT***GG	3'; murine anti-NIP VH	42-bp homologous to 3FCG4F 21-bp homologous to IGF
3FCG4F	***ACTCTCACAGTCTCTTCAGCCTCCACCAAGGGCCCATCGGTC***	5'; rhesus macaque IgG CH1	42-bp homologous to FVH3G4R 21-bp homologous to IGF
IGF	TCC***TCAGCCTCCACCAAGGGCCCA***	5'; rhesus macaque IgG CH1	21-bp homologous to FVH3G4R 21-bp homologous to 3FCG4F
IgG1R	GAC***GGTCCCCCCAGGAG***	3'; rhesus macaque IgG1 CH1	14-bp homologous to G2C1RN
G2C1RN	***GATGGTCCCCCCAGGAGTTCAGCTGGGCACGGTGGGCACGTGGAACGACATGGGAGCCCAACTGTCTTGTCCACCTTGG***	3'; rhesus macaque IgG2 CH1	79-bp homologous to G2C2FN 14-bp homologous to IgG1R
G2C2FN	***CCAAGGTGGACAAGACAGTTGGGCTCCCATGTCGTTCCACGTGCCCACCGTGCCCAGCTGAACTCCTGGGGGGACCATC***	5'; rhesus macaque IgG2 CH2	79-bp homologous to G2C1RN
G2C2R	***CACCTGTGGCTCTCGGGGCTGCCCTTTGGTTTTGGAGACAGTT***TTCT	3'; rhesus macaque IgG2 CH2	43-bp homologous to G2C3F
G2C3F	***AACTGTCTCCAAAACCAAAGGGCAGCCCCGAGAGCCACAGGTG***	5'; rhesus macaque IgG2 CH3	43-bp homologous to G2C2R
G3C1R	***ATGGGGGTGTGAACTCAACTCTCTTGTCCACCTTGG***	3'; rhesus macaque IgG3 CH1	36-bp homologous to G3CHR 15-bp homologous to G3CHF
G3CHR	***CTGGGCATGGTG****GGCATGGGGGAGTTGTGTCACCAC****ATGGGGGTGTGAACTCAACTCTCTTGTCCACCTTGG***	3'; rhesus macaque IgG3 hinge	36-bp homologous to G3C1R 51-bp homologous to G3CHF 12-bp homologous to G3C2F
G3CHF	***AGTTCACACCCCCAT****GTGGTGACACAACTCCCCCATGCC****CACCATGCCCAG****CACCTGAACTCCTGGGGGGAC***	5'; rhesus macaque IgG3 hinge	33-bp homologous to G3C2F 51-bp homologous to G3CHF 15-bp homologous to G3C1R
G3C2F	***CACCATGCCCAG****CACCTGAACTCCTGGGGGGAC***	5'; rhesus macaque IgG3 CH2	33-bp homologous to G3CHF 12-bp homologous to G3CHR
G3C2R	***GCTCTCGGGGCTGCCCTTTGGCTTTGGAGA***TGGTTT	3'; rhesus macaque IgG3 CH2	30-bp homologous to G3C3F
G3C3F	***TCTCCAAAGCCAAAGGGCAGCCCCGAGAGC***CGCAGG	5'; rhesus macaque IgG3 CH3	30-bp homologous to G3C2R
IG4CR1	***ATGCTGGGCATG***GGGGTGTGAACTCAACTCTCTTGT	3'; rhesus macaque IgG4 CH1	12-bp homologous to IG4CF2
IG4CF2	***CATGCCCAGCAT***GCCCAGCACCTGAACTCCTGG	5'; rhesus macaque IgG4 CH2	12-bp homologous to IG4CR1
IG4R2	***GCTCTCGGGGCTGCCCTTTGGCTTTGGAGATGG***	3'; rhesus macaque IgG4 CH2	33-bp homologous to IG4F3
IG4F3	***CCATCTCCAAAGCCAAAGGGCAGCCCCGAGAGC***	5'; rhesus macaque IgG4 CH3	33-bp homologous to IG4R2
IgNotI	ATTA**GCGGCCGC**ATAATGGGTGACAATGACATCCACTTTGCCTTTCTCTCCACA***GGTGTGCATTCCCAGGTCCAATTGCAGCAGCCT***	5'; murine anti-NIP VH[b]	Containing *NotI* site (5'-GCGGCCGC-3') Containing full 33-bp sequence of FVH5FW
IgXhoI	ACTCA**CTCGAG*****GGATCC*****ATTACTAGTAGCAGGTGCCGTCCACCTCCGCCATGATCTGCGTGTAGTGGTTGTGCAGA***	3'; rhesus macaque IgG CH3[c]	Containing *XhoI* site (5'-CTCGAG-3') Containing partial 65-bp sequence of FCG4R Containing full 22-bp sequence of IGC2

[a]Ending with or before the last single digit/letter with -FW or -F, or ending with *NotI*, forward direction; ending with –R or *XhoI*, reverse direction; IgC2, reverse direction.

[b]Bold and underline, restriction endonuclease sequences; bold and italic, with or without underline, overlapping ("homologous") region (with underline, identical; without underline, complementary in reverse direction) with the relevant primer(s) indicated in "Sequence characteristics" column.

[c]For non-flanking ("internal") primers, the 5' or the 3' end represents that at the 5'or 3' intron-exon junction, respectively.

NIP-rhIGHG2, NIP-rhIGHG3, and NIP-rhIGHG4 are 1,390, 1,369, 1,423, and 1,366, respectively. These constructs encode four corresponding rhesus macaque IgH subclasses. As mentioned above, the final fragment contains two unique *BsmI* (or *NotI*) and *BamHI* (or *XhoI*) RE sites whose sequences were embedded in the two far end flanking primers (i.e. the outermost 5' and 3' primers) and were introduced into the constructs by PCRs.

SOE-PCRs were carried out by Expand High Fidelity polymerase (Roche Diagnostics North America, Indianapolis, IN) or Ex Taq DNA polymerase (Clontech Laboratories Inc., Mountain View, CA) in a total of 50 or 100 µl final reaction volume containing 10-200 ng plasmid DNA, 10-50 pmol (each) primers, 200-250 µM (each) dNTPs, 1.5-2.5 mM $MgCl_2$, and 2-2.5 U of DNA Taq polymerase. DNA concentration of samples was calculated using the formula C (pmol/µL) = (75 x A260 x d)/(bp x l), in which A260 is the absorbance at 260 nm, d is the dilution factor, bp is the length of DNA in basepair, and l is cuvette width in cm. PCR conditions were as follows: after initial denaturation at 95°C for 5-10 min to melt strands into single strands, cDNAs were amplified for 25-40 cycles, with each cycle consisting of 94°C for 30 sec-1 min to melt strands, 56°C for 30 sec-1 min to anneal primers, and 72°C for 30 sec-2 min and 30 sec to extend strands. To ensure complete extension, a final step at 72°C for 5-10 min was applied. The negative controls consisted of the reaction mixture with no template DNAs.

Adjustment of PCR conditions and parameters, including optimization of time in each step and of the annealing temperature (from 52-60^{0}C, with 0.5^{0}C or 1^{0}C increment, to promote annealing), as well as additional cloning steps in pCR2.1-TOPO TA vector (see below for procedures) for some of the gene segments and fragments, were needed to minimize non-specific products and to improve the success of SOE-PCR ligation and amplification. The concentrations of the two primers in each primer pair were close to each other and ranged from 20-200 nM per

reaction (in each reaction, specific primers were used dependent on which PCR was being performed, as described above). To allow for better annealing and extension of overlaps in some reactions – such as those for generation of IgG3, which were with additional hinge primers – PCRs that used equimolar concentrations of DNA fragments were run without primers and low annealing temperature during early cycles (i.e. the first 5-10 cycles), followed by a higher annealing temperature with fresh PCR mixtures in the remaining 20-30 cycles. Whenever possible, fragments and sub-fragments (intermediate fragments) were put into cloning plasmid vectors to serve as a source of DNA templates. Flanking primers were sometimes added after two to three cycles to reduce competition for the available reagents in the reactions. To determine the optimal SOE-PCR reaction conditions and parameters, varying magnesium concentrations were also applied in a series of SOE-PCR reactions. The molar ratios of the two DNA segment or fragment templates used in annealing SOE-PCRs were generally equal (1:1, with total DNA amount was at least 0.7 μg/50 ml PCR); but in some cases, variable ratios such as 1:2, 1:3, or 1:5, dependent upon their sizes, were applied in order for the desired fragments to be better annealed.

2.2.3. Cloning and sequence analysis of the NIP-rhIGHG cDNA constructs

To assess the fidelity of PCR reactions and to improve the purity of the fused fragments (i.e. to minimize the appearance of non-specific side products), SOE-PCR products were cloned into pCR2.1-TOPO cloning vector (Fig. 2.4). As described above, the resultant cDNA hybrids were introduced at the 5’ end of V coding gene and the 3’ end of C coding gene region with *BsmI* and *BamHI* (B-B) restriction sites, respectively, in one subset of the molecules, or with *NotI* and *XhoI* (N-X) restriction sites, respectively, in another subset. These restriction sites were

intentionally incorporated (embedded) in the appropriate primers and were unique, as they were not present in any of the examined IgH cDNA genes. These sites will allow for cloning of the cDNA into specialized expression vectors (see below). After SOE-PCR annealing and amplification, an appropriate volume of SOE-PCR reactions containing the final chimeric IgG fusion genes were subjected to electrophoresis on a 1-2% agarose gel (dependent upon the fragment sizes) diluted in TBE buffer (Sigma–Aldrich Co., St. Louis, MO) and containing 0.1-0.2 mg/ml ethidium bromide (Sigma–Aldrich Co., St. Louis, MO). The DNAs were subsequently visualized using an ultraviolet transilluminator, and the bands of interest (showing expected size) were individually excised and purified using QIAquick Gel Extraction kit (Qiagen Inc., Valencia, CA) using a microcentrifuge. Purified NIP-rhIGHG PCR products were then cloned within EcoRI sites into pCR 2.1-TOPO TA cloning vector (Invitrogen, Carlsbad, CA), which contains an ampicillin resistance gene. For optimal incorporation, different molar ratios (vector:insert) were applied, including 1:1, 1:3, 1:5, 1:10, 2:1, 3:1, and 5:1 (higher ratios were for difficult cloning). The amount of vector to start with ranged between 10-20 ng and was calculated as [(ng vector x kb insert)/kb vector] x (moles insert/moles vector) = ng insert (http://www.promega.com/biomath/Default.htm). Resultant plasmids were subsequently transformed into Top10 *Escherichia coli* (E. coli) chemically competent cells using One Shot Chemical Transformation kit (Invitrogen, Carlsbad, CA), following the manufacturer's protocols. The competent cells were then spread onto LB agar plates containing 50 μg/ml of ampicillin and 1 μg of X-Gal for screening for suitable colonies. Insert-positive clones were then picked and further cultured (expanded) by incubation overnight in LB culture tubes containing 50 μg/ml of ampicillin at 37°C in a shaking rotary incubator (200-230 rpm).

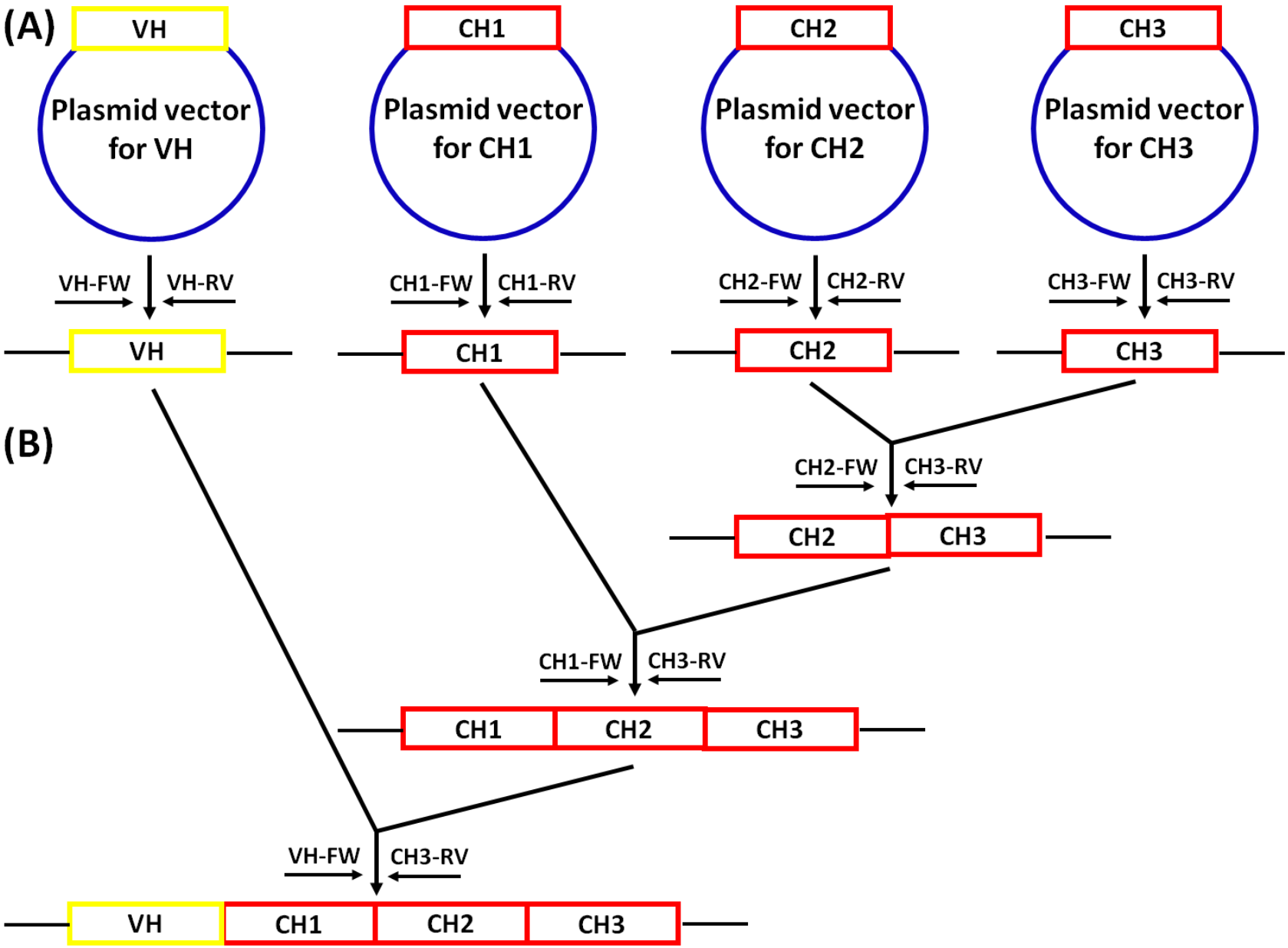
(A)
VH
CH1
CH2
CH3
Plasmid vector for VH
Plasmid vector for CH1
Plasmid vector for CH2
Plasmid vector for CH3
VH-FW
VH-RV
CH1-FW
CH1-RV
CH2-FW
CH2-RV
CH3-FW
CH3-RV
VH
CH1
CH2
CH3
(B)
CH2-FW
CH3-RV
CH2
CH3
CH1-FW
CH3-RV
CH1
CH2
CH3
VH-FW
CH3-RV
VH
CH1
CH2
CH3

(C)

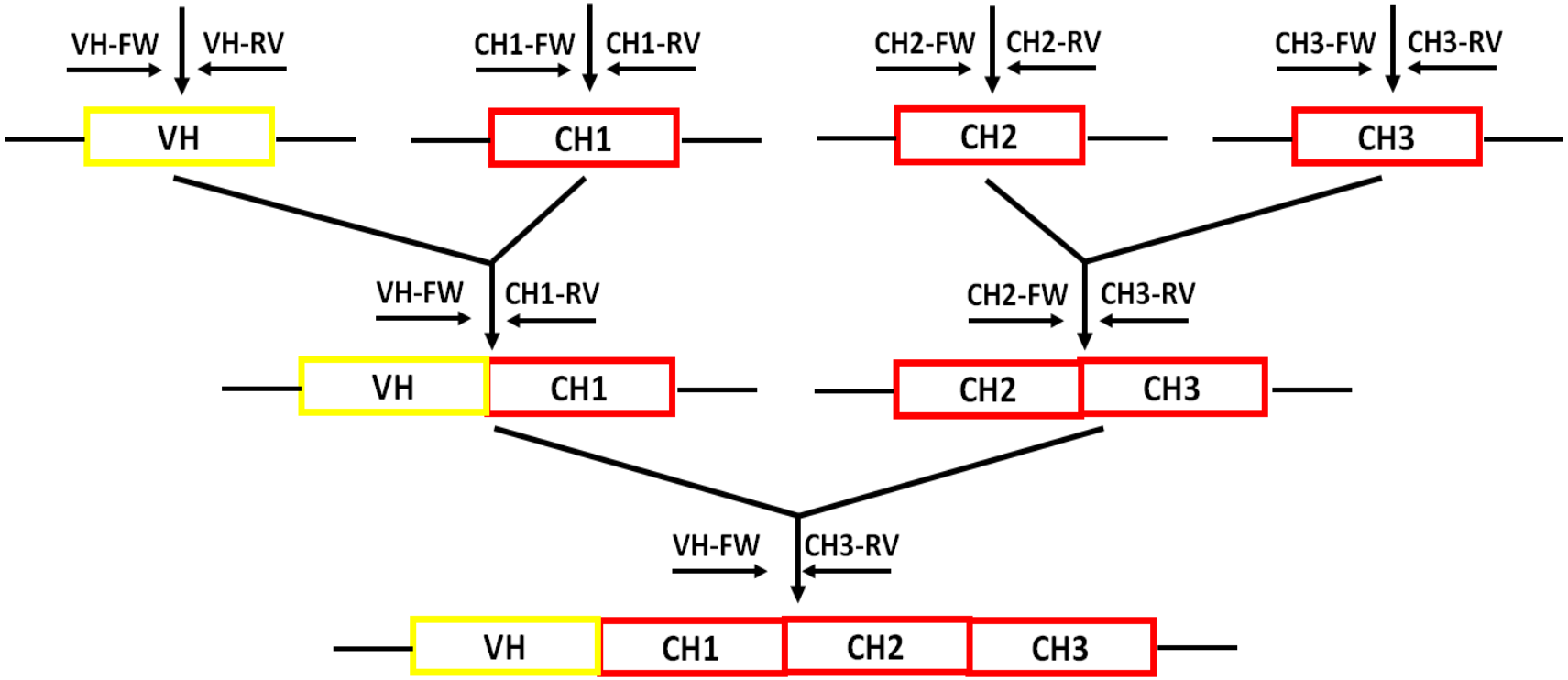
VH-FW
VH-RV
CH1-FW
CH1-RV
CH2-FW
CH2-RV
CH3-FW
CH3-RV
VH
CH1
CH2
CH3
VH-FW
CH1-RV
CH2-FW
CH3-RV
VH
CH1
CH2
CH3
VH-FW
CH3-RV
VH
CH1
CH2
CH3

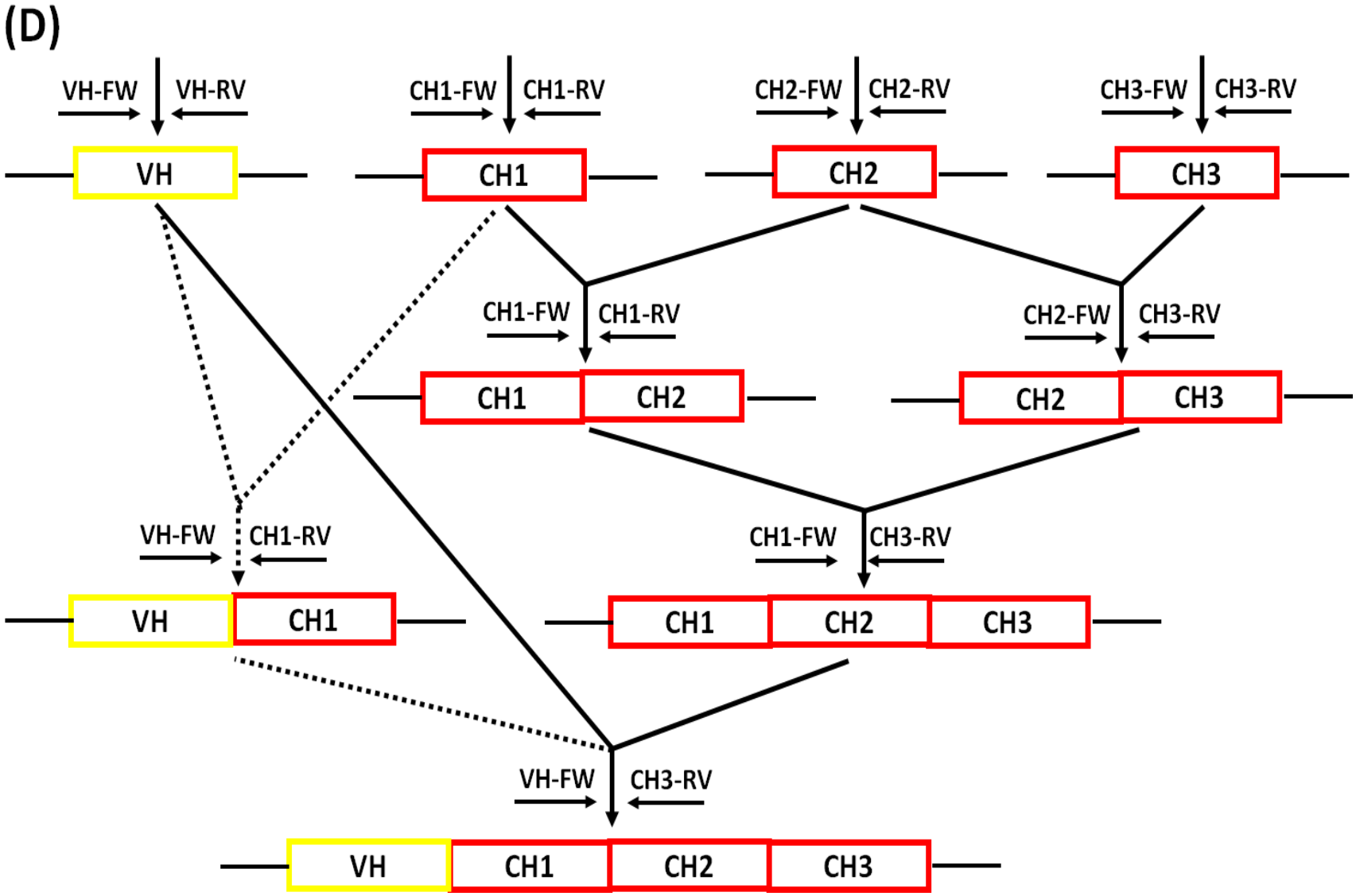
(D)
VH-FW
VH-RV
CH1-FW
CH1-RV
CH2-FW
CH2-RV
CH3-FW
CH3-RV
VH
CH1
CH2
CH3
CH1-FW
CH1-RV
CH2-FW
CH3-RV
CH1
CH2
CH2
CH3
VH-FW
CH1-RV
CH1-FW
CH3-RV
VH
CH1
CH1
CH2
CH3
VH-FW
CH3-RV
VH
CH1
CH2
CH3

Fig. 2.3. Flowchart diagrams outlining different experimental strategies for generation of recombinant NIP-rhIGHG cDNA constructs by SOE-PCRs (not drawn to scale). (A) PCR amplification of individual mouse VH (represented as the yellow-line, enlarged box) and rhesus macaque IgG CH (represented as red-line, enlarged boxes) fragments (i.e. CH1, CH2, and CH3) encoding corresponding domains of recombinant IgGs to be generated. These fragments are represented in the 5' to 3' orientation. cDNAs coding for these VH and CH domains were amplified from the appropriate plasmid vectors (shown are not the real names of the plasmids), retrieved from our plasmid repository. The direction of the primers used to amplify these fragments are illustrated as short black horizontal arrows (shown are not the real names of the primers). Straight short black lines represent flanking sequences. (B) A representative strategy of SOE-PCR joining (see Fig. 1.8 for the principle) of DNA fragments. The fragments were jointed by SOE-PCRs using the appropriate primer sets, as indicated. Arrows indicate the direction of the primers used to amplify the fragments. (C) An alternative strategy. (D) Additional strategies.

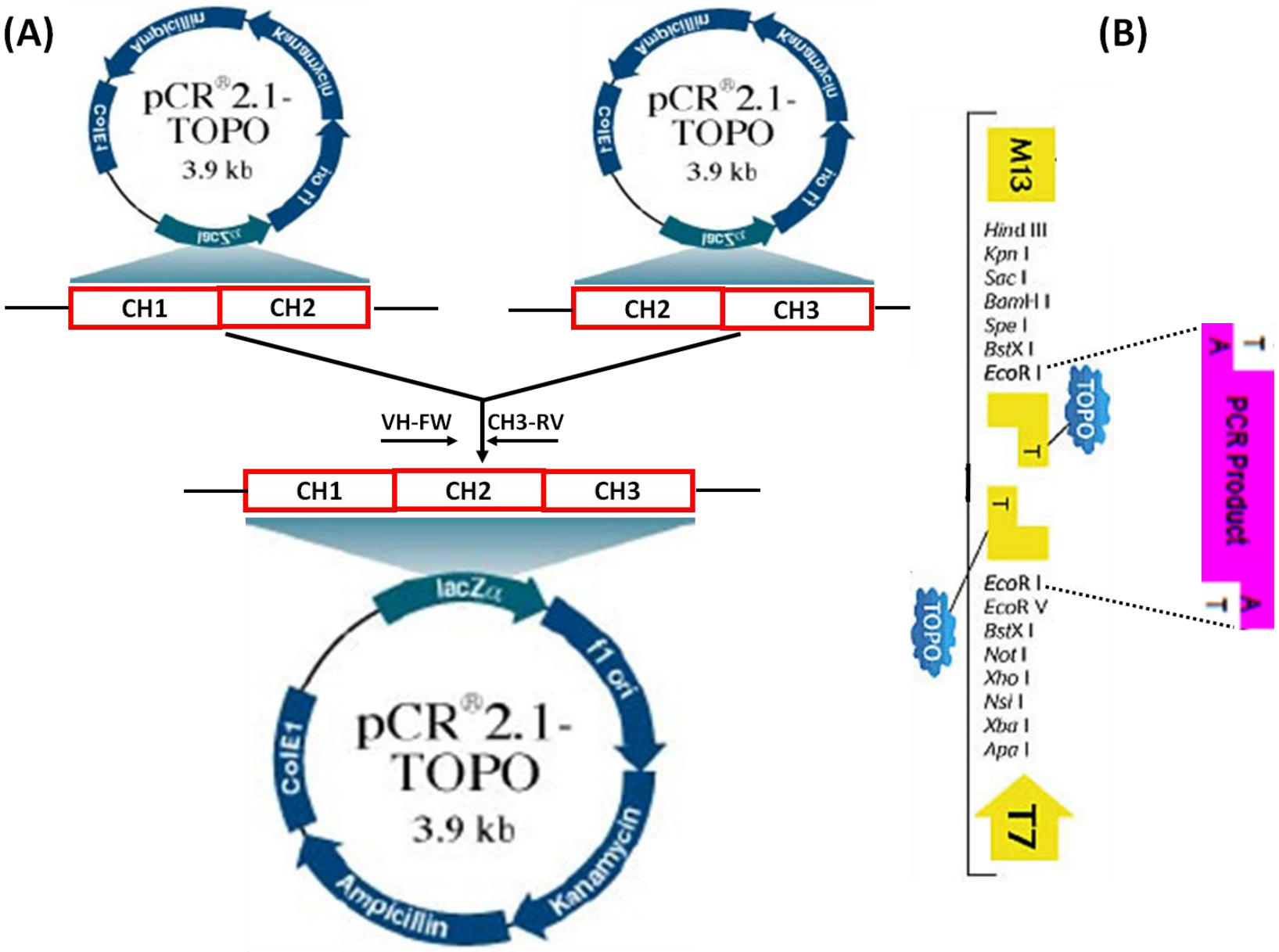
(A)
pCR®2.1-TOPO
3.9 kb
CH1
CH2
CH2
CH3
VH-FW
CH3-RV
CH1
CH2
CH3
lacZα
f1 ori
Kanamycin
Ampicillin
ColE1
(B)
M13
Hind III
Kpn I
Sac I
BamH I
Spe I
BstX I
EcoR I
TOPO
T
PCR Product
A
EcoR I
EcoR V
BstX I
Not I
Xho I
Nsi I
Xba I
Apa I
T7

Fig. 2.4. Ligation of PCR products into pCR2.1 TOPO TA cloning vector. (A) These fragments are used as an example to show the procedure of TOPO cloning for ligation of PCR products (as to assess the fidelity of PCRs). The recognition sites for a number of restriction endonucleases (the unique multiple cloning site, which is used to clone in DNA fragments of interest) are embedded within the lacZ coding sequence. Because the lacZ peptide will be functionally disrupted or inactivated by the presence of the DNA insert, the lacZ coding gene sequence is used as a selectable marker. (B) Schematic representation of ligation of PCR product ligates into TOPO vector in the presence of Topoisomerase (hence the name of the vector). Some figure pieces are reproduced from the internet.

NIP-rhIGHG insertion, proper orientation, and accuracy of sequences were confirmed by RE digestion and DNA sequencing (Fig. 2.5). Briefly, the minipreps DNA Purification System kit (Promega Corporation, Madison, WI) was used to purify plasmid DNAs extracted from grown clones in LB medium, and the obtained plasmid DNAs were digested with *EcoRI* (New England Biolabs, Beverly, MA). *EcoRI*-digested plasmids were then electrophoresed on a 1% agarose gel to verify the presence of the desired insert based on the size of the inserted fragments. Bands containing NIP-rhIGHG constructs with the correct size were extracted using a QIAquick gel extraction kit (Qiagen Inc., Valencia, CA) and the recombinant plasmids were sequenced to confirm cloning correctness. All DNA sequences were determined using the ABI Prism Dye Termination Cycle Sequencing kit and on an ABI model 3100 automated sequencing apparatus (PerkinElmer, Wellesley, MA). Sequencing primers were those used for PCR amplifications and the forward and reverse M13 primers.

Further sequencing analysis was also applied to sequences of the resultant constructs. MacVector software (Accelrys Inc., San Diego, CA) and the free BioEdit program (http://www.mbio.ncsu.edu/bioedit/bioedit.html) were used to identify overlapping regions and to edit sequences. Sequences were aligned using the CLUSTAL function of the MEGALIGN, part of the LASERGENE software package (DNASTAR Inc., Madison, WI). The prediction of potential N-glcosylation sites was conducted by analyzing the full length sequence of the obtained molecules using the online tool NetNGlyc 1.0 Server (http://www.cbs.dtu.dk/services/NetNGlyc/), which is based on identifying Asn-Xaa-Ser/Thr consensus sequences (Julenius et al., 2005). Drawing plasmids was performed using the free Plasm plasmid drawing software (http://biofreesoftware.com/plasm). Standardized nomenclature, labels, and numbering of IMGT®, the international ImMunoGeneTics information system®

(http://www.imgt.org or http://imgt.cines.fr) (Lefranc et al., 2009) were used to identify IgSF gene segments, as well as to display and discuss sequencing data based on human reference sequences. Two-dimensional representation, or IMGT Colliers de Perles on one layer was obtained with the IMGT Collier-de-Perles tool in the IMGT/DomainGapAlign (http://www.imgt.org/3Dstructure-DB/cgi/Collier-de-Perles.cgi) (Ehrenmann et al., 2010). Allelic polymorphisms and characteristic positions of the C-like domains were described using the IMGT unique numbering for C domain [C-DOMAIN of IG and T cell receptors (TR)] (Lefranc et al., 2005).

2.2.4. pLNOH2 and P2561/2/3 expression vector systems and the murine IgH-defective myeloma J558L cell line

For expression vectors, we used the pLNOH2 (or pLNOH2γ3) (Norderhaug et al., 1997) plasmid vector (kindly provided by Drs. Lars Norderhaug and Inger Sandlie, University of Oslo and Ab Design AS, Nesoddtangen, Norway) (Fig. 2.6). This vector is derived from the expression vector pcDNA3 (Invitrogen, Carlsbad, CA) and contains essential elements for transcription and translational regulation. Specifically, it consists of a CMV promoter (P) situated at the 5' end of a gene cassette containing an Ig leader (L) (signal peptide) region sequence of murine Ig genes (to permit secretion of the fusion protein), a murine VH gene encoding an Igλ domain with specificity for the hapten NIP inserted between RE sites *BsmI* and *BsiWI*, followed by an intron. The intron comprises splice acceptor (GU) and splice donor (AG) signals for correct processing of mRNA. The vector also harbors a gene restriction cassette, located downstream of the murine V gene and inserted between RE sites *HindIII* and *BamHI*, encoding the CH fragment of human IgG3 sequence (*IGHG3*), followed by a strong

polyadenylation signal and transcription termination sequence in the 3’ end (pA). These C and V region genes together encode complete IgG H chains. The vector further contains unique restriction sites for easy subcloning of V and C region genes as cassettes, and can be used to express an anti-NIP VH gene segment in combination with any CH region genes of different IgG subclasses exchanged as *HindIII-BamHI* fragments (Norderhaug et al., 1997). For selection and stable expression of transformant cells, the vector also carries a neomycin resistance gene, which is under the control of CMV promoter. The vector also possesses an ampicillin resistance marker gene (Amp) (for selection in E. coli), f1 origin of replication (f1), and SV40 origin of replication (to allow for transient expression). The use of the vector allows both transient and stable expression in mammalian cells.

To improve stability of expression vectors in transfected cells, we also used a modified version of the vector pLSXN (BD Biosciences, San Jose, CA), which contains long terminal repeats (LTR) that allow for the gene of interest to integrate into the host cell chromosomes for stable expression (Fig. 2.8). Constitutive transcription of cloned genes inserted into this plasmid vector is driven by CMV promoter. Promoter and enhancer sequences controlling expression of the gene of interest in the multiple cloning site are also inserted in the 5’ viral LTR of this vector. pLSXN also contains a neomycin resistance gene, controlled by SV40 early promoter (PSV40e), that allows antibiotic transfectant selection in eukaryotic cells. Additionally, pLXSN consists of Col E1 origin of replication and E. coli Amp resistance gene for propagation and antibiotic selection in bacteria. We amplified by PCR using primers that incorporated desirable RE sites a portion of the pcDNA3.1 constructs that contains cDNA of NHP FcγIIIRa (or another gene of interest), a CMV promoter, L signal peptide, a bovine growth hormone polyadenylation signal, and an f1 origin. This PCR portion was then sequentially transferred to the multiple cloning site

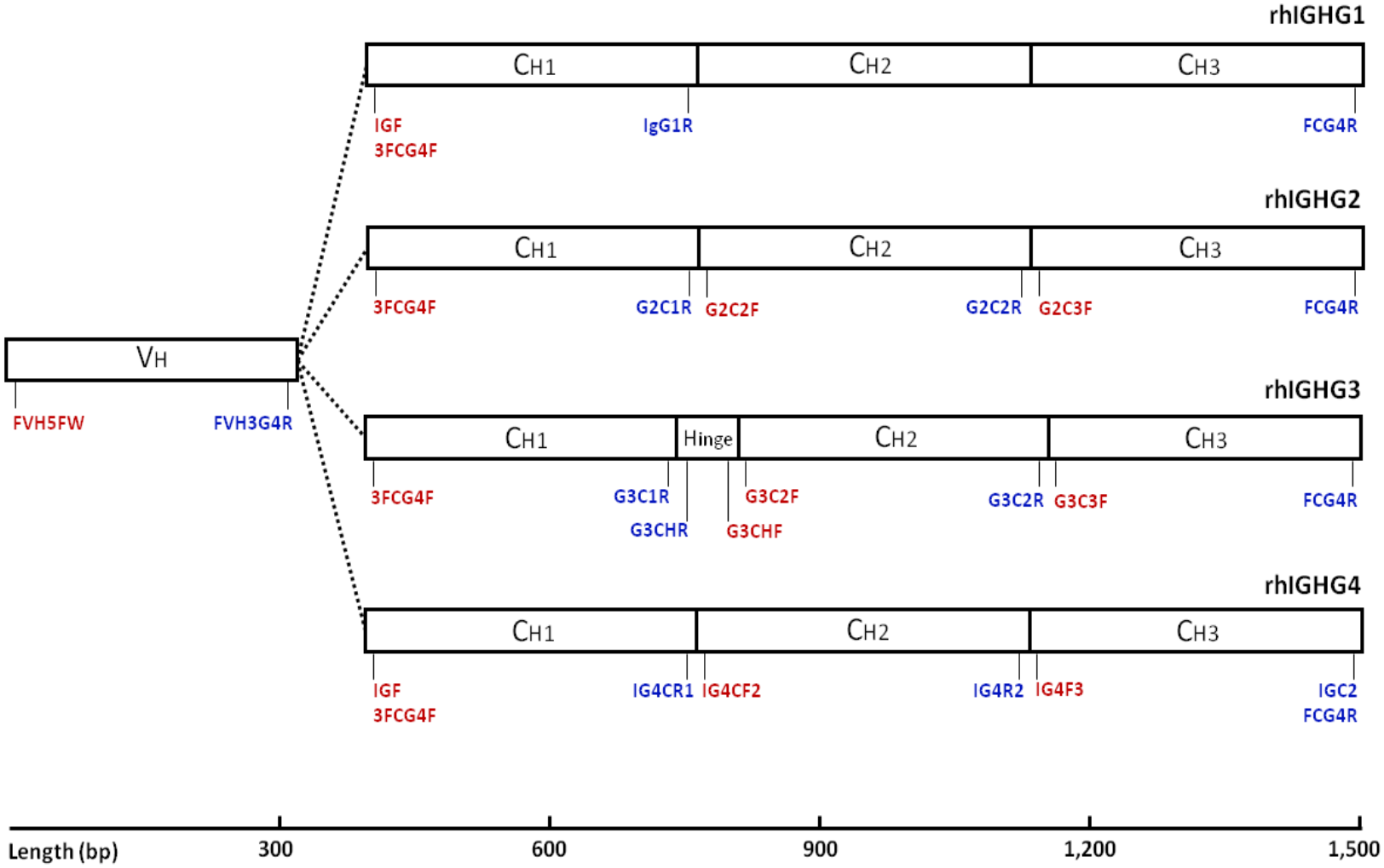
rhIGHG1
CH1
CH2
CH3
IGF
3FCG4F
IgG1R
FCG4R
rhIGHG2
CH1
CH2
CH3
3FCG4F
G2C1R
G2C2F
G2C2R
G2C3F
FCG4R
VH
FVH5FW
FVH3G4R
rhIGHG3
CH1
Hinge
CH2
CH3
3FCG4F
G3C1R
G3CHR
G3C2F
G3CHF
G3C2R
G3C3F
FCG4R
rhIGHG4
CH1
CH2
CH3
IGF
3FCG4F
IG4CR1
IG4CF2
IG4R2
IG4F3
IGC2
FCG4R
Length (bp)
300
600
900
1,200
1,500

Fig. 2.5. Schematic representation of the PCR- and SOE-PCR-amplified *IGHG* fragments that make up of the four recombinant NIP-rhIGHG (Igγ) cDNA constructs. CH1, the hinge (for Igγ3), CH2, and CH3 amplified fragments of each Igγ cDNA construct, as well as the VH amplified fragment to be connected to all of these constructs, are shown. Each amplified fragment is represented as an enlarged box, as indicated. The VH fragment, which was derived from murine myeloma and specific to NIP (5-iodo-4-hydroxy-3-nitrophenyl acetyl), was joined by SOE-PCRs to a complete rhesus macaque IgH fragment, which were constructed also by SOE-PCRs. Name and relative location (indicated by vertical black bars) of primers used to amplify different fragments in these SOE-PCRs are depicted. The final recombinant constructs were amplified in SOE-PCRs using the primers flanking the VH 5' end (FVH5FW) and the CH3 3' end (FCG4R, or IGC2 in the case of NIP-rhIGHG4), as indicated. Each primer was designed to flank the appropriate gene fragments; the sequences of the primers used are given in Table 2.1. The trans-membrane exons at the 3' end of the mRNA of the Igγ chains are not depicted. The Igγ3 hinge is not drawn to scale. Illustrated below the scheme is a bar representing relative length distance scale (in bp) in the 5' to 3' orientation for the fragments. The intron-exon organization of the IGHG genes was inferred from the human and rhesus macaque sequences publicly available. The necessary splice sites found at intron boundaries and the sequences of the introns were removed.

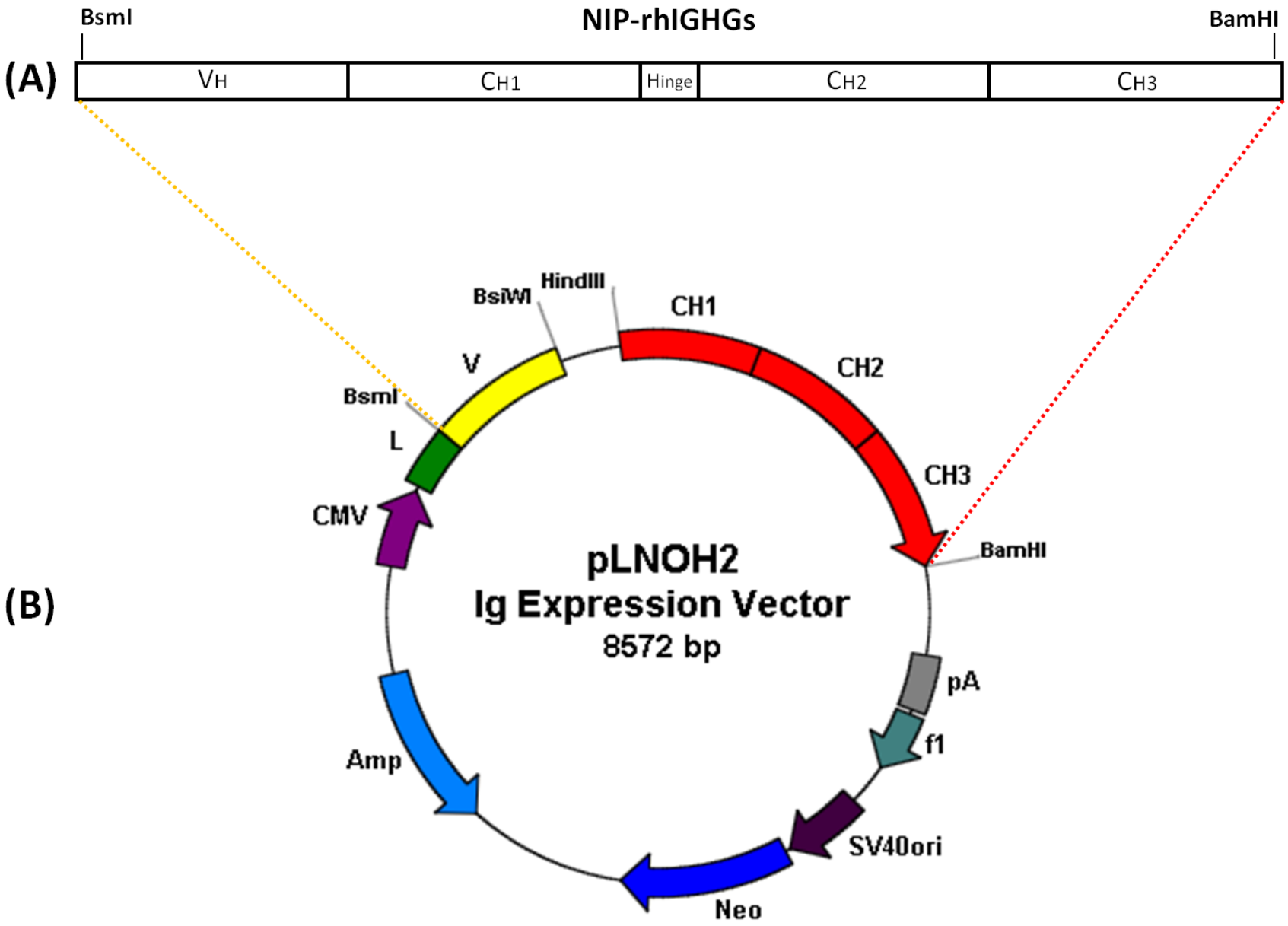
(A)
BsmI
NIP-rhIGHGs
BamHI
VH
CH1
Hinge
CH2
CH3
(B)
BsiWI
HindIII
CH1
V
CH2
BsmI
L
CH3
CMV
BamHI
pLNOH2
Ig Expression Vector
8572 bp
pA
f1
Amp
SV40ori
Neo

Fig. 2.6. Schematic representation of the structure of a representative recombinant NIP-rhIGHG cDNA construct (shown is the NIP-rhIGH3 cDNA construct) and simplification of the architecture of the expression plasmid vector pLNOH2, highlighting regions of functional significance and relevant features (not drawn to scale). (A) Schematic representation of structure of recombinant NIP-rhIGHG3 cDNA construct. A mouse VH fragment with NIP specificity that contained a *BsmI* restriction site at the 5' end was joined by SOE-PCRs to rhesus macaque Igγ3 CH fragment constructed also by SOE-PCRs and contained a *BamHI* restriction site at the 3' end. Only restriction sites at the ends of the constructs are depicted. The trans-membrane exons at the 3' end of mRNA of IgH chains are not illustrated. The hybrid chain was subcloned into the expression plasmid vector pLNOH2 onto *BsmI* and *BamHI* sites. The hinge is not drawn to scale. (B) Simplification of the map of specialized pLNOH2 expression vector, highlighting regions of relevant features (not drawn to scale). This double-stranded closed-circular DNA molecule vector is derived from vector pcDNA3 (Invitrogen, Carlsbad, CA) (Norderhaug et al., 1997). Expression is driven by a cytomegalovirus promoter (CMV) and leader (L) (signal peptide) sequence (L permits secretion of the expressed protein). The vector contains, adjacent to L sequence, an anti-NIP murine VH gene cloned in *BsmI* and *BsiWI* restriction sites, followed by a human genomic Igγ3 CH gene cassette, which can be replaced by those of different subclasses of rhesus macaques onto the *HindIII* and *BamHI* sites, as indicated. CH1, CH2, and CH3 refer to the corresponding domains in Igγ3 CH genes. Polyadenylation signal (pA; recognition sequence for polyadenylation) of the vector is inserted downstream of the Igγ CH coding sequence to ensure proper and efficient processing of mRNA transcript in eukaryotic cells. The vector backbone also contains an f1 ori (f1) for single-stranded DNA production (plasmid origin of replication), as well as an SV40 promoter (SV40ori) for plasmid replication in mammalian cells.

Plasmid DNA replication occurs in one direction, as illustrated by the f1 ori arrow. Located downstream of SV40ori region in the vector is a gene cassette for neomycin resistance (Neo), which is controlled by SV40 promoter and allows for G418 antibiotic selection of stable expression by transfected eukaryotic cells. Structurally similar to gentamycin and generally toxic to eukaryotic and prokaryotic cells, the aminoglycoside antibiotic G418 is useful for selection of cells stably transfected with Neo gene (presence of insert DNA will disrupt functional activities and allow for selection). The pLNOH2 vector also comprises an ampicillin resistance gene (Amp) for propagation and antibiotic selection in bacteria (E. coli). The curve arrows on the genes illustrate the direction of transcription. VH gene is oriented so that its direction of transcription is opposite to that of the Amp gene. *BsmI* and *BamHI* sites, located downstream of CMV promoter/L sequence and Igγ CH cassette, respectively, are unique and can be used for directional insertion of constructs of interest as *BsmI-BamHI* restriction fragments. The *BsmI-BamHI* restriction fragments of NIP-rhIGHG inserts are ~1.37 kb-1.42 kb in size, varying dependent on IgH subclasses. The vector sequence totals ~8.6kb in length and all sites illustrated are unique (occur only once in within the plasmid sequence). The orientation and sequence of DNA inserts in the recombinant plasmids were confirmed by RE digestions and/or nucleotide sequencing. This map was constructed using the plasmid drawing software Plasm (http://biofreesoftware.com/plasm) and based on information described in Brekke and Thommesen, 2003, and Norderhaug et al., 1997.

of pLXSN (BD Biosciences, San Jose, CA) (Rogers et al., 2006), generating the P2561/2/3 expression vectors. These recombinant plasmid vectors facilitate selection of transformants on culture media containing ampicillin, and enable stable integration into nuclear chromosomal cellular DNA.

For production of intact recombinant IgGs, we employed a well-characterized and genetically stable mammalian host cell line, the BALB/c murine IgH-loss-variant myeloma (i.e. Ab-producing cells) J558L cells (Oi et al., 1983; kindly provided by Dr. Sherie L. Morrison, University of California, Los Angeles, Los Angeles, CA). Although being a murine plasmacytoma, these cells do not produce intact mouse Ig Abs as they express no endogenous IgH chain [due to a spontaneous loss of IgH chain from their parental myeloma cell line J558 (Morrison, 1985)]. However, these cells continue to constitutively synthesize and secret an IgL λ1 chain specific for NIP (Oi et a., 1983), which can form complete Ig molecules with NIP affinity when combined with anti-NIP (i.e. containing anti-NIP VH) IgH chains. The cells can also recombine two transfected DNA molecules in an appropriate manner (in about 30% of cells that received and integrated intact copies of both DNA molecules) (Fell et al., 1989). Thus, once transfected with an IgH chain expression vector, such as that encoded in pLNOH2 plasmid, the cell machinery will synthesize and assemble IgL and IgH chains (chain-assembly), ultimately secreting endogenously intact Ig molecules. Additionally, murine IgH-chain defective myeloma cells are capable of producing greater amounts (and with higher protein concentration) of ectopic fusion protein compared to other cell lines, including CHO or HEK293 cells (Howard et al., 2002). The cells were maintained in Iscove's modified Dulbecco's medium (IMDM) supplemented with 10% fetal bovine serum (FBS), penicillin G sodium 100 IU/ml, and streptomycin sulfate 100 μg/ml under standard conditions in 25-ml or 75-ml sterile filter screw-

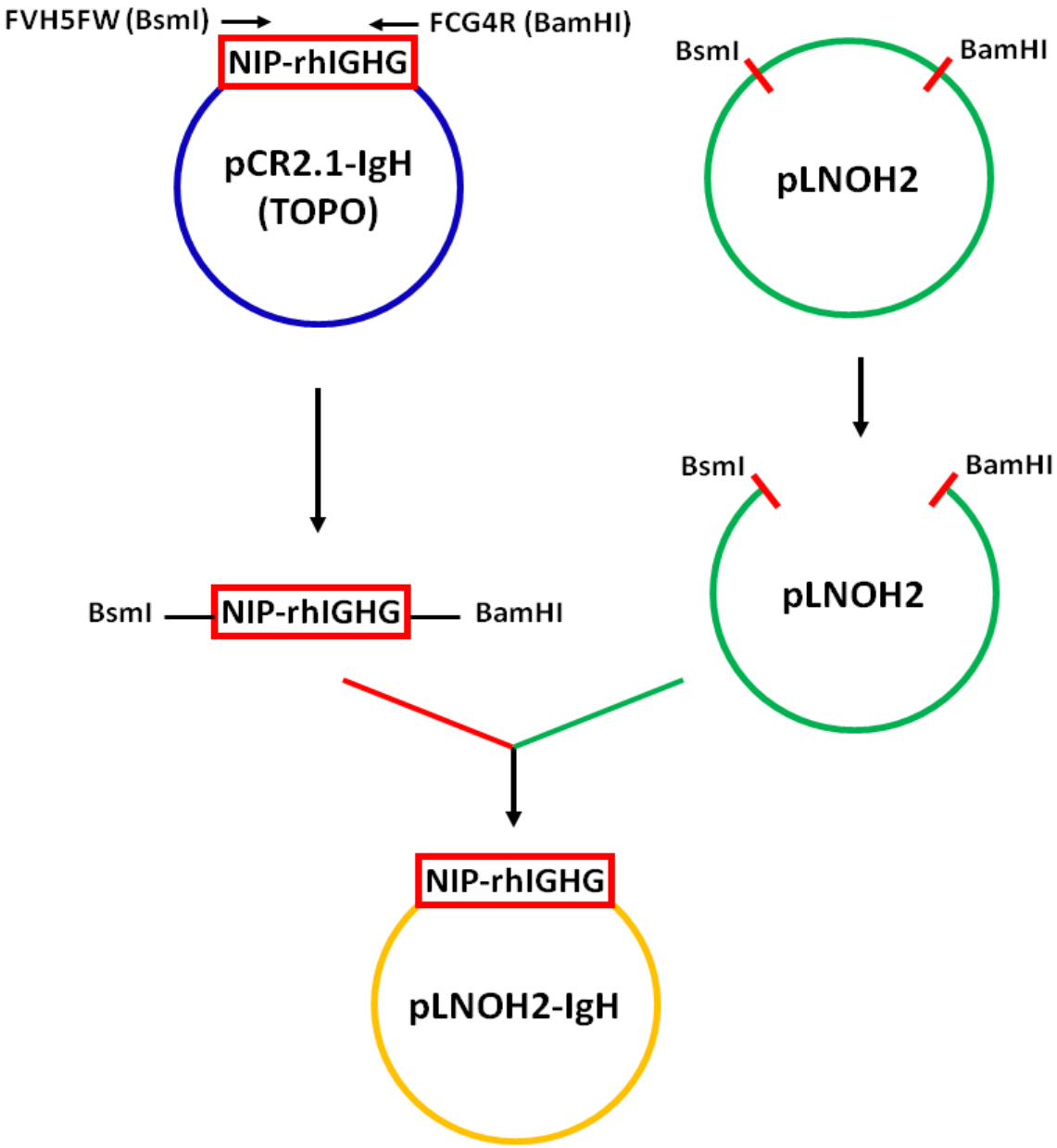
FVH5FW (BsmI)
FCG4R (BamHI)
NIP-rhIGHG
pCR2.1-IgH
(TOPO)
BsmI
BamHI
pLNOH2
BsmI
NIP-rhIGHG
BamHI
BsmI
BamHI
pLNOH2
NIP-rhIGHG
pLNOH2-IgH

Fig. 2.7. Schematic representation of generation of recombinant expression plasmid vector pLNOH2-IgH (not drawn to scale). NIP-rhIGHG constructs were PCR-amplified from appropriate TOPO vectors using forward primer FVH5FW (containing *BsmI* restriction site in its 5' end) and reverse primer FCG4R (containing *BamHI* restriction site in its 5' end), as indicated. The resultant PCR products were then ligated into pLNOH2 vector previously digested with both *BsmI* and *BamHI* REs. The recombinant constructs are therefore encoded within *BsmI-BamHI* sites of the resulting recombinant expression vector.

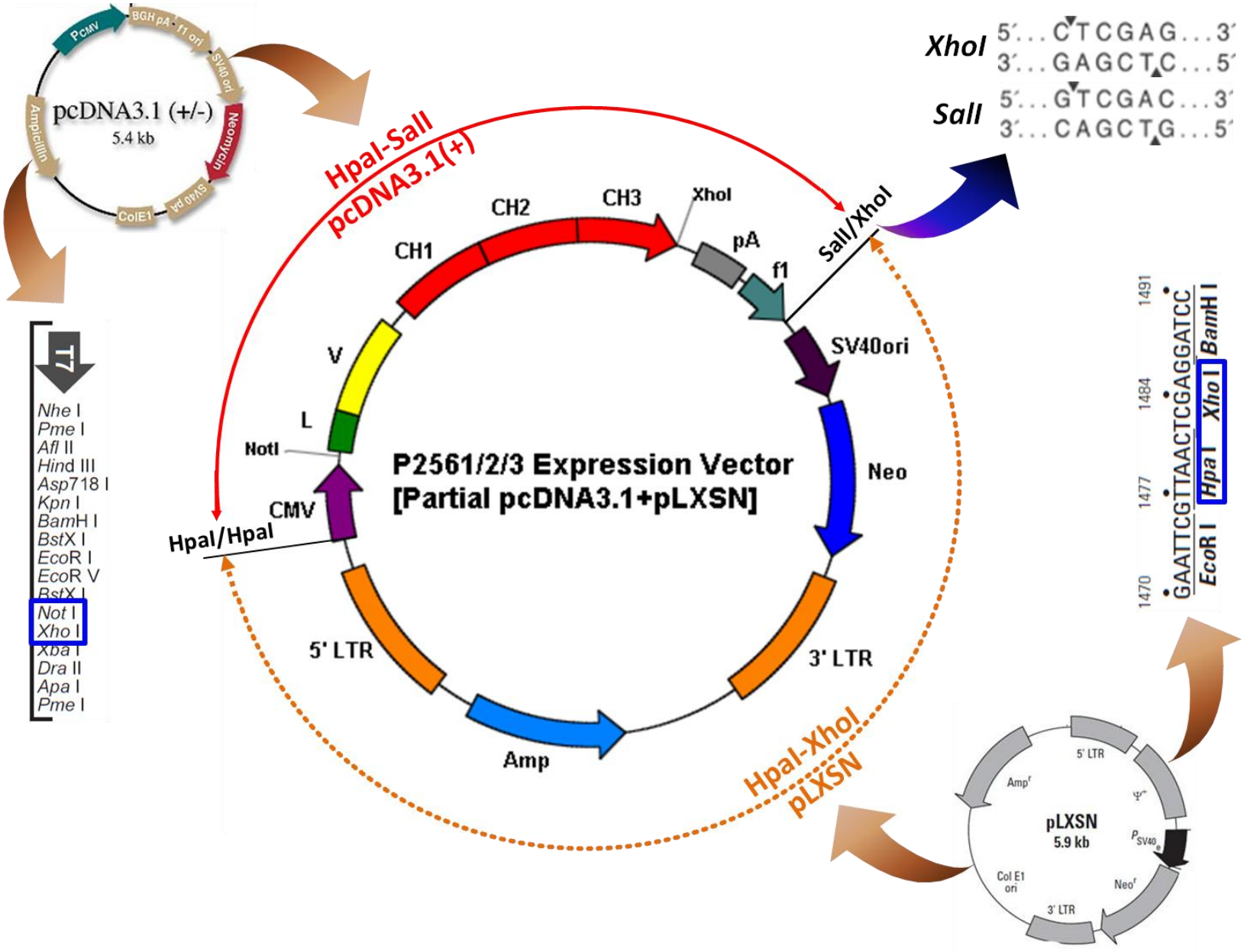
pcDNA3.1 (+/-)
5.4 kb
PCMV
BGH pA
f1 ori
SV40 ori
Neomycin
SV40 pA
ColE1
Ampicillin
T7
Nhe I
Pme I
Afl II
Hind III
Asp718 I
Kpn I
BamH I
BstX I
EcoR I
EcoR V
BstX I
Not I
Xho I
Xba I
Dra II
Apa I
Pme I
HpaI-SalI
pcDNA3.1(+)
XhoI 5′...CTCGAG...3′
3′...GAGCTC...5′
SalI 5′...GTCGAC...3′
3′...CAGCTG...5′
CH1
CH2
CH3
XhoI
pA
f1
SalI/XhoI
V
L
NotI
CMV
HpaI/HpaI
P2561/2/3 Expression Vector
[Partial pcDNA3.1+pLXSN]
SV40ori
Neo
5' LTR
3' LTR
Amp
HpaI-XhoI
pLXSN
1491
1484
1477
1470
GAATTCGTTAACTCGAGGATCC
EcoR I HpaI XhoI BamH I
pLXSN
5.9 kb
5' LTR
Amp
Col E1 ori
Neo
3' LTR

Fig. 2.8. Simplification of the architecture of the expression plasmid vector P2561/2/3, highlighting regions of functional and relevant features (not drawn to scale). The vector contains a unique multiple cloning site for cDNA insertion and a variety of promoters, including strong retroviral promoters, to facilitate expression of inserted cDNA constructs. This double-stranded closed-circular DNA molecule vector was made up by ligating NIP-rhIGHG-containing *HpaI-SalI* restriction fragment (~1.1 kb in size) of recombinant expression pcDNA3.1(+) vector into retroviral vector pLXSN to *HpaI* and *XhoI* restriction sites (~5.9 kb in size, after digestion). RE *HpaI*, which cuts between nucleotide location 163-164 or 1,477-1,478 in pcDNA3.1(+) or pLXSN vector, respectively, is a blunt-end ligation. RE *SalI*, which cuts between nucleotide location 1,272-1,273 in pcDNA3.1(+) vector, and RE *XhoI*, which cuts between nucleotide location 1,484-1,485 in pLXSN vector, have their overhangs matched (ligation would destroy these cut sites). Expression is driven by a cytomegalovirus promoter (CMV)/leader (L) sequence, which are derived from pcDNA3.1(+) vector (L signal peptide allows secretion of protein). In addition to recombinant NIP-rhIGHG constructs, the *HpaI-SalI*-digested restriction fragments that were cut out from the recombinant pcDNA3.1(+) vectors also comprise of the pcDNA3.1(+)-derived polyadenylation signal (pA; recognition sequence for polyadenylation), located downstream of Igγ CH coding sequence to direct proper and efficient processing of mRNA transcript in eukaryotic cells, as well as of f1 ori (f1; plasmid origin of replication),which is for single-stranded DNA replication. Plasmid DNA replication occurs in one direction, as illustrated by the f1 ori arrow. The P2561/2/3 vector maintains from pLXSN retroviral vector SV40 early promoter (SV40ori) for plasmid replication in mammalian cells, the gene cassette for neomycin resistance (Neo), located downstream of and controlled by SV40ori promoter, which allows for G418 antibiotic selection of stable expression by transfected eukaryotic cells, as well

as ampicillin resistance gene (Amp) for propagation and antibiotic selection in bacteria (E. coli). Therefore, only bacteria containing the vector are capable of growing in the presence of ampicillin, and cell clones selected by Neo resistance indicate those cells in which an endogenous gene was disrupted due to the proviral insertion. pLXSN vector also contains, in the 5' viral long terminal repeat (LTR) sequence, a viral promoter and enhancer sequences that direct expression of the genes of interest inserted in its multiple cloning site. Thus, P2561/2/3 vector permits expression of DNA constructs inserted into the multiple cloning site, which is sandwiched between the 5′ and 3′ LTR sequences, under the controls of a variety of promoters (i.e. retroviral LTR, CMV, or SV40ori). The curve arrows on the genes illustrate the direction of transcription. VH gene is oriented so that its direction of transcription is opposite to that of Amp gene. As with expression vector pLNOH2 regarding *BsmI* and *BamHI* sites, *NotI* and *XhoI* sites in P2561/2/3 vector, which are located downstream of CMV promoter and Igγ CH cassette, respectively, are unique; these sites separate CMV promoter from Neo gene sequence and can be used for directional insertion of recombinant constructs of interest as *NotI-XhoI* restriction fragments (none of these constructs has *NotI* or *XhoI* site). *NotI-XhoI* restriction fragments of NIP-rhIGHG inserts are ~1.37 kb-1.42 kb in size, varying dependent on IgH subclasses. P2561/2/3 vector sequence totals ~8.4 kb (~7.0 kb if without insertion of a recombinant construct) in length and all sites indicated are unique (occur only once in within plasmid sequence). pLXSN vector (~5.9 kb in size), through its retroviral 5' LTR and 3' LTR sequences, between which the gene of interest are cloned, facilitates integration of the insert into chromosomes for stable expression and, therefore, making it easy for isolation and providing higher yield than if using expression vectors pLNOH2 or pcDNA3.1(+) alone (both of which have almost the same yield). The orientation and sequence of DNA inserts in recombinant

plasmids were confirmed by RE digestions and DNA sequencing. This map was constructed using the plasmid drawing software Plasm (http://biofreesoftware.com/plasm) and based on information described in Rogers et al., 2006, and on Clontech website (http://www.synthesisgene.com/vector/pLXSN.pdf). Some figure pieces are reproduced from the internet.

caps flasks, and grown at 37°C with 5% CO2 atmosphere.

2.2.5. Generation of expression vectors for NIP-rhIGHG chimeric constructs

To construct NIP-rhIGHG IgH expression vectors, we excised and replaced VH and human IgG3 CH genes in pLNOH2γ3 plasmid with cDNA containing anti-NIP VH of pLNOH2γ3 fused to the entire Chinese rhesus macaque *IGHGs* (IgG CH) as a single fragment. pLNOH2 was sequentially digested with *BsmI* and *BamHI* or *NotI* and *XhoI* RE pair (New England BioLabs, Ipswich, MA) to remove murine VH and human *IGHG3* genes from the parent vector (Fig. 2.7 and 2.9). A verified TOPO clone containing cDNA constructs encoding sequence of recombinant NIP-rhIGHG was similarly excised (i.e. under sequential digestion with the same two REs) to release the constructs. Resultant ~1.5-kb *BsmI-BamHI*-digested gene fragments obtained from TOPO clones were purified and subcloned into pLNOH2 to the unique *BsmI* and *BamHI* RE sites, downstream of CMV promoter and in proper orientation, to create constructs pLNOH2-rhIGHG1, pLNOH2-rhIGHG2, pLNOH2-rhIGHG3, and pLNOH2-rhIGHG4. Only pLNOH2 plasmids with correct DNA sequences, which are the original anti-NIP VH fused with each of the four rhesus macaque IGHG subclasses, were used for transferring of expression vector and mammalian cell transfection.

To improve the stability of expression vectors in transfected cells, the above mentioned P2561/2/3 expression vectors were used. Firstly, the original NIP-rhIGHG constructs were PCR-amplified from verified pCR2.1-TOPO vector clones (that carry the original engineered NIP-rhIgG constructs) using forward IgNotI and reverse IgXhoI primers (Table 2.1). These amplifications added *NotI* and *XhoI* RE sites into the 5’ end and the 3’ end, respectively, of original NIP-rhIGHG cDNA constructs. Next, the modified *NotI-XhoI*-containing NIP-rhIGHG

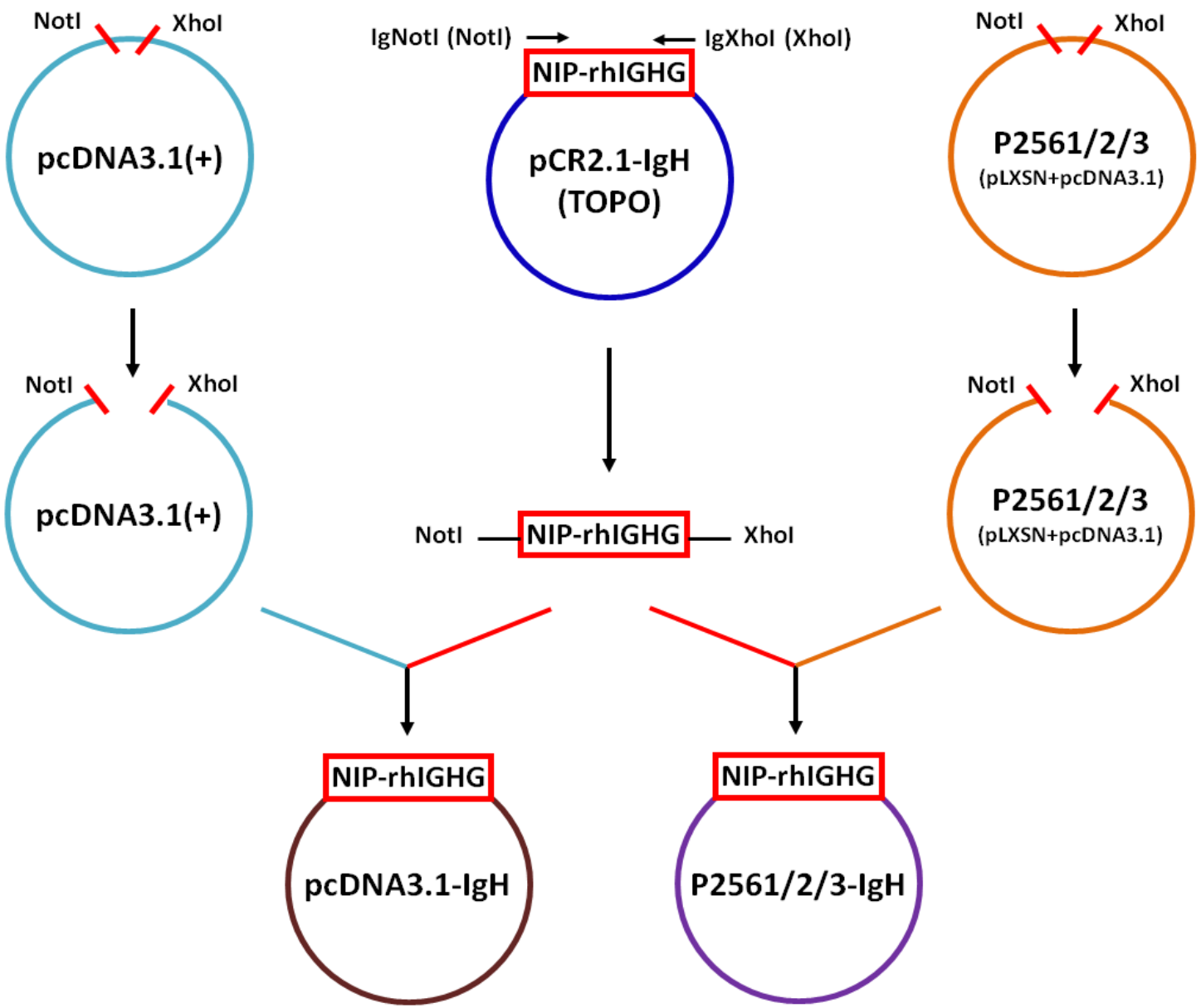
NotI
XhoI
pcDNA3.1(+)
IgNotI (NotI)
IgXhoI (XhoI)
NIP-rhIGHG
pCR2.1-IgH
(TOPO)
NotI
XhoI
P2561/2/3
(pLXSN+pcDNA3.1)
NotI
XhoI
pcDNA3.1(+)
NotI
NIP-rhIGHG
XhoI
NotI
XhoI
P2561/2/3
(pLXSN+pcDNA3.1)
NIP-rhIGHG
pcDNA3.1-IgH
NIP-rhIGHG
P2561/2/3-IgH

Fig. 2.9. Schematic representation of generation of recombinant expression plasmid vectors pcDNA3.1-IgH and P2561/2/3-IgH (not drawn to scale). The NIP-rhIGHG constructs were PCR-amplified from appropriate TOPO vectors using forward primer IgNotI (containing *NotI* restriction site in its 5' end; Table 2.1) and the reverse primer IgXhoI (containing *XhoI* restriction site in its 5' end; Table 2.1), as indicated. Resultant PCR products were then ligated into pcDNA3.1(+) or P2561/2/3 vectors previously digested with both *NotI* and *XhoI* REs. Recombinant constructs are therefore encoded within *NotI-XhoI* sites of resulting recombinant expression vectors.

cDNA constructs were ligated into ampicillin-resistant pCR2.1 TOPO TA cloning vector (Invitrogen, Carlsbad, CA), within *EcoRI* sites, following the procedure as described previously. Then the ~1.5 kb fragments (with confirmed correct sequence) were released from pCR 2.1 TOPO clones (that carry the modified engineered NIP-rhIGHGs) by sequential digestion with *NotI* and *XhoI* REs (New England BioLabs, Ipswich, MA), and cleaned up on a 1% agarose gel. These *NotI*-*XhoI*-containing fragments were subsequently subcloned into expression vectors P2561/2/3 using the unique *NotI* and *XhoI* RE sites, downstream CMV promoter and in proper orientation, to yield plasmid constructs P2561/2/3-rhIGHG1, P2561/2/3-rhIGHG2, P2561/2/3-rhIGHG3, and P2561/2/3-rhIGHG4. Thus, the final IgG gene cassettes contained at their 5' end a *NotI* site (between CMV promoter and Ig leader) and at their 3' end a *XhoI* site (between Ig CH region stop codon and poly(A) signal sequence).

In addition to using P2561/2/3 vectors, the ~1.5-kb *NotI*-*XhoI*-digested fragments were also subcloned – to the unique *NotI* and *XhoI* RE sites – onto pcDNA3.1 expression vector by similar procedures, yielding constructs pcDNA3-rhIGHG1, pcDNA3-rhIGHG2, pcDNA3-rhIGHG3, and pcDNA3-rhIGHG4.

Thus, two subsets of recombinant pCR2.1-TOPO cloning vectors were digested with a pair of REs – *BsmI* and *BamHI* or *NotI* and *XhoI* – as appropriately (Fig. 2.7 and 2.9). Excised restriction cDNA hybrid constructs were accordingly engineered into plasmids pLNOH2, pcDNA3.1, and P2561/2/3 digested with corresponding pair of REs to make final recombinant expression vectors. Insertion and orientation were analyzed by PCR and RE digestion, and subsequently confirmed by DNA sequencing in both forward and reverse directions.

All ligation reactions were performed overnight at 14°C in the presence of T4 DNA ligase (Roche Diagnostics North America, Indianapolis, IN). Resultant NIP-rhIGHG-containing

plasmid DNAs were then transformed into and amplified in Top10 *E. coli* competent cells selected on ampicillin (Invitrogen, Carlsbad, CA) by heat shock, as previously described (except that no X-Gal was included in LB plates). Colonies were first screened for the presence of insertion by PCR directly on raw extracts from clones. Subsequently, miniprep DNAs derived from the PCR-screened positive colonies, which were purified by plasmid mini-preparations (Qiagen Inc., Valencia, CA), were verified for insertion and proper orientation by RE digestion using *BsmI* and *BamHI* REs, and by DNA sequencing. After verification, good clones were expanded and prepared with an EndoFree plasmid maxi kit (Qiagen Inc., Valencia, CA). The maxiprep yields from these expression vectors varied among 1.5-2.5 μg/ml (with the use of an initial culture volume of 5 ml).

2.2.6. Production of transient and stable J558L transfectoma cell lines expressing recombinant NIP-rhIGHG chimeras

To determine whether pLNOH2, pcDNA3.1, and P2561/2/3 vectors that contained cDNA constructs encoding NIP-rhIGHG IgH subclass chimeras and containing CMV promoter, murine Ig leader, and poly-A signal sequences could express complete IgGs, we transfected each of them into J558L cells. Transfection was performed by electroporation using closed-circle DNA plasmids and G418-resistant clones would grow out. Transfectoma cell lines were produced on small-scale expression for specificity analysis purpose. Only plasmids with correct DNA sequences were used for transfection. Before transfection, production of murine IgL λ chain by J558L cells was confirmed by ELISA.

Briefly, after antibiotic-resistant bacterium cells retaining the constructs were selected, NIP-rhIGHG-containing plasmid vectors were purified and prepared in large quantities using

using EndoFree Plasmid Maxi kits (Qiagen Inc., Valencia, CA). The quantity and quality of DNA were assessed by DNA gel electrophoresis and by optical density at 260/280 nm. Twenty micrograms of each supercoiled plasmid expression vector DNAs, including those of pLNOH2, which served as positive controls (known to react with rhesus macaque IgGs), were pulsed into 5 x 10^6 to 1 x 10^7 J558L cells resuspended in 200-300 μl ice-cold PBS (without $Ca2^{++}$ and $Mg2^{++}$) placed in 1 cm x 0.4 cm x 4.5 cm plastic microcuvettes that had been equipped with aluminum electrodes. Two to three pulses at 1 second intervals with 300 V were applied using the gene pulser Electroporator II (Invitrogen, Carlsbad, CA), setting at 1000 μF (at a capacitance setting of 25 μF) and infinite resistance (giving a ~30-40 msec pulse). Following 10 min of incubation on ice, the cells were suspended in pre-warmed 10-20 ml of complete IMDM [i.e. Iscove's modified Dulbecco's medium containing 2 mM L-glutamine, 100 IU/ml penicillin G sodium, 100 μg/ml streptomycin sulfate, 5 mM HEPES (Sigma–Aldrich Co., St. Louis, MO), and 5-10% fetal bovine serum (FBS)]. The cells were allowed to recover by incubation for 24-48 hrs at 37^0C in a 5% CO2 atmosphere.

At 72 h post-transfection, stable transfectants were selected by resistance under the final concentration of 0.8-1.0 mg/ml (400-2,000 μg/ml) geneticin (antibiotic G418; Invitrogen, Carlsbad, CA) in complete IMDM medium and were allowed to grow to saturation for four weeks or until a concentration of 3-4 x 10^6 cells/ml was achieved. During incubation, cell supernatants were harvested and replaced at 5, 10, 14, 21, and 28 days post-transfection. Supernatants were also obtained from the cells that were allowed to grow to saturation for up to six weeks. Cell supernatants were centrifuged (20,000 g for 30 min) to remove cellular debris before using in subsequent assays. Because usually production of Abs gradually decline due to transient nature of transfection, cell cultures were terminated after six weeks.

2.2.7. Detection of Igλ and complete (assembled) recombinant NIP-rhIGHG chimeric antibodies

Ab production and binding activity to specific antigen of anti-NIP murine Igλ chain and complete recombinant IgG (NIP-rhIgGs) in transfected J558L cell supernatants were determined by capture enzyme linked immunosorbent assay (ELISA). Secreted IgGs were detected by either immobilized affinity purified goat anti-monkey IgG(H+L)-specific Abs (KPL, Baltimore, MD; Cat. #071-11-021; for detection of IgH γ), or an immobilized goat anti-mouse Ig λ Abs (Southern Biotech, Birmingham, AL; Cat. #1060-01; IgL-specific Ab, for detection of IgL λ), or immobilized NIP-BSA (KPL, Baltimore, MD; NIP-specific IgGs, containing both anti-NIP VL and VH regions; for detection of whole IgG Ab). For goat anti-mouse Igλ ELISAs, bound Igλ was detected by HRP-conjugated secondary Ab goat anti-mouse λ (Invitrogen, Carlsbad, CA). For anti-IgH γ-specific or anti-whole chimeric IgG Abs, bound Abs were detected by horse radish peroxidase (HRP)-conjugated anti-monkey IgGs (KPL, Baltimore, MD; Cat. #074-11-021). All Ab reagents were diluted in blocking buffer.

Briefly, 96-well high-binding polyvinyl microtiter ELISA plates were coated with 50 μl goat anti-mouse Ig λ Ab (Invitrogen, Carlsbad, CA) at 4 or 8 μg/ml or with NIP-BSA (KPL, Baltimore, MD) at 8 or 15 μg/ml in coating buffer (KPL, Baltimore, MD). Following incubation at 4°C overnight, plates were washed with PBS containing 0.05% Tween-20 and unoccupied wells were blocked with 5% FCS (or BSA) diluted in PBS at 37°C for 30 min. After washing the plates, undiluted cell culture supernatants of G418 resistant transfectants and the appropriate controls [positive control: purified murine myeloma IgG3 λ (Sigma–Aldrich Co., St. Louis, MO; Cat. # M9019; negative controls: culture media plus 5% FCS] were added to pre-coated plates (100 μl/well) for triplicate wells. For Igλ assays, culture supernatant from untransfected J558L

cells (test samples), purified mouse myeloma IgG1 with a λ-chain (Sigma–Aldrich Co., St. Louis, MO) (positive control), or 5% FCS in either culture media or PBS [or 0.05% (vol/vol) of PBS-Tween 20] (negative control), was added (100 μl/well), and incubated at 37°C for 1 h. For IgH/IgG assays, supernatants from transfected J558L cells (test samples), from unstranfected cells (negative controls), or from cells transfected with pLNOH2 (positive controls), were added (100 μl/well), and incubated overnight at 4°C. Following washing four times with PBS containing 0.05% Tween 20 to remove unbound Ab, the bound Abs were detected by adding (100 μl/well) 1/1,000-1/10,000 diluted, appropriate HRP-labeled secondary Abs [HRP-conjugated goat anti-mouse Igλ (Invitrogen, Carlsbad, CA) for detection of IgL λ and IgG, and HRP-conjugated anti-monkey IgH γ (KPL, Baltimore, MD) for detection of IgH and IgG]. Plates were incubated for 1 h at 37°C, washed four times, and the bound peroxidase was revealed by adding OPD and ABTS/H_2O_2 (Sigma–Aldrich Co., St. Louis, MO) for color development, followed by addition of stop solution. Absorbance was measured at 405 or 492 nm after 15-30 min using an automated Benchmark microplate reader (Bio-Rad, Hercules, CA). Tests were done in triplicate wells and triplicates were averaged.

2.3. Results

2.3.1. Four NIP-rhIGHG cDNA hybrid constructs were successfully generated by SOE-PCRs and were properly incorporated into pCR2.1-TOPO cloning vector

cDNA segments encoding anti-NIP murine VH and rhesus macaque individual CH domains CH1, CH2, and CH3 (the hinge is embedded in CH1 and CH2 domains, as previously described) of each of four rhesus macaque IgG subclasses were successfully amplified by PCRs from the appropriate plasmid vectors (data not shown). Complete IgH cDNA hybrid encoding

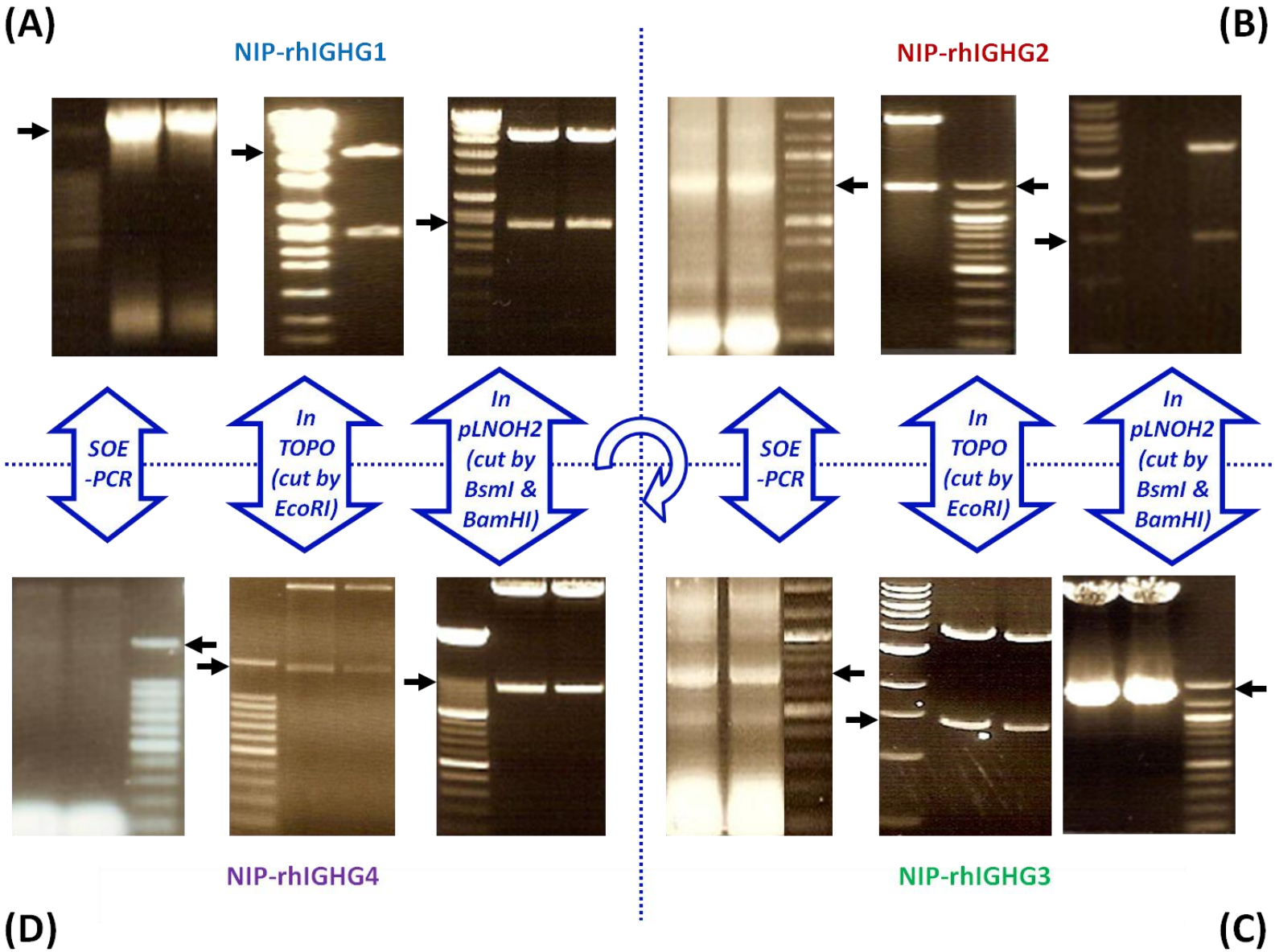
(A)
NIP-rhIGHG1
(B)
NIP-rhIGHG2
SOE -PCR
In TOPO (cut by EcoRI)
In pLNOH2 (cut by BsmI & BamHI)
SOE -PCR
In TOPO (cut by EcoRI)
In pLNOH2 (cut by BsmI & BamHI)
NIP-rhIGHG4
NIP-rhIGHG3
(D)
(C)

Fig. 2.10. Gel electrophoresis separation of DNA products resulting from SOE-PCR annealing and amplification or digestion of clones of recombinant gene constructs of NIP-rhIGHG1 (A), NIP-rhIGHG2 (B), NIP-rhIGHG3 (C), and NIP-rhIGHG4 (D) that were ligated into cloning and expression vectors. RE digestions were used to confirm that the recombinant constructs had each been inserted into the correct region of vectors and in the correct orientation (which were subsequently confirmed by DNA sequencing). SOE-PCR-generated products or fragments obtained from RE-digested DNA plasmids were separated on 1-2% agarose gels, adjacent to DNA molecular weight standards. The gels were stained with ethidium bromide and were visualized and photographed under UV light. Each quadrant in this figure contains a representative gel for, from left to right, annealing and amplification of subclass recombinant gene construct using the two flanking primers at the 5' end of VH and the 3' end of CH3 by a single SOE-PCR, RE with single enzyme *EcoRI* of pCR2.1 TOPO TA transformed clones, and restriction digestion with double enzymes *BsmI* and *BamHI* of pLNOH2 transformed clones. Arrows indicate where DNA fragments are expected to be shown (correct-sized bands). In each gel, both lanes shown correspond to the same DNA product, except for the middle gels in (A) and (B), which have only one lane shown. For lanes with two bands, the above released band corresponds to the digested vector and the below released band corresponds to the inserted DNA fragment. The DNA molecular weight standards are represented by lanes with multiple bands. As being shown, in each quadrant, the size (in kilobase-pairs, kb) of DNA fragments after RE digestions are the same as those of the SOE-PCR products, which are 1.39 (A), 1.37 (B), 1.42 (C), and 1.37 (D). The size (kb) of plasmid vectors after digestions are 3.9 (pCR2.1 TOPO cloning vector) and 7.2 (pLNOH2 expression vector). Only representative clones containing

bands of expected sizes are shown. Lanes showing no bands correspond to undetectable DNA products.

each IgG subclass was created by several sequential SOE-PCRs. Agarose gel analysis of these SOE-PCR products (Fig. 2.10) showed DNA bands of approximately 1.39, 1.37, 1.42, and 1.37 kb, representing the four corresponding recombinant IgH hybrids, IgHγ1, IgHγ2, IgHγ3, and IgHγ4, respectively. When performed with the annealing temperature of 56^0C or 58^0C and a magnesium concentration of 2.5 mM, SOE-PCRs using the two outermost flanking primers were generally found to yield minimal non-specific (due to sequence differences) products while producing desired amplification fragments.

For cloning and sequencing, resultant hybrid cDNA genes were subsequently ligated into pCR2.1-TOPO TA cloning vector. These ligations resulted in two subsets of recombinant cloning vectors: one containing cDNAs carrying *BsmI-BamHI* restriction sites and the another carrying *NotI-XhoI* restriction sites. Insertion and orientation were checked by PCR and RE digestion. Digestion of resultant recombinant cloning vectors with *EcoRI* (Fig. 2.10) or *BsmI* and *BamHI* pair (data not shown) for the *BsmI-BamHI* subset, as well as with *EcoRI* or *NotI* and *XhoI* pair (Fig. 2.11) for the *NotI-XhoI* subset, yielded bands of similar sizes as those of SOE-PCR products of corresponding cDNA hybrids. These results verified the correct size and proper orientation of the hybrids incorporated in pCR2.1 TOPO TA clones.

Correct sequence and orientation of the hybrids were also confirmed by DNA sequencing in both forward and reverse directions across the inserted points. Alignment of deduced amino acid sequences of IgH γ CH1, CH2, and CH3 domains belonging to four IgG isotypes (IgG1, IgG2, IgG3, and IgG4) gene fragments from human (*Homsap*) and rhesus macaque (*Macmul*) is shown in Fig. 2.12. Each rhesus macaque CH domains contains a similar number of amino acids as that found in human counterparts, which is 98, 109-110, and 107, in CH1, CH2, and CH3 domains, respectively. Majority of differences were located in the hinge region for all compared

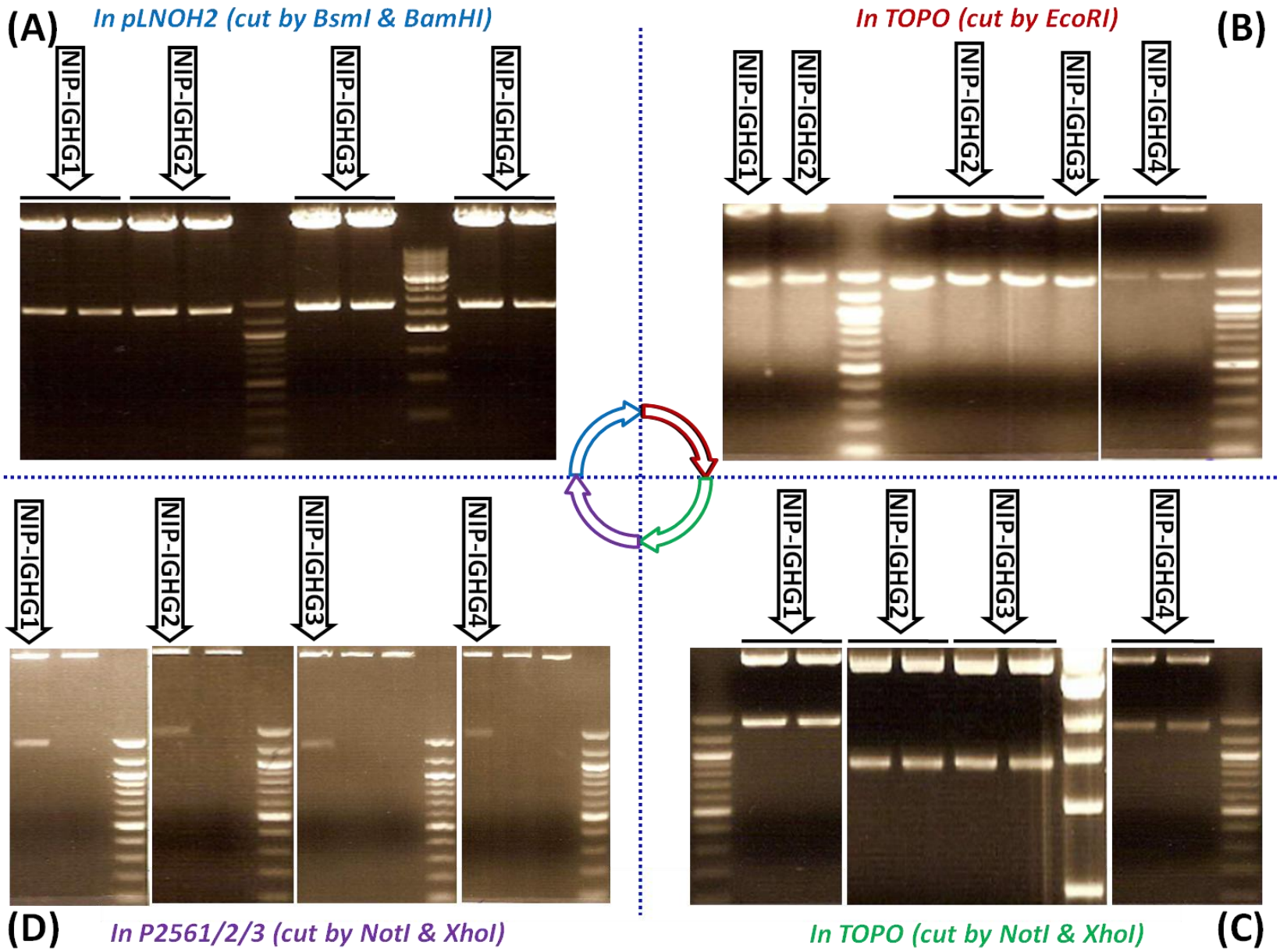
(A)
In pLNOH2 (cut by BsmI & BamHI)
NIP-IGHG1
NIP-IGHG2
NIP-IGHG3
NIP-IGHG4
(B)
In TOPO (cut by EcoRI)
NIP-IGHG1
NIP-IGHG2
NIP-IGHG2
NIP-IGHG3
NIP-IGHG4
NIP-IGHG1
NIP-IGHG2
NIP-IGHG3
NIP-IGHG4
(D)
In P2561/2/3 (cut by NotI & XhoI)
NIP-IGHG1
NIP-IGHG2
NIP-IGHG3
NIP-IGHG4
In TOPO (cut by NotI & XhoI)
(C)

Fig. 2.11. Gel electrophoresis separation of DNA fragments resulting from digestions of clones of recombinant gene constructs of NIP-rhIGHG1, NIP-rhIGHG2, NIP-rhIGHG3, and NIP-rhIGHG4 that were ligated into cloning and expression vectors. RE digestions were used to confirm that recombinant gene constructs had each been inserted into the correct region of vectors and in the correct orientation (which were subsequently confirmed by sequencing). Fragments obtained from RE-digested DNA plasmids were separated on 1-2% agarose gels, adjacent to DNA molecular weight standards. The gels were stained with ethidium bromide and were visualized and photographed under UV light. Shown in this figure are a representative gel for restriction digestion with double enzymes *BsmI* and *BamHI* of pLNOH2 transformed clones (A), with single enzyme *EcoRI* of pCR2.1 TOPO TA transformed clones (B), with double enzymes *NotI* and *XhoI* of pCR2.1 TOPO TA transformed clones (C), and with double enzymes *NotI* and *XhoI* of P2561/2/3 transformed clones (D). As being shown, each lane displays two bands, of which the above released band corresponds to the digested vector and the below released band corresponds to inserted DNA fragment. Number of lanes corresponding to each construct varies, as indicated by the horizontal lines. The vertical arrows with short notations show lanes corresponding to the indicated constructs. The DNA molecular weight standards are represented by lanes with multiple bands. In each quadrant, the size (in kilobase-pairs, kb) of the DNA fragments after RE digestions are 1.39, 1.37, 1.42, and 1.37 for NIP-rhIGHG1, NIP-rhIGHG2, NIP-rhIGHG3, and NIP-rhIGHG4 construct, respectively. The size (kb) of the plasmid vectors after digestions are 3.9 (pCR2.1-TOPO), 7.2 (pLNOH2), and 7.0 (P2561/2/3). Only representative clones containing bands of the expected sizes are shown. Lanes showing only one band (with size similar to that of the relevant vector) correspond to clones without successful DNA ligation.

sequences (Table. 2.2). Two-dimensional structure and secondary structure according to IMGT were also displayed (Fig. 2.13). As discussed previously, these IMGT Collier de Perles graphical two-dimensional representations provide useful information for relating structure to potential function (Bertrand et al., 2004). The sequence of anti-NIP V regions of the resultant rhesus macaque IgHs was identical to each other and to the original sequence (data not shown).

Taken together, these data indicate that all four chimeric NIP-rhIGHG cDNA gene constructs were accurately and successfully created by SOE-PCRs and were properly incorporated into pCR2.1 TOPO TA cloning vectors.

2.3.2. Four NIP-rhIGHG cDNA hybrid constructs were successfully engineered into pLNOH2, pcDNA3.1(+), and P2561/2/3 expression vectors

As shown in Fig. 2.11, pLNOH2 plasmids digested by *BsmI* and *BamHI* gave rise to individual bands of approximately 1.39, 1.37, 1.42, and 1.37 kb, which were the same size as that of corresponding SOE-PCR products. Analysis of the restriction digests with *NotI* and *XhoI* (Fig. 2.11) confirmed that the cDNA hybrids were successfully engineered into pLNOH2. Similar restriction digests with *BsmI* and *BamHI* pair or with *NotI* and *XhoI* RE pair indicated that the hybrids were recombined into P2561/2/3 (Fig. 2.11) and pcDNA3.1 (data not shown) vectors. The correct insertion and proper orientation were also confirmed by sequencing cDNA hybrids (data not shown). DNA sequencing data of NIP-rhIGHG hybrid genes were consistent with DNA sequences of VH (data not shown) and rh*IGHG*s genes listed in Genbank (Fig. 2.12).

Taken together, these data demonstrate that all four chimeric NIP-rhIGHG cDNA gene constructs were accurately and successfully engineered into pLNOH2, pcDNA3.1, and P2561/2/3 expression vectors.

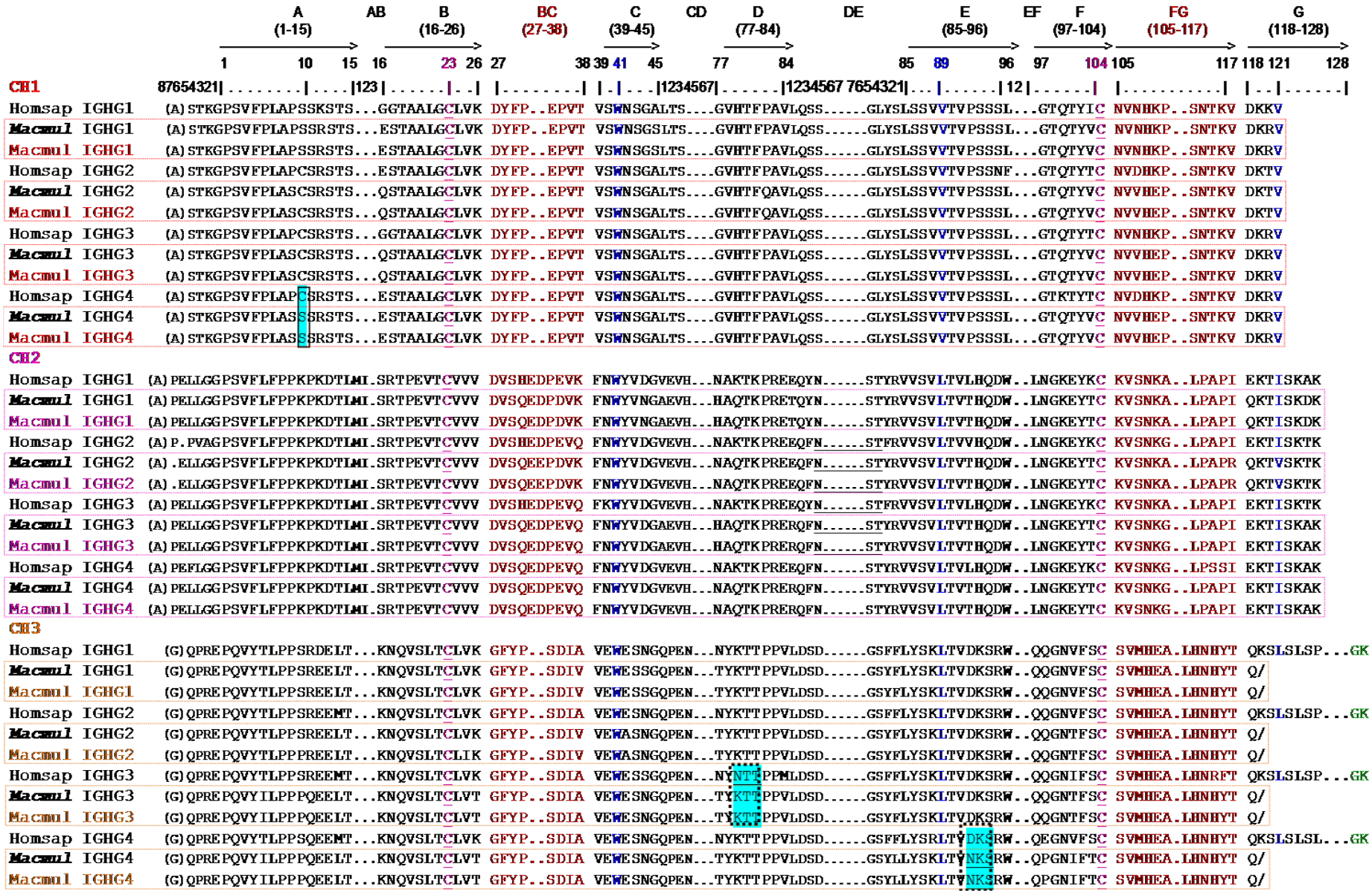
A (1-15)
AB
B (16-26)
BC (27-38)
C (39-45)
CD
D (77-84)
DE
E (85-96)
EF
F (97-104)
FG (105-117)
G (118-128)
CH1
CH2
CH3
Homsap IGHG1
Macmul IGHG1
Macmul IGHG1
Homsap IGHG2
Macmul IGHG2
Macmul IGHG2
Homsap IGHG3
Macmul IGHG3
Macmul IGHG3
Homsap IGHG4
Macmul IGHG4
Macmul IGHG4

Fig. 2.12. Alignment of deduced amino acid sequences of IgH CH1, CH2, and CH3 domains of four IgG isotypes (IgG1, IgG2, IgG3, and IgG4) from human (*Homsap*) and rhesus macaques (*Macmul*). The top upper line illustrates the domain beta strands, as indicated by the letters and numbering positions, with a horizontal arrow; the double letters represent the turns (AB, DE, and EF) and the loops (BC and FG) between the sandwich fold beta strands, or the transversal strand (CD) (Lefranc et al., 2005). The second and third upper lines indicate the C-DOMAIN IMGT unique numbering. Conserved Cys residues (i.e. positions 23 and 104) are colored in magenta; conserved Trp (position 41) and hydrophobic residues (positions 89 and 121) are illustrated in blue. Residues of the beta strand loops (BC and FG) are shown in dark red. Two sequences for each individual domain of rhesus macaques were included for each IgH domain and are bordered in single-line enlarged boxes, as indicated. In each box, the above sequence (black "*Macmul*" text) indicates the published sequences and the below sequence (colorful "*Macmul*" text) indicates the sequences generated in the present study. The GenBank access codes for the published sequences included are AAQ57550.1 (IGHG1), AAQ57562.1 (IGHG2), AAQ57556.1 (IGHG3), and AAQ57568.1 (IGHG4) (Scinicariello et al., 2004). Between parentheses is the first amino acid that results from the splicing of each preceding exon. Underlined Cs indicate Cys residues that have the potential to form intra-chain disulfide bonds. Potential N-linked glycosylation sites (N-x-S/T; x denotes any amino acid) are underlined. Dot-line small-sized boxes represent residual differences between rhesus macaques and humans with regard to amino acids that are known to be functionally important, including those of potential N-linked glycosylation sites (n=2), or with regard to Cys (which is known to have the potential to form intra-chain disulfide bonds) (n=1). The last nine amino acids in the non-human primate species are not present in the figure, and slashes indicate the positions where our sequences are ended.

Dots illustrate the IMGT gaps (missing amino acids, according to the IMGT unique numbering) inserted to maximize alignment. This display is according to the IMGT unique numbering for C-DOMAIN and C-LIKE DOMAIN and is based on the IMGT protein display (Lefranc et al., 2005).

Table 2.2. Deduced amino acid sequences of the hinge of IgH CH1, CH2, and CH3 domains of four IgG isotypes (IgG1, IgG2, IgG3, and IgG4) from human (*Homsap*) and rhesus macaque (*Macmul*)[a].

	IGHG1	IGHG2	IGHG3	IGHG4
Homsap	(E)PKSCDKTHT*CPPC*P(A)PELLGGP[e]	(E)RK*CCVECPPC*P(A)PPVAGP	[H1] (E)LKTPLGDTTHT*CPRCP(*A)PELLGGP [H2] *(E)PSKCDTPPPCPRCP* [H3] *(E)PSKCDTPPPCPRCP* [H4] *(E)PSKCDTPPPCPRCP*	(E)SKYGPP*CPSC*P(A)PEFLGGP
Macmul	(E)IKTCGGGSKPPT*CPPC*P(A)PELLGGP	(G)LP*CRSTCPPC*P(A)ELLGGP	(E)FTPPCGDTTPP*CPPCP(*A)PELLGGP	(E)FTPP*CPPC*P(A)PELLGGP
Macmul	(E)IKTCGGGSKPPT*CPPC*P(A)PELLGGP	(G)LP*CRSTCPPC*P(A)ELLGGP	(E)FTPPCGDTTPP*CPPCP(*A)PELLGGP	(E)FTPP*CPPC*P(A)PELLGGP

[a]Two sequences for each hinge of rhesus macaques were included for each IgH isotype: the above sequence (black "*Macmul*" text) indicates the published sequences (Scinicariello et al., 2004) and the below sequence (colorful "*Macmul*" text) indicates the sequences generated in the present study. The hinge is composed of three distinct regions: the upper hinge (the fragment in front of the italic, underlined text), the core hinge (the italic, underlined text fragment), followed by the lower hinge/CH2 terminus [although the "lower hinge" is encoded by the C-terminus of the CH2 exon, it is considered to be part of the hinge due to the intermolecular interactions (Burton and Woof, 1992)]. Human IgG3 hinge has four sequence repetitions, with three times the [(E)PSKCDTPPPCPRCP] sequence is repeated. Between parentheses is the first amino acid that results from the splicing of each preceding exon. Underlined C, Cys involved in the formation of intrachain disulfide bridges. The GenBank access codes for the published sequences included are AAQ57550.1 (IGHG1), AAQ57562.1 (IGHG2), AAQ57556.1 (IGHG3), and AAQ57568.1 (IGHG4) (Scinicariello et al., 2004).

2.3.3. Four chimeric NIP-rhIGHG IgH chains with NIP-specificity of the original murine VH were successfully expressed by J558L cells

ELISA plates were coated with purified anti-monkey IgG, which recognizes different Ab epitopes of the whole IgG(H+L) or IgH. Therefore, affinity purified anti-monkey IgG(H+L) recognized recombinant IgH or IgG subclasses, which were bound to and were detectable by HRP-conjugated anti-monkey IgG [due to the bivalent nature of IgGs (two IgH chains in a single IgG)]. As shown in Fig. 2.16, the average OD reading at 405 nm in supernatants collected from cells transfected with chimeric IgH fusions was much higher than that of negative controls using the whole IgG- or IgH-specific conjugate, indicating that chimeric IgGs are bound by anti-monkey IgG Abs. These OD values were similar to or in several cases even higher than those of positive controls (Fig. 2.16). We found no expressed IgH nor IgG in IMDM medium transfectoma supernatants, which served as negative controls as well. Supernatants of pLNOH2 (served as a positive control) reacted with immobilized purified anti-monkey IgG, while the medium control (IMDM) or supernatant of untransfected J558L cells was non-reactive with the purified Ab (Fig. 2.16). These results confirm the chimeric IgH identity through its anti-monkey IgH-specific reactivity upon transfection and selection in J558L cells.

2.3.4. Four NIP-rhIGHG intact IgG subclass Abs that retained binding specificity of the original V regions were successfully produced by J558L cells

To verify that secreted recombinant rhesus macaque IgH chains were assembled with NIP-specific murine IgL λ chains, we carried out another set of sandwich ELISAs where NIP-BSA was immobilized on plates and bound IgGs were detected by HRP-conjugated anti-monkey IgG Abs. Before transfection, production of murine IgL λ from J558L cells was confirmed by

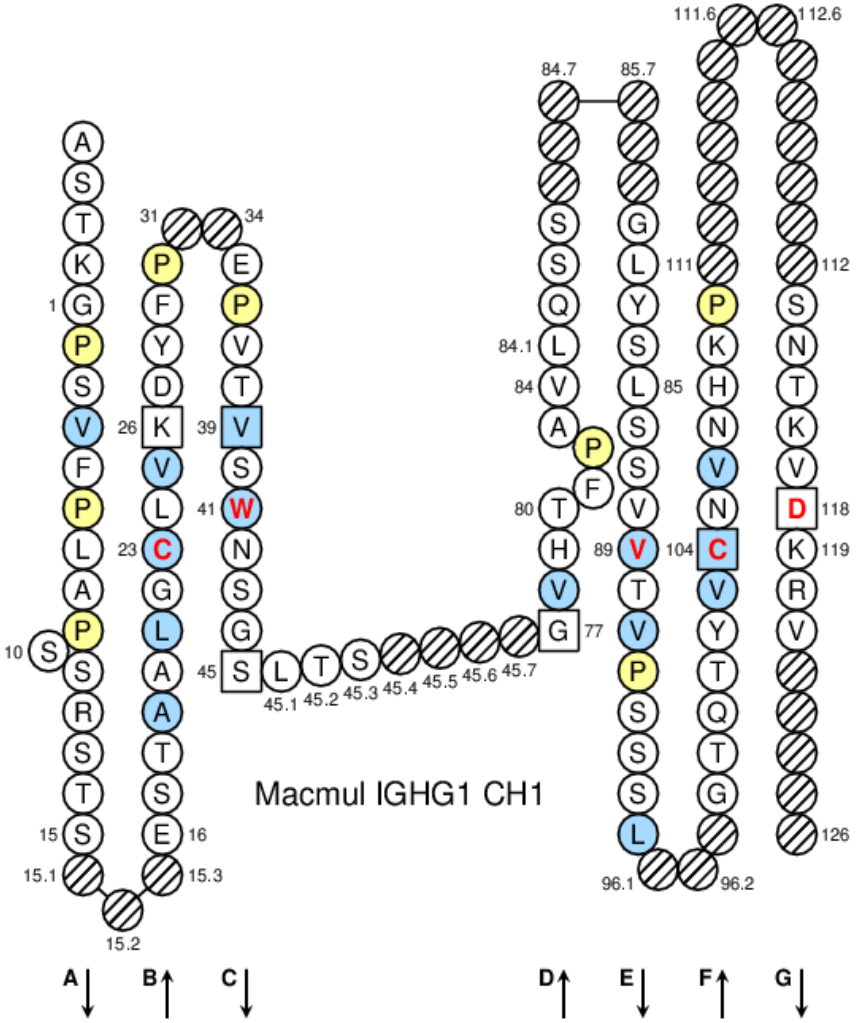
Macmul IGHG1 CH1
A
B
C
D
E
F
G

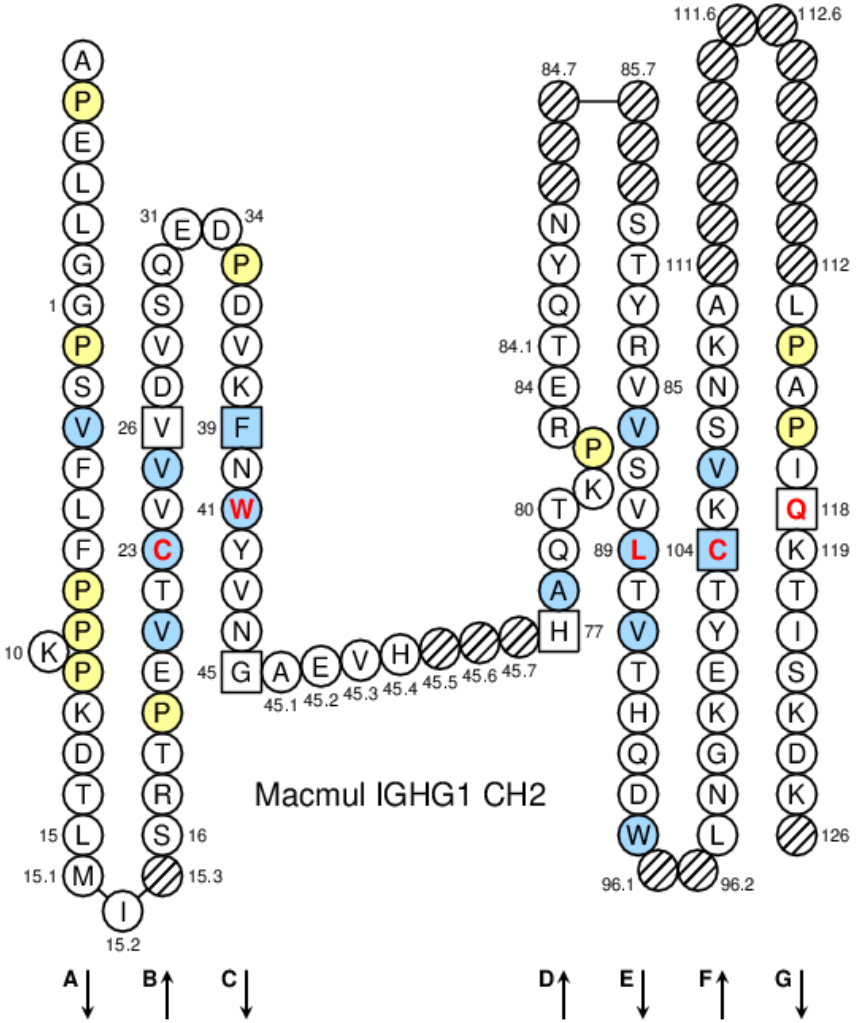
Macmul IGHG1 CH2
A
B
C
D
E
F
G

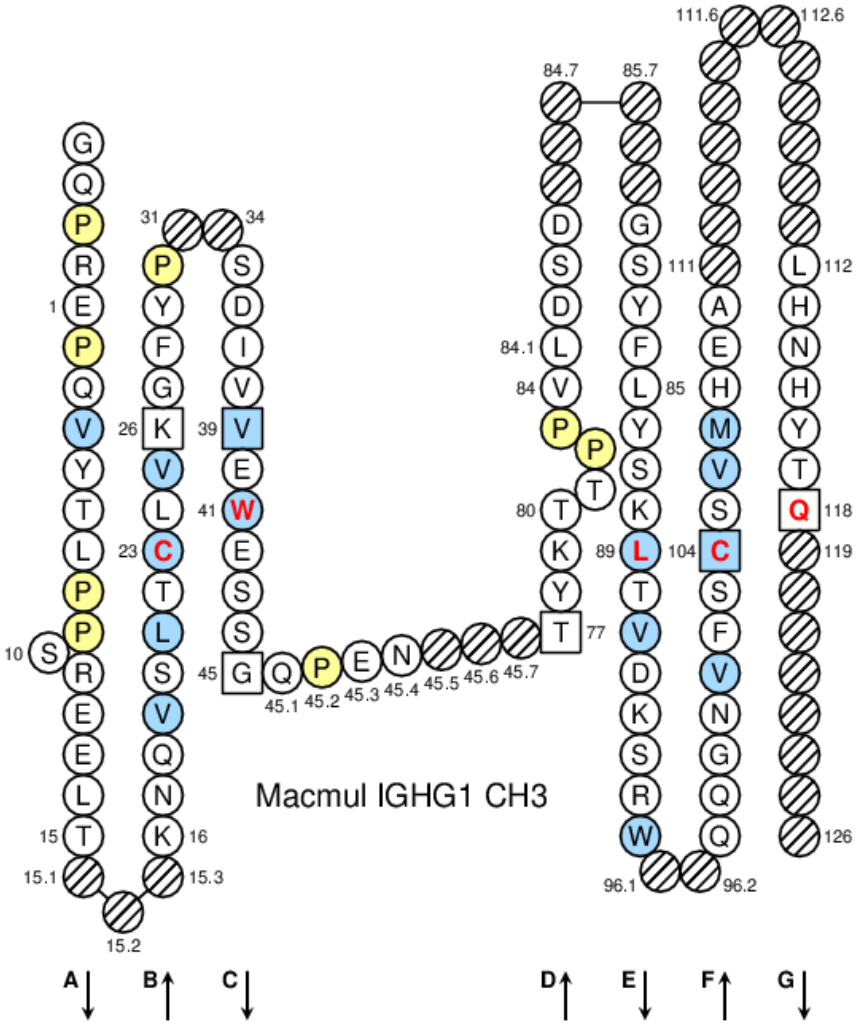
Macmul IGHG1 CH3
A
B
C
D
E
F
G

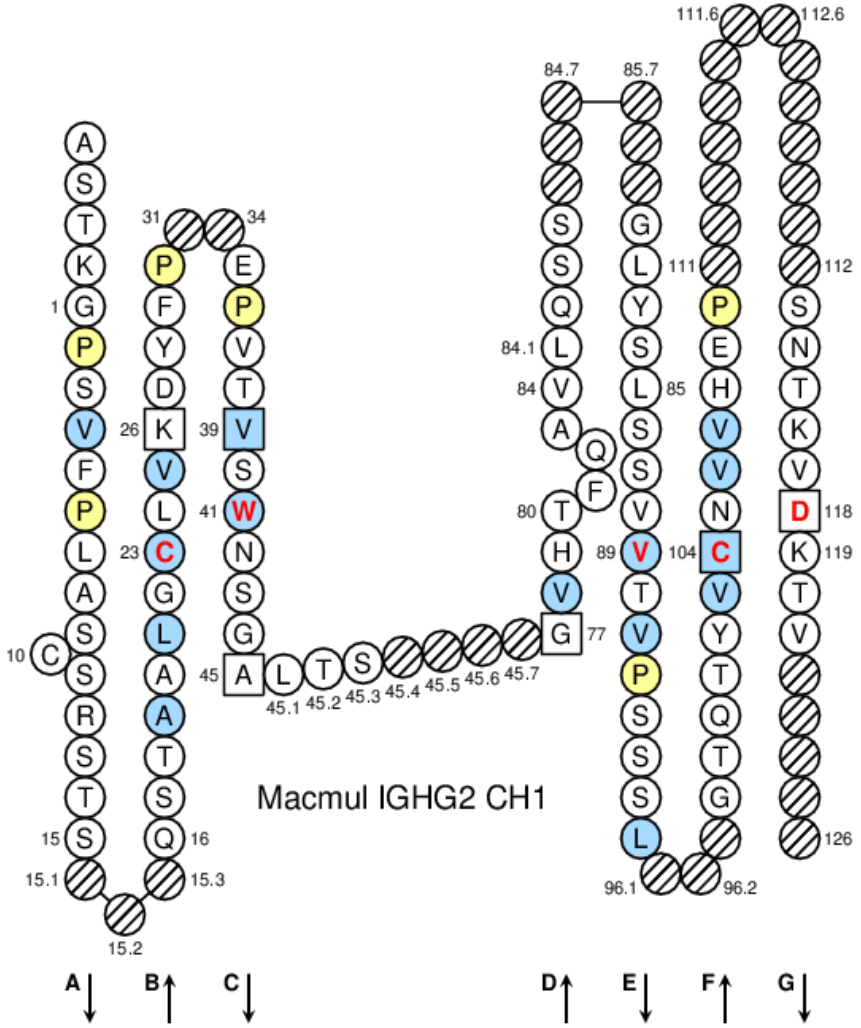
Macmul IGHG2 CH1
A
B
C
D
E
F
G

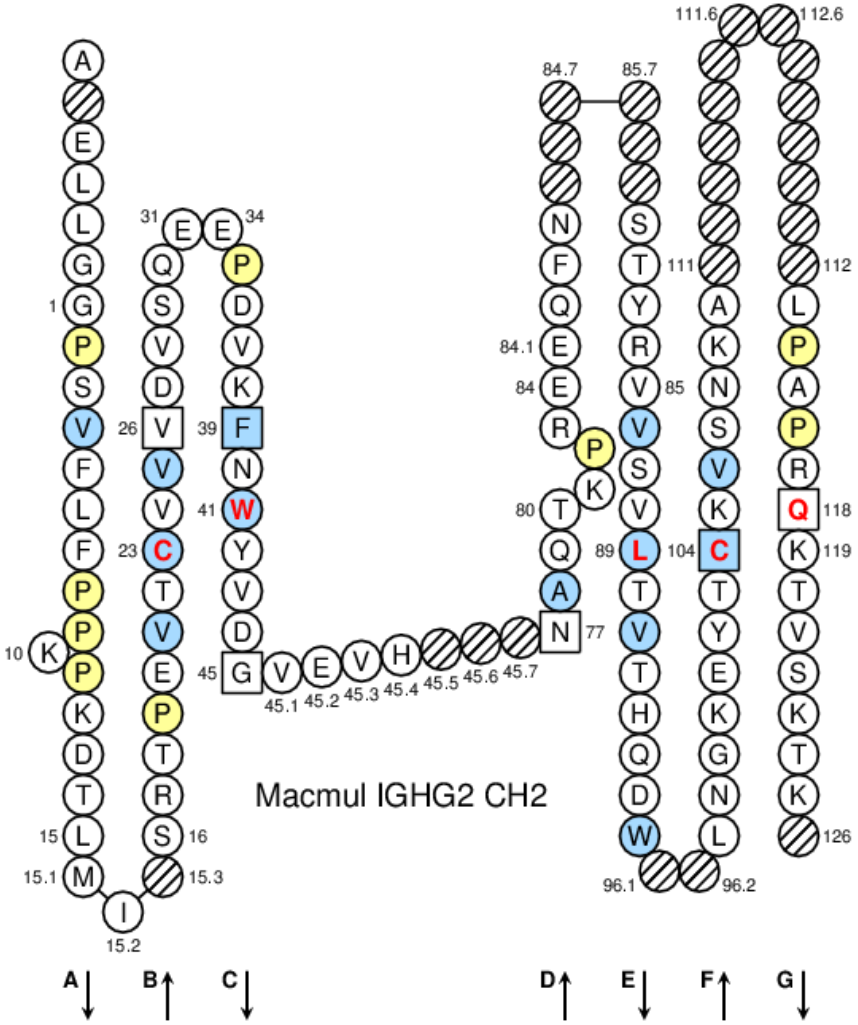
Macmul IGHG2 CH2
A
B
C
D
E
F
G

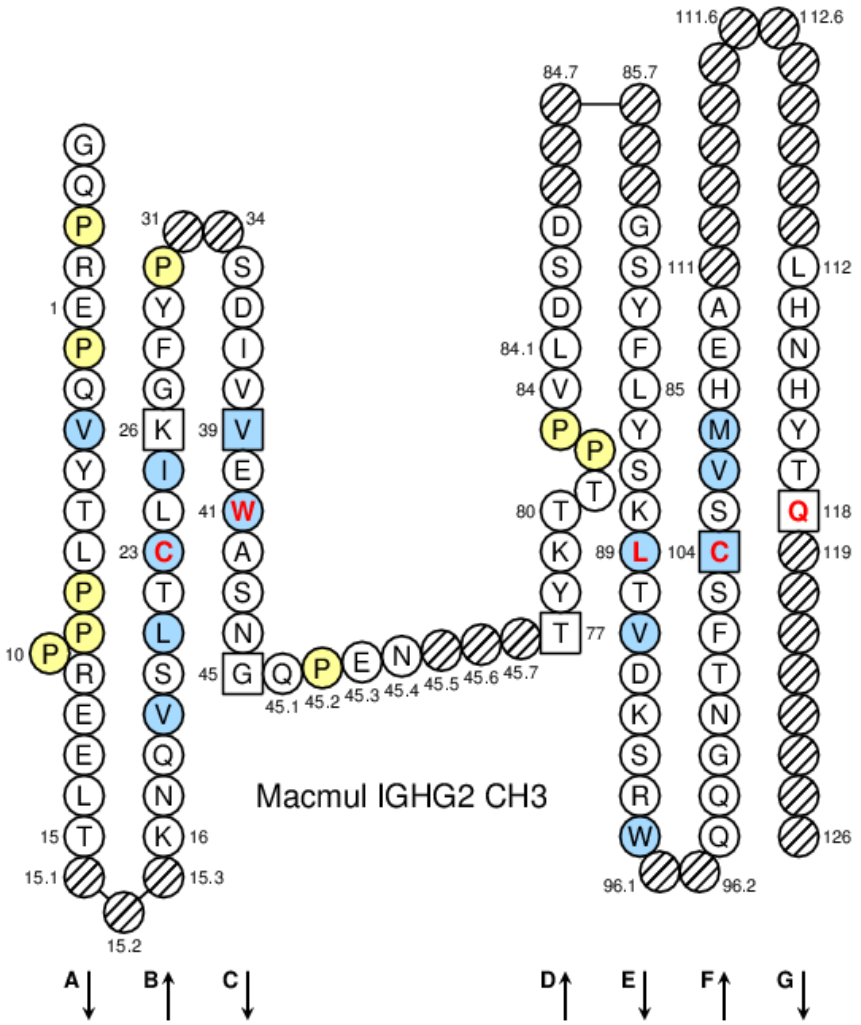
Macmul IGHG2 CH3
A
B
C
D
E
F
G

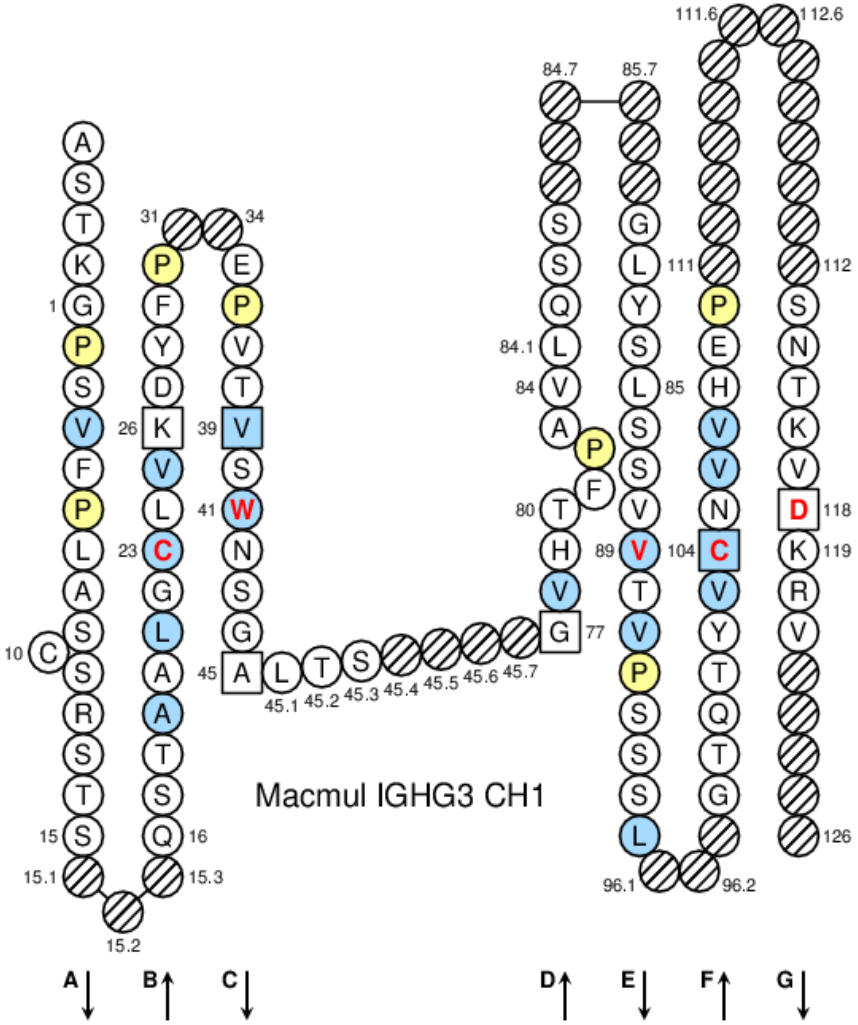
Macmul IGHG3 CH1
A
B
C
D
E
F
G

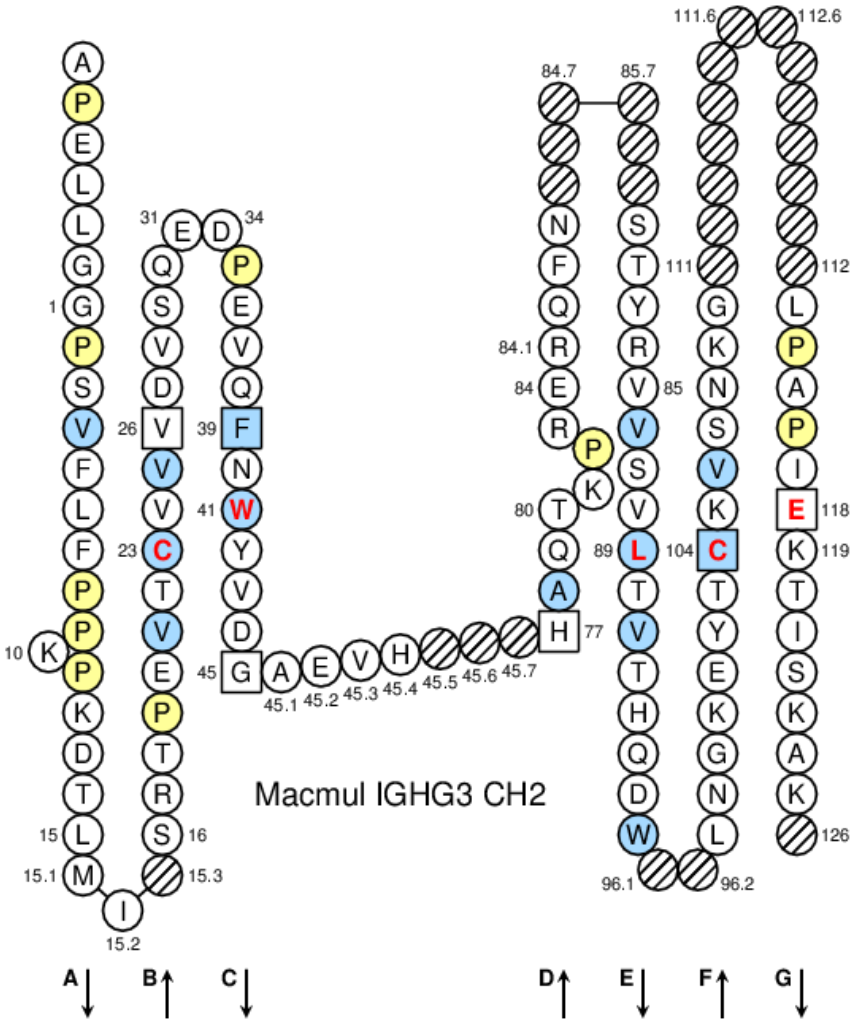
Macmul IGHG3 CH2
A
B
C
D
E
F
G

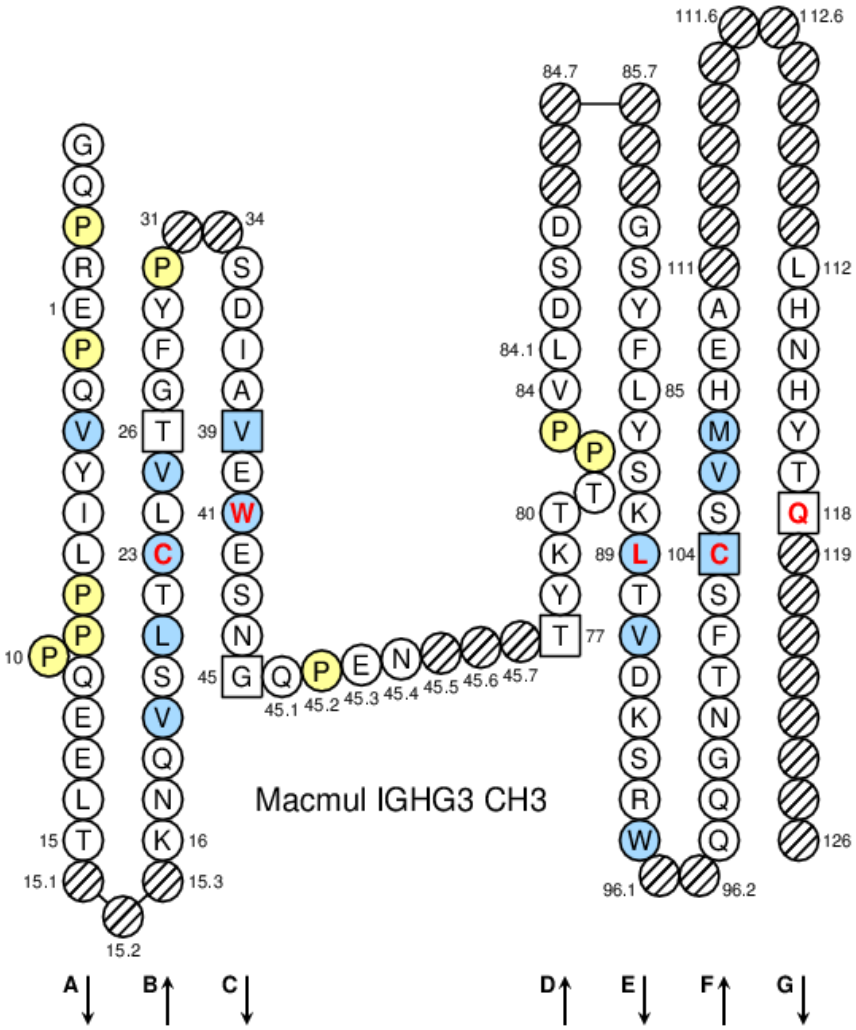
Macmul IGHG3 CH3
A
B
C
D
E
F
G

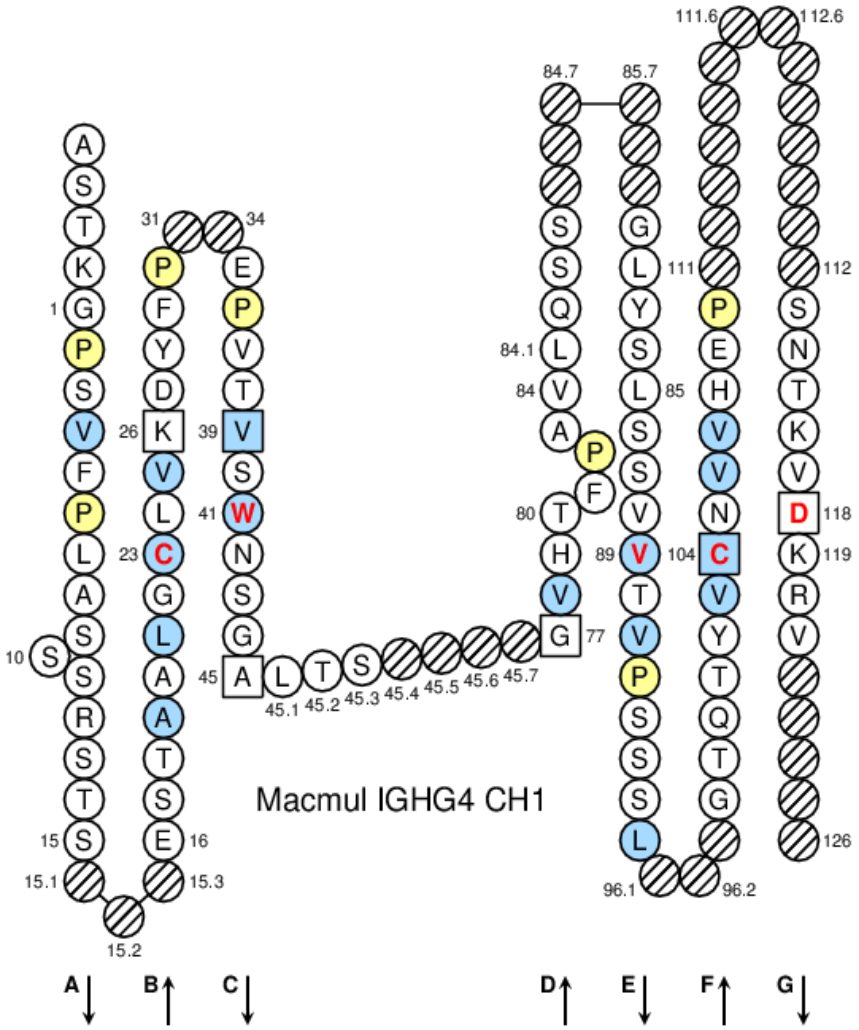
Macmul IGHG4 CH1
A
B
C
D
E
F
G

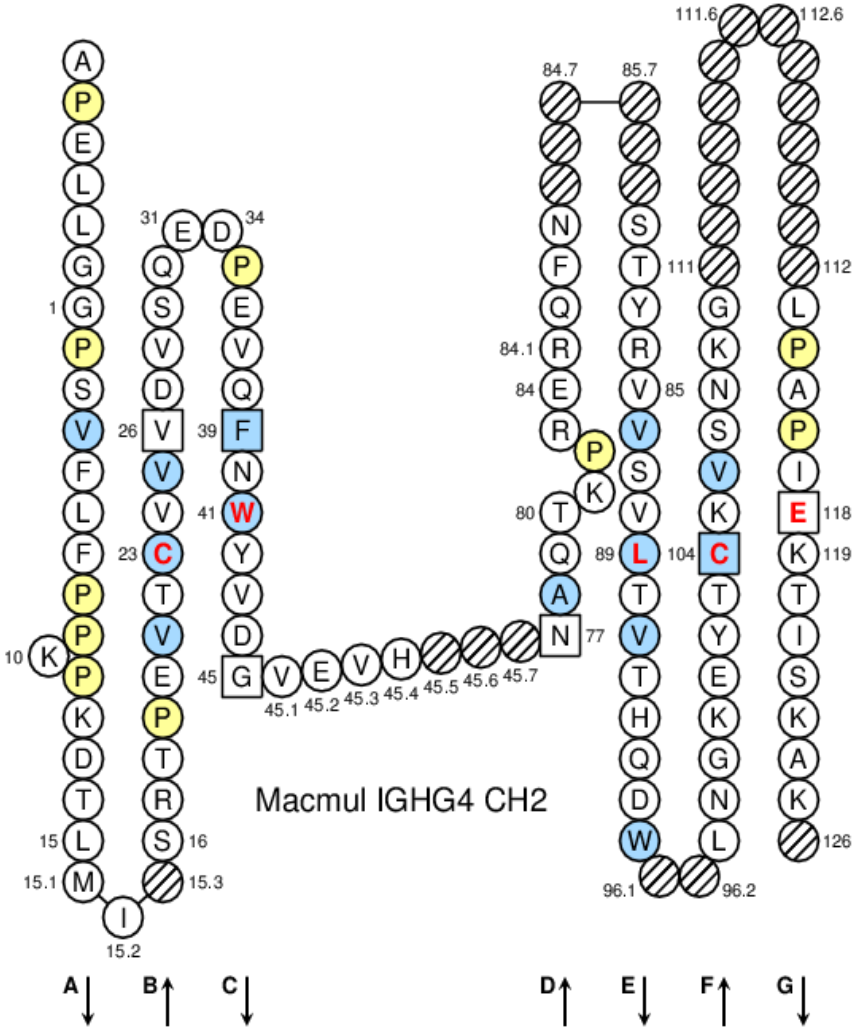
Macmul IGHG4 CH2
A
B
C
D
E
F
G

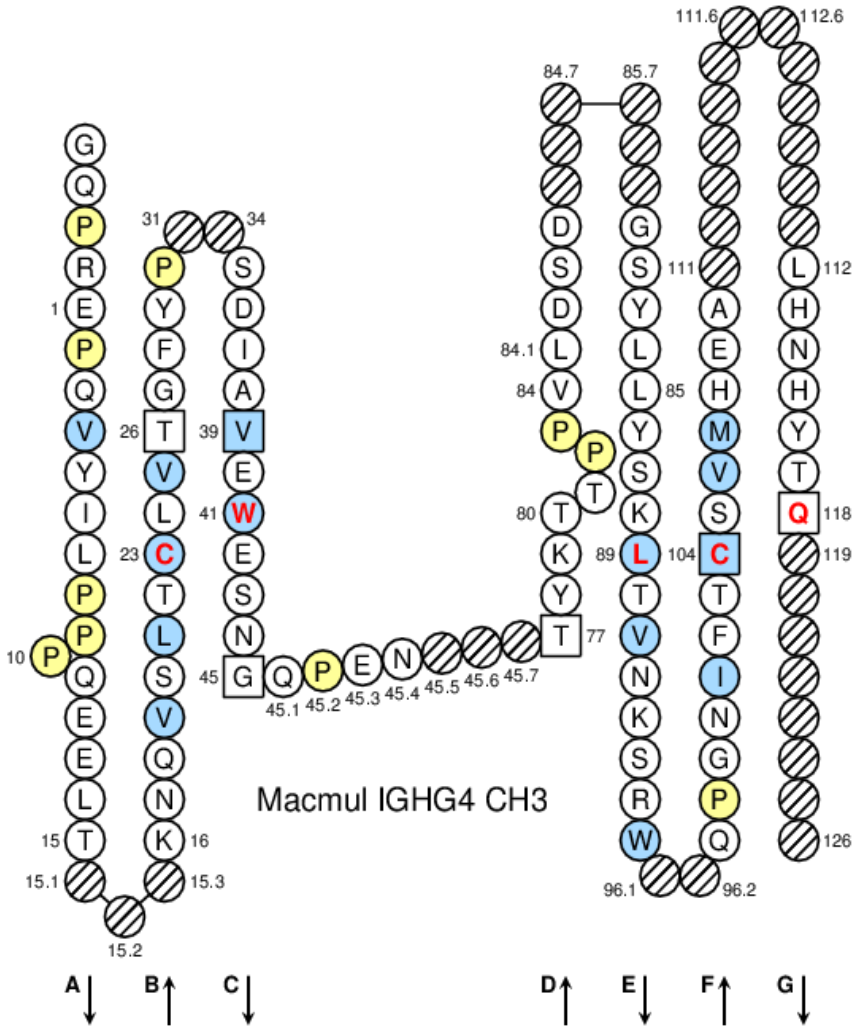
Macmul IGHG4 CH3
A
B
C
D
E
F
G

Fig. 2.13. Two-dimentional representation, or IMGT Colliers de Perles, of rhesus macaque (*Macmul*) CH domain sequences of each of the four IGHG subclass molecules. Shown are Colliers de Perles representation on one layer obtained with the IMGT/Collier-de-Perles tool in the IMGT/DomainGapAlign (http://www.imgt.org/3Dstructure-DB/cgi/Collier-de-Perles.cgi) (Ehrenmann et al., 2010). Colliers de Perles is the two-dimentional graphical representations of IG and TR V, C domains, highlighting conserved amino acids. The C-DOMAIN IMGT Colliers de Perles is based on the IMGT unique numbering for C- and C-LIKE DOMAIN and allows sequence comparison of Ig superfamily (IgSF) domains in different species (one layer Colliers de Perles), as well as localization of amino acids involved in FcR binding, in C1q binding, and in N-glycosylation sites (two layer Colliers de Perles) (Lefranc et al., 2005). The conserved Cys (position 23), and Cys (position 104), are indicated. Blue circles or squares represent core positions at which hydrophobic amino acids (I, V, L, F, C, M, A) and W are found in more than 50% of analyzed IgSF sequences. All Pro residues are shown in yellow. Squares illustrate homology with the corresponding positions in the V-DOMAINs (positions 26, 39, 104, and 118) or delimitation of the characteristic transversal CD strand of the C-LIKE-DOMAINs (positions 45 and 77). The BC loop, CD transversal strand, and FG loop are limited by amino acids displayed in squares. Hatched circles indicate missing positions according to the IMGT unique numbering for C-DOMAIN and C-LIKE-DOMAIN (Lefranc et al., 2005). Arrows indicate the beta strand direction.

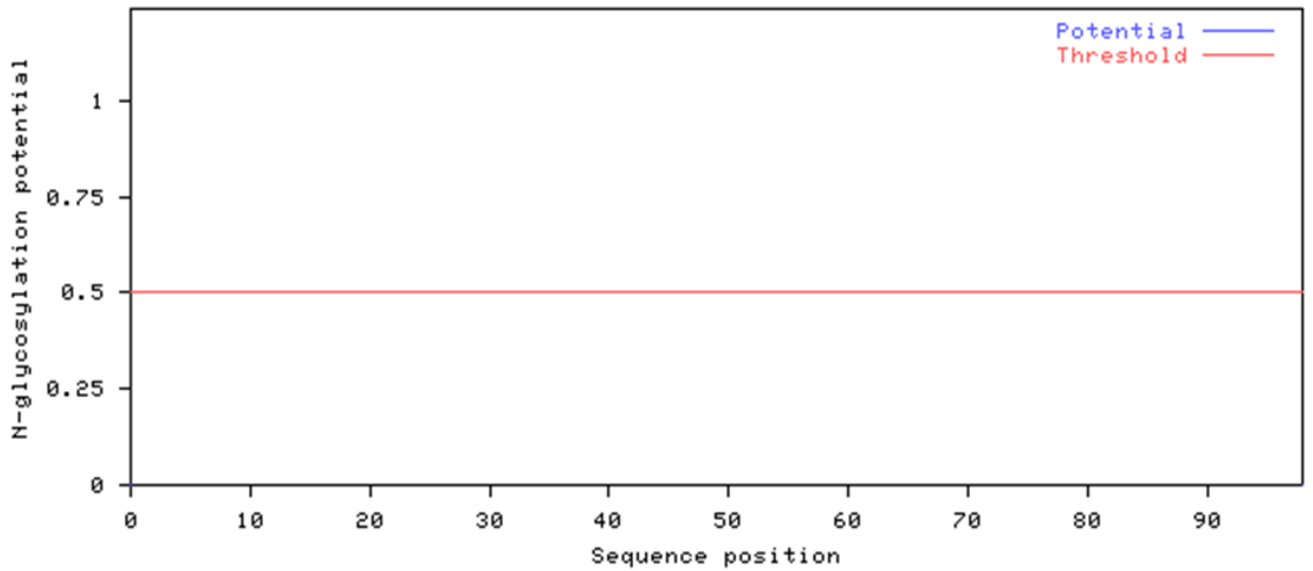
Potential
Threshold
N-glycosylation potential
1
0.75
0.5
0.25
0
0
10
20
30
40
50
60
70
80
90
Sequence position

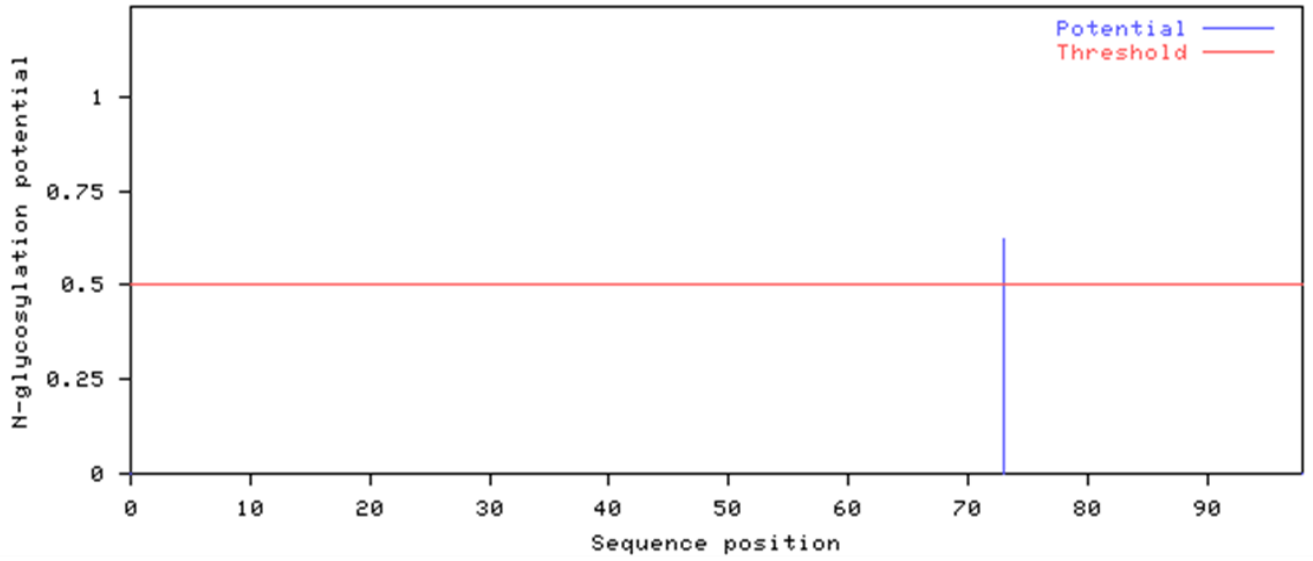
Potential
Threshold
N-glycosylation potential
1
0.75
0.5
0.25
0
0
10
20
30
40
50
60
70
80
90
Sequence position

Fig. 2.14. Prediction of potential N-glcosylation sites for CH3 domains of human (above) and rhesus macaque (below) IgG4 sequences, conducted by the use of the online tool NetNGlyc 1.0 Server (http://www.cbs.dtu.dk/services/NetNGlyc/), which is based on identifying Asn-Xaa-Ser/Thr consensus sequences (Julenius et al., 2005). Unlike in humans (above), in rhesus macaques (below), IgG4 has one additional computationally-predicted N-glycolsylation site at CH3.

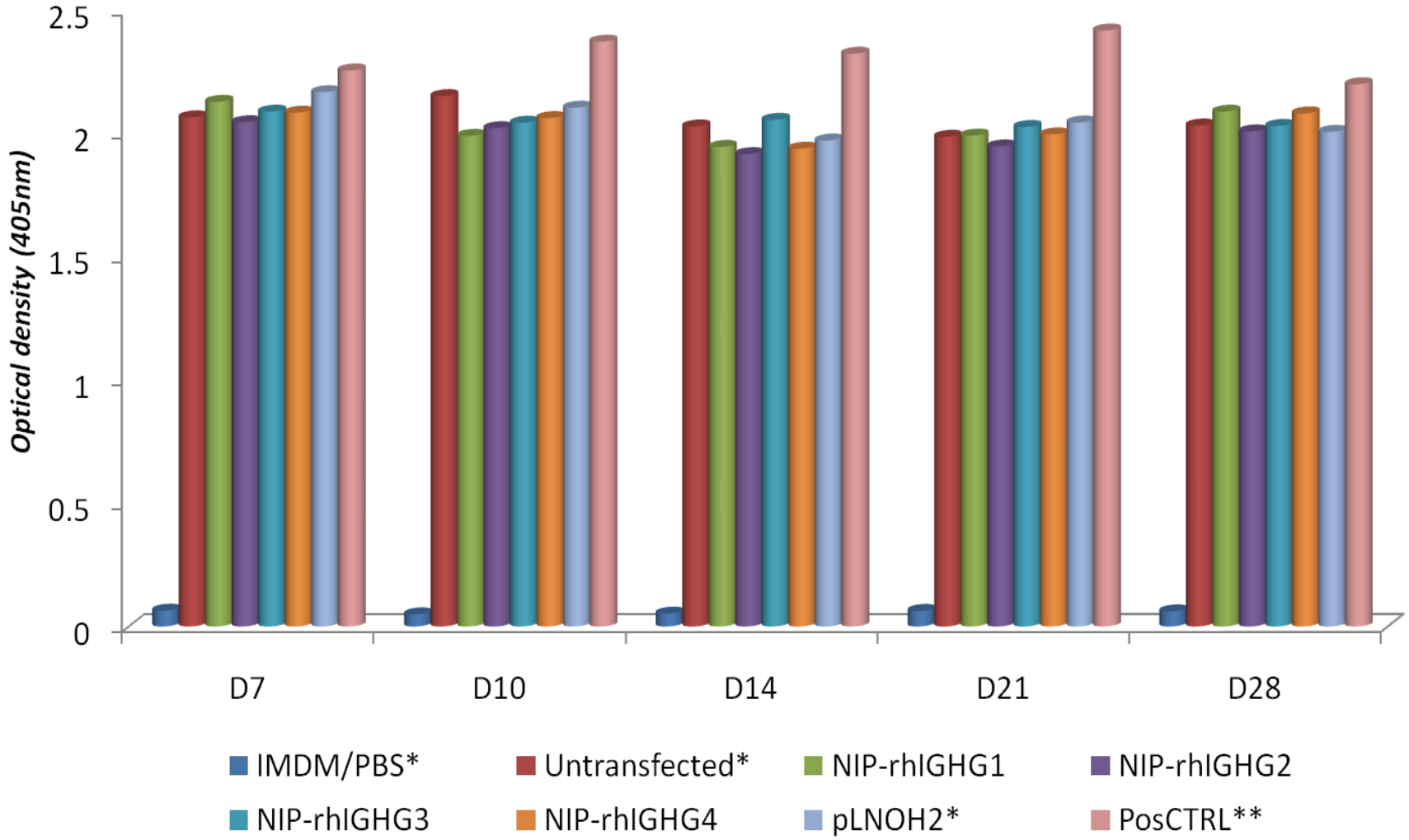
Optical density (405nm)
2.5
2
1.5
1
0.5
0
D7
D10
D14
D21
D28
IMDM/PBS*
Untransfected*
NIP-rhIGHG1
NIP-rhIGHG2
NIP-rhIGHG3
NIP-rhIGHG4
pLNOH2*
PosCTRL**

Fig. 2.15. Expression by J558L cells of NIP-specific mouse Igλ associated with secreted recombinant IgHs as detected by sandwich ELISA for its binding to purified anti-mouse IgL λ Abs produced in goat (NIP anti-λ ELISA). For detecting an antigen or Ab, sandwich ELISA is a sensitive and specific technique that uses two Abs, both of which are specific to the antigen or the Ab of interest and bind it at non-overlapping epitopes. Undiluted supernatants collected at different time points from J558L cells transfected with recombinant pLNOH2 expression vector containing NIP-rhIGHG1, NIP-rhIGHG2, NIP-rhIGHG3, or NIP-rhIGHG4 chimeric construct, from unstransfected cells (represents a negative control), or from cells transfected with the original pLNOH2 vector, which encodes human IgH and is specific for NIP, were incubated on ELISA plates coated with goat anti-mouse λ (Southern Biotech, Birmingham, AL; Cat. #1060-01). IgL λ was detected by HRP-conjugated secondary Ab goat anti-mouse λ (Southern Biotech, Birmingham, AL; Cat. #1060-05). Absorbance was measured at 405 nm using an automated microplate reader. Purified mouse IgG3 λ (Sigma–Aldrich Co., St. Louis, MO; Cat. # M9019) was added as a positive control. IMDM, the cell culture medium, and PBS, were also included to serve as additional negative and blank controls. Day numbers indicate numbers of days after transfection when supernatants were harvested for testing. Values are means of duplicate wells. The assays were performed twice and yielded similar results. *Data shown for IMDM/PBS, Untransfected, and pLNOH2 were from the NIP-rhIGHG3 experiments, which were used as representative; IMDM/PBS, Untransfected, and pLNOH2 values obtained from the NIP-rhIGHG1, NIP-rhIGHG2, and NIP-rhIGHG4 experiments were similar. PosCTRL**, purified mouse IgG3 λ (Sigma–Aldrich Co., St. Louis, MO; Cat. # M9019).

ELISA (data not shown).

As shown in Fig. 2.17, supernatants collected from cells transfected with recombinant IgH hybrids that were captured with NIP-BSA were readily detectable with HRP-conjugated anti-monkey IgGs. Supernatant from cells transfected with pLNO2 vector (human IgG3), which represented a positive control, also bound NIP-BSA. No binding was observed for supernatants from untransfected cells. These data indicate that intact IgG subclass Abs were assembled, as secreted recombinant Ab molecules featured both the VL/VH IgL NIP-specificity and the anti-monkey IgH-specific reactivity.

For all gene hybrids, Ab secretion level was with a peak on day 10 after transfection (Fig. 2.16, 2.17, and 2.18). Furthermore, protein production proceeded as early as at day 5 (Fig. 2.16 and 2.17). Six weeks after transfection, ELISA assays showed that the transfectomas producing good quantities of IgGs were still active (i.e. secreting Abs) (data not shown). Expression levels varied dependent on subclasses and the yield was generally highest for IgG2, followed by IgG3 then IgG4, and lowest for IgG1 (Fig. 2.18). During the examining period of time (up to six weeks post-transfection), production of murine λ IgL by J558L cells was confirmed by ELISA (Fig. 2.15). In these assays, ELISA plates were coated with goat anti-mouse λ [purified anti-mouse λ Abs produced in goat (NIP-specific anti-VL/VH λ Abs)] and bound IgL λ was detected by HRP-conjugated secondary Ab goat anti-mouse λ.

Taken together, production of recombinant IgGs recognized by both anti-NIP (i.e. Fab) and anti-monkey (i.e. Fc/IgH) Abs suggest that upon transfection with chimeric NIP-rhIGHG vectors, the IgH-deficient myeloma J558L cells produce complete H_2L_2 complete IgG molecules, resulting from pairing of transfected recombinant IgH with IgL λ endogenously expressed by the cells. Secreted Abs were with the pre-defined specificity (intact binding capability) against NIP.

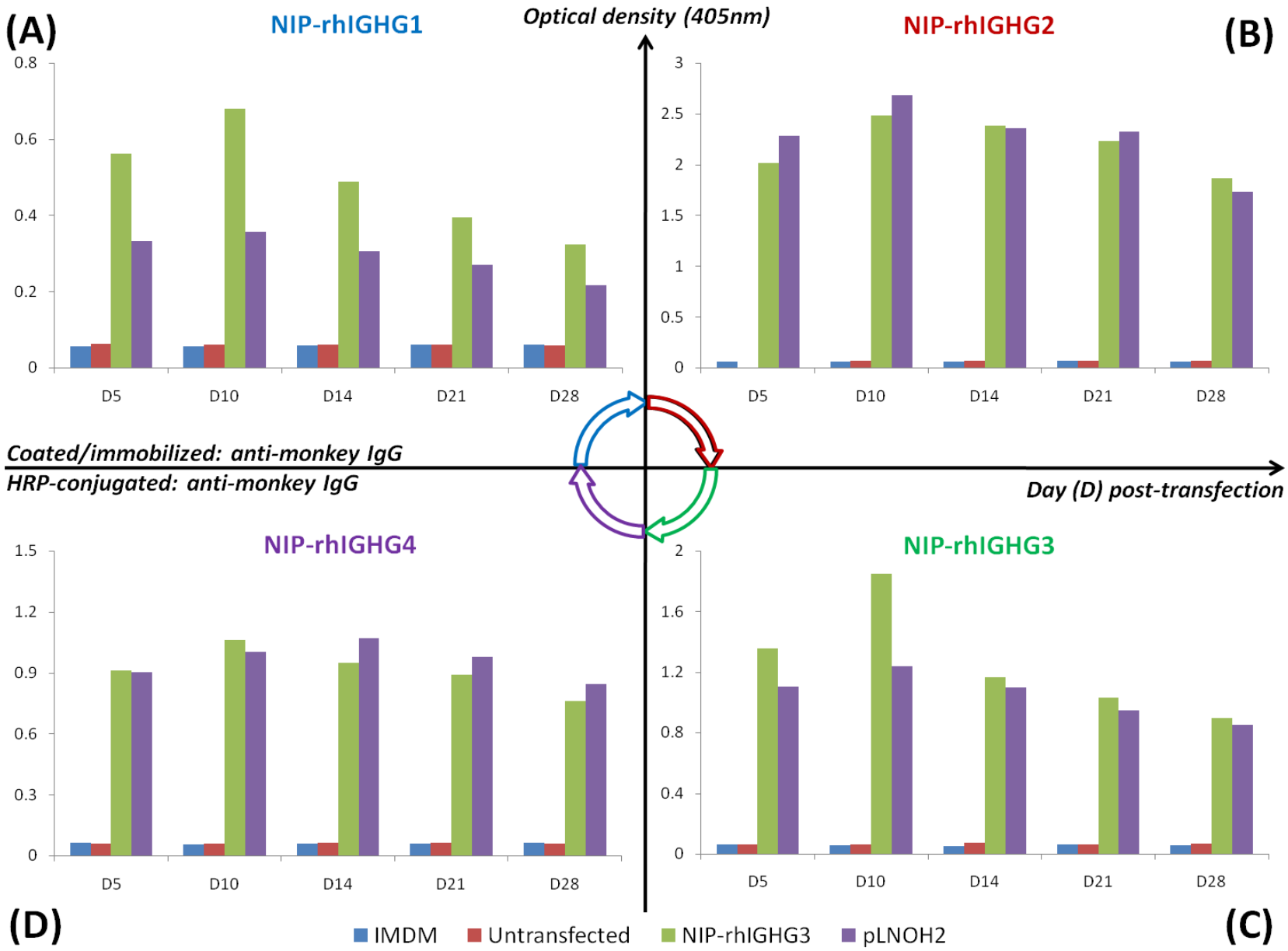
(A)
NIP-rhIGHG1
Optical density (405nm)
NIP-rhIGHG2
(B)
0.8
0.6
0.4
0.2
0
3
2.5
2
1.5
1
0.5
0
D5
D10
D14
D21
D28
Coated/immobilized: anti-monkey IgG
HRP-conjugated: anti-monkey IgG
Day (D) post-transfection
NIP-rhIGHG4
NIP-rhIGHG3
1.5
1.2
0.9
0.6
0.3
0
2
1.6
1.2
0.8
0.4
0
(D)
(C)
IMDM
Untransfected
NIP-rhIGHG3
pLNOH2

Fig. 2.16. Production of recombinant NIP-rhIGHG IgH chains of different IgG subclasses as determined by sandwich ELISA for their binding to an affinity purified anti-monkey IgG produced in goat (monkey-specific anti-gamma ELISA). For detecting an antigen or Ab, sandwich ELISA is a sensitive and specific technique that uses two Abs, both of which are specific to the antigen or the Ab of interest and bind it at non-overlapping epitopes. Undiluted supernatants collected at different time points from J558L cells transfected with a recombinant pLNOH2 expression vector containing the NIP-rhIGHG1 (A), NIP-rhIGHG2 (B), NIP-rhIGHG3 (C), or NIP-rhIGHG4 (D) chimeric construct, from unstransfected cells (represents a negative control), or from cells transfected with the original pLNOH2 vector, which encodes human IgH chain and is specific for NIP [represents a positive control (known to react with rhesus macaque IgG)], were incubated on ELISA plates coated with affinity purified goat anti-monkey IgG(H+L) (KPL, Baltimore, MD; Cat. #071-11-021) as the capture Ab. Bound Abs were detected by HRP-conjugated secondary Abs goat anti-monkey IgG (whole IgG- or IgH-specific) (KPL, Baltimore, MD; Cat. #074-11-021) for rhesus macaques. Due to rhesus macaque IgG bivalency, if they bind to immobilized purified goat anti-monkey IgG, they will also bind to HRP-conjugated goat anti-monkey secondary Abs. Absorbance was measured at 405 nm using an automated microplate reader. IMDM, the cell culture medium, was also included to serve as an additional negative control. Day numbers indicate numbers of days after transfection when supernatants were harvested for testing. Values are means of duplicate wells. The assays were performed twice and yielded similar results.

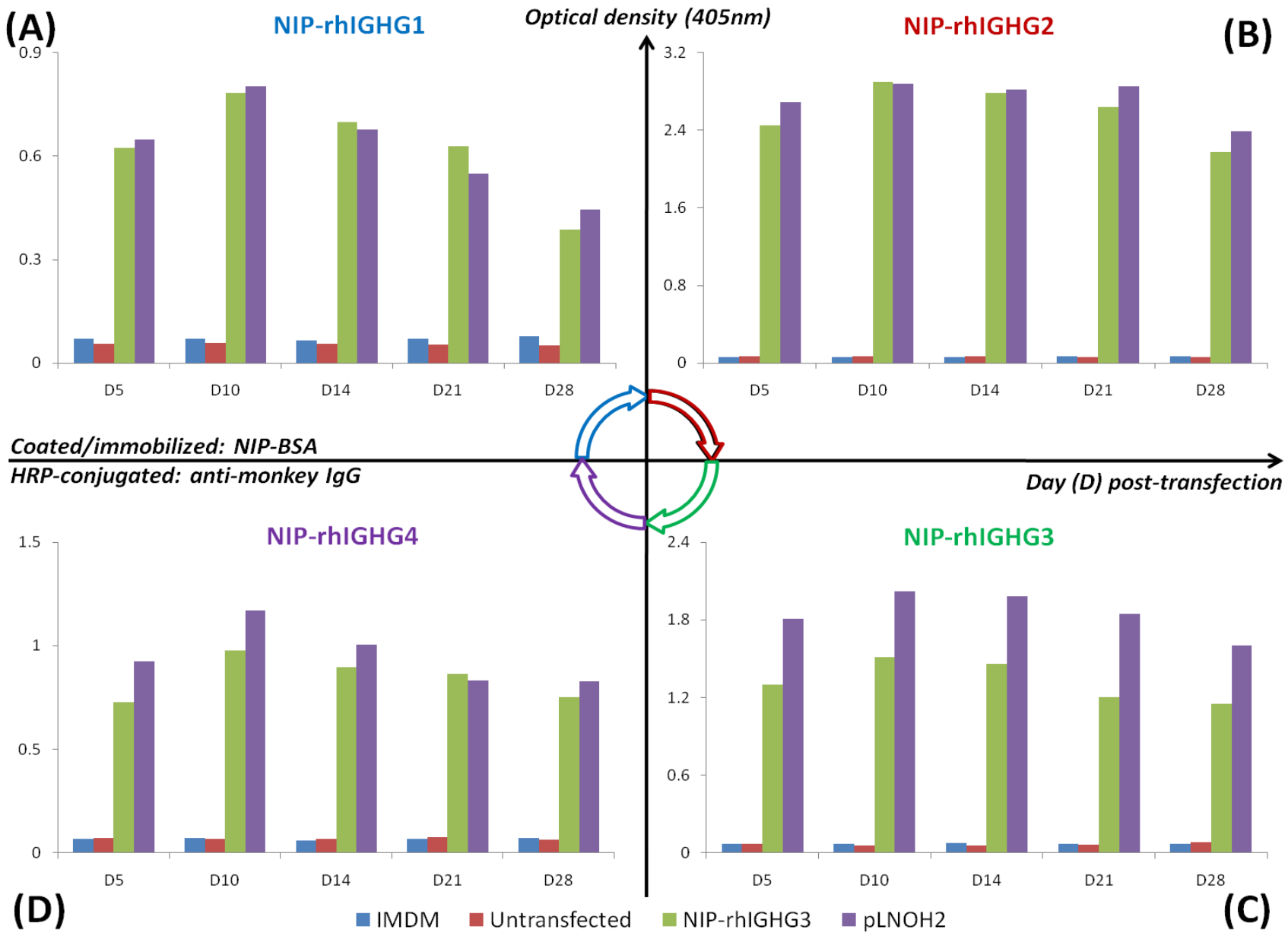
(A)
NIP-rhIGHG1
Optical density (405nm)
NIP-rhIGHG2
(B)
0.9
0.6
0.3
0
3.2
2.4
1.6
0.8
0
D5
D10
D14
D21
D28
Coated/immobilized: NIP-BSA
HRP-conjugated: anti-monkey IgG
Day (D) post-transfection
NIP-rhIGHG4
NIP-rhIGHG3
1.5
1
0.5
0
2.4
1.8
1.2
0.6
0
(D)
(C)
IMDM
Untransfected
NIP-rhIGHG3
pLNOH2

Fig. 2.17. Production of complete recombinant NIP-rhIGHG Abs of different IgG subclasses as determined by capture (indirect) ELISA for their binding to NIP-BSA (NIP coupled to BSA) antigen (NIP-specific anti-gamma ELISA). Expression of rhesus macaque IgH and its ability to pair with NIP-specific mouse IgL λ were tested using capture ELISAs. Undiluted supernatants collected at different time points from J558L cells transfected with a recombinant pLNOH2 expression vector containing NIP-rhIGHG1 (A), NIP-rhIGHG2 (B), NIP-rhIGHG3 (C), or NIP-rhIGHG4 (D) chimeric construct, from unstransfected cells (represents a negative control), or from cells transfected with the original pLNOH2 vector, which encodes human IgH chain and is specific for NIP (known to react with rhesus macaque IgG and represents a positive control), were incubated on ELISA plates coated with NIP-BSA (Biosearch Technologies, Birmingham, AL; Cat. #N-5040-10; 8-15 μg/ml). Bound Abs were detected by HRP-conjugated secondary Abs goat anti-monkey IgG (whole IgG- or IgH-specific) (KPL, Baltimore, MD; Cat. #074-11-021) for rhesus macaques. Absorbance was measured at 405 nm using an automated microplate reader. IMDM, the cell culture medium, was also included to serve as an additional negative control. Day numbers indicate numbers of days after transfection when supernatants were harvested for testing. Values are means of duplicate wells. The assays were performed twice and yielded similar results.

Thus, four chimeric NIP-rhIGHG intact IgGs that retained binding specificity of the original anti-NIP V regions were successfully produced.

2.4. Discussion

One of the major reasons for lack of IgG functional *in vitro* studies for the rhesus macaque model is the unavailability of specific serological reagents, whereas human Abs poorly or rarely interact with rhesus macaque effector leukocytes. To circumvent this pitfall, we have engineered recombinant Abs representing each of the four IgG subclasses of rhesus macaques. Previously, our laboratory has utilized molecular cloning techniques to identify and characterize IgG genes in rhesus macaques. From these studies, four IgG subclasses are discovered and are found to be variable most in the hinge region, although isotypic variation in amino acid sequences is also identified in CH1, CH2, and CH3 domains (Scinicariello et al., 2004). In addition to isotypic variation, intra-species allelic polymorphism also appears among individual animals. Of particular note from these findings is the addition in rhesus macaque IgG4 CH3 domain of a potential N-glycosylation site, from which possible related structural and/or functional changes remain to be elucidated. These characterized *IGHG* genes in rhesus macaques have provided the knowledge to generate their recombinant Abs.

In this study, we describe the procedures for engineering four chimeric recombinant murine-rhesus macaque IgGs. Here the ~1.4-1.5 kb *BsmI-BamHI*- and *NotI-XhoI*-containing IgH chain cDNA cassettes (which contained a murine VH region specific for the hapten NIP) of each of the four rhesus macaque IgG CH subclasses, were constructed by SOE-PCRs and subsequently cloned into pLNOH2 and P2561/2/3 expression vectors, respectively. Resultant IgH expression vectors were then transfected by electroporation into a murine myeloma cell line,

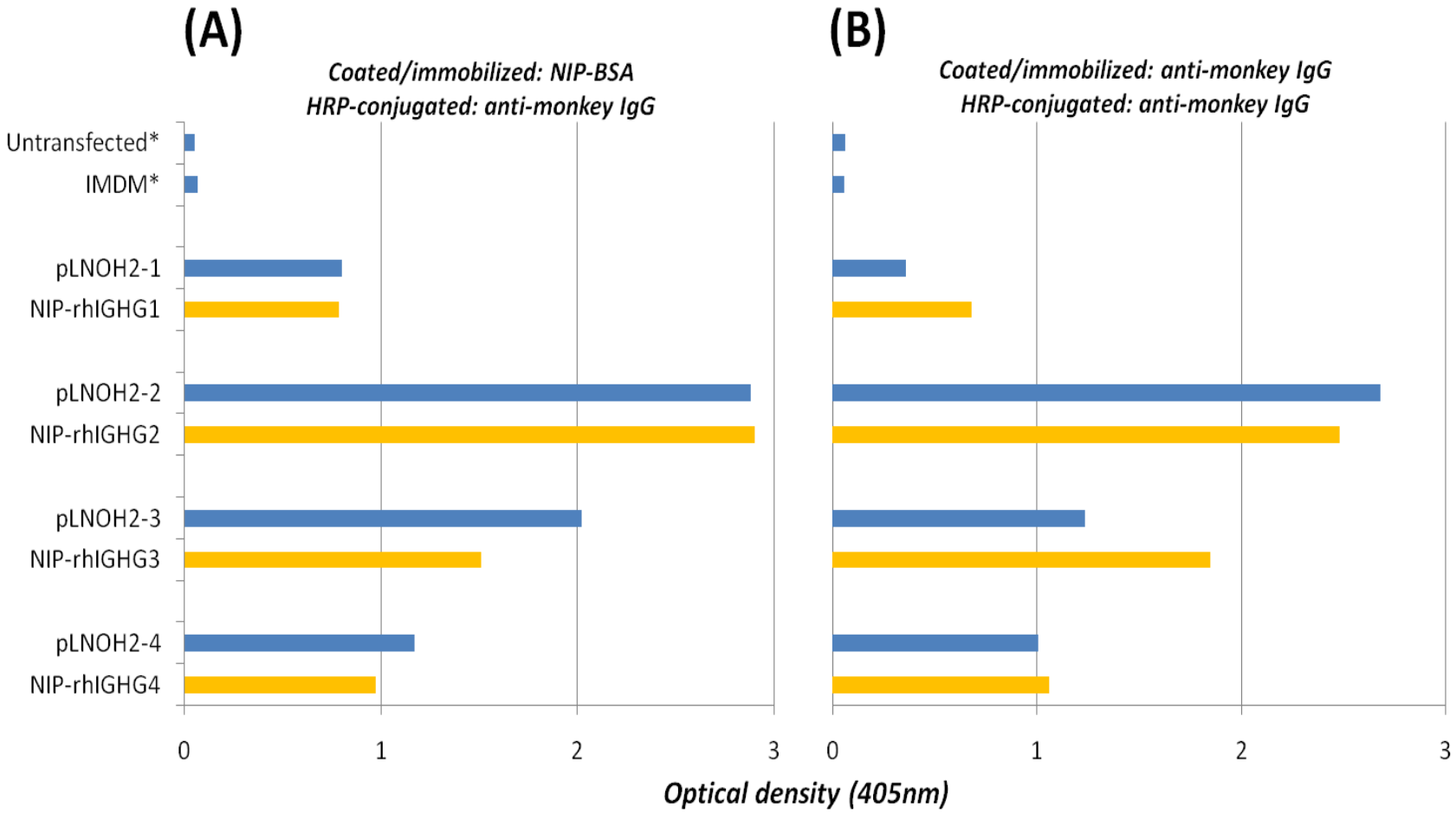
(A)
Coated/immobilized: NIP-BSA
HRP-conjugated: anti-monkey IgG
Untransfected*
IMDM*
pLNOH2-1
NIP-rhIGHG1
pLNOH2-2
NIP-rhIGHG2
pLNOH2-3
NIP-rhIGHG3
pLNOH2-4
NIP-rhIGHG4
0
1
2
3
(B)
Coated/immobilized: anti-monkey IgG
HRP-conjugated: anti-monkey IgG
0
1
2
3
Optical density (405nm)

Fig. 2.18. Different yields in production of recombinant NIP-rhIGHG Abs of different IgG subclasses as determined by ELISA for their binding to NIP-BSA antigen [(A); NIP-specific anti-gamma ELISA] or to an affinity purified anti-monkey IgG produced in goat [(B); monkey-specific anti-gamma ELISA]. Undiluted supernatants collected at day 10 post-transfection from J558L cells transfected with recombinant pLNOH2 expression vector containing the NIP-rhIGHG1, NIP-rhIGHG2, NIP-rhIGHG3, or NIP-rhIGHG4 chimeric construct, from unstransfected cells (represents a negative control), or from cells transfected with the original pLNOH2 vector, which encodes human IgH chain and is specific for NIP (known to react with rhesus macaque IgG and represents a positive control), were incubated on ELISA plates coated with NIP-BSA (Biosearch Technologies, Birmingham, AL; Cat. #N-5040-10; 8-15 μg/ml) (A) or with with purified goat anti-monkey IgG (KPL, Baltimore, MD; Cat. #071-11-021) (B). Bound Abs were detected by HRP-conjugated secondary Abs goat anti-monkey IgG (whole IgG- or IgH-specific) (KPL, Baltimore, MD; Cat. #074-11-021) for rhesus macaque. Absorbance was measured at 405 nm (the X-axis) using an automated microplate reader. IMDM, the cell culture medium, was also included to serve as an additional negative control. Values are means of duplicate wells. The assays were performed twice and yielded similar results. *Data shown for IMDM and Untransfected were from the NIP-rhIGHG3 experiments, which were used as representative; IMDM and Untransfected values obtained from the NIP-rhIGHG1, NIP-rhIGHG2, and NIP-rhIGHG4 experiments were similar).

J558L, which express the NIP-specific IgL chain. Surviving cells were selected by G418 antibiotics and IgG production was determined by ELISA. Successful production and identity of intact recombinant IgGs were confirmed by their capability of binding the hapten NIP and being bound by purified goat anti-monkey Abs. All resultant recombinant molecules were confirmed for sequence accuracy.

The recombinant DNA method is a powerful tool for construction of Ab genes and production of genetically engineered Abs with novel or modified structural and/or functional properties for applications in both basic and applied research. With more and more Ig gene sequences and specifically constructed vectors for subsequent cloning and expression become available, the process of producing recombinant Igs can nowadays be faster and more flexible. cDNA-based vector systems have been also used to express chimeric murine (V)-human (C) Abs under CMV promoter direction (McLean et al., 2000; Preston et al., 1998; Norderhaug et al., 1997). Also, *in vitro* Ab expression requires cloning of Ig (V and C) gene fragments into eukaryotic cell expression plasmids containing specifically constructed functional sequences, including those encoding an Ig promoter (for transcription control), an Ig intron leader (allowing for secretion of fusion protein), a poly(A) signal (for transcription termination), an origin of replication, and antibiotic resistance markers (for clone selection) (Tiller et al., 2008; Wrammert et al., 2008). Several such Ig expression vectors have been developed (Tiller et al., 2008; McLean et al., 2000; Persic et al., 1997). However, Ig expression vectors lacking intron sequences have generally yielded a low level of secreted Abs (Gillies et al., 1989; Neuberger and Williams, 1988). In this study, we took advantages of these techniques to successfully create and produce four complete recombinant chimeric cDNA gene constructs consisting of rhesus

macaque IgG CH region genes in combination with the murine VH region genes whose protein product direct against the NIP hapten.

Amplification of rhesus macaques IgG CH gene segments was carried out with degenerate primers designed from known conserved regions of IgG CH sequences in humans and optimized for sufficient (re)amplification SOE-PCRs. Also, these primers were designed so that they would not only amplify Ig gene fragments, but also appropriately add unique, desirable RE sites that overlapped with adjunct fragments or with the cloning and expression vectors – yet absent in IgG gene constructs (Persic et al., 1997) – for easy exchange of Ig gene cassettes and allowing for straightforward subsequent cloning of DNA constructs. These primers have allowed murine V region genes to be fused in frame to rhesus macaque C regions genes to create a single, complete IgH chain fragment for cloning and ligation. Additionally, the primers employed were also appropriately provided with sequence extensions for overlap reactions or were embedded with necessary Ig functional element sequences for transcription, transport, and translation.

The creation of recombinant IgH gene fragment in this study relied on the method for splicing two pieces of DNA, SOE-PCR (Yolov and Shabarova, 1990; Yon and Fried, 1989). As previously described, this technique is a powerful tool for fusing two short DNA fragments whose total length is not greater than 3-4 kb (Kuwayama 2002; Pont-Kingdon, 1997), which is ideal for creating IgH gene region. Using sequential SOE-PCRs, we have successfully assembled individual DNA fragments with overlapping sequences to generate four recombinant cDNA fusion constructs, each encoding a rhesus macaque IgG CH subclass. Constructed plasmids were examined by restriction analysis and confirmed by DNA sequence analysis for their sequence accuracy and insert orientation. As described in the Materials and Methods section, since the two DNA template fragments were introduced at their adjacent end an overlapping sequence, each of

them can act as a giant "primer" on the other one. These reactions resulted in the fused DNA species to be created in the mixture of early SOE-PCR products. Due to the low concentration of the complementary DNA fragments and their shorter sequence (thus, lower melting temperature), appearance of the fused DNA species at this stage of SOE-PCR reactions (i.e. amplification, not reamplification) would be most successful at a relatively low annealing temperature. Indeed, when performed with the annealing temperature of 56^0C or 58^0C and a magnesium concentration of 2.5 mM, SOE-PCRs that used the two outermost flanking primers were generally found to yield minimal nonspecific products while producing desired amplification fragments. This melting temperature range should be considered when designing degenerate primers.

In some particular instances, however, such as with IgG3 with which additional primers were used, creating a complete recombinant cDNA fragments using these approaches was not straightforward: many non-specific DNA species were yielded while little or no desired DNA product was produced. In such cases, redesigning internal primers by increasing their overlap length (of up to 47-99 nt long; Shevchuk et al., 2004) could improve the (re)amplification success rate. This observation is consistent with previous findings (Shevchuk et al., 2004). Alternatively, modification of SOE-PCR strategy by adding the flanking primer pairs after running of several reactions (i.e. these early runs are with no primers to allow for fusion DNA species to pair) could be applied (Shevchuk et al., 2004). Also, in general, we observed that the use of equimolar concentrations of DNA template fragments tended to reduce the presence of non-specific products. We also note that use of Clontech DNA polymerase generally improves the success of amplification compared to using the Taq-based polymerases. Cloning of amplified

SOE-PCR products of IgG CH cDNA fragments into plasmid vectors was also necessary, given the slight sequence differences between the IgG subclasses.

In this study, we used an established pLNOH2 expression plasmid vector that not only contains all the essential elements necessary for transcription – including the appropriate intronic sequences and the needed splicing signals at the intron boundaries – but also consists of unique restriction sites for easy subcloning or straightforward substitution of IgG CH region genes (Norderhaug et al., 1997). We have also demonstrated the expression and assembly of full-length IgH and IgL to form complete rIgs by a specialized mammalian cell line. The IgH was cloned and expressed using a eukaryotic plasmid expression vector. Successful recognition of rIgs by whole IgG-specific or IgH-specific conjugate indicate that IgH chains were correctly assembled with the IgL chains that were endogenously secreted by J558L cells (these cells express no endogenous IgH, hence no intact Abs are secreted). These data proved that IgL and IgH chains were produced and were able to covalently associate to make intact (H_2L_2) IgG molecules. These results also indicate that all expressed proteins, throughout the incubation period, were correctly folded. Additional experiments, however, are needed to examine if the Abs were glycosylated correctly.

Previous work in our laboratory has used cDNA-based expression systems to produce functional recombinant Abs and FcRs (Rogers et al., 2008 and 2006). An early Ig expression system was applied to express recombinant Abs composing of NIP-binding V regions and macaque IgA CH region genes; the resultant recombinant Abs were able to bind NIP (Rogers et al., 2008). In this study, we improved the use of this early Ig expression system by employing unique RE sites and made the P2561/2/3 Ig expression system. This system can be used to create recombinant Abs possessing rhesus macaque or other NHP polymorphic Ig CH genes for

functional characterization of recently recognized high levels of intraspecies variability. Also, because our functional Ig gene constructs were transfected into a murine myeloma (i.e. Ab-producing cells) that endogenously express IgL λ chains, the steps involved in cloning of IgL chains could be bypassed, thus avoiding some SOE-PCR and subsequent cloning procedures, which are often obstacles in recombinant Ab production. Furthermore, successful production of complete chimeric IgG subclasses reactive with purified anti-monkey IgG directed whole IgG or IgH and capable of specifically binding to the NIP-BSA hapten, as described in this study, confirms that murine IgL λ chain (V and C regions) was successfully engineered into rhesus macaque IgH chains while still retained specificity of the original V regions. Since the hapten NIP is directed by murine IgL λ chain but not by rhesus macaque IgH regions, the use of this specificity would avoid potential detection problems associated with intra- and/or inter-species sequence variability within IgH CH domains. Thus, this system would be a useful tool for engineering complete recombinant IgG Abs with pre-defined specificity and desired CH regions.

In conclusions, the Ig cloning and expression systems, and the genetically engineered recombinant IgG chimeras created in this study, represent both the foundations and the tools for further studies of IgG effector functions, such as activating pathogen-clearance cell-killing effector mechanisms through binding corresponding FcγRs, and IgG preferential serum usage during various immune responses in the rhesus macaque model. These materials can also be utilized for basic studies of Ab structure-function relationship. These potential studies will be discussed in more details later in this dissertation.

Acknowledgments

Support for Doan C. Nguyen was provided by the Molecular Basis of Disease program at Georgia State University.

CHAPTER 3

RHESUS MACAQUE IGG FC RECEPTORS: CHARACTERIZATION AND ALLELIC POLYMORPHISMS OF ENCODING GENES AND GENERATION OF RECOMBINANT cDNA EXPRESSION VECTORS

(PARTIAL CONTENT OF THIS CHAPTER WAS PUBLISHED AS:

NGUYEN ET AL., IMMUNOGENETICS 2011;63:351–62)

3.1. Summary

Macaque models are invaluable for AIDS research. Initial development of HIV-1 vaccines relies heavily on SIV-infected rhesus macaques. Neutralizing Abs, a major component of anti-HIV protective responses, ultimately interact with FcRs on phagocytic and NK cells to eliminate the pathogen. Despite the major role that FcRs play in protective responses, limited information is available on these molecules in rhesus macaques. In this study, rhesus macaque CD64 (FcγRI) and CD32 (FcγRII) homologues were genetically characterized. Presence of CD64, CD32, and CD16 (FcγRIII) allelic polymorphisms were also determined in a group of nine animals. Results from this study show that the predicted structures of rhesus macaque CD64 and CD32 are highly similar to their human counterparts. Rhesus macaque and human CD64 and CD32 extracellular domains are 94–95% and 88–90% homologous, respectively. Although all Cys residues are conserved between the two species, rhesus macaque CD32 exhibits two additional N-linked glycosylation sites, whereas CD64 lacks three of them, when compared to humans. Three CD64, five CD32, and three CD16 distinct allelic sequences were indentified in the nine animals examined, indicating a relatively high level of polymorphism in rhesus macaque

FcγRs. Recombinant FcγR gene cDNA constructs were successfully generated and engineered into cloning and expression vectors using novel refined plasmid systems. These constructs can be cloned into HeLa cells for production of recombinant FcγRs, which will be a useful tool for functional studies, including those related to IgG/FcγR interactions and initiation of cellular immune responses. Collectively, these results validate rhesus macaques as models for vaccine development and Ab responses, while at the same time, underscoring the need to take into account the high degree of genetic heterogeneity present in this species when designing experimental protocols.

3.2. Materials and methods

3.2.1. Blood samples, total RNA isolation, reverse transcription, and cDNA synthesis of FcγR genes

Fig. 3.1. shows the major steps involved in identifying and cloning rhesus macaque FcγR genes, and in generation of their recombinant cloning and expression plasmid vectors. Heparinized blood samples were collected from nine healthy rhesus macaque (*Macaca mulatta*) of different ages housed at the Language Research Center of Georgia State University, Atlanta, GA. Animal blood collection was done according to local and federal guidelines. Total RNA was extracted from whole blood using QiaAmp RNA Blood Mini kit (Qiagen Inc., Valencia, CA). Total RNA (~1–3 μg) was then reverse transcribed into single-stranded cDNA using either oligo (dT)15 or random primers, followed by primer extension with the AMV reverse transcriptase (Roche Diagnostics North America, Indianapolis, IN), in a total reaction volume of 15–30 μl. Next, the resulting first-strand cDNA products were serially diluted and PCR-amplified with Expand High Fidelity polymerase (Roche Diagnostics North America, Indianapolis, IN) using

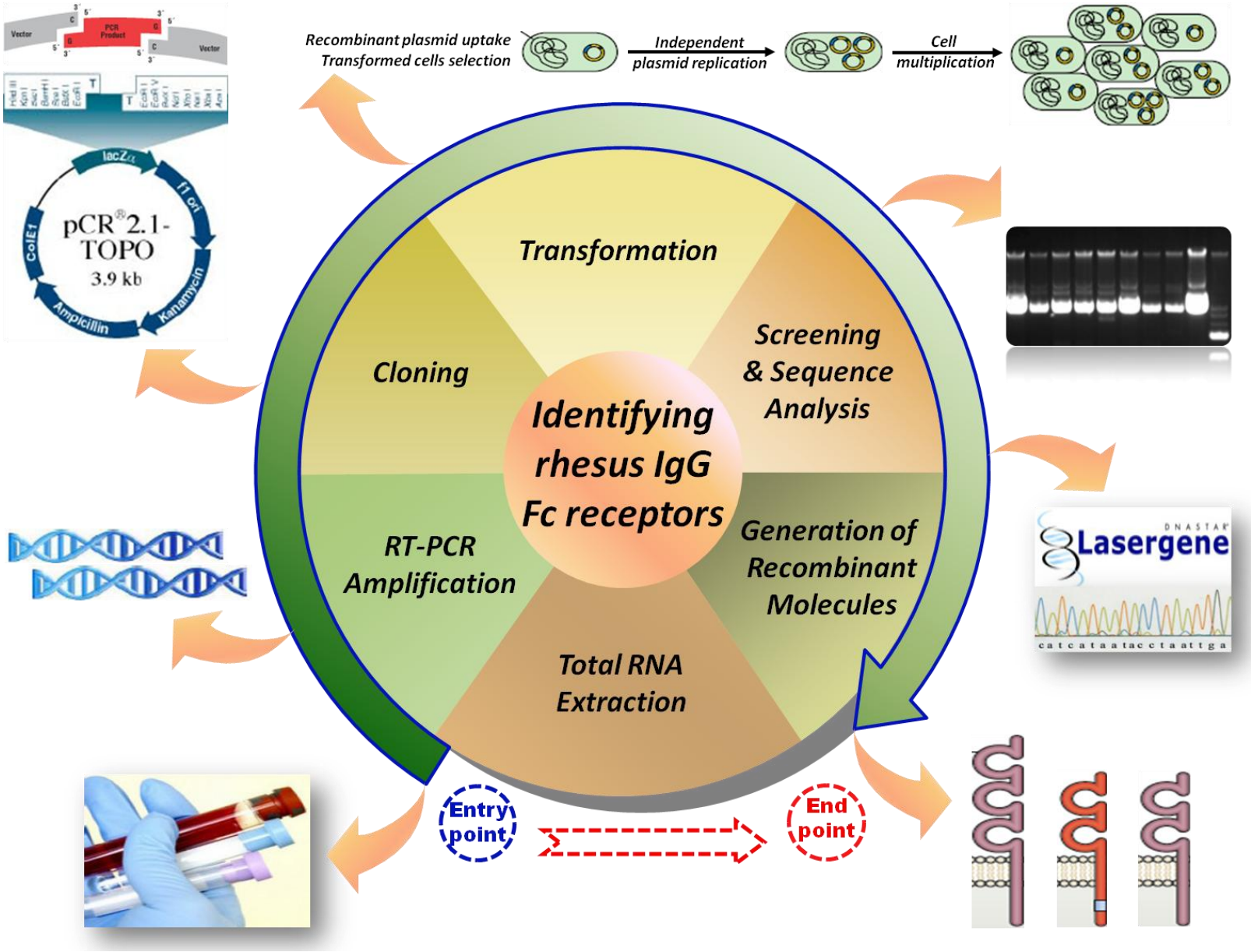
Recombinant plasmid uptake
Transformed cells selection
Independent
plasmid replication
Cell
multiplication
pCR®2.1-
TOPO
3.9 kb
Transformation
Screening
& Sequence
Analysis
Generation of
Recombinant
Molecules
Total RNA
Extraction
RT-PCR
Amplification
Cloning
Identifying
rhesus IgG
Fc receptors
Lasergene
Entry
point
End
point

Fig. 3.1. Flowchart representation illustrating major steps involved in identifying and cloning rhesus macaque FcγR genes, as well as in generation of recombinant FcγR cloning and expression plasmid vectors. Individual cDNA gene fragments were first isolated and amplified from total RNA extracted from whole blood cells by RT-PCR and PCR using primers that were designed based on known conserved regions of corresponding human FcγR gene sequences. Resulting cDNA genes were cloned into pCR2.1 TOPO TA cloning vector containing a selectable marker sequence, which was used for selection of transformed clones that picked up constructs and replicated in competent bacterium cells cultured in medium containing X-gals and ampicillin antibiotic. All constructs were verified by DNA sequencing before further steps. For generating recombinant molecules, cDNA constructs were firstly amplified from cloning vectors by PCR using primers that incorporated appropriate restriction sites (that were used to ligate a desired contruct into an expression vector, where it fits exactly between the two restriction sites). To make a large quantity of the constructs, resulting recombinant expression vector was then transformed back into competent bacterium cells so that they were multiplicated by these cells following their division and replication. An appropriate amount of recombinant DNAs were made available and ready for mammalian cellular transfection. Some figure pieces are reproduced from Smith and Clatworthy, 2010, and from the internet.

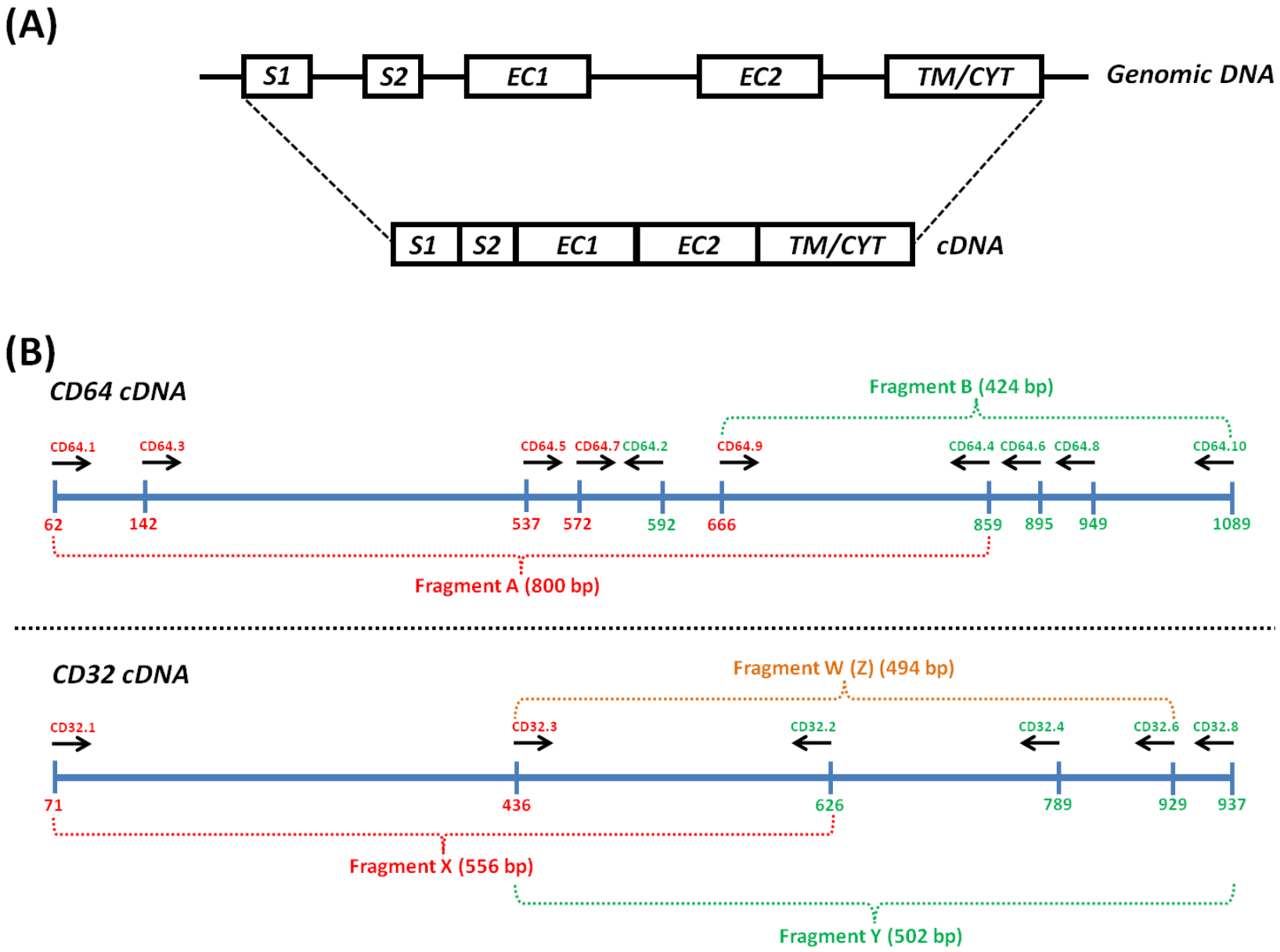
(A)
S1
S2
EC1
EC2
TM/CYT
Genomic DNA
S1
S2
EC1
EC2
TM/CYT
cDNA
(B)
CD64 cDNA
Fragment B (424 bp)
CD64.1
CD64.3
CD64.5
CD64.7
CD64.2
CD64.9
CD64.4
CD64.6
CD64.8
CD64.10
62
142
537
572
592
666
859
895
949
1089
Fragment A (800 bp)
CD32 cDNA
Fragment W (Z) (494 bp)
CD32.1
CD32.3
CD32.2
CD32.4
CD32.6
CD32.8
71
436
626
789
929
937
Fragment X (556 bp)
Fragment Y (502 bp)

Fig. 3.2. Schematic representation of FcγRIIIa genomic and cDNA structure and of gene fragments encoding the extra cellular domains of FcγRI and FcγRII molecules, as well as strategy for creating recombinant cDNA fragments. (A) Schematic representation of FcγRIIIa genomic and cDNA structure (not drawn to scale). S, signal sequence (encoded in 2 exons); EC, extracellular Ig-like domains; TM/CYT, transmembrane/cytoplasmic domains. The intron-exon organization of the FcγR genes was inferred from the human and rhesus macaque sequences publicly available. The necessary splice sites found at intron boundaries and the sequences of the introns were removed. (B) Diagrammatic representation of gene fragments encoding the extra cellular domains of FcγRI and FcγRII molecules and strategy for creating recombinant cDNA fragments. Name, direction (horizontal black arrows), and relative positioning/location (colorful numbers) of primers as well as corresponding amplified PCR products are depicted. The final recombinant constructs were amplified in SOE-PCRs using the outermost flanking primers. The sequences of primers used are given in Table 3.1.

appropriate oligonucleotide primer pairs (see below) in a total of 50 or 100 µl reaction volume. PCR conditions were as follows: after initial denaturation at 95°C for 10 min, the cDNAs were amplified for 40 cycles, with each cycle consisting of 94°C for 1 min, 56°C for 1 min, and 72°C for 2 min and 30 s. To ensure complete extension, a final step at 72°C for 10 min was applied. At least two independent RT-PCR reactions using the same total RNA were performed, and from 10 to 15 independent cDNA clones per individual macaque and from each of two separate PCR reactions were analyzed. These steps were performed to rule out that the putative allelic polymorphisms were due to a PCR amplification artifact.

3.2.2. Design of primers

Primers for amplification of macaque FcγRI (CD64) and FcγRII (CD32) genes were designed from the corresponding human sequences (assuming conserved homology between primates) (Fig.3.2). The terminal sense and antisense FcγRII/FcγRI primers are located within the start of the leader region (exon 1) and within the end of the cytoplamic region (FcγRII exon 5 and FcγRI exon 6), respectively, of the cDNAs shared by multiple human FcγRIIa/FcγRIa sequences (Table 3.1). Internal primers for each of these two receptors were situated within exon 4, which encodes the [D2] domain of CD32, or exon 5, which encodes the [D3] domain of CD64. Using these primer sets, the PCR amplification product should span most of the FcγRII or FcγRI-targeted cDNAs (covering from exon 1 to the most 3′ exon). Specifically, the CD32.1 and CD32.2 primer pair was used to generate a 566-bp product spanning the first part of FcγRII, beginning from the leader region. CD32.3 and CD32.8 primer pair would amplify a 502-bp fragment that had a 191-bp overlapping sequence with the fragment produced by CD32.1 and CD32.2, and that spanned the second part of FcγRII, including the CO-TM-CYT region.

Similarly, two FcγRI fragments that had a 194-bp overlapping sequence were amplified by the use of CD64.1 and CD64.4 (yielding an 800-bp fragment) and CD64.9 and CD64.10 (generating a 424-bp fragment) primer pairs. For FcγRIII, primers included FCG3aF (located within the start of the leader region) and FCG3aR (located within the end of the cytoplamic region). All primers were designed to generate FcγRIIa, FcγRIa, and FcγRIIIa homologue products, and were used for each individual animal of the nine macaques examined.

3.2.3. Cloning and sequencing of amplified FcγR cDNAs

Appropriate volume of PCR reactions were run on a 2% agarose gel and the bands of interest (showing expected size) were excised and purified using QIAquick Gel Extraction kit (Qiagen Inc., Valencia, CA) using a microcentrifuge. The purified PCR products were then cloned into the pCR2.1 TOPO TA cloning vector (Invitrogen, Carlsbad, CA) for sequencing analysis purpose. The plasmids were transformed into Top10 E. Coli chemically competent cells using TOPO TA Cloning and One Shot Chemical Transformation following the manufacturer's protocols (Invitrogen, Carlsbad, CA). Subsequently, 10–15 inserted, positive colonies from each sample were picked and incubated overnight in LB culture tubes at 37°C in a shaking rotary incubator (200–230 rpm). The minipreps DNA Purification System kit (Promega Corporation, Madison, WI) was used to purify plasmid DNA, and the plasmid DNA was then screened on a 1% agarose gel after digestion with EcoRI to confirm the inserted fragment size. All DNA sequences were determined using the ABI Prism Dye Termination Cycle Sequencing kit and on an ABI model 3100 automated sequencing apparatus (PerkinElmer, Wellesley, MA). Sequencing primers were those used for PCR amplifications and the forward and reverse M13 primers.

Table 3.1. Primers used for amplification of rhesus macaque FcγR[a] cDNAs.

Primer Name	Sequence (5'-3')	Product size (bp)	Position	Location	Accession number[c]
FCG3aF (fw)[b]	ATGTGGCAGCTGCTCCTCCCA	765	(-51)-(-31)	L-encoded region	DQ423379.1
FCG3aR (rv)	TCATTTGTCTTGAGGGTCCTT		(714)-(694)	CYT-encoded region	DQ423379.1
CD32.1 (fw)	TTTTGCTGCTGCTGGCTTCTGC	556	(-32)-(-11)	L-encoded region	BC020823.1
CD32.2 (rv)	ATGCTGGGCACTTGGACAGTGATG		(527)-(504)	[D2]-encoded exon 4	BC020823.1
CD32.3 (fw)	AAGGACAAGCCTCTGATCAAGGTC	502	(337)-(360)	[D2]-encoded exon 4	XM_001118066.2
CD32.8 (rv)	TGACATGGTCGTTGGGAGGAAG		(838)-(817)	CYT-encoded region	BC020823.1
CD64.1 (fw)	GACAGCTCTGCTCCTTTGGGTTC	800	(-40)-(-18)	L-encoded region	NM_000566.3
CD64.4 (rv)	AGGACATTTCCGTCTTCTGTGG		(758)-(737)	[D3]-encoded exon 5	NM_000566.3
CD64.9 (fw)	AATCTGGTCACCCTGAGCTGTG	424	(565)-(586)	[D3]-encoded exon 5	NM_000566.3
CD64.10 (rv)	AATGTCTGTCTTCTTGAAGGCTGG		(988)-(965)	CYT-encoded region	NM_000566.3

[a]Abbreviation and full gene designations are the following: FcγRI: IgG Fc high affinity I receptor (CD64); FcγRII: IgG Fc low affinity II receptor (CD32); FcγRIII (or FCG3a): IgG Fc low affinity III receptor (CD16).

[b]fw, forward direction; rv, reverse direction.

[c]GenBank accession number for the reference sequences used for designing primers.

3.2.4. Construction of rhesus macaque FcγR cloning vector

The complete CD64 and CD32 extracellular domain cDNA gene fragments were generated by SOE-PCR ligating two separate fragments containing overlapping short sequences, which were produced by PCRs using the appropriate primer pairs (CD64.1 and CD64.10, and CD32.1 and CD32.8; Fig. 3.2 and Table 3.1). The CD16 cDNA fragment was directly amplified from relevant sequencing-verified plasmids. To facilitate transfer of these FcγR cDNA fragments from TOPO TA cloning vector into expression vectors, *HindIII* and *BamHI* restriction sites were introduced to their 5' and 3' ends, respectively, by PCRs using forward FCG3FHind and reverse FCG3RBam primers (Table 3.2 and Fig. 3.3) on the appropriate cloning vector previously generated. Also, additional FcγR cDNA fragments were incorporated with *NotI* and *XhoI* restriction sites to their 5' and 3' ends, respectively, following a similar strategy with the use of FcγR.NotI and FcγR.XhoI primers (Table 3.2 and Fig. 3.4). Resultant FcγR cDNAs (i.e. consisting of the two added restriction sites: *HindIII* and *BamHI*, or *NotI* and *XhoI*) were then run on a 1% gel, extracted, and put into pCR2.1 TOPO TA cloning vectors, and were subsequently transformed into Top10 E. Coli chemical competent cells for cloning again, following previously described procedures.

3.2.5. Construction of rhesus macaque FcγR expression plasmid systems using pcDNA3.1(+) (HindIII/BamHI), as well as pcDNA3.1(+) (Not/Xho) and P2561/2/3 (Not/Xho) vectors

To create expression vectors, the newly RE-added FcγR cDNA gene fragments were excised from the pCR2.1-TOPO TA cloning vector clones with correct sequences by sequential digestion with *HindIII* and *BamHI* and cleaned up on a 1% agarose gel (Fig. 3.3). Plasmids were purified using the QIAprep spin miniprep kit (Qiagen Inc., Valencia, CA) and bands containing

Table 3.2. Primers used for generation of rhesus macaque FcγR recombinant DNA constructs by SOE-PCR amplifications.

Primer name[a]	Sequence (5'-3' direction)[b]	Specificity	Sequence characteristics[c]
FcγR.FHind (fw)	AGAT**AAGCTT**GAT***ATG*****GTGGCAGCTGCTCCTCCCA**	5'; FcγRIIIa	Containing *HindIII* site (5'-AAGCTT-3') Containing full 21-bp sequence of FCG3aF Containing an ATG start codon
FcγR.RBam (rv)	TCTA**GGATCC*****TCATTTGTCTTGA*****GGGTCCTT**	3'; FcγRIIIa	Containing *XhoI* site (5'-GGATCC-3') Containing full 21-bp sequence of FCG3aR Containing a TGA stop codon
CD32.NotI (fw)	ATTA**GCGGCCGC**ATA***ATG***ACTATGGAGACCCAAATGTCTCA GAATGTATGTCCCAGAAACCTGTGGCTGCTTCAACCATTGAC AG***TTTTGCTGCTGCTGGCTTCTGC***	5'; FcγRII	Containing *NotI* site (5'-GCGGCCGC-3') Containing full 22-bp sequence of CD32.1 Containing an ATG start codon
CD32.XhoI (rv)	ACTCGA**CTCGAG**TTATTAGTTATTACTGT***TGA*****CATGGTCGTT GGGAGGAAG**	3'; FcγRII	Containing *XhoI* site (5'-CTCGAG-3') Containing full 22-bp sequence of CD32.8 Containing a TGA stop codon
CD64.NotI (fw)	ATTA**GCGGCCGC**ATA***ATG***TGGTTCTT***GACAGCTCTGCTCCTT TGGGTTC***	5'; FcγRI	Containing *NotI* site (5'-GCGGCCGC-3') Containing full 23-bp sequence of CD64.1 Containing an ATG start codon
CD64.XhoI (rv)	ACTCGA**CTCGAG**TTATTACTACGTGGCCCCCTGGGGCTCCTT CCGGTGCACCCCTTCCTGCAGCTGTTCTTCTTTTTGTTCCTGA CATTTCAGCTCTTCTTCTA***AATGTCTGTCTTCTTGAAGGCTGG***	3'; FcγRI	Containing *XhoI* site (5'-CTCGAG-3') Containing full 24-bp sequence of CD64.10 Containing a TGA stop codon

[a]fw, forward direction; rv, reverse direction.

[b]Bold and underline, restriction endonuclease sequences; bold and italic, with or without underline, overlapping ("homologous") region with the relevant primer indicated in "Sequence characteristics" column.

[c]An (ATG) start codon needed for proper initiation of translation and a stop (TGA) codon necessary for proper termination.

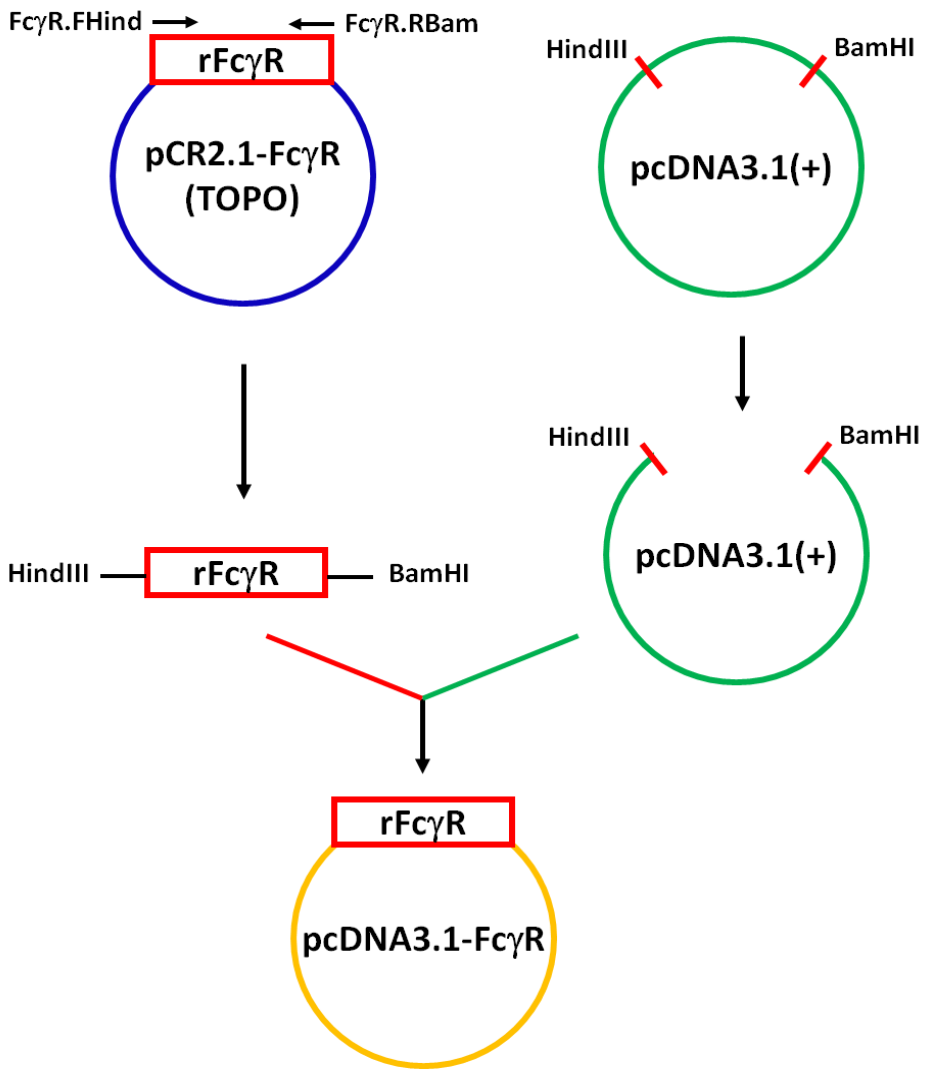

Fig. 3.3. Schematic representation of major steps in generation of recombinant expression plasmid vector pcDNA3.1-FcγR-*Hind/Bam* (not drawn to scale). The FcγR constructs were PCR-amplified from the appropriate TOPO vectors using forward primer FcγR.FHind (containing *HindIII* restriction site in its 5' end) and reverse primer FcγR.RBam (containing *BamHI* restriction site in its 5' end), as indicated. Resultant PCR products were then incorporated into pcDNA3.1 vector previously digested with both *HindIII* and *BamHI* REs. Recombinant constructs are therefore encoded within the *HindIII-BamHI* sites of resulting recombinant expression vector.

FcγR DNAs of the correct size were extracted using a QIAquick gel extraction kit (Qiagen Inc., Valencia, CA). The extracted cDNAs were then cloned into the *HindIII*- and *BamHI*-digested (i.e. within the multiple cloning site) expression vector pcDNA3.1(+), which contain SV40 ori and CMV promoter (Invitrogen, Carlsbad, CA). Similar procedures were applied on expression vectors pcDNA3.1(+) and P2561/2/3 using *NotI* and *XhoI* instead of *HindIII* and *BamHI* REs, as appropriately (Fig. 3.4). Ligations were performed using T4 DNA ligase (Roche Diagnostics North America, Indianapolis, IN) overnight at 14^0C. Resultant FcγR expression vectors were then transformed into Top10 E. Coli chemical competent cells (Invitrogen, Carlsbad, CA) by heat shock, as previously described in production of recombinant IgGs. Miniprep DNAs derived from the colonies were screened for successful insertion and correct orientation by PCR and RE digestions of plasmids using appropriate enzymes, followed by confirmation by DNA sequencing in both forward and reverse directions across fusion points with selected FcγR primers (and/or pcDNA3.1 T7 and T7 reverse primers). All constructs verified by sequence analysis were produced in large quantities of expression vectors using EndoFree Plasmid Maxi kits (Qiagen Inc., Valencia, CA), to be used for transfection into HeLa cells by electroporation method.

3.2.6. Sequence analysis

MacVector software (Accelrys Inc., San Diego, CA) and BioEdit program (http://www.mbio.ncsu.edu/bioedit/bioedit.html) were used to identify overlapping regions and edit sequences. Sequences were aligned with each other within the same receptor group and with other known counterparts using the CLUSTAL function of the MEGALIGN, part of the LASERGENE software package (DNASTAR Inc., Madison, WI). Construction of the

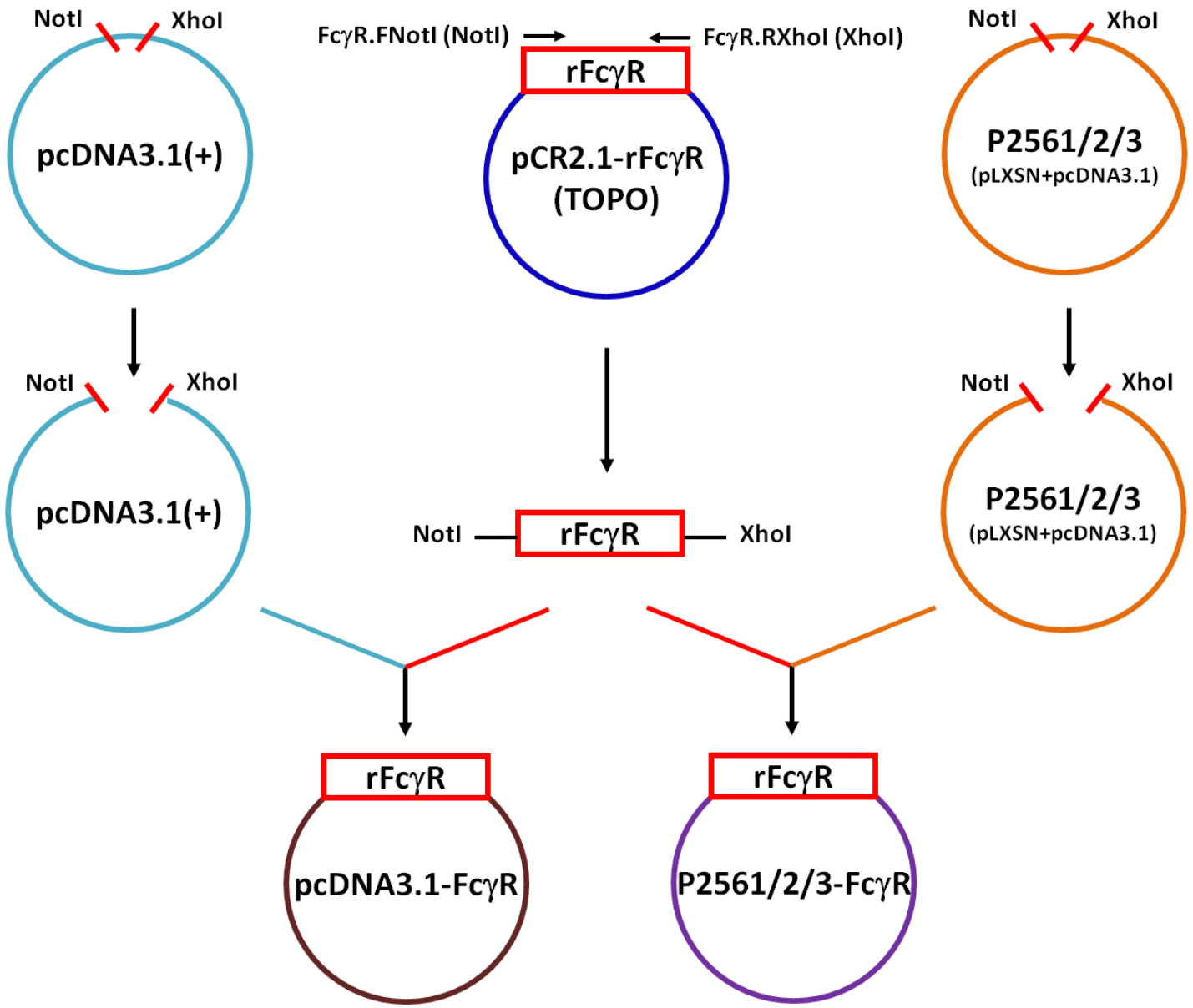
NotI
XhoI
pcDNA3.1(+)
FcγR.FNotI (NotI)
FcγR.RXhoI (XhoI)
rFcγR
pCR2.1-rFcγR
(TOPO)
NotI
XhoI
P2561/2/3
(pLXSN+pcDNA3.1)
NotI
XhoI
pcDNA3.1(+)
NotI
rFcγR
XhoI
NotI
XhoI
P2561/2/3
(pLXSN+pcDNA3.1)
rFcγR
pcDNA3.1-FcγR
rFcγR
P2561/2/3-FcγR

Fig. 3.4. Schematic representation of major steps involved in generation of the recombinant expression plasmid vectors pcDNA3.1-FcγR-*NotI/XhoI* and P2561/2/3-FcγR (not drawn to scale). The FcγR constructs were PCR-amplified from the appropriate TOPO vectors using forward primer FcγR.NotI (containing *NotI* restriction site in its 5' end) and reverse primer FcγR.XhoI (containing *XhoI* restriction site in its 5' end), as indicated. Resultant PCR products were then ligated into pcDNA3.1(+) or P2561/2/3 vectors previously digested with both *NotI* and *XhoI* REs. The recombinant constructs are therefore encoded within the *NotI-XhoI* sites of resulting recombinant expression vectors.

phylogenetic tree was also based on the use of the LASERGENE's MEGALIGN part. Prediction of potential glycosylation site was performed online using EnsembleGly website (http://turing.cs.iastate.edu/EnsembleGly/; Caragea et al., 2007). Standardized nomenclature, labels, and numbering of IMGT®, the international ImMunoGeneTics information system® (http://www.imgt.org) (Lefranc et al., 2009) were used to display and discuss sequencing data based on human reference sequences. Allelic polymorphisms and characteristic positions of the C-like domains were described using the IMGT unique numbering for C domain (C-DOMAIN of IG and T cell receptors (TR) and C-LIKE-DOMAIN of IgSF other than IG and TR) (Lefranc et al., 2005).

3.3. Results

We identified macaque FcγR at the cDNA level and examined whether allelic polymorphisms were present by analyzing PCR-amplified cDNA sequences. These sequences were obtained from reverse transcription of whole blood total RNA extracts, followed by PCR amplification using primers complementary to human sequences located within the beginning L and the ending CO-TM-CYT exons. All PCR amplifications were successful in each of the nine animals examined. The introduction of PCR artifacts was minimized by the use of a high-fidelity polymerase with proofreading ability, and by carrying out separate PCRs and multiple clone selections for each individual animal. The cDNA sequences determined in the present study are available as GenBank accession numbers HQ423386- HQ423388 (FcγRIII), HQ423389-HQ423393 (FcγRII), and HQ423394-HQ423396 (FcγRI).

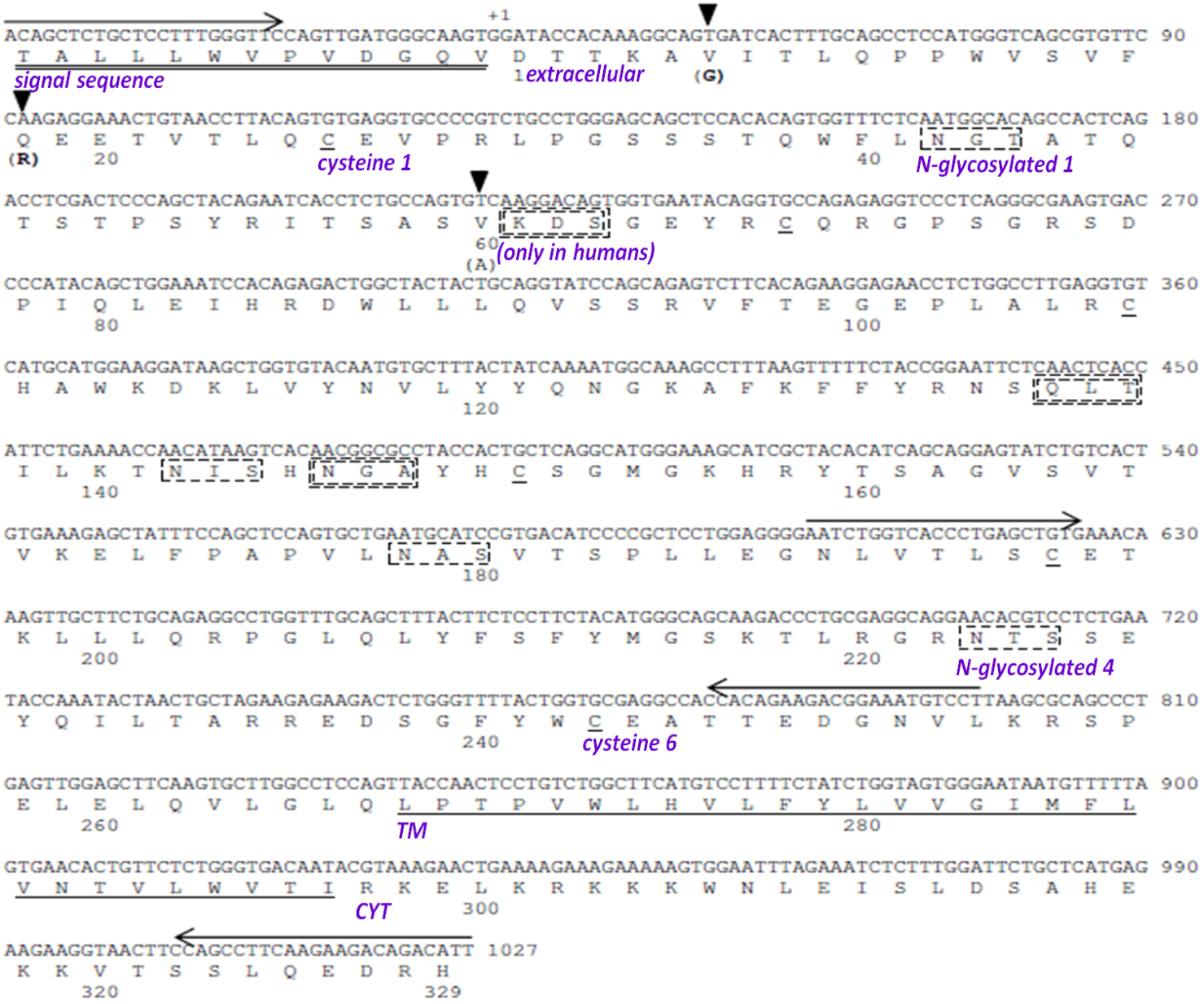
signal sequence
extracellular
(G)
(R)
cysteine 1
N-glycosylated 1
(only in humans)
(A)
N-glycosylated 4
cysteine 6
TM
CYT

Fig. 3.5. Nucleotide and deduced amino acid sequences of rhesus macaque Fcγ receptor I (FcγRI, CD64) (GenBank accession number: HQ423396). Nucleotides are numbered at right and amino acids are numbered throughout. The amino acid numbering is in accordance with the IMGT unique numbering system for Ig C-like domains (Lefranc et al., 2005). Following the N-terminal signal sequence (a 13 amino acid part is shown doubly underlined) is the extracellular portion of ~270 amino acids in length. The predicted start site of the mature protein is indicated by the number "1" below the amino acid A. +1, above the nucleotide sequence, indicates the start of the extracellular chain. Underlined Cs indicates cysteines (n=6) that have potential to form intra-chain disulfide bonds. Potential N-linked glycosylation sites (n=4; Caragea et al., 2007) (N-x-S/T) are represented by single-line broken boxes. Boxes with broken double line (n=3) denote potential N-linked glycosylation sites recognized in humans only. The underlined sequence represents the CO-TM region. The two over-line arrows at the beginning and the end of the nucleotide sequence represent the binding regions and directions for the designed CD64.1 (forward) and CD64.10 (reverse) primers, respectively. The other two over-line arrows in the middle of the sequence denote internal primers [CD64.9 (forward) and CD64.4 (reverse), in that order]. Arrowheads indicate the allelic positions at which the polymorphic residues (represented by amino acids displayed below and in parentheses) identified in this work are present.

3.3.1. Rhesus macaque FcγRI (CD64) and FcγRII (CD32) cDNA clones exhibit the typical mRNA primary structure of their human counterpart

Using the primer sets which were designed based on human FcγRII gene sequences, we identified an almost full-length macaque FcγRII homologue cDNA. The molecule contains 865 bp, encoding a 288-amino acid protein (Fig. 3.6; shown is a representative sequence). The structure of the deduced amino acid sequence was inferred by analogy to published human sequences. It was found extensively similar to that described for human FcγRIIa mRNA structure, typical of type I membrane IgSF C-like domain proteins. The first 12-amino acid stretch, which formed the partial putative N terminal leader (L) region, is followed by a predicted mature protein. The mature protein is composed of an extracellular portion of 176 amino acids, which, as previously described for the human counterpart receptor, contains two extracellular domains, namely [D1] and [D2].

As expected, four cysteines (C26, C68, C107, and C151), that have potential to form the characteristic C-like intradomain disulfide bonds, are conserved in the extracellular portion (1st-CYS 23 and 2nd-CYS 104 in the IMGT unique numbering; Lefranc et al., 2005). The conserved C-like domain structure suggests that disulfide bonds are formed between C26 and C68 and between C107 and C151 in [D1] and [D2], respectively. The conserved C-like extracellular portion is followed by a relatively short segment of 32 amino acids (AA) that, by analogy to human CD32a, represents the connecting region (CO) of 10 AA and the transmembrane region (TM) of 22 AA. The remaining amino acids of the deduced sequence form the partial C-terminal cytoplasmic (CYT) region. Three potential N-linked glycosylation sites are conserved between humans and macaques, two of which, [D1] N97 and [D2] N95 (IMGT unique numbering; Lefranc et al., 2005) are present in the extracellular portion, whereas the third one, [CYT] N10,

located in the CYT region, has probably no functional significance (Table 3.3). Macaques carry two additional N linked glycosylation sites [D2] N77 and N88 (resulting from amino acid changes) compared to humans (Table 3.3 and Fig. 3.6). However, these two positions are polymorphic: the first one, [D2] 77, in rhesus macaques, the N glycosylation site being or not present, whereas the second one, [D2] 88, is polymorphic in humans, and may have an N-glycosylated site as shown in the '2fcb' 3D structure (IMGT/3Dstructure-DB; Ehrenmann et al. 2010). As in humans, two YxxL signatures, separated by 11 amino acids and representing a typical immunoreceptor tyrosine-based activation motif (ITAM; YxxLx(7–12)YxxL), are present in the CYT region.

Similar to FcγRII, macaque FcγRI cDNA clones also show a typical human FcγRI mRNA organization (Fig. 3.5). The obtained 1,027-bp-encoded 342-amino acid polypeptide starts with a putatively partial leader region of 13 residues, followed by the extracellular region consisting of three domains [D1], [D2], and [D3] and is 267 amino acids in length, ending with a CO region (7AA), a TM region (23 AA) and a partial CYT region. As in humans, six cysteines (C26 and C68, C107 and C151, as well as C195 and C243), each pair of which (1st-CYS 23 and 2nd-CYS 104 in the IMGT unique numbering; Lefranc et al., 2005) forms disulfide bonds of the [D1], [D2] and [D3] domain, respectively, are conserved in macaques. However, only four potential N-linked glycosylation sites, [D1] N44, [D2] N95, [D3] N6 and N80 (Table 3.3 and Fig. 3.5), are present in macaques as compared to the seven present in humans.

Together, these results show that rhesus macaque FcγRII and FcγRI cDNA clones exhibit the typical mRNA primary structure/organization of their corresponding human receptor.


+1
signal sequence
extracellular portion
cysteine 1
N-glycosylated 1
(not in humans)
cysteine 4
TM
CYT
N-glycosylated 5
ITAM

Fig. 3.6. Nucleotide and deduced amino acid sequences of rhesus macaque Fcγ receptor II (FcγRII, CD32) (GenBank accession number: HQ423393). Nucleotides are numbered at right and amino acids are numbered throughout. The amino acid numbering is in accordance with the IMGT unique numbering system for Ig C-like domains (Lefranc et al., 2005). Following the N-terminal signal sequence (a 12 amino acid part is shown doubly underlined) is the extracellular portion of ~180 amino acids in length. The predicted start site of the mature protein is indicated by the number "1" below the amino acid A. +1, above the nucleotide sequence, indicates the start of the extracellular chain. Underlined Cs (n=4) indicates cysteines that have the potential to form intra-chain disulfide bonds. Potential N linked glycosylation sites (n=5; Caragea et al., 2007) (N-x-S/T; x denotes any amino acid) are represented by broken boxes, of which those with broken double-line (n=2) denote potential N-linked glycosylation sites not recognized in humans. The underlined sequence corresponds to the CO-TM region. Closed boxes illustrate the two YxxL signatures, separated by 11 amino acids in the intracellular cytoplasmic tail, which represent a typical immunoreceptor tyrosine-based activation motif (ITAM; YxxLx(7–12)YxxL) in the molecule. The two over-line arrows at the beginning and the end of the nucleotide sequence represent the binding regions and directions for the designed CD32.1 (forward) and CD32.8 (reverse) primers, respectively. The other two over-line arrows in the middle of the sequence denote internal primers [CD32.3 (forward) and CD32.2 (reverse), in that order]. Arrowheads indicate the allelic positions at which the polymorphic amino acids (represented by amino acids displayed below and in parentheses) identified in this work are present. The closed black circle indicates a functional polymorphic amino acid in human CD32 (131 H/R), known to define the specificity of human CD32 for IgG2.

3.3.2. The rhesus macaque CD64 and CD32 extracellular C-like, ligand-binding portion shares high homology with that of human CD64 and, to a lesser degree, CD32, respectively

We compared the FcγRI and FcγRII deduced amino acid sequences obtained from all nine macaques examined with the corresponding sequences in humans. The IMGT Collier de Perles representation of CD32 and CD64 [D1] and [D2] domains are shown in Fig. 3.7. This representation allows to locate amino acids within a topological context by bridging the gap between linear amino acid sequences and 3D structures (Kaas et al., 2007). Figures 3.9, 3.10, 3.11, and 3.12 show that rhesus macaque deduced proteins display totally conserved intron–exon boundaries and exhibit high homology in sequence compared to their human counterparts. For the extracellular portion alone, amino acid comparisons between these two primate species revealed a high level of similarity, which were ~88–90% for CD32 (18–22 changes in the entire 176-amino-acid extracellular region) and ~94–95% for CD64 (14–16 changes in the entire 267-amino-acid extracellular region) (percentage ranged depending on the alleles considered in comparison). For macaque CD32, these amino acid differences are distributed equally (n=8 to 11) between [D1] and [D2] domains (Fig. 3.10). However, for CD64, while each of the two first domains [D1] and [D2] show relatively equivalent number (n=6 to 8) of amino acid differences(compared to humans), its third domain [D3] displays the least change (n=2) (Fig. 3.9). The TM region in macaque CD32 and CD64 share ~83% (number of amino acid differences, n=5) and 93% (n=2) identity with that in humans, respectively. Thus, the number of macaque/human amino acid differences in these two receptors is substantially lower in the TM region than in the C-like domains.No attempt was made for comparing the L or CYT region sequences, as when designing primer sets, we did not aim to confirm the full length of the receptors (several residues at L and CYT terminals were not present in the final cloning

products). As mentioned above, two additional potentially glycosylated N are observed in macaque CD32 (Fig. 3.6). In contrast, two residues of this type are replaced by other amino acids in CD64 (Fig. 3.5). Furthermore, replacement of human [D2] T101 (148) in CD64 with A in macaques results in breaking of the potential N-linked glycosylation motif of [D2] N99 in the receptor. These amino acid changes are present in all animals examined, with the exception of the polymorphic amino acid CD32 [D2] 77 (128 in sequence).

All but one of the human CD32a amino acids known to be crucial for IgG binding (Maxwell et al., 1999) are conserved in macaque CD32. These residues include: [D2] K29 and P30 (BC loop), S79 and D82 (D strand), and Y113 (FG loop) (113, 114, 130, 133, and 157 in sequence, respectively), which presumably directly contact the IgG Fc ligand; [D2] L36, P87 and I108 (115, 134, and 155 in sequence), which presumably have the ability to affect conformation of the loops; [D2] H80 (131 in sequence) (D strand), the established low-responder polymorphic allele (Fig. 3.6). The only exception is at position [D2] 81 (132 in sequence): it is L in humans but M in macaques. [D2] M81 is found in all nine macaques examined. It is noteworthy that all nine examined macaques display [D2] H80 (131 in sequence) (Fig. 3.10), the well known IgG2 low-responder polymorphic allele in humans (Warmerdam et al., 1991). Because no human CD64a crystal structure has been solved to date (Ellsworth et al., 2010), and thus no specific residues crucial for ligand binding have been established, it is not possible to identify potential conserved IgG-binding amino acids in the macaque CD64 sequence. However, at least three binding interface residues in [D2], W3, W26, and K77 (87, 110, 128 in sequence) found to be totally invariant among all human FcγRs (Radaev et al., 2001), are completely conserved in all nine macaque CD64 proteins (Fig. 3.9). These amino acids are also conserved in most macaque CD32 proteins examined (Fig. 3.10).

Table 3.3. Correspondence between sequence positions and IMGT unique numbering for potential N-linked glycosylation sites in rhesus macaque FcγRs[a].

Position	CD32 domains					CD64 domains			
	[D1]		[D2]		[CYT]	[D1]	[D2]	[D3]	
In sequences	61	128	135	142	213	42	142	178	223
In IMGT	97	77	88	95	10	44	95	6	80
Compared to human	Conserved	Polymor-phic	Polymor-phic	Conserved	Conserved	Conserved	Conserved	Conserved	Conserved

[a]Abbreviation and full gene designations are the following: FcγRI: IgG Fc high affinity I receptor (CD64); FcγRII: IgG Fc low affinity II receptor (CD32); FcγRIII: IgG Fc low affinity III receptor (CD16).

Table 3.4. Location and type of allelic polymorphism present in rhesus macaque FcγRs[a].

FcγR (total novel polymorphism)[c]	[D1] amino acid positions (number of animals)[b]							[D2] amino acid positions (number of animals)						
	6 (5)[d]	18 (15.2)	55 (90)	60 (96)	75 (117)	79 (121)	92 (8)	93 (9)	119 (40)	125 (46)	126 (47)	128 (77)	133 (82)	140 (93)
CD16 (2)	-----	-----	-----	-----	L/P (1)	-----	A/T (2)	-----	-----	-----	-----	-----	-----	-----
CD32 (9)	-----	-----	M/R (4)	-----	-----	V/I (1)	-----	T/P (3)	A/T (1)	K/I (5)	S/A (1)	N/K (5)	N/D (4)	Q/R (4)
CD64 (3)	V/G (1)	Q/R (1)	-----	V/A (1)	-----	-----	-----	-----	-----	-----	-----	-----	-----	-----

[a]Abbreviation and full gene designations are the following: FcγRI: IgG Fc high affinity I receptor (CD64); FcγRII: IgG Fc low affinity II receptor (CD32); FcγRIII: IgG Fc low affinity III receptor (CD16).

[b]Number of individual animals (among of the nine animals examined) whose sequences exhibit polymorphism.

[c]Number of novel allelic polymorphic amino acids that were identified in this work.

[d]Numbers in parentheses indicate the IMGT positions per domain (Lefranc et al., 2005).

Together, these data show that the extracellular C-like, ligand-binding portion of rhesus macaque CD64 and CD32 shares extensive homology with that of human CD64 and, to a lesser degree, CD32, respectively.

3.3.3. A relatively high level of intra-species polymorphism is present in macaque FcγR sequences

Nine (M55R, V79I, T93P, A119T, K125I, S126A, N128K, N133D, and Q142R) or three (V6G, Q18R, and V60A) allelic polymorphic residues were identified from all examined macaque FcγRII or FcγRI alleles, respectively (Table 3.4). In CD64, all variable residues occur in membrane-distal [D1], whereas in CD32, most (seven out of nine) allelic polymorphic sites are clustered on a short segment in the membrane-proximal [D2] domain (Table 3.4, Fig. 3.10, and Fig. 3.12). Unlike FcγRII and FcγRI, the macaque FcγRIII sequence and a number of its allelic polymorphisms have recently been described (Miller et al., 2007; Rogers et al., 2006b). In the present study, two previously unreported CD16 allelic variants at the amino acid level were identified from the nine macaques examined: most macaques carry [D1] L117 (75 in sequence) and [D2] A8 (92 in sequence), whereas one of the animals exhibits [D1] P117 and two animals exhibit [D2] T8 in their CD16 domains (Table 3.4, Fig. 3.11, and Fig. 3.12).

Among the nine macaques examined, five (CD32) and three (CD64 and CD16) distinct allelic sequences, differing by at least one amino acid, were recognized (Fig. 3.9 and 3.10, and data not shown).

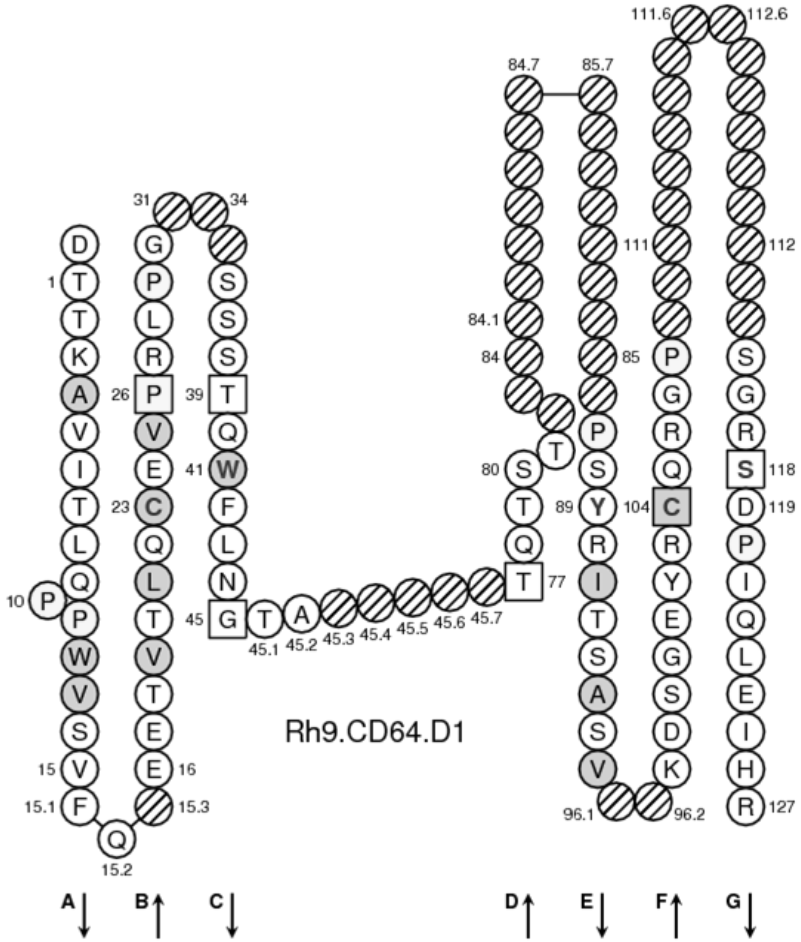
Rh9.CD64.D1
A
B
C
D
E
F
G

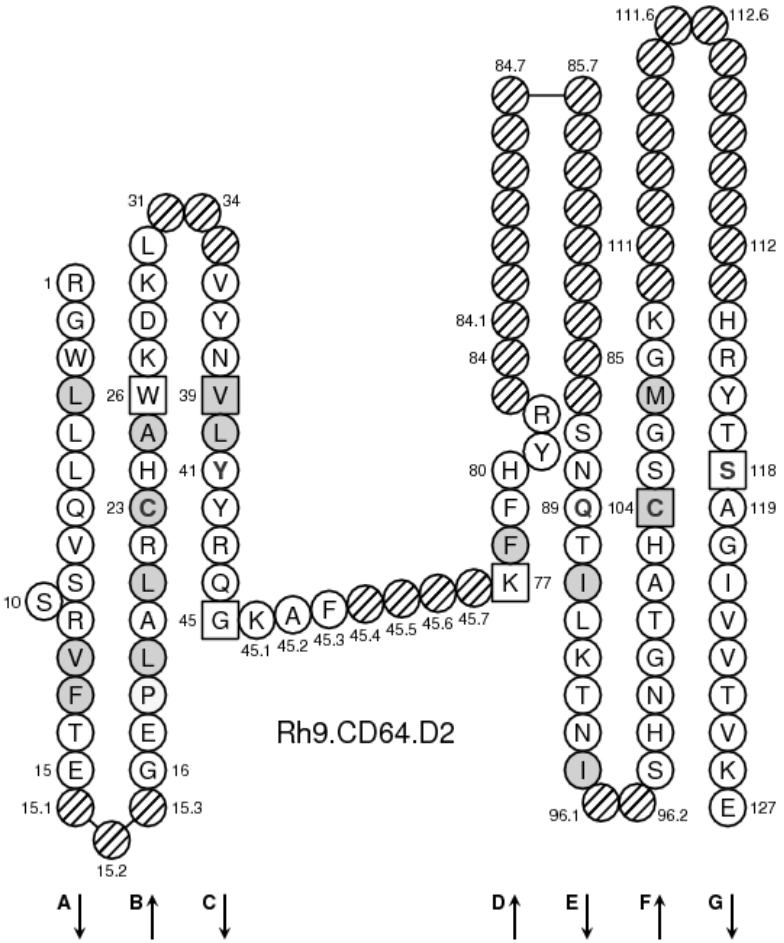
Rh9.CD64.D2
A
B
C
D
E
F
G

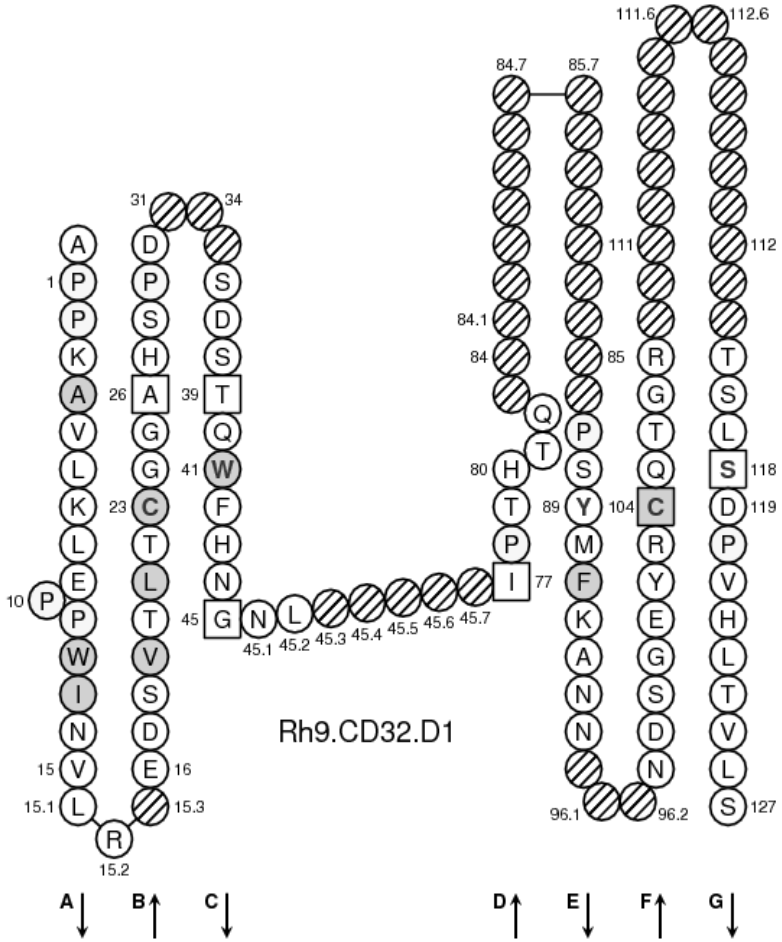
Rh9.CD32.D1
A
B
C
D
E
F
G

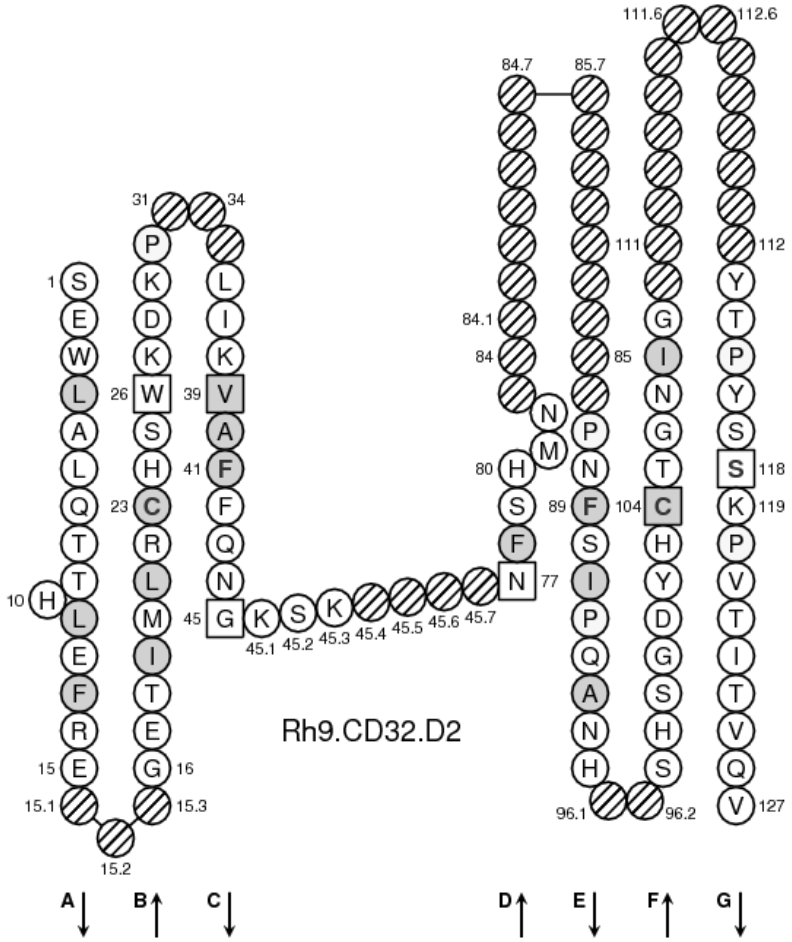
Rh9.CD32.D2
A
B
C
D
E
F
G

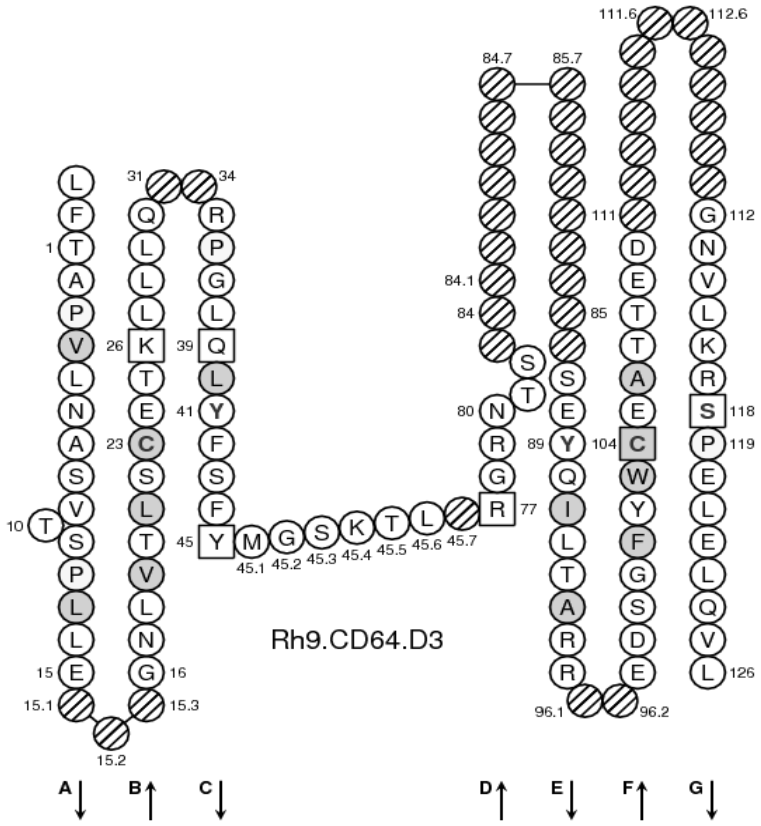

Fig. 3.7. IMGT Colliers de Perles of rhesus macaque CD32 (FcγRII) C like [D1] (I), and [D2] (II) as well as CD64 (FcγRI) C-like [D1] (III), [D2] (IV) and [D3] (V) domains (on one layer; obtained with the IMGT/Collier-de-Perles tool in the IMGT/DomainGapAlign) (Ehrenmann et al., 2010). Colliers de Perles is the 2D graphical representations of IG and TR V, C domains, highlighting conserved amino acids. The conserved C (position 23), and C (position 104), are indicated. Shaded circles or squares represent positions at which hydrophobic amino acids (I, V, L, F, C, M, A) and W are found in more than 50% of analyzed IgSF sequences. The BC loop, CD transversal strand, and FG loop are limited by amino acids displayed in squares. Hatched circles indicate missing positions according to the IMGT unique numbering for C-DOMAIN and C-LIKE-DOMAIN (Lefranc et al., 2005). Arrows indicate the beta-strand direction.

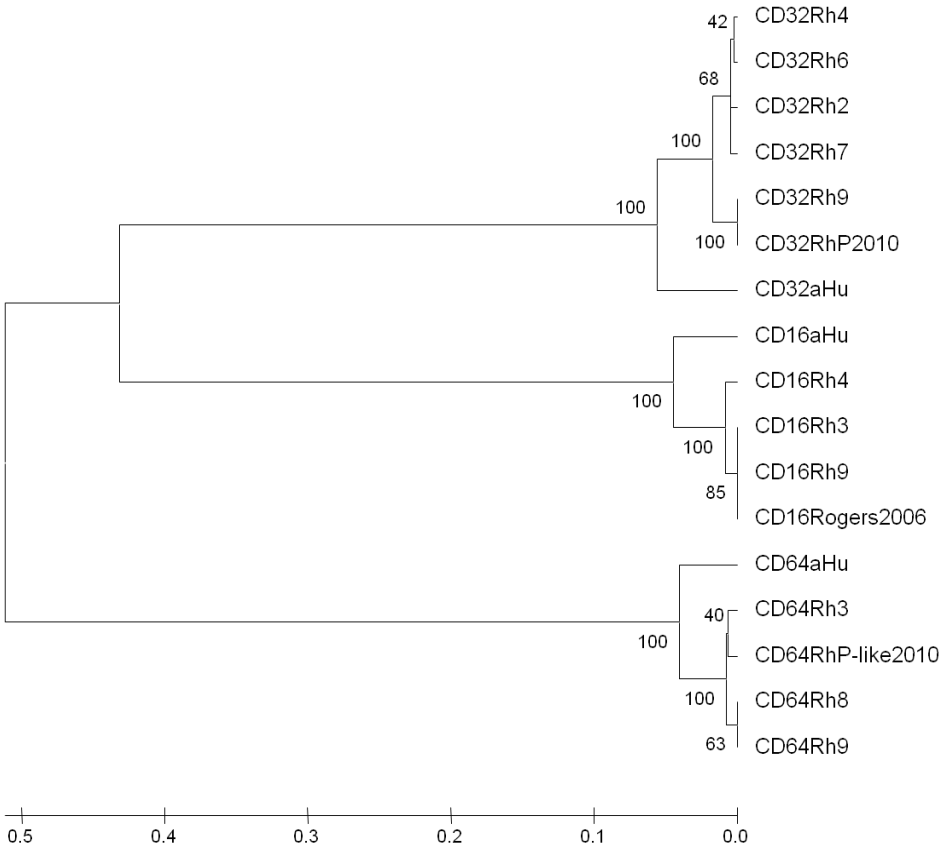

Fig. 3.8. A phylogenetic tree indicating the amino acid sequence similarity among independent allelic variants of macaque FcγR molecules identified in this study. Also included are a representative human corresponding receptor and a computationally predicted CD32 and CD64-like sequences (see Figures 3.5 and 3.6 for GenBank accession numbers of these sequences). Phylogenetic distances were computed from the CD32 and CD64 amino acid sequences aligned in Figures 3.6 and 3.5. For CD16, a representative human ("CD16aHu"; GenBank accession number: AK291451.1) and macaque CD16 are included ("CD16Rogers2006"; GenBank accession number: ABD83659). The numbers next to the branches indicate the percentage of replicate trees. The evolutionary distance bar denotes the number of substitutions per site.

```
                        A        AB     B          BC        C     CD       D        E          F        FG           G
                     (1-15)           (16-26)   (27-38)   (39-45)        (77-84)  (85-96)    (97-104) (105-117)   (118-128)
                    ──────────────>  ──────────>          ──────>        ──────>  ──────────>  ──────>           ──────────>
                    1         10  15  16      26  27      36  39   45       77   84  85 89    96 97    104 105       117 118    127
             87654321 | ........|....|123|.........| |........|  |.....|1234567|......| |...|......| .......| |...........| |.........|
Human D1        D T TKAVITLQPPWVSVFQ.EETVTLHCEVL HLPG...SSS  TQWFLNGTA.....TQTST... ..PSYRITSASV NDSGEYRC QRGL......SGR SDPIQLEIHR
Rhe9  D1        - - ----------------.------Q---P R---...---  ---------.......-----.. ..---------- K------- ---P......--- ----------
Rhe3  D1        - - ---G------------.------Q---P R---...---  ---------.......-----.. ..----------A K------- ---P......--- ----------
Rhe8  D1        - - ---------------R.------Q---P R---...---  ---------.......-----.. ..---------- K------- ---P......--- ----------
RheP  D1        - - ---------L------.------Q---P R---...---  ---------.......-----.. ..----------A K------- ---P......--- ----------

Human D2          (G)WLLLQVSSRVFTE...GEPLALRCHAW KDKL...VYN  VLYYRNGKAF....KFFHWN.. ..SNLTILKTNI SHNGTYHC SGMGK....HRYT SAGISVTVKE
Rhe9  D2          (D)-------------...---------- ----...---  -----Q----....----YR.. ..--Q------- -----A-- -----....---- ----V-----
Rhe3  D2          (D)-------------...---------- ----...---  -----Q----....----YR.. ..--Q------- -----A-- -----....---- ----V-----
Rhe8  D2          (D)-------------...---------- ----...---  -----Q----....----YR.. ..--Q------- -----A-- -----....---- ----V-----
RheP  D2          (D)-------------...---------- ----...---  -----Q----....----YR.. ..--Q------- -----A-- -----....---- ----V-----

Human D3        LFT APVLNASVTSPLLE...GNLVTLSCETK LLLQ..RPGL  QLYFSFYMGSKTL.RGRNTS.. ..SEYQILTARR EDSGLYWC EAATED.GNVLKR SPELELQVL
Rhe9  D3        --- --------------...---------- ----..----  -------------.------.. ..---------- ----F--- --T---.------ ---------
Rhe3  D3        --- --------------...---------- ----..----  -------------.------.. ..---------- ----F--- --T---.------ ---------
Rhe8  D3        --- --------------...---------- ----..----  -------------.------.. ..---------- ----F--- --T---.------ ---------
RheP  D3        --- --------------...---------- ----..----  -------------.------.. ..---------- ----F--- --T---.------ ---------

Human CO-TM-CY  GLQLPTP VWFHVLFYLAVGIMFLVNTVLWV TIRKELKRKKKWDLEISLDSGHEKKVISSLQEDRH
Rhe9  CO-TM-CY  ------- --L------V------------ ------------N-------A-----T--------
Rhe3  CO-TM-CY  ------- --L------V------------ ------------N-------A-----T--------
Rhe8  CO-TM-CY  ------- --L------V------------ ------------N-------A-----T--------
RheP  CO-TM-CY  ------- --L------V------------ ------------N-------A-----T--------
```

Fig. 3.9. Alignment of the deduced amino acid sequences of rhesus macaque CD64 (FcγRI) (GenBank accession numbers: HQ423394-HQ423396) (obtained by cloning and sequencing whole blood cDNAs) with a human CD64a representative (shown as "Human"; GenBank accession number: AK291451.1). The deduced amino acid sequences of the macaque CD64 are compared and residues that differ from the human CD64a sequence are shown. Included are only macaque sequences carrying independent allelic polymorphic amino acids (n=3), in which each allele has a single polymorphic site or a unique combination of polymorphic sites. A computationally predicted macaque CD64-"like" ["RhesusP"; GenBank accession number (updated 6/1/2010): XR_013029] was also counted in. Hyphens illustrate identical residues and dots represent the IMGT gaps (missing amino acids) inserted to maximize alignment.

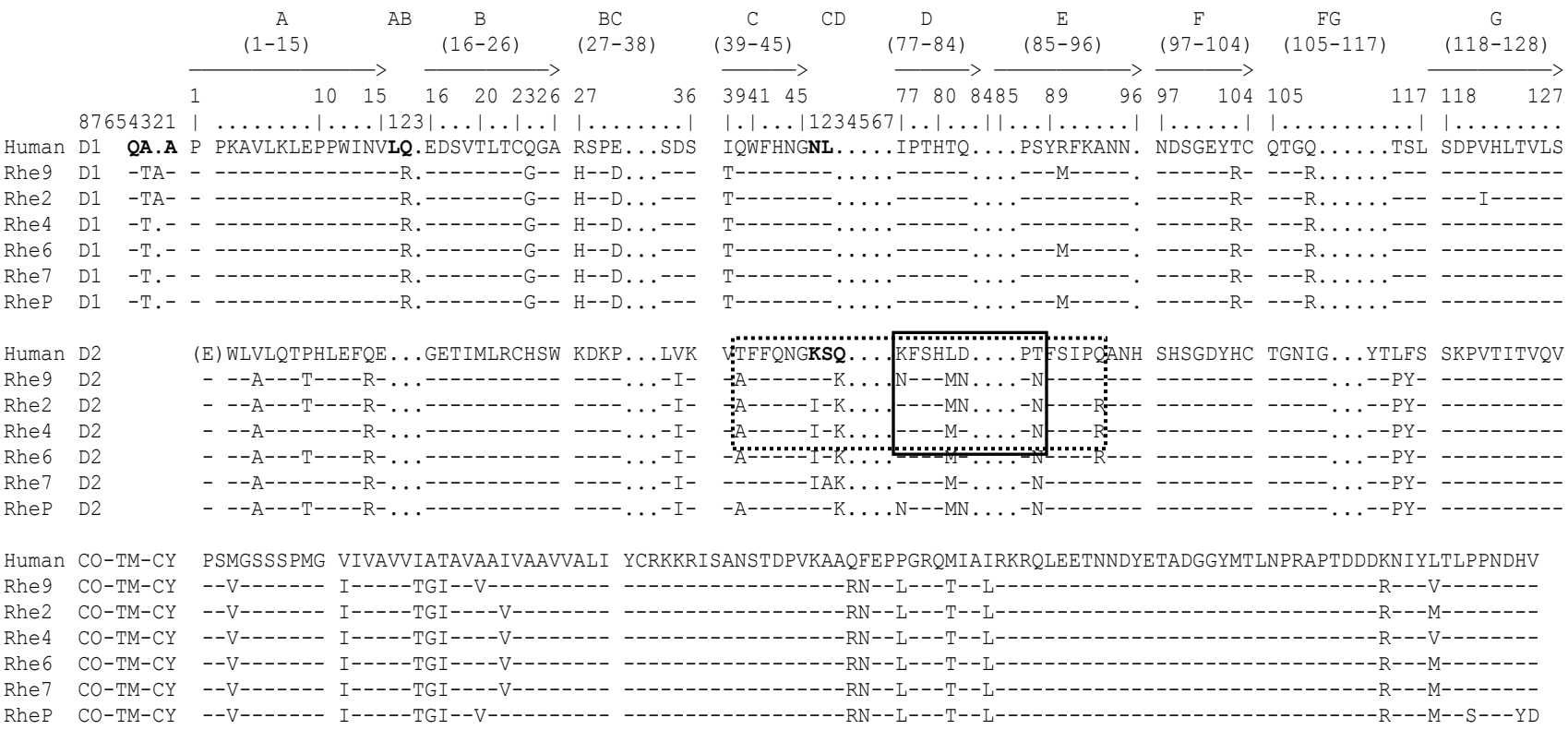
A (1-15) AB B (16-26) BC (27-38) C (39-45) CD D (77-84) E (85-96) F (97-104) FG (105-117) G (118-128)
Human D1 QA.A P PKAVLKLEPPWINVLQ.EDSVTLTCQGA RSPE...SDS IQWFHNGNL.....IPTHTQ....PSYRFKANN. NDSGEYTC QTGQ.....TSL SDPVHLTVLS
Rhe9 D1 -TA- - ----------R.--------G-- H--D...--- T--------.....------....---M-----. ------R- ---R......--- ----------
Rhe2 D1 -TA- - ----------R.--------G-- H--D...--- T--------.....------....---------. ------R- ---R......--- ---I------
Rhe4 D1 -T.- - ----------R.--------G-- H--D...--- T--------.....------....---------. ------R- ---R......--- ----------
Rhe6 D1 -T.- - ----------R.--------G-- H--D...--- T--------.....------....---M-----. ------R- ---R......--- ----------
Rhe7 D1 -T.- - ----------R.--------G-- H--D...--- T--------.....------....---------. ------R- ---R......--- ----------
RheP D1 -T.- - ----------R.--------G-- H--D...--- T--------.....------....---M-----. ------R- ---R......--- ----------
Human D2 (E)WLVLQTPHLEFQE...GETIMLRCHSW KDKP...LVK VTFFQNGKSQ....KFSHLD....PTFSIPQANH SHSGDYHC TGNIG...YTLFS SKPVTITVQV
Rhe9 D2 - --A---T----R-...---------- ----...-I- -A-------K....N---MN....-N-------- -------- -----...--PY- ----------
Rhe2 D2 - --A---T----R-...---------- ----...-I- -A-----I-K....----MN....-N----R--- -------- -----...--PY- ----------
Rhe4 D2 - --A--------R-...---------- ----...-I- -A-----I-K....----M-....-N----R--- -------- -----...--PY- ----------
Rhe6 D2 - --A---T----R-...---------- ----...-I- -A----I-K....----M-....-N----R--- -------- -----...--PY- ----------
Rhe7 D2 - --A--------R-...---------- ----...-I- -------IAK....----M-....-N-------- -------- -----...--PY- ----------
RheP D2 - --A---T----R-...---------- ----...-I- -A-------K....N---MN....-N-------- -------- -----...--PY- ----------
Human CO-TM-CY PSMGSSSPMG VIVAVVIATAVAAIVAAVVALI YCRKKRISANSTDPVKAAQFEPPGRQMIAIRKRQLEETNNDYETADGGYMTLNPRAPTDDDKNIYLTLPPNDHV
Rhe9 CO-TM-CY --V------- I-----TGI--V---------- ----------RN--L---T--L--------R---V--------
Rhe2 CO-TM-CY --V------- I-----TGI----V--------- ----------RN--L---T--L--------R---M--------
Rhe4 CO-TM-CY --V------- I-----TGI----V--------- ----------RN--L---T--L--------R---V--------
Rhe6 CO-TM-CY --V------- I-----TGI----V--------- ----------RN--L---T--L--------R---M--------
Rhe7 CO-TM-CY --V------- I-----TGI----V--------- ----------RN--L---T--L--------R---M--------
RheP CO-TM-CY --V------- I-----TGI--V---------- ----------RN--L---T--L--------R---M--S---YD

Fig. 3.10. Alignment of the deduced amino acid sequences of rhesus macaque CD32 (FcγRII) (GenBank accession numbers: HQ423389-HQ423393) obtained by cloning and sequencing whole blood cDNAs with a human CD32a representative (shown as "Human"; GenBank accession number: BC020823.1). The deduced amino acid sequences of macaque CD32 are compared and amino acids that differ from the human CD32a sequence are shown. Included are only macaque sequences carrying independent allelic polymorphic amino acids (n=5), in which each allele has a single polymorphic site or a unique combination of polymorphic sites. A computationally predicted macaque CD32 ["RhesusP"; GenBank accession number (updated 6/1/2010): XM_001118066.2] was also counted in. Hyphens indicate identical residues and dots represent the IMGT gaps (missing amino acids) inserted to maximize alignment. The broken-line box represents the region where macaque polymorphic sites are clustered. The unbroken-line box indicates the eight-amino acid stretch bearing multiple N substitutions (see text for details).

Thus, these results suggest a relatively high level of intra-species heterogeneity of CD32 and, to a lesser extent, CD64 and CD16, in rhesus macaques.

3.3.4. Susscessful generation of recombinant FcγR gene cDNA constructs as well as their cloning and expression vectors

The cDNAs that encode the extracellular domains of rhesus macaque CD64, CD32, and CD16, were successfully annealed and amplified by PCRs or SOE-PCRs (Fig. 3.13). These cDNA constructs were subsequently ligated properly into pCR2.1 TOPO TA cloning. Sequencing-verified cloning vectors were digested with appropriate REs to release each FcγR, which was subsequently subcloned into pcDNA3.1(+) (Invitrogen, Carlsbad, CA) on *HindIII* and *BamHI* RE sites, downstream of and in-frame with the promoter sequence, yielding the constructs pcDNA3-FcγRs-Hind-Bam (Fig. 3.3). Similar procedures were carried out for pcDNA3.1(+) (Invitrogen, Carlsbad, CA) and *NotI* and *XhoI* REs, creating pcDNA3-FcγRs-*Not*-*Xho* recombinant expression vectors (Fig. 3.4). Additional expression plasmids, termed P2561/2/3-FcγRs-*Not*-*Xho*, were also made by ligating the *NotI*-*XhoI*-digestive FcγR cDNAs into P2561/2/3 plasmids excised with the same REs (Fig. 3.4).

The insert was verified for correct size and proper orientation by RE digestion (Fig. 3.13). RE analysis using *EcoRI*, *HindIII* and *BamHI* pair, as well as *NotI* and *XhoI* pair, revealed agarose gel band(s) [a double band pattern was observed when the FcγR cDNAs also contained the same RE site(s)] corresponding to the expected molecular weight/size of about 1.1, 0.9, or 0.8 kb for CD64, CD32, or CD16, respectively, indicating that each of the constructs has been inserted into the expression vectors (Fig. 3.13). Selected recombinant plasmids were subsequently produced in large quantities using EndoFree Plasmid Maxi kits (Qiagen Inc.,

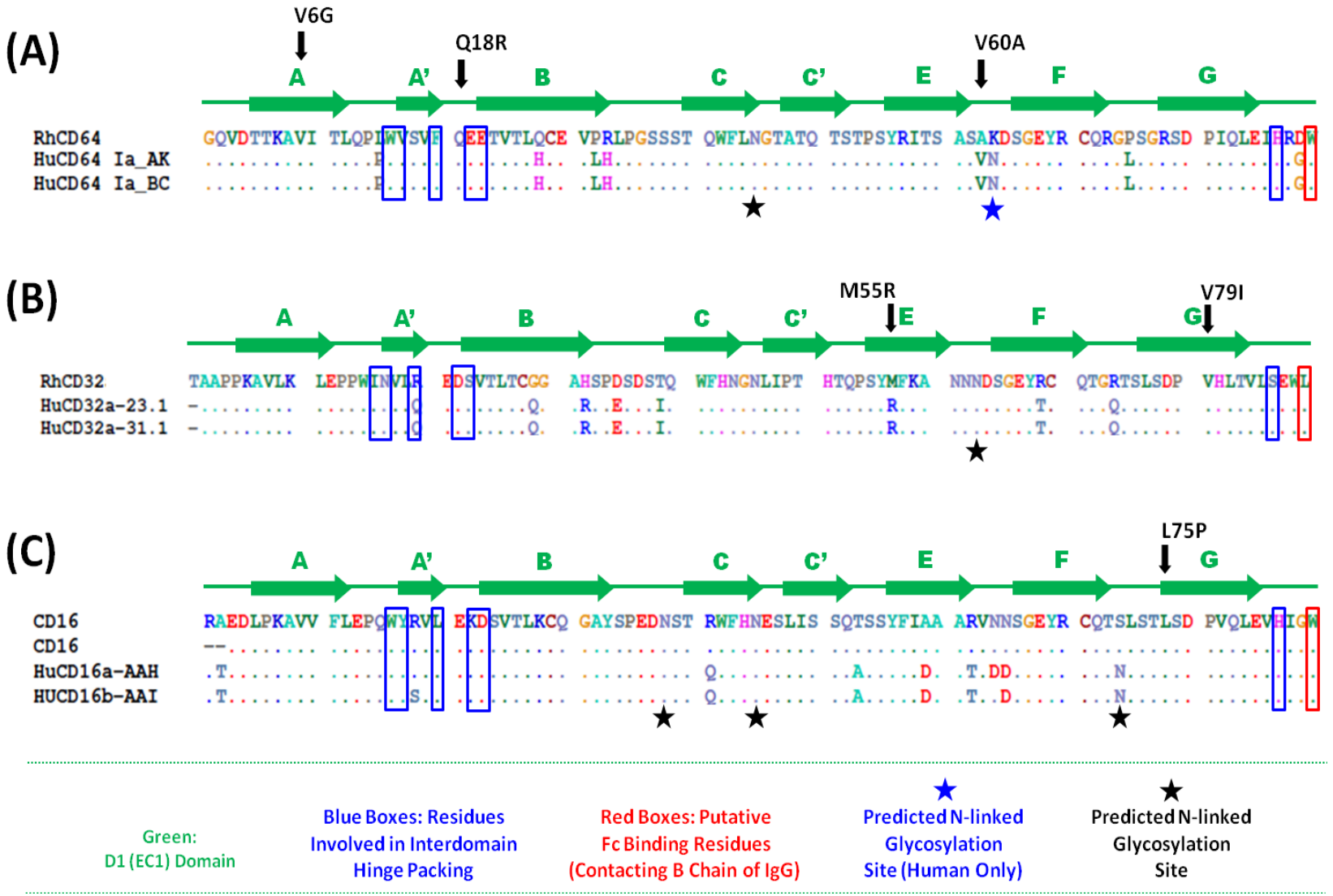
(A)
V6G
Q18R
V60A
A
A'
B
C
C'
E
F
G
RhCD64
HuCD64 Ia_AK
HuCD64 Ia_BC
(B)
M55R
V79I
RhCD32
HuCD32a-23.1
HuCD32a-31.1
(C)
L75P
CD16
CD16
HuCD16a-AAH
HUCD16b-AAI
Green: D1 (EC1) Domain
Blue Boxes: Residues Involved in Interdomain Hinge Packing
Red Boxes: Putative Fc Binding Residues (Contacting B Chain of IgG)
Predicted N-linked Glycosylation Site (Human Only)
Predicted N-linked Glycosylation Site

Fig. 3.11. Schematic representation illustrating the extracellular domain 1 ([D1], or EC1) putative secondary structure of a representative sequence from each of three rhesus macaque FcγR classes in alignment with those in humans: no variation at known human functional positions is found in the animal molecules. (A) FcγRI (CD64), (B) FcγRII (CD32), (C) FcγRIII (CD16). The black texts above each sequence secondary structure depict the variations found in rhesus macaques, with the vertical arrows showing their relative positioning. Blue boxes, residues involved in interdomain hinge packing; red boxes, putative Fc binding residues (contacting B chain of IgG); blue star, predicted N-linked glycosylation site (human only); black star, predicted N-linked glycosylation site. Rh, rhesus macaque; Hu, human. These representations were constructed based on Radaev et al., 2001; Zhang et al., 2000; and Maxwell et al., 1999.

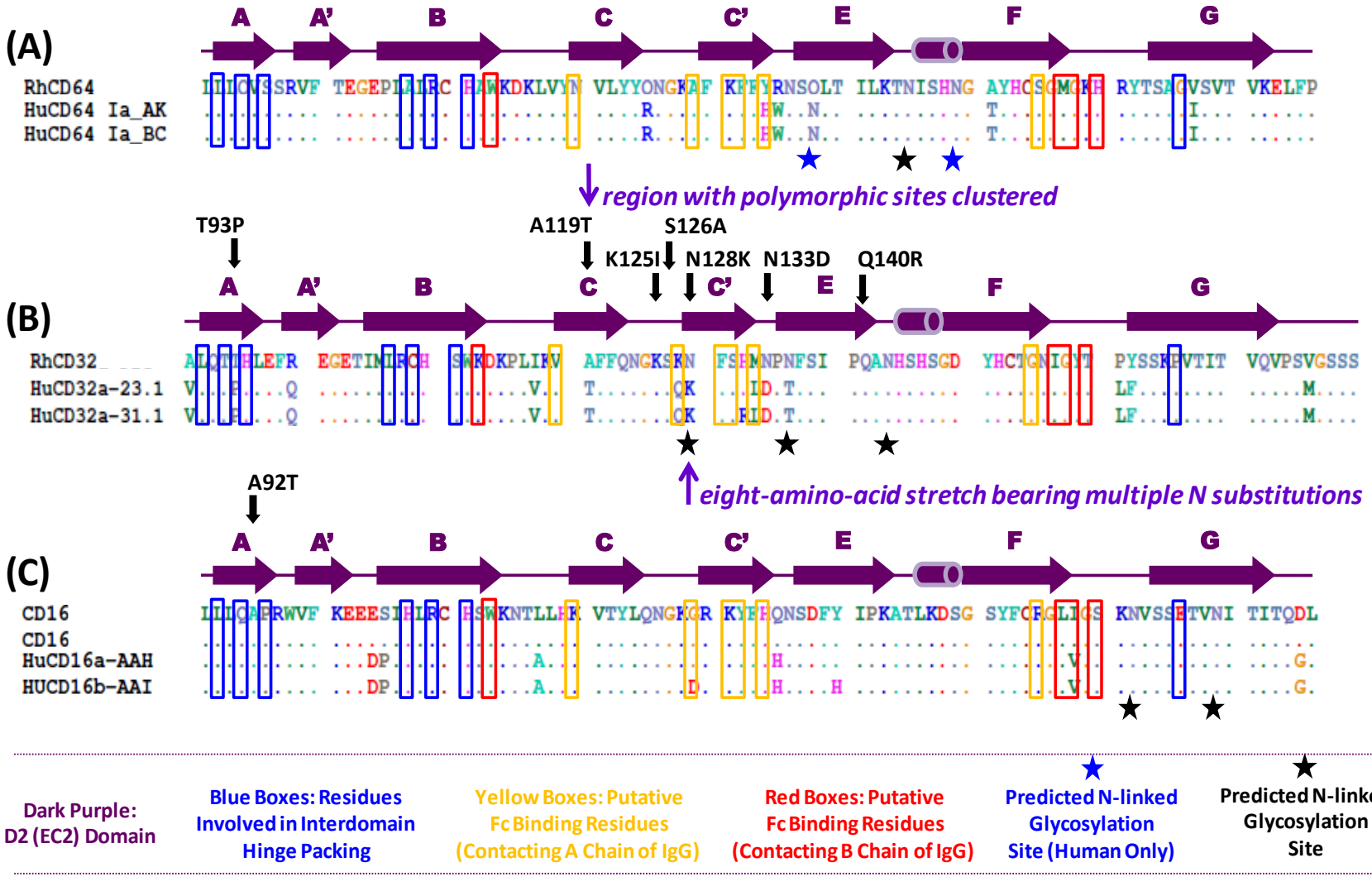
(A)
A
A'
B
C
C'
E
F
G
RhCD64
HuCD64 Ia_AK
HuCD64 Ia_BC
region with polymorphic sites clustered
T93P
A119T
S126A
K125I
N128K
N133D
Q140R
(B)
RhCD32
HuCD32a-23.1
HuCD32a-31.1
eight-amino-acid stretch bearing multiple N substitutions
A92T
(C)
CD16
CD16
HuCD16a-AAH
HUCD16b-AAI
Dark Purple: D2 (EC2) Domain
Blue Boxes: Residues Involved in Interdomain Hinge Packing
Yellow Boxes: Putative Fc Binding Residues (Contacting A Chain of IgG)
Red Boxes: Putative Fc Binding Residues (Contacting B Chain of IgG)
Predicted N-linked Glycosylation Site (Human Only)
Predicted N-linked Glycosylation Site

Fig. 3.12. Schematic representation illustrating the extracellular domain 2 ([D2], or EC2) putative secondary structure of a representative sequence from each of three rhesus macaque FcγR classes in alignment with those in humans: no variation at known human functional positions is found in the animal molecules. (A) FcγRI (CD64), (B) FcγRII (CD32), (C) FcγRIII (CD16). The black texts above each sequence secondary structure depict the variations found in rhesus macaques, with the vertical arrows showing their relative positioning. Blue boxes, residues involved in interdomain hinge packing; yellow boxes, putative Fc binding residues (contacting A chain of IgG); red boxes, putative Fc binding residues (contacting B chain of IgG); blue star, predicted N-linked glycosylation site (human only); black star, predicted N-linked glycosylation site. Rh, rhesus macaque; Hu, human. These representations were constructed based on Radaev et al., 2001; Zhang et al., 2000; and Maxwell et al., 1999.

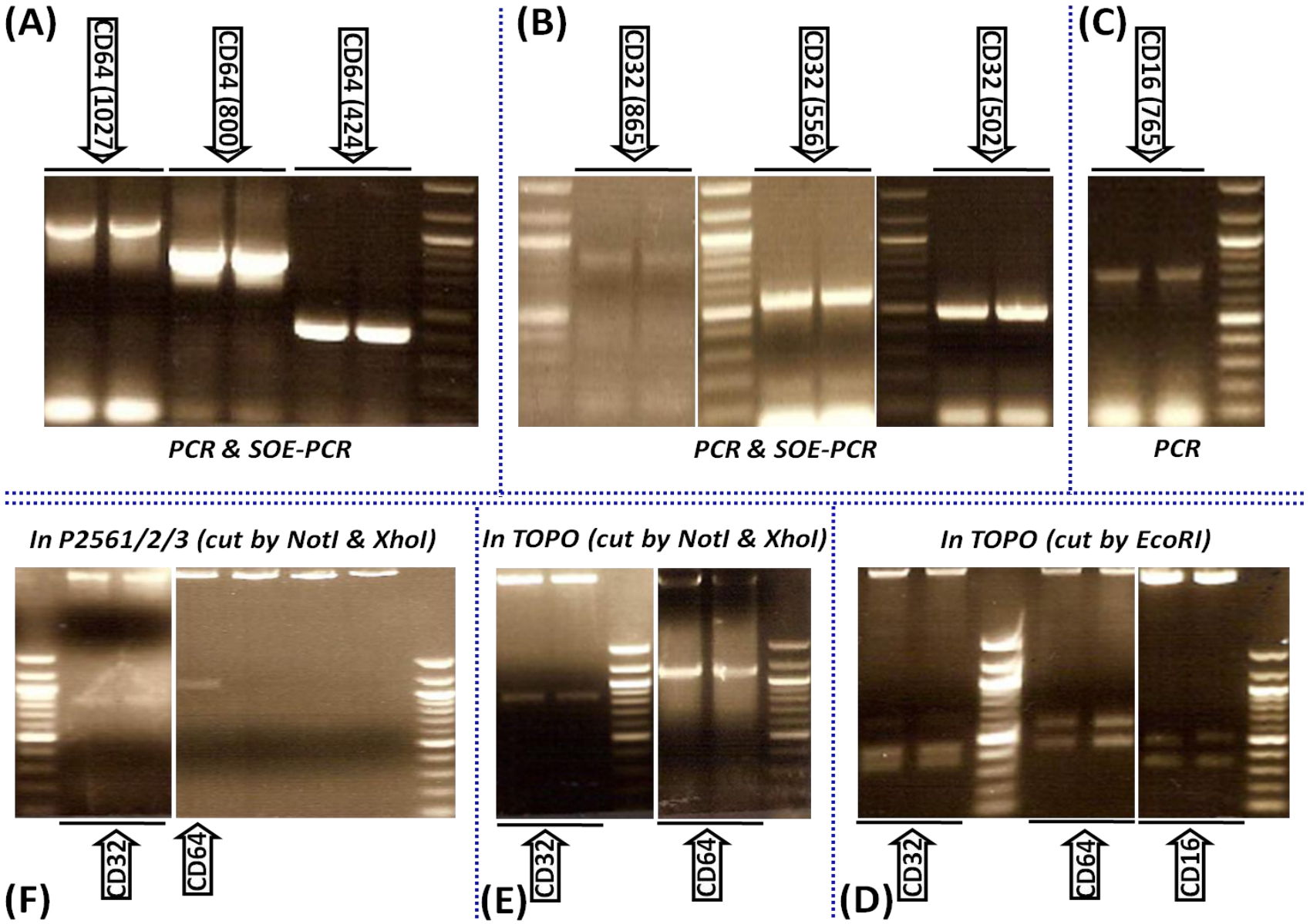
(A)
CD64 (1027)
CD64 (800)
CD64 (424)
PCR & SOE-PCR
(B)
CD32 (865)
CD32 (556)
CD32 (502)
PCR & SOE-PCR
(C)
CD16 (765)
PCR
In P2561/2/3 (cut by NotI & XhoI)
CD32
CD64
(F)
In TOPO (cut by NotI & XhoI)
CD32
CD64
(E)
In TOPO (cut by EcoRI)
CD32
CD64
CD16
(D)

Fig. 3.13. Gel electrophoresis separation of DNA products resulting from PCR and SOE-PCR annealing and amplification or digestion of clones of recombinant gene constructs of FcγRI (A), FcγRII (B), and FcγRIII (C), as well as gel electrophoresis separation of DNA fragments resulting from digestions of clones of recombinant FcγR gene constructs in pCR2.1 TOPO TA cloning vector cut by *EcoRI* (D), in pCR2.1 TOPO TA cloning vector cut by *NotI* and *XhoI* (E), and in P2561/2/3 expression vector cut by *NotI* and *XhoI* (F). PCR- and SOE-PCR-generated products or fragments obtained from RE-digested DNA plasmids were separated on 1-2% agarose gels, adjacent to DNA molecular weight standards. The gels were stained with ethidium bromide and were visualized and photographed under UV light. RE digestions were used to confirm that the recombinant gene constructs had each been inserted into correct region of the vectors and in correct orientation (which were subsequently confirmed by DNA sequencing). Number of lanes corresponding to each construct varies, as indicated by the horizontal lines. For lanes with two bands, the above released band corresponds to the digested vector and the below released band corresponds to the inserted DNA fragment. Lanes showing only one band (with size similar to that of the relevant vector) correspond to clones without successful DNA ligation. The DNA molecular weight standards are represented by lanes with multiple bands. Only representative clones containing bands of the expected sizes are shown. The vertical arrows with short notations show lanes corresponding to the indicated constructs.

Valencia, CA), to be used for cellular transfection. DNA sequencing analysis confirmed the accuracy and orientation of all these constructs in the expression vectors (data not shown).

Taken together, these data indicate that the FcγR cDNA genes were successfully engineered into cloning and expression vector systems.

3.4. Discussion

The well-recognized protective nature of antibody responses in HIV-infection (Mascola and Montefiori, 2010), along with the need to test candidate vaccines in the SIV-infected rhesus macaque model, underscores the importance of characterizing Fc receptors in this species. Indeed, recent findings indicate the importance of exploiting antibody responses that depend on the interactions with Fc receptors to increase vaccine efficacy. Well-characterized anti-HIV neutralizing monoclonal antibodies and even some non neutralizing antibodies show markedly increased viral inhibitory activity when operating through an FcγR mediated mechanism (Forthal and Moog, 2009). Using a different host-pathogen model system, it has been shown that antigen-antibody complexes enhance antiviral cytotoxic T cell responses through FcγR-mediated binding to dendritic cells (Michaud et al., 2010). Clearly, the breadth of FcγR functions appears more extensive than what initially assumed. Therefore, the characterization of Fc receptors in rhesus macaques is necessary to correctly and fully utilize this major animal model.

Although the FcγRII and FcγRI-“like” sequences have recently been predicted computationally, results from our study provide the first analysis of FcγRII and FcγRI macaque homologues along with their intraspecies allelic polymorphisms. The predicted cDNA structure of the macaque CD32 and CD64 represents the typical primary structure of their human counterparts, suggesting similar nature interactions with IgG molecules. Macaque FcγR exhibit

characteristic FcγR structural features. In particular, the length of a domain and the number of amino acids present between cysteine pairs, both of which are responsible for the folding pattern, is shorter in FcγR (~88 and 42–44 residues, respectively) as compared to IG proteins (~110 and no fewer than 80 residues, respectively) (Maxwell et al., 1999; Williams and Barclay, 1988). The high amino acid sequence identity of the FcγR domains between humans and macaques is consistent with the highly conserved nature of the individual C-like FcγR binding domains. Nevertheless, not all amino acids from the Fc binding region and the interdomain region packing are completely conserved in the macaque CD32 or CD64 sequences. One example is the addition of two predicted N linked glycosylation sites at [D2] 77 and 88 in macaque CD32, and the lack of three of these sites at [D1] 97, [D2] 88 and 99 in CD64, as compared to their human counterparts. It is noteworthy that all these amino acid changes are recognized in the computer-predicted sequences, as well as in every individual animal examined, except for the polymorphic [D2] 77. Given that N-glycosylation sites have the ability to affect structure/folding, cell-cell adhesion, leukocyte expression patterns, and ligand-binding properties of FcγR (Rogers et al., 2006; van Sorge et al., 2003), it might be predicted that these inter-species variations in glycosylation pattern might have a functional consequence on macaque CD32 and CD64 proteins.

The majority of amino acids known to be crucial for CD32 ligand binding in humans (Maxwell et al., 1999) are conserved in rhesus macaques. However, the human [D2] L81 is substituted by M81 in all nine animals. As L and M are both amino acids with a hydrophobic side chain and both favor the formation and stabilization of domain structures, it is reasonable to speculate that no major alteration in the hydrophilic/hydrophobic profile results from this change. Nevertheless, it is noteworthy that this position is located downstream next to the

functionally polymorphic amino acid [D2] H/R80 (131). This residue defines the specificity of CD32 for IgG in humans (Warmerdam et al., 1991). Interestingly, all nine macaques investigated display H131, the IgG2 low-responder polymorphic allele. It remains to be seen, however, if this substitution affects IgG-binding affinity and/or specificity of the receptor.

Because the C-terminal membrane-proximal [D2] domain is the principal IgG-binding domain, its polymorphisms may influence binding properties. The N-terminal membrane-distal [D1] domain, on the other hand, mainly plays a supporting role in domain–domain interaction; thus, its variations might only affect the orientation of the spatial domain (Radaev and Sun, 2002). In macaque CD64 proteins, all four (including RhesusP) polymorphic amino acids occur in [D1] (three in A strand and AB turn and the fourth one at position 93) (at amino acid 6–60), whereas in CD32 proteins, most (seven of nine) allelic polymorphic sites are clustered on a short segment in the middle of D2 (at amino acid 120–140 segment). Thus, these regions might be capable of mutating easily, indicating the impact of the evolutionary forces and the active functions of the receptors. In CD32 molecules, this short segment represents the type of small-region, broad variation occurrence that might render the CD32 amino acid 120–140 segment a mutation hot spot. Even more interesting is the presence of a shorter stretch of eight amino acids located within another segment (residues 128 to 135): four of the eight residues are polymorphic, three of these four polymorphic residues are N, and two of these three N residues are potential glycosylated ones, thus indicating that this segment/stretch represents the most actively functional and evolutionarily instable area of the molecule. Although the polymorphic variations identified in the present study, including the two novel CD16 variants, are entirely located in the ligand-binding regions, no single, specific variation is at a location known to be crucial for IgG binding in the corresponding human molecules. However, even a single amino acid change may

significantly alter the ligand-binding affinity of FcγR. IgG-FcγR interactions are complex and multi-facial, and therefore, until binding studies are carried out, it is difficult to predict the functional implications of these allelic variations.

Under natural evolutionary selection, polymorphisms, when occurring co-locally in both FcγR molecules and their native Fc ligand within the binding areas, have the potential to optimize functional activity and increase the binding fitness of both interacting players (Kim et al., 2001). Also, because of the extensive contact surface and multiple interactive residues, interactions between different FcRs and homodimeric Fc fragment of IgG (ligand) subclasses are complex. For instance, both the CH2 and CH3 domains of IgGs are involved in binding, with participated amino acids bind with different affinity depending on particular IgG subclass and the corresponding FcγR class members (Shields et al., 2001; Burton and Woof, 1992). Additionally, these interactions are asymmetrical (i.e. overlapping but not identical residues in both Fc fragments may take part in binding). Recent work from our group demonstrates the existence in macaques of a high level of IgA and IgG intra-species polymorphisms, particularly in the IgG2 and IgG4 subclasses (Rogers et al., 2008; Scinicariello et al., 2004; Scinicariello and Attanasio, 2001). The amino acid changes are primarily located at CH2 domain or the hinge region, including the lower hinge where all FcγRs bind and are responsible for most of the IgG effector functions and properties (Radaev and Sun, 2002). Thus, as both FcγR and IgG are highly polymorphic in macaques, the binding fitness and effector functions associated with these molecules might vary from individual to individual (i.e. intra-species) and might differ from those present in humans (i.e. inter-species). In order to adequately assess the binding properties and the ability to mediate effector functions of NHP FcγRs, therefore, not only the polymorphism of FcγRs themselves are ascribed, but also their ligand IgG genetic heterogeneity

must also be taken into account. Whether or not the sequence differences in FcγRs in rhesus macques (compared to humans) might be compensated by substitutions in their corresponding IgGs, leading to the unique properties and functions of the monkey IgG molecules, is difficult to predict and remains to be experimentally determined. Additionally, since particular allelic variations can be associated with disease susceptibility and/or severity and may influence the outcome of treatment with monoclonal antibodies (van Sorge et al., 2003; Cartron et al., 2002), this high heterogeneity characteristics must be considered when designing studies and interpreting data obtained using macaques for assessing immunogenicity and protective efficacy of HIV vaccines or vaccines for other infectious diseases, for studying the genetic basis of IgG-mediated human diseases, and for evaluating Ab- or FcγR-derived immunotherapeutic approaches.

In this study, we have successfully constructed recombinant cDNAs for all three classes of rhesus macaque FcγRs through two expression vector systems. In the first system, each rhesus macaque FcγR class cDNA was amplified by RT-PCRs and annealed by SOE-PCRs using primers with restriction sites for *HindIII* and *BamHI*, followed by cloning into pCR2.1 TOPO TA vector, and subsequent RE digestion verification and DNA sequencing confirmation. The FcγR cDNA was then excised from pCR2.1 TOPO TA cloning vector with *HindIII* and *BamHI* REs and engineered into expression vector pcDNA 3.1(+) (pre-digested with *HindIII* and *BamHI* REs), which contains CMV promoter and poly(A) signal to drive FcγR expression. An alternative system, where instead of *HindIII* and *BamHI* sites, *NotI* and *XhoI* RE sites were used. This first system was applied for expression of rhesus macaque FcR genes recently identified in our laboratory, including those encoding CD16 (Rogers et al., 2006) or the FcR for IgA (CD89) (Rogers et al., 2008). Transfection with this vector into HeLa or COS-7 cells, however, failed to

yield cell clones stably and/or sufficiently expressing recombinant FcγRs (Nguyen, D.C, unpublished data). Therefore, we developed a second expression vector system, which was a "combined" vector derived from the retrovirus vector pLXSN, containing LTR (as previously described; Fig. 2.8), that allow for the inserted gene to integrate into the host cell chromosomes. This vector was created by transferring a portion of the vector consisting of the FcR gene – as well as pcDNA3.1(+) promoter and poly(A) signal – into the pLXSN vector. The use of this "combined" vector, termed P2561/2/3, has previously proved to be capable of stably expressing recombinant FcγRs (Rogers et al., 2008 and 2006). P2561/2/3 system used in the present study, however, differs from the system previously used in our laboratory (Rogers et al., 2008 and 2006) by its unique RE sites. This improved expression vector system has also been used for generation of recombinant IgGs, as described in the previous chapter.

Cloning procedures are often the "bottleneck" in the use of the recombinant DNA method. Although in this study, no transfected cell clones were created at this time for evaluation of production of recombinant FcγRs, the successful construction of expression vectors is an important step before further studies can be undertaken. The gene expression cDNA constructs created in this study, which were designed (through the design of the primers) to incorporate unique [i.e. those are not present in FcγR genes, and rare (Persic et al., 1997)] *NotI-XhoI* restriction sites outside the gene coding regions for FcγRs, capable of facilitating easy cloning and exchange of IgSF gene constructs, can be readily cloned into another particular expression plasmid vector using RE digestion-ligation. For instance, future studies using the vector systems created from this study (and once protein FcγRs are produced) include those for mapping of binding interaction with ligands (IgGs) to specific epitopes, for interactions of FcγRs with the signaling chains, and for comparative studies of rhesus macaque/human IgG/FcγR interactions.

Acknowledgments

This work was supported in part by NIH grant R21 AI078855, by the Research Program Enhancement from the GSU Office of Research and Sponsored Programs and by the Georgia Research Alliance. The authors thank the Language Research Center of Georgia State University, Dr. Michael Hart and Matthew Davis for providing and collecting all rhesus macaque blood samples used in this study. Support for Doan C. Nguyen was provided by the Molecular Basis of Disease program at Georgia State University.

CHAPTER 4

17β-ESTRADIOL RESTORES ANTIBODY RESPONSES TO AN INFLUENZA VACCINE IN A POSTMENOPAUSAL MOUSE MODEL

(PARTIAL CONTENT OF THIS CHAPTER WAS PUBLISHED AS:

NGUYEN ET AL., VACCINE 2011;29:2515–8)

4.1. Summary

Post-menopausal women belong to an age group that is highly susceptible to influenza infection and its most serious complications. Data on the immunogenicity of influenza vaccines in these women is, however, limited. In this study, we assessed the antibody response to influenza vaccination in a postmenopausal mouse model. An inactivated-detergent-split vaccine from the A/New Caledonia/20/99 (H1N1) influenza virus strain was given to three groups of mice: ovariectomized (OVEX), OVEX with 17β-estradiol replacement (OVEX + E2), and sham-OVEX. The OVEX+ E2 group produced influenza virus-specific serum antibodies, including neutralizing antibodies, at significantly higher levels ($p < 0.001$) than did OVEX mice. These levels matched those observed in the sham-OVEX group, indicating that ovariectomy negatively modulates the antibody response to the influenza vaccine, whereas 17β-estradiol replacement restores this response to levels observed in intact animals. Our findings suggest that immunogenicity and efficacy of influenza vaccines need to be evaluated in postmenopausal women, including those receiving hormone replacement therapy.

4.2. Introduction

Influenza remains a serious public health problem, which generates heavy burdens by annual epidemics and sporadic pandemics (Fiore et al., 2010). In the United States, influenza-associated hospitalizations increase with increasing age (Dao et al., 2010). Co-morbidities and serious complications, including pneumonia, respiratory failure, and sepsis, are common in older individuals (Lee et al., 2010). Post-menopausal women belong to the age group highly susceptible to influenza complications. Currently, the most effective method in influenza control and prevention is the use of vaccines (Fiore et al., 2010). In the elderly, because of poor immune responses due to immunosenescence, the rate of immunization failure for influenza vaccines may be as high as 50% (Gravenstein et al., 1989). Unlike other infections, such as bacterial infections and sepsis, in which females are more resistant than males (Straub, 2007), women are more susceptible than men to influenza virus infection (WHO, 2010).

Sex hormones are known to modulate the development and function of the immune system (Karpuzoglu et al., 2009; Bouman et al., 2005). As compared to men and pre-menopausal women, postmenopausal women and women subjected to surgical menopause are more susceptible to some specific disorders, including infectious diseases, and exhibit T and B cell impairment (Kumru et al., 2004). The use of hormone replacement therapy and estrogen replacement therapy in postmenopausal women is associated with retaining or improving both B and T cell immune functions, as well as with partly preventing or restoring some of the immune impairments associated with the post-menopause status (Gameiro et al., 2010). However, the modulatory effect of estrogen on immunity to human recommended vaccines, particularly after menopause, is largely uncharacterized.

We hypothesized that estrogen modulates the antibody response to influenza vaccine preparations and tested this hypothesis in the present study.

4.3. Materials and methods

4.3.1. Mice, bilateral ovariectomy, and estrogen deliver

Pathogen-free adult (8–12 weeks of age) female BALB/c mice (Charles River Laboratories, Inc., Wilmington, MA), were housed and maintained in a pathogen-free environment on a phytoestrogen-free diet. The animals were divided into three groups: OVEX (subjected to ovariectomy), OVEX+ E2 (supplemented with exogenous estrogen) and Intact (sham-OVEX, not subjected to ovariectomy) (Fig. 4.1). Each group consisted of 23–24 mice, in which half of the mice were immunized, and the other half served as control. Surgical ovariectomy was performed under anesthesia to remove both left and right ovaries and animals were allowed to recover for at least one week before initiation of the experiments. 17β-estradiol (E2) (Sigma–Aldrich Corp., St. Louis, MO) was dissolved in 100% ethanol and diluted to its final concentrations (1 nM) in phosphate-buffered saline (PBS). The animals received 1 nM E2 in drinking water (Gordon et al., 1986). The continuous delivery of E2 began after surgeries and lasted until the conclusion of the experiment. All animals were housed and all experimental procedures were carried out according to local and federal guidelines.

4.3.2. Immunization

Mice were immunized subcutaneously with a primary (Day 0) and booster (Day 28) 3 μg dose of an inactivated-detergent split influenza vaccine containing 333 μg/ml of the surface protein hemagglutinin (HA) of A/New Caledonia/20/99 virus (H1N1) obtained from Dr. David

Burt (ID Biomedicals, now GlaxoSmithKline Biologicals, Canada). Serum samples were collected at weeks 2–3 pre-immunization, immediately before vaccination (Day 0), 3 weeks after the first (3rd week post-prime) and the second (3rd week post-booster) doses, and 3 (3rd month) and 6 (6th month) months after the second dose (Fig. 4.2). Animals were monitored for adverse reactions to immunization such as redness, swelling, or the formation of granulomas at the site of injection.

4.3.3. Evaluation of specific serum antibody response

Antibody responses were evaluated by performing a set of assays using serum samples collected at different time-points. The assays included enzyme-linked immunosorbent assay (ELISA), HA-specific hemagglutination inhibition (HI), micro-neutralization (MN), and single-radial hemolysis (SRH). Individual serum samples were used for all assays, with the exception of MN assay, for which pooled serum samples were used. The whole live homologous A/New Caledonia/20/99 virus was used for HI and MN assays. Viruses were propagated in the allantoic cavity of 10-day-old embryonated hens' eggs at 34°C for 2 days. Virus stocks were aliquoted and stored at −70 ◦C until use. ELISAs were performed to detect IgM, IgG, IgG1, and IgG2a specific for viral HA by standard end-point dilution as previously described (Katz et al., 1997). Test sera were treated with receptor-destroying enzyme (RDE; purified neuraminidase from Vibrio cholerae, Denka Seiken Co. Ltd., Tokyo, Japan). Control negative mouse sera (five to seven samples) were included in each ELISA to establish negative endpoint cut-offs. Titers for immune sera were calculated as the reciprocal of the highest dilution of test sera that gave an absorbance reading value greater than twice the mean absorbance with one standard deviation of the control sera at an equivalent dilution. A four-fold or two-fold increase in titer, for individual and pooled

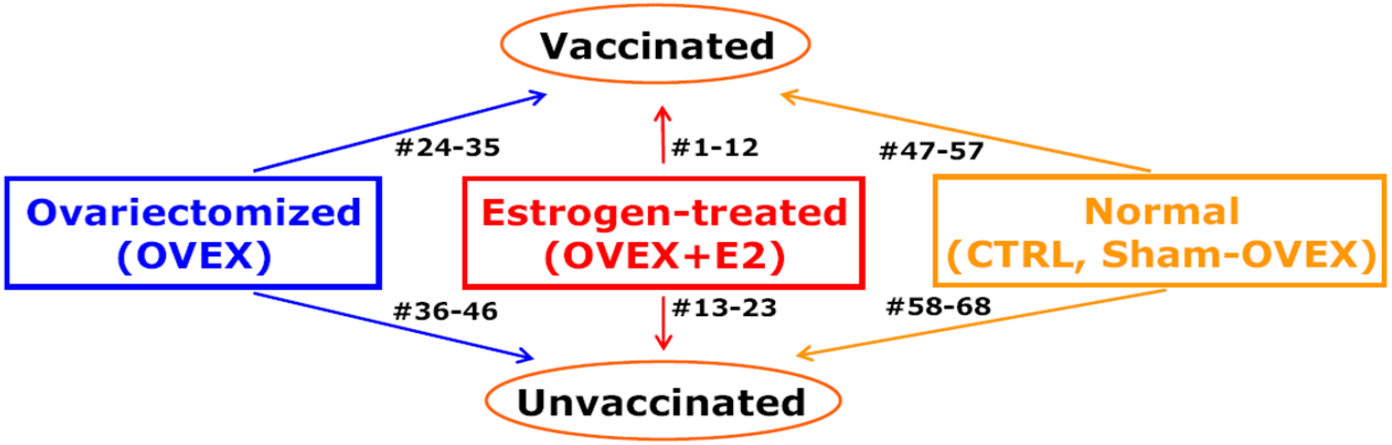

Fig. 4.1. Grouping of animals. Numbers denote individual animal numbering (for label purpose).

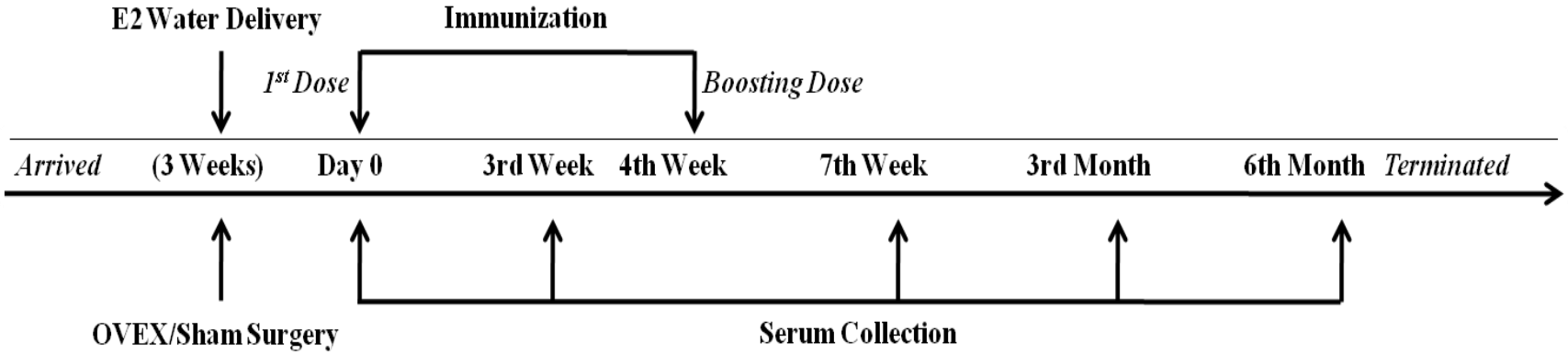

Fig. 4.2. Immunization and blood collection timeline.

serum comparison, respectively, was considered statistically significant for specific enhancement. Sera were tested for HI antibody using whole live homologous A/New Caledonia/20/99 virus (8 HA units per 50 μl PBS), by a standard HI assay (Stephenson et al., 2004). A four-fold or greater increase in HI titer was considered indicative of significant enhancement.

Neutralizing antibody activity was determined according to the MN assay as previously described (Stephenson et al., 2004). The presence of viral protein was detected by ELISA with a monoclonal antibody to the influenza A NP (Katz et al., 1997). MN titers were expressed as reciprocal of the highest dilution of serum that gave 50% neutralization of 100 TCID50 of virus in Marbin Darby canine kidney cells. Sera were considered positive for antibody if titers of ≥80 were obtained in both assays; a fourfold or greater increase in MN titer was considered indicative of specific enhancement. The SRH assay was performed using chicken red blood cells as previously described (Stephenson et al., 2004). A 25% erythrocyte suspension was coated with an amount of 5,000 HAU per ml of homologous A/New Caledonia/20/99 virus. Plates were prepared by incorporating 0.6 ml of virus-treated erythrocytes together with 8.4 ml of 1% melted agar (Sigma–Aldrich Co., St. Louis, MO). An SRH zone of 25mm2 was considered protective (to 50% subjects) and an increase of equal or greater than 50% in the zone represented a significant antibody rise.

4.3.4. Data analysis

Serum HI antibody titers underwent log 2 transformation; the initial serum dilution was 1/10, and undetectable titers were assigned a value of 5. Comparison of Ig titers was referred to log10 transformation of ELISA end-point titers. The SPSS program (SPSS Inc., Chicago, IL)

version 12 was used for statistical analysis. Analysis among multi-group data was carried out using ANOVA, followed by Tukey's honestly significant differences test, or Tamhane's T2 test when the test of homogeneity of variances (Levene's statistic) indicated that the variance between the groups was not equal. Non-parametric data were compared by Mann–Whitney U-test after Kruskal–Wallis analysis of variance. The null hypothesis was rejected at $p > 0.05$.

4.4. Results

All immunized mice produced anti-HA specific IgG and IgM responses following the primary dose. Antibody titers substantially increased after the booster dose (Fig. 4.3), with IgG being the predominant antibody class observed. The rise in specific antibody titers of both Ig classes post-prime was specific (from four- to seven-fold and significantly higher with $p < 0.001$) in the OVEX+ E2 and Intact when compared to the OVEX mice. Antibody levels increased substantially post-booster immunization ($p < 0.001$). No significant difference ($p = 0.557$) in antibody titers was observed between the OVEX+ E2 and Intact mouse groups for both time points and for both Ig classes. Specific IgG1 and IgG2a subclass antibodies were substantially induced. IgG1 levels were in general higher than IgG2a levels, regardless of the presence of E2. No statistically significant change was observed in titer for all three groups of mice of the same time points within each subclass of Ig.

Animals from all groups generated a limited, but detectable HI antibody titers 3 weeks post-primary immunization. After the boosting dose, however, serum HI antibody titers dramatically increased (up to 128-fold) for all groups (Fig. 4.3). At this time point, the titers from

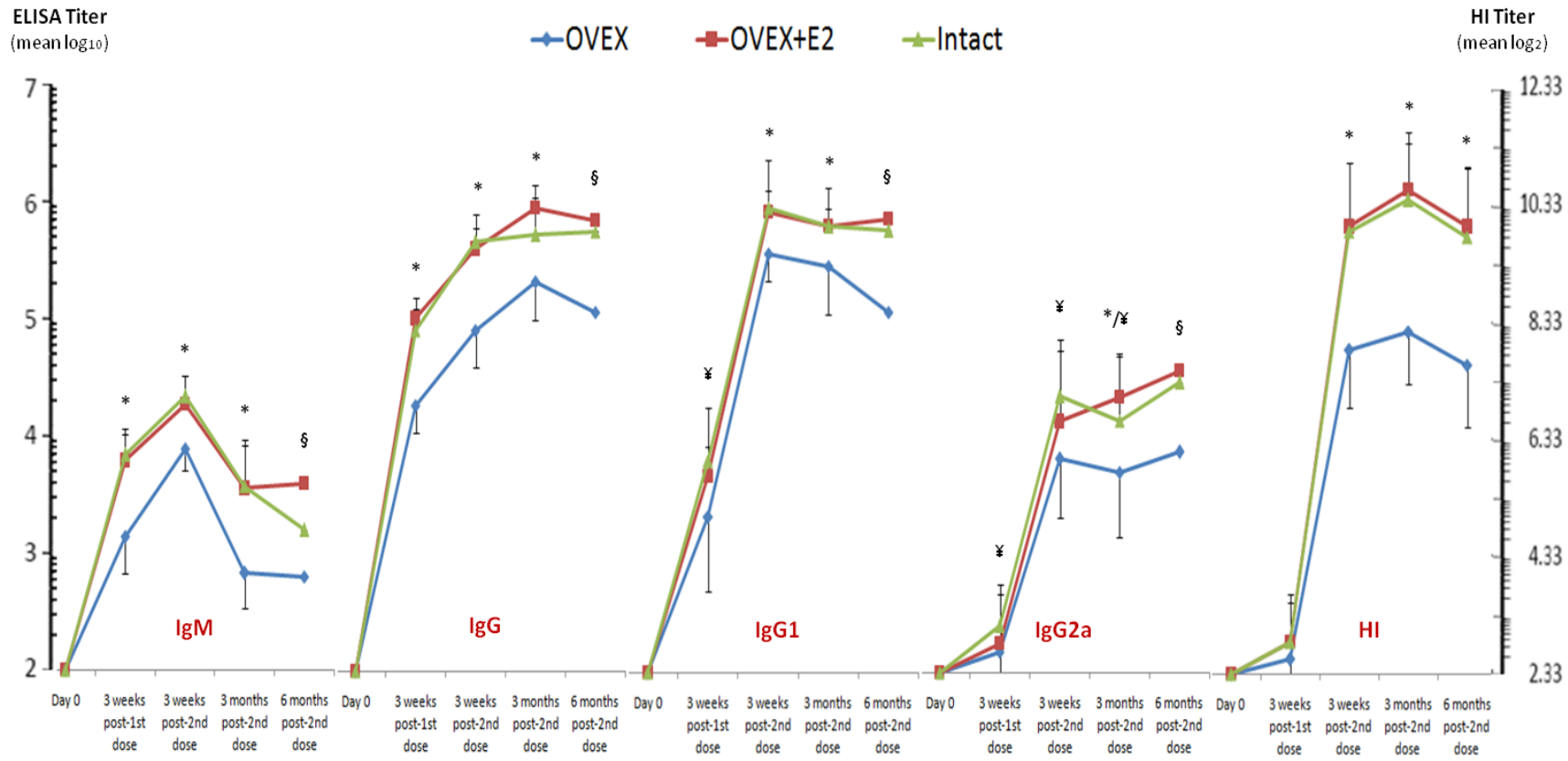
ELISA Titer
(mean log10)
OVEX
OVEX+E2
Intact
HI Titer
(mean log2)
7
6
5
4
3
2
12.33
10.33
8.33
6.33
4.33
2.33
IgM
IgG
IgG1
IgG2a
HI
Day 0
3 weeks post-1st dose
3 weeks post-2nd dose
3 months post-2nd dose
6 months post-2nd dose

Fig. 4.3. Specific protective antibodies were induced and restored in the presence of 17β-estradiol (E2) through six months after the boosting immunization. Titers expressed as values of mean $\log_2$ (for HI titer) or mean $\log_{10}$ (for ELISA IgM/IgG titers)±standard deviation (SD); titers of 2.33 (mean $\log_2$) and 2.00 (mean $\log_{10}$) for HI titer and ELISA IgM/IgG titers, respectively, were the detection limit. [¥]No statistically significant change was observed in titer for all three groups of mice at the same time points within each subclass of Ig. [*]Changes in titer of the OVEX+ E2 and Intact groups of mice as compared to that of the OVEX group of mice [specifically increased, and with statistical significance ($p < 0.05$)] and of the OVEX+ E2 and Intact groups of mice as compared to each other [no statistically significant change ($p > 0.5$)]; all considered at the same time point. [*/¥]Increase in titer with ($p < 0.05$; OVEX+ E2 group) and without ($p > 0.05$; Intact group) statistical significance as compared to the OVEX group of mice. [§]Pooled sera (no SD and no statistical comparison).

the OVEX+ E2 and Intact mouse groups were similar, and at least four-fold higher than those from the OVEX group ($p = 0.001$). As a four-fold increase in HI titer is considered protective, our results demonstrate a specific and significant elevation of HI antibody levels in the OVEX+ E2 and Intact mice as compared to the OVEX group. Results from the SRH assay show that the hemolytic areas produced by the OVEX+ E2 or Intact sera were 62% and 65% greater than those obtained with OVEX sera respectively, while these two former areas differed only by 2% and the unvaccinated sera yielded no hemolytic zone (Fig. 4.4).

Together, these results show the presence of similar antibody levels in the OVEX+ E2 and Intact groups, and the presence of significantly higher antibody levels in these groups as compared to the OVEX group.

Maintenance of long-term vigorous immune responses is important for overall vaccine efficacy. Therefore, we evaluated anti HA antibody titers produced three and six months after the booster immunization using the same set of assays used to detect antibody levels at earlier time points. Fig. 4.3 and Table 4.1 show the level and kinetics of these responses. IgG levels peaked three months post boost for HI and MN antibodies, whereas IgM reached maximum levels three-week post-boost, with no exceptions for all groups. Influenza virus-specific serum antibodies were present three and six months post-boost regardless of the presence of estrogen (Fig. 4.3). IgG1 and IgG2a levels were maintained through six months after the boosting immunization. Again, antibody responses were not significantly different ($p > 0.05$) between the OVEX+ E2 and Intact groups, but were specifically and significantly higher ($p < 0.001$) than those in the OVEX group three and six months post-boost. Similarly, results from SRH assay showed a significantly higher antibody levels in the OVEX+ E2 and Intact groups as compared to the OVEX group: the hemolytic area produced by the OVEX+ E2 or Intact sera was greater than that

yielded by the OVEX sera by 66% and 68%, respectively (for the three-month time point), and by 74% and 87%, respectively (for the six-month time point); all these zones were greater than 25 mm^2 (data not shown). No significant differences between the OVEX+ E2 and the Intact groups (their hemolytic areas differed by 1% or 7% at three- and six-month, respectively) were seen. Results from the SRH assay cannot be used to obtain quantitative determinations. However, SRH results were used to confirm the finding that the OVEX+ E2 group produced antibody responses at levels produced by the Intact group.

All tested serum antibody (IgG, IgM, HI, and MN) titers at all times points from all control (unvaccinated) mice of the three groups were below detectable level (data not shown).

Together, these results suggest that exogenous administration of estrogen restores production of specific antibody responses, but does not influence the T_H1/T_H2 pattern, at least up to six months after administration of the booster dose.

4.5. Discussion

Gender dimorphism in responses against pathogens and in autoimmune diseases has been observed in both humans and rodent models (Klein et al., 2010; McCombe et al., 2009). Indeed, the presence of estrogen and androgen receptors on progenitor and mature cells of the immune system suggests an important role for sex hormones in hematopoiesis and development of innate and adaptive immunity (Cunningham and Gilkeson, 2010; Rahman and Christian, 2007). The influence of 17β-estradiol on B-cell activity and development of antibody-mediated autoimmune diseases has been characterized (Grimaldi et al., 2005). However, it is recognized that information on the role that 17β-estradiol play in the modulation of antibody responses to vaccines is limited (Klein et al., 2010). Results from our study directly indicate a modulatory role

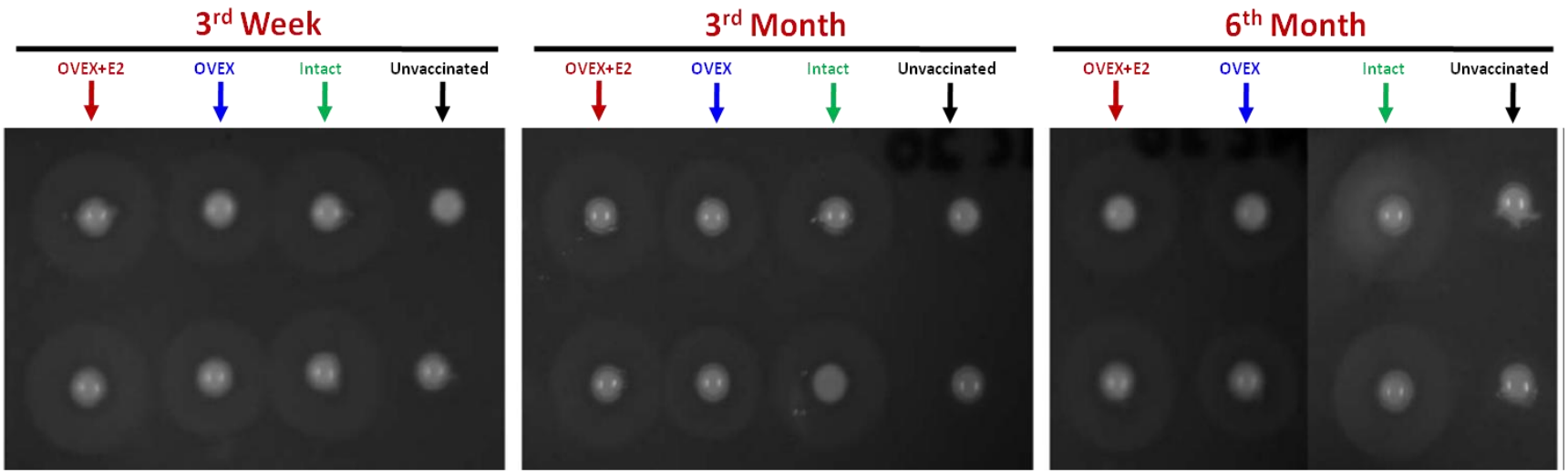

Fig. 4.4. Effect of 17β-estradiol (E2) on influenza-specific antibody production as measured by Single Radial Hemolysis (SRH) assay. Specific antibodies were restored in the presence of estrogen from three weeks through six months after the boosting immunization. BALB/c mice were s.c. immunized with monovalent influenza vaccine antigen of A/New Caledonia/20/99 (H1N1) virus strain. Serum samples were collected one-, three-, and six-months after the boost (Two-Dose Vaccination) immunization. Agarose gels were used and results are read directly by measuring diameter of lysis ring that is directly proportional to the concentration of antibodies in test sera. Each sample was tested in duplicate.

Table 4.1. Neutralizing antibody titers in ovariectomized (OVEX) mice, OVEX mice subjected to 17β-estradiol (E2) replacement (OVEX + E2) and Intact mice.

	MN titer	
Mouse group[a]	Three months post-2nd vaccine dose	Six months post-2nd vaccine dose
OVEX[b]	640[c]	320
OVEX + E2[b]	5,120[d]	2,560[d]
Intact[b]	5,120[d]	2,560[d]

[a]Each group of 11–12 BALB/c mice were s.c. immunized with 3 μg/dose of the HA antigen.

[b]All MN assays used pooled sera (no SD).

[c]Titers expressed as the reciprocal of the highest dilution of serum that gave 50% neutralization of 100 TCID50 of virus in MDCK cells.

[d]Increased in titer of equal or greater than fourfold as compared to the OVEX group of mice of the same time course and of less than fourfold as compared to each other indicated with this same note ([d]).

for E2 replacement on the response to an influenza vaccine in a post-menopausal animal model. In a similar model, E2 replacement resulted in improved protection against herpes simplex virus-2 (HSV-2) genital challenge as compared to placebo and progesterone (Bhavanam et al., 2008) and estrogen administered in conjunction with a specific vaccine HSV-2 improved protection (Pennock et al., 2009). Thus, it is reasonable to postulate that postmenopausal women might respond differently to vaccine administration and that E2 replacement might up-modulate responses to vaccines in these women.

The ability of E2 to restore specific anti-influenza HA antibody responses, which provide the essential protective role in influenza infection, in ovariectomized animals could be related to up-modulation of T_H2 activity, as estrogen is known to exhibit reciprocal regulatory effects on T helper cells by inhibiting T_H1 cytokine production and promoting that of T_H2 cells (Salem, 2004). Alternatively, this finding could be a result of the skewed-T_H2 responses that are known to be produced by Balb/c mice (Sacks et al., 2008). In our study, although anti-HA specific IgG1 (T_H2-related) was higher than IgG2a (T_H1-related) and anti-HA specific IgG1 increased earlier than IgG2a in all groups of mice, neither ovariectomy nor E2 levels had an effect on IgG1/IgG2a levels. The mechanisms underlying the ability of estradiol to up-modulate the response to the influenza vaccine are most likely complex and may involve pathways mediated by estrogen receptors as well as receptor independent pathways. Clarification of these mechanisms, as well as assessment of protective efficacy through challenge studies, will provide insight for the design of estradiol-based intervention strategies to increase the efficacy of influenza vaccines in postmenopausal women.

The incidence of influenza infection, as well as related morbidity and mortality, may differ between males and females, are often related to age and may vary between countries. For

example, the outcome of influenza virus infection is generally worse for females, but the magnitude of these differences varies across geographical regions (WHO, 2010). Most reports of cases of seasonal influenza do not analyze data for sex differences, and when sex differences are analyzed there is no assessment of the interaction between sex and age. Although humoral immune responses to influenza vaccines have been found to be consistently higher in women than in men, clinical studies focusing on the effectiveness of these vaccines do not assess neither the role of sex nor the interaction between sex and age (Klein et al., 2010). Thus, studies carried out in animal models provide needed insight to understand the role that menopause plays in the response to vaccines. As life expectancy increases worldwide, the size of the postmenopausal population will increase accordingly. At the same time, influenza epidemics and pandemics are expected to continue representing a major global health threat. Older individuals are known to be at risk of serious influenza-associated complications while, at the same time, responding poorly to vaccines. Postmenopausal women would have the added disadvantage of impaired responses caused by a changing hormonal environment. Therefore, results from our study highlight the importance of taking into account the postmenopausal status when evaluating vaccine efficacy and designing strategies to control epidemic and pandemic influenza.

Acknowledgements

We thank Jacqueline M. Katz for kindly providing reagents for the *in vitro* assays. This work was supported in part by the Research Program Enhancement from the GSU Office of Research and Sponsored Programs and by the Georgia Research Alliance. Support for Feda Masseoud was provided by the Molecular Basis of Disease program at Georgia State University.

References

Bhavanam S, Snider DP, Kaushic C. Intranasal and subcutaneous immunization under the effect of estradiol leads to better protection against genital HSV-2 challenge compared to progesterone. Vaccine. 2008;26:6165–72.

Bouman A, Heineman MJ, Faas MM. Sex hormones and the immune response in humans. Hum Reprod Update. 2005;11:411–23.

Cunningham M, Gilkeson G. Estrogen receptors in immunity and autoimmunity. Clin Rev Allergy Immunol. 2011;40:66-73.

Dao CN, Kamimoto L, Nowell M, Reingold A, Gershman K, Meek J, et al. Adult hospitalizations for laboratory-positive influenza during the 2005–2006 through 2007–2008 seasons in the United States. J Infect Dis. 2010;202:881–8.

Fiore AE, Uyeki TM, Broder K, Finelli L, Euler GL, Singleton JA, et al. Prevention and control of influenza with vaccines: recommendations of the advisory committee on immunization practices (ACIP). MMWR Recomm Rep 2010;59:1–62.

Gameiro CM, Romao F, Castelo-Branco C. Menopause and aging: changes in the immune system – a review. Maturitas. 2010;67:316-20.

Gordon MN, Osterburg HH, May PC, Finch CE. Effective oral administration of 17 beta-estradiol to female C57BL/6J mice through the drinking water. Biol Reprod. 1986;35:1088–95.

Gravenstein S, Duthie EH, Miller BA, Roecker E, Drinka P, Prathipati K, et al. Augmentation of influenza antibody response in elderly men by thymosin alpha one. A double-blind placebo-controlled clinical study. J Am Geriatr Soc. 1989;37:1–8.

Grimaldi CM, Hill L, Xu X, Peeva E, Diamond B. Hormonal modulation of B cell development and repertoire selection. Mol Immunol. 2005;42:811–20.

Karpuzoglu E, Zouali M. The multi-faceted influences of estrogen on lymphocytes: toward novel immuno-interventions strategies for autoimmunity management. Clin Rev Allergy Immunol. 2011;40:16-26.

Katz JM, Lu X, Young SA, Galphin JC. Adjuvant activity of the heat-labile enterotoxin from enterotoxigenic Escherichia coli for oral administration of inactivated influenza virus vaccine. J Infect Dis. 1997;175:352–63.

Klein SL, Jedlicka A, Pekosz A. The Xs and Y of immune responses to viral vaccines. Lancet Infect Dis. 2010;10:338–49.

Kumru S, Godekmerdan A, Yilmaz B. Immune effects of surgical menopause and estrogen replacement therapy in peri-menopausal women. J Reprod Immunol. 2004;63:31–8.

Lee N, Choi KW, Chan PK, Hui DS, Lui GC, Wong BC, et al. Outcomes of adults hospitalised with severe influenza. Thorax. 2010;65:510–5.

McCombe PA, Greer JM, Mackay IR. Sexual dimorphism in autoimmune disease. Curr Mol Med. 2009;9:1058–79.

Pennock JW, Stegall R, Bell B, Vargas G, Motamedi M, Milligan G, et al. Estradiol improves genital herpes vaccine efficacy in mice. Vaccine. 2009;27:5830–6.

Rahman F, Christian HC. Non-classical actions of testosterone: an update. Trends Endocrinol Metab. 2007;18:371–8.

Sacks DL, Sher A, Riley EM, Wynn TA. The immune response to parasites. In: Paul WE, editor. Fundamental Immunology. 6th ed. Philadelphia: Lippincott Williams and Wilkins; 2008. p. 1105–7.

Salem ML, Estrogen. a double-edged sword: modulation of T_H1- and T_H2- mediated inflammations by differential regulation of T_H1/T_H2 cytokine production. Curr Drug Targets Inflamm Allergy. 2004;3:97–104.

Stephenson I, Wood JM, Nicholson KG, Charlett A, Zambon MC. Detection of anti-H5 responses in human sera by HI using horse erythrocytes following MF59-adjuvanted influenza A/Duck/Singapore/97 vaccine. Virus Res. 2004;103:91–5.

Straub RH. The complex role of estrogens in inflammation. Endocr Rev. 2007;28:521–74.

WHO, Department of Gender. Women and Health: Sex, Gender and Influenza; 2010, http://whqlibdoc.who.int/publications/2010/9789241500111_eng.pdf. Accessed 3/13/2012.

CHAPTER V

CONCLUSIONS AND FUTURE DIRECTIONS

Phylogenetically positioned closely to humans, rhesus macaques are being increasingly used as an animal model for studies involving a variety of human diseases, as well as for assessing Ab-based therapeutics and vaccines, especially for HIV/AIDS research (Staprans et al., 2010; Hérodin et al., 2005). The design and interpretation of experimental data related to these studies often require the evaluation of humoral responses and are typically based on the assumption that rhesus macaque Ab molecules and their interactions with Fc receptors mimic those present in humans. This assumption has not been fully evaluated. The information available on rhesus macaque Ab molecules and corresponding Ig Fc receptors is steadily increasing (Warncke et al., 2012; Jacobsen et al., 2011; Rogers et al., 2008, 2006a, and 2004; Scinicariello et al., 2004; Scinicariello and Attanasio, 2001; Calvas et al., 1999). The findings that rhesus macaques exhibit a high level of Ab constant region polymorphism (Rogers et al., 2008; Scinicariello et al., 2004; Scinicariello and Attanasio, 2001) suggest that their interactions with corresponding FcRs might be heterogenous, and that the structural and functional properties of their Ab products may not be of direct equivalence of those in humans. Indeed, recent data demonstrated a direct correlation of key amino acid differences with distinct functional activities (including ADCC and CDC) and FcγR binding affinity of the human and cynomolgus IgG subclasses (Warncke et al., 2012; Jacobsen et al., 2011). However, the IgG effector functions and pathogen clearance mechanisms in this model are largly unexplored – mostly due to lack of specific Ab reagents. In this study, we have engineered and produced recombinant IgG chimeras that were able to specifically recognize the NIP and were bound by

affinity purified goat anti-monkey IgG(H+L) Abs. These recombinant Abs would be powerful new tools for evaluation of various IgG functional properties, including activation of cell-killing mechanisms through binding with FcγRs such as ADCC, CDC, and phagocytosis, as well as other Ig characteristics, such as their half-life and protease susceptibility.

To assess their ability in triggering specific effector functions, these recombinant IgG molecules will be subjected to FcγR binding and other immune cell-related studies (Fig. 5.1). Such FcγR binding properties and effector functional activities of these NIP-rhIgG chimeras will be assessed in *in vitro* studies using methods established in our laboratory (Rogers et al., 2006). For these purpose, we retained the murine Ig V gene directed against the NIP hapten, an established specificity for Ig effector functions studies. HeLa cell lines expressing rhesus macaque FcγRs already generated (Rogers et al., 2006; Rogers et al., 2004) or to be generated (using the expression vector systems described in this dissertation) will be used in these functional studies. We expect these rhesus macaque recombinant IgG subclasses to exhibit the effector functions of the related appropriate human IgG CH regions, including FcγR binding and activation of relevant immune effector cells. We also predict some binding affinity and effector functional differences that might result from distint amino acid sequences of IgG subclasses among these two species. Confirmation of the presence and potency of such IgG effector functions with these newly created chimeric recombinant Abs will allow for their better use in further studies.

Monoclonal Abs capable of specifically recognizing each of the rhesus macaque IgG subclasses represent valuable tools for further characterization of Ab responses and vaccine efficacy in this model. The relative level of IgG subclasses synthesized and present in rhesus macaque serum, which provide insights into the mechanisms that drive Ab production in this

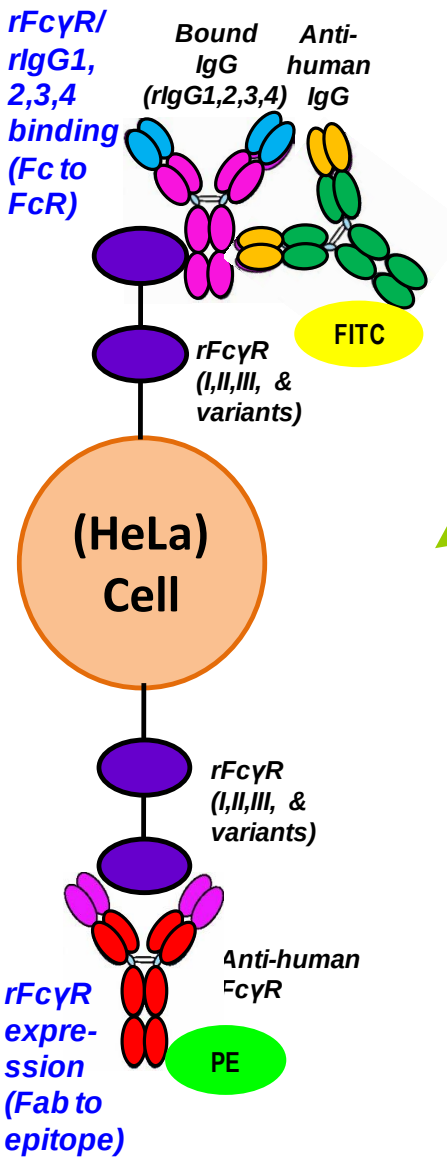

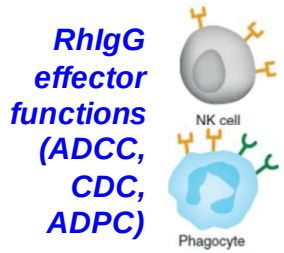

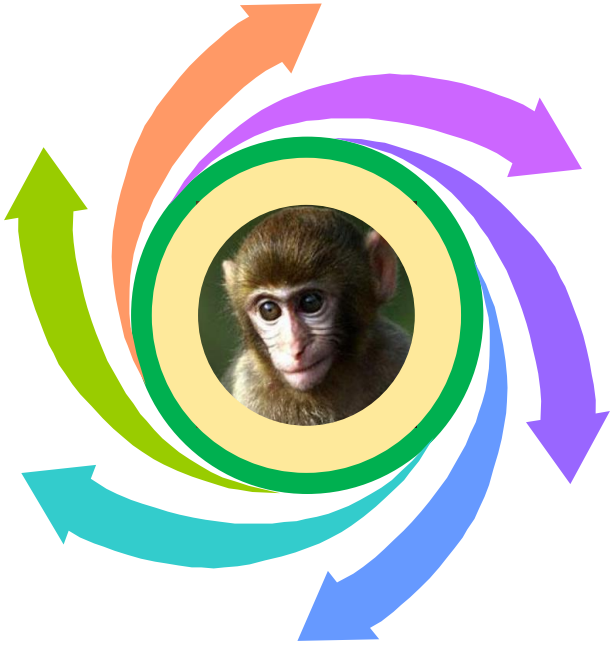

Future Studies

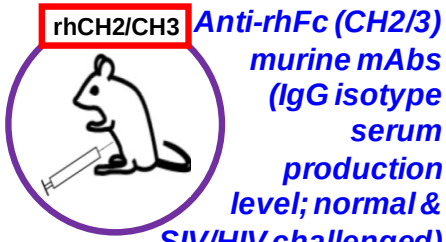

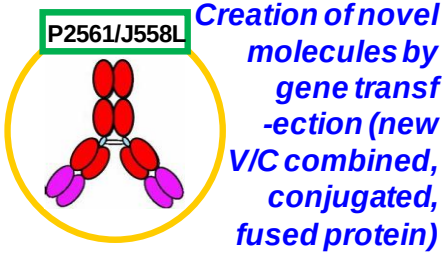

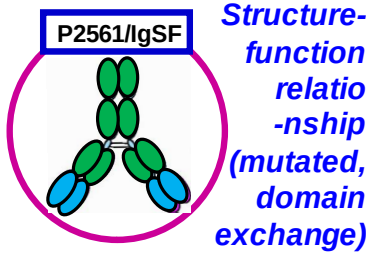

Fig. 5.1. Future studies and directions. See texts for details.

model, remain unknown. Given the availability of the cloning and expression plasmids containing the CH2/CH3 exon cDNA constructs (coding for the Fc region) created in this study, murine mAbs able to specifically recognize rhesus macaque IgG subclass Fc regions may be rapidly generated. Such Ab generation can be completed through DNA immunization of mice, an approach previously described by our group (Attanasio et al., 1997) (Fig. 5.1). Resultant murine mAbs can then be utilized to define the relative IgG isotype expression levels in normal and SIV/SHIV-infected rhesus macaque individuals.

In this study, we have developed a flexible vector system and strategies for cloning and expression of Ig genes in order to produce in mammalian cells functional Igs, including those from NHP animals. As presented in the present study, complete, fully assembled IgG Abs that retain original antigenic specificity can be created and produced from separate IgH and IgL chains. This Ig expression system is uselful for engineering Abs with desired properties to be used to assess the IgG structure-function relationship or to evaluate vaccines or Ab-based therapeutic development. For example, the system might be used to enable generation of novel Abs with V domains of particular specificity, including clinically relevant specificity – instead of the NIP, such as those specific to antigens originated from SIV, HIV, or influenza viruses [including the lethal H5N1 (Simmons et al., 2007)], as well as from Mycobacterium tuberculosis (Fig. 5.1). These agents can be simply created by exchanging the Ig V gene of interest with that of the system. Such recombinant IgG variants might even be used for passive transfer or SIV/HIV challenge studies in rhesus macaques. Such *in vivo* evaluation will provide insights not only to better define the interplay between the humoral immune system and the cell-based effector innate immunity, but also to clarify the role of specific Ab-dependent cell-killing effector functions in *in vivo* protection against these pathogens (including HIV, SIV, and

influenza virus antigens). Those studies would, in turn, provide insights related to the *in vivo* administration of therapeutic Abs.

Through genetic manipulation of Ig (not necessarily IgG) CH region genes, the effector functions of recombinant Abs can be modified to allow for desired immune effector responses while retaining antigen binding potency and specificity. To this end, the recombinant plasmid constructs created in this study may be subjected to manipulation for IgG-related basic and applied research purposes, including evaluating the pharmacologic values of recombinant Abs in the rhesus macaque model. Modifications could also be adapted to generate recombinant Abs with additional V and/or C functional properties, as well as for optimization (enhancement or neutralization) of particular Fc-mediated effector functions or other functional activities, to be used in Ab–antigen interaction studies or as therapeutic agents (Fig. 5.1). Moreover, such materials and approaches can be utilized for studying IgG structure/function relationships, such as changes in FcγR binding affinity due to amino acid differences by intra-species allelic polymorphisms in CH domains or in the hinge region. These constructs might also be used for production of well-conserved, immunogenic protein antigens for vaccine studies as well.

In light of the finding that despite the extensive sequence identity and almost complete overlap of amino acids involved in Ab Fc binding, human and macaque CD16 molecules differ as it relates to number of isoforms (no CD16b has been identified in macaques) and cell-type expression patterns (as compared to human neutrophils, known to express CD16, rhesus macaque neutrophils do not appear to express this protein) (Rogers et al., 2006b), and that distint FcγR expression patterns and different binding properties between cynomolgus and human FcγRs and IgGs molecules have been recently revealed (Warncke et al., 2012; Jacobsen et al., 2011), further characterizations of FcγR classes in rhesus macaques are necessary. The cellular

expression patterns of the rhesus macaque FcγRs identified in this dissertation – including CD64 and CD32 receptors – have been partially completed (Nguyen, D.C, unpublished data). As previously discussed, the results obtained with genetic characterization of FcγRs validate rhesus macaques as an animal model for vaccine development and Ab response studies, while at the same time, underscoring the need to take into account their high degree of genetic heterogeneity when designing experimental protocols for such studies. These results were also the basis for creation of recombinant FcγR cDNA molecules.

A major application using a cloned (recombinant) DNA molecule is the expression of it into a recombinant protein product. Our long term goals upon identification of the rhesus macaque homologues of human FcγR molecules at the genetic level are to characterize those molecules at the protein level, including determining their expression patterns on leukocyte populations and binding properties to both human and rhesus macaques IgG subclasses. As discussed previously, FcγRs vary in their affinity for different IgG subclasses. Moreover, interspecies differences between Igs as well as between FcRs of NHP models as opposed to humans might lead to variation in types immune effector responses induced by immune complexes (ICs)-FcRs (Warncke et al., 2012; Jacobsen et al., 2011). These differences might be ascribed onto different host defense strategies and disease susceptibility or progression of the rhesus macaque model against invading pathogens. Better understanding of these responses would serve to improve interpretation of immunology-related studies conducted in these models, particularly in rhesus macaques. Such studies could provide valuable insight for development of therapeutic agents directed at Ig and their Fc cell surface receptors. Therefore, it is important to develop expression systems for FcγRs and assays for binding affinity of cell bound receptors (and possibly, secreted FcγR portions), particularly given the fact that it is currently unknown

whether or at what extent human IgGs bind rhesus macaque effector cells. Recombinant forms of rhesus macaque FcγRs must, thus, be engineered. The first step towards these goals is to create recombinant FcγR cDNA constructs and incorporated them into cloning and expression vectors. We have employed the expression system and strategies developed and validated in this study to successfully create such FcγR cDNA constructs and vectors. Indeed, our strategies can also be adapted to be used for other rhesus macaque or other NHP IgSF molecule members as well.

The recombinant IgG chimeras, as well as the cDNA plasmid vectors of IgG subclasses and corresponding FcγR molecules created in this study, therefore, represent both the foundations and the fundamental tools for further studies about IgG effector functions and Ab structure-function relationship in the rhesus macaque model (Fig. 5.1). Such studies will further validate and improve the use of rhesus macaques as a valuable model for studies that require assessment of IgG and FcγR functional properties and their interactions.

CHAPTER VI

REFERENCES

Amzel LM, Poljak RJ. Three-dimensional structure of immunoglobulins. Annu Rev Biochem. 1979;48:961-97.

An Z. Monoclonal antibodies - a proven and rapidly expanding therapeutic modality for human diseases. Protein Cell. 2010;1:319-30.

Arnold JN, Wormald MR, Sim RB, Rudd PM, Dwek RA. The impact of glycosylation on the biological function and structure of human immunoglobulins. Annu Rev Immunol. 2007;25:21-50.

Attanasio R, Jayashankar L, Engleman CN, Scinicariello F. Baboon immunoglobulin constant region heavy chains: identification of four IGHG genes. Immunogenetics. 2002;54:556-61.

Attanasio R, Pehler K, Scinicariello F. DNA-based immunization induces anti-CD4 antibodies directed primarily to native epitopes. FEMS Immunol Med Microbiol. 1997;17:207-15.

Attanasio R, Stunz GW, Kennedy RC. Folding patterns of immunoglobulin molecules identified by urea gradient electrophoresis. J Biol Chem. 1994;269:1834-8.

Attarwala H.TGN1412: From Discovery to Disaster. J Young Pharm. 2010;2:332-6.

Bachmann MF, Zinkernagel RM. The influence of virus structure on antibody responses and virus serotype formation. Immunol Today. 1996;17:553–8.

Bengtén E, Wilson M, Miller N, Clem LW, Pilström L, Warr GW. Immunoglobulin isotypes: structure, function, and genetics. Curr Top Microbiol Immunol. 2000;248:189-219.

Bertrand G, Duprat E, Lefranc MP, Marti J, Coste J. Characterization of human FCGR3B*02 (HNA-1b, NA2) cDNAs and IMGT standardized description of FCGR3B alleles. Tissue Antigens 2004;64:119–31.

Binstadt BA, Geha RS, Bonilla FA. IgG Fc receptor polymorphisms in human disease: implications for intravenous immunoglobulin therapy. J Allergy Clin Immunol. 2003;111:697–703.

Brekke OH, Michaelsen TE, Sandlie I. The structural requirements for complement activation by IgG: does it hinge on the hinge? Immunol Today. 1995;16:85-90.

Brekke OH, Thommesen JE. Tailoring Natural Effector Functions: Antibody Engineering Beyond Humanization. In: Methods in Molecular Biology, Vol. 207: Recombinant Antibodies for Cancer Therapy: Methods and Protocols. Edited by: M. Welschof and J. Krauss, Humana Press Inc., Totowa, NJ. 2003;207:383-91.

Bruggemann M. Evolution of the rat immunoglobulin gamma heavy chain gene family. Gene. 1988;74:473-9.

Burmester G, Pezzutto A. Color Atlas of Immunology . Georg Thieme Verlag. 2003.

Burton DR. Antibodies, viruses and vaccines. Nat Rev Immunol. 2002;2:706-13.

Burton DR, Woof JM. Human antibody effector function. Adv Immunol. 1992;51:1-84.

Burton DR. Human and mouse monoclonal antibodies by repertoire cloning. Trends Biotechnol. 1991;9:169-75.

Calvas P, Apoil P, Fortenfant F, Roubinet F, Andris J, Capra D, Blancher A. Characterization of the three immunoglobulin G subclasses of macaques. Scand J Immunol. 1999;49:595–610.

Caragea C, Sinapov J, Silvescu A, Dobbs D, Honavar V. Glycosylation site prediction using ensembles of Support Vector Machine classifiers. BMC Bioinform. 2007;8:438.

Carlsson HE, Schapiro SJ, Farah I, Hau J. Use of primates in research: A global overview. Amer J Prim. 2004;63:225-37.

Carter P. Improving the efficacy of antibody-based cancer therapies. Nat Rev Cancer. 2001;1:118-29.

Cartron G, Dacheux L, Salles G, Solal-Celigny P, Bardos P, Colombat P, Watier H. Therapeutic activity of humanized anti-CD20 monoclonal antibody and polymorphism in IgG Fc receptor FcgammaRIIIa gene. Blood 2002;99:754–8.

Casadevall A, Dadachova E, Pirofski LA. Passive antibody therapy for infectious diseases. Nat Rev Microbiol. 2004;2:695-703.

Cavacini LA, Kuhrt D, Duval M, Mayer K, Posner MR. Binding and neutralization activity of human IgG1 and IgG3 from serum of HIV-infected individuals. AIDS Res Hum Retroviruses. 2003;19:785-92.

Cavacini LA, Emes CL, Power J, Desharnais FD, Duval M, Montefiori D, Posner MR. Influence of heavy chain constant regions on antigen binding and HIV-1 neutralization by a human monoclonal antibody. J Immunol. 1995;155:3638-44.

Clark M. Antibody Engineering IgG Effector Mechanisms. Chem Immunol. 1997;65:88–110.

Collin M, Shannon O, Bjorck L. IgG glycan hydrolysis by a bacterial enzyme as a therapy against autoimmune conditions. Proc Natl Acad Sci U. S. A. 2008;105:4265-70.

Coloma MJ, Trinh KR, Wims LA, Morrison SL. The hinge as a spacer contributes to covalent assembly and is required for function of IgG. J Immunol. 1997;158:733-40.

Daëron M. Fc receptor biology. Annu Rev Immunol. 1997;15:203–34.

Daza-Vamenta R, Glusman G, Rowen L, Guthrie B, Geraghty DE. Genetic divergence of the rhesus macaque major histocompatibility complex. Genome Res. 2004;14:1501-15.

Ehrenmann F, Kaas Q, Lefranc MP. IMGT/3Dstructure-DB and IMGT/DomainGapAlign: a database and a tool for immunoglobulins or antibodies, T cell receptors, MHC, IgSF and MhcSF. Nucleic Acids Res. 2010;38:D301–7.

Ehrlich PH, Moustafa ZA, Justice JC, Harfeldt KE, Gadi IK, Sciorra LJ, Uhl FP, Isaacson C, Ostberg L. Human and primate monoclonal antibodies for in vivo therapy. Clin Chem. 1988;34:1681-8.

Ellsworth JL, Hamacher N, Harder B, Maurer M, Bukowski TR, Lantry M, Noriega C, Rixon MW, Fox B, Lewis K, Meengs B, Rollins E, Greeff K, Meyer J, Birks C. Generation of a high-affinity Fcgamma receptor by Ig-domain swapping between human CD64A and CD16A. Protein Eng Des Sel. 2010;23:299–309.

Fell HP, Yarnold S, Hellstrom I, Hellstrom KE, Foldger KR. Homologous recombination in hybridoma cells: Heavy chain chimeric antibody produced by gene targeting. Proc Natl Acad Sci U S A. 1989;86:8507-11.

Forthal DN, Moog C. Fc receptor-mediated antiviral antibodies. Curr Opin HIV AIDS 2009;4:388–93.

Furebring C, Speckner A, Mach M, Sandlie I, Norderhaug L, Borrebaeck CA, Turesson H, Ohlin M. Antibody-mediated neutralization of cytomegalovirus: modulation of efficacy induced through the IgG constant region. Mol Immunol. 2002;38:833-40.

Gardner MB, Luciw PA. Macaque models of human infectious disease. ILAR J. 2008;49:220-55.

Gibbs RA, Rogers J, Katze MG, Bumgarner R, Weinstock GM, Mardis ER, Remington KA, Strausberg RL, Venter JC, Wilson RK, Batzer MA, Bustamante CD, Eichler EE, Hahn MW, Hardison RC, Makova KD, Miller W, Milosavljevic A, Palermo RE, Siepel A, Sikela JM, Attaway T, Bell S, Bernard KE, Buhay CJ, Chandrabose MN, Dao M, Davis C, Delehaunty KD, Ding Y, Dinh HH, Dugan-Rocha S, Fulton LA, Gabisi RA, Garner TT, Godfrey J, Hawes AC, Hernandez J, Hines S, Holder M, Hume J, Jhangiani SN, Joshi V, Khan ZM, Kirkness EF, Cree A, Fowler RG, Lee S, Lewis LR, Li Z, Liu YS, Moore SM, Muzny D, Nazareth LV, Ngo DN, Okwuonu GO, Pai G, Parker D, Paul HA, Pfannkoch C, Pohl CS, Rogers YH, Ruiz SJ, Sabo A, Santibanez J, Schneider BW, Smith SM, Sodergren E, Svatek AF, Utterback TR, Vattathil S, Warren W, White CS, Chinwalla AT, Feng Y, Halpern AL, Hillier LW, Huang X, Minx P, Nelson JO, Pepin KH, Qin X, Sutton GG, Venter E, Walenz BP, Wallis JW, Worley KC, Yang SP, Jones SM, Marra MA, Rocchi M, Schein JE, Baertsch R, Clarke L, Csürös M, Glasscock J, Harris RA, Havlak P, Jackson AR, Jiang H, Liu Y, Messina DN, Shen Y, Song HX, Wylie T, Zhang L, Birney E, Han K, Konkel MK, Lee J, Smit AF, Ullmer B, Wang H, Xing J, Burhans R,

Cheng Z, Karro JE, Ma J, Raney B, She X, Cox MJ, Demuth JP, Dumas LJ, Han SG, Hopkins J, Karimpour-Fard A, Kim YH, Pollack JR, Vinar T, Addo-Quaye C, Degenhardt J, Denby A, Hubisz MJ, Indap A, Kosiol C, Lahn BT, Lawson HA, Marklein A, Nielsen R, Vallender EJ, Clark AG, Ferguson B, Hernandez RD, Hirani K, Kehrer-Sawatzki H, Kolb J, Patil S, Pu LL, Ren Y, Smith DG, Wheeler DA, Schenck I, Ball EV, Chen R, Cooper DN, Giardine B, Hsu F, Kent WJ, Lesk A, Nelson DL, O'brien WE, Prüfer K, Stenson PD, Wallace JC, Ke H, Liu XM, Wang P, Xiang AP, Yang F, Barber GP, Haussler D, Karolchik D, Kern AD, Kuhn RM, Smith KE, Zwieg AS, Rhesus Macaque Genome Sequencing and Analysis Consortium. Evolutionary and biomedical insights from the rhesus macaque genome. Science. 2007;316:222-34.

Gillies SD, Lo KM, Wesolowski J. High-level expression of chimeric antibodies using adapted cDNA variable region cassettes. J Immunol Methods. 1989;125:191-202.

Greenwood J, Clark M, Waldmann H. Structural motifs involved in human IgG antibody effector functions. Eur J Immunol. 1993;23:1098-104.

Gottlieb AB, Kang S, Linden KG, Lebwohl M, Menter A, Abdulghani AA, Goldfarb M, Chieffo N, Totoritis MC. Evaluation of safety and clinical activity of multiple doses of the anti-CD80 monoclonal antibody, galiximab, in patients with moderate to severe plaque psoriasis. Clin Immunol. 2004;111:28-37.

Green JM, Schreiber AD, Brown EJ. Role for a glycan phosphoinositol anchor in Fc gamma receptor synergy. J Cell Biol. 1997;139:1209-17.

Hérodin F, Thullier P, Garin D, Drouet M. Nonhuman primates are relevant models for research in hematology, immunology and virology. Eur Cytokine Netw. 2005;16:104–16.

Ho SN, Hunt HD, Horton RM, Pullen JK, Pease LR. Site-directed mutagenesis by overlap extension using the polymerase chain reaction. Gene. 1989;77:51-9.

Hogarth PM. Fc receptors are major mediators of antibody based inflammationin autoimmunity. Curr Opin Immunol. 2002;14:798–802.

Howard MR, Lodge AP, Reed JE, McNamee CJ, Moss DJ. High-level expression of recombinant Fc chimeric proteins in suspension cultures of stably transfected J558L cells. Biotechniques. 2002;32:1282-6, 1288.

Jacobsen FW, Padaki R, Morris AE, Aldrich TL, Armitage RJ, Allen MJ, Lavallee JC, Arora T. Molecular and functional characterization of cynomolgus monkey IgG subclasses. J Immunol. 2011;186:341-9.

Janeway CAJr, Travers P. Immunobiology: The immune system in health and disease. Oxford, Blackwell Scientific Publications. 1996, 2nd Edn.

Jefferis R, Lund J. Interaction sites on human IgG-Fc for FcgammaR: current models. Immunol Lett. 2002;82:57–65.

Jefferis R, Lund J, Pound JD. IgG-Fc-mediated effector functions: molecular definition of interaction sites for effector ligands and the role of glycosylation. Immunol Rev. 1998;163:59-76.

Joag SV, Adams RJ, Foresman L, Galbreath D, Zink MC, Pinson DM, McClure H, Narayan O. Pathogenesis of SIVmac infection in Chinese and Indian rhesus macaques: effects of splenectomy on virus burden. Virology 1994;200:436–46.

Julenius K, Mølgaard A, Gupta R, Brunak S. Prediction, conservation analysis, and structural characterization of mammalian mucin-type O-glycosylation sites. Glycobiology. 2005;15:153-64.

Kaas Q, Ehrenmann F, Lefranc MP. IG, TR and IgSF, MHC and MhcSF: what do we learn from the IMGT Colliers de Perles? Brief Funct Genomic Proteomic. 2007;6:253–64.

Keller MA, Stiehm ER. Passive immunity in prevention and treatment of infectious diseases. Clin Microbiol Rev. 2000;13:602-14.

Kim H, Matsunaga C, Yoshino A, Kato K, Arata Y. Dynamical structure of the hinge region of immunoglobulin G as studied by 13C nuclear magnetic resonance spectroscopy. J Mol Biol. 1994;236:300-9.

Kim TD, Cho SE, Yang CH, Kim J. Analysis of Fc gammaRIII and IgG Fc polymorphism reveals functional and evolutionary implications of protein-protein interaction. J Mol Evol. 2001;53:1–9.

Kipriyanov SM, Le Gall F. Generation and production of engineered antibodies. Mol Biotechnol. 2004;26:39-60.

Köhler G, Milstein C. Continuous cultures of fused cells secreting antibody of predefined specificity. Nature. 1975;256:495-7.

Kuwayama H, Obara S, Morio T, Katoh M, Urushihara H, Tanaka Y. PCR-mediated generation of a gene disruption construct without the use of DNA ligase and plasmid vectors. Nucleic Acids Res. 2002;30:E2.

Lackner AA, Veazey RS. Current concepts in AIDS pathogenesis:Insights from the SIV/macaque model. Ann Rev Med. 2007;58:461-76.

Laffly E, Sodoyer R. Monoclonal and recombinant antibodies, 30 years after ... Hum Antibodies. 2005;14:33-55.

Lefranc MP, Giudicelli V, Ginestoux C, Jabado-Michaloud J, Folch G, Bellahcene F, Wu Y, Gemrot E, Brochet X, Lane J, Regnier L, Ehrenmann F, Lefranc G, Duroux P. IMGT, the international ImMunoGeneTics information system. Nucleic Acids Res. 2009;37:D1006–12.

Lefranc M-P, Lefranc G. The Immunoglobulin Facts Book. San Diego, CA. Academic Press 2001;3-90.

Lefranc MP, Pommié C, Kaas Q, Duprat E, Bosc N, Guiraudou D, Jean C, Ruiz M, Da Piédade I, Rouard M, Foulquier E, Thouvenin V, Lefranc G. IMGT unique numbering for immunoglobulin and T cell receptor constant domains and Ig superfamily C-like domains. Dev Comp Immunol. 2005;29:185–203.

Ling B, Veazey RS, Luckay A, Penedo C, Xu K, Lifson JD, Marx PA. SIV(mac) pathogenesis in rhesus macaques of Chinese and Indian origin compared with primary HIV infections in humans. AIDS 2002;16:1489–96.

Liu F, Bergami PL, Duval M, Kurth D, Posner M, Cavacini L. Expression and functional activity of isotype and subclass switched human monoclonal antibody reactive with the base of the V3 loop of HIV-1 gp120. AIDS Res Hum Retroviruses 2003;19:597-607.

Lögdberg L, Kaplan E, Drelich M, Harfeldt E, Gunn H, Ehrlich P, Dottavio D, Lake P, Ostberg L. Primate antibodies tocomponents of the human immune system. J Medical Pimatol. 1994;23:285–97.

Loset GA, Roux KH, Zhu P, Michaelsen TE, Sandlie I. Differential segmental flexibility and reach dictate the antigen binding mode of chimeric IgD and IgM: implications for the function of the B cell receptor. J Immunol. 2004;172:2925-34.

Lund J, Takahashi N, Pound JD, Goodall M, Nakagawa H, Jefferis R. Oligosaccharide-protein interactions in IgG can modulate recognition by Fc gamma receptors. FASEB J. 1995;9:115-9.

Marthas ML, Lu D, Penedo MC, Hendrickx AG, Miller CJ. Titration of a SIVmac251 stock by vaginal inoculation of Indian and Chinese origin rhesus macaques: transmission efficiency, viral loads, and antibody responses. AIDS Res Hum Retroviruses 2001;17:1455–66.

Mascola JR, Montefiori DC. The role of antibodies in HIV vaccines. Annu Rev Immunol. 2010;28:413–44.

Maxwell KF, Powell MS, Hulett MD, Barton PA, McKenzie IF, Garrett TP, Hogarth PM. Crystal structure of the human leukocyte Fc receptor, Fc gammaRIIa. Nat Struct Biol. 1999;6:437–42.

McLean GR, Nakouzi A, Casadevall A, Green NS. Human and murine immunoglobulin expression vector cassettes. Mol Immunol. 2000;37:837-45.

Michaelsen TE, Aase A, Westby C, Sandlie I. Enhancement of complement activation and cytolysis of human IgG3 by deletion of hinge exons. Scand J Immunol. 1990;32:517-28.

Michaud HA, Gomard T, Gros L, Thiolon K, Nasser R, Jacquet C, Hernandez J, Piechaczyk M, Pelegrin M. A crucial role for infected-cell/antibody immune complexes in the enhancement of

endogenous antiviral immunity by short passive immunotherapy. PLoS Pathog. 2010;6:e1000948.

Miletic VD, Frank MM. Complement-immunoglobulin interactions. Curr Opin Immunol. 1995;7:41-7.

Miller CJ, Genescà M, Abel K, Montefiori D, Forthal D, Bost K, Li J, Favre D, McCune JM. Antiviral antibodies are necessary for control of simian immunodeficiency virus replication. J Virol. 2007;81:5024–35.

Morrison SL. Transfectomas provide novel chimeric antibodies. Science. 1985;229:1202-7.

Morrison SL, Smith RIF, Wright A. Structural determinants of human IgG function. The Immunologist. 1994;2;119-224.

Murphy KM, Paul Travers P, Walport M. Immunobiology, 7th Edition, Garland Publishing, 2008.

Nakamura T, Kloetzer WS, Brams P, Hariharan K, Chamat S, Cao X, LaBarre MJ, Chinn PC, Morena RA, Shestowsky WS, Li YP, Chen A, Reff ME. In vitro IgE inhibition in B cells by anti-CD23 monoclonal antibodies is functionally dependent on the immunoglobulin Fc domain. Int J Immunopharmacol. 2000;22:131-41.

Nath BM, Schumann KE, Boyer JD. The chimpanzee and other non-human-primate models in HIV-1 vaccine research. Trends Microbiol. 2000;8:426-31.

Neuberger MS, Williams GT. The intron requirement for immunoglobulin gene expression is dependent upon the promoter. Nucleic Acids Res. 1988;16:6713-24.

Newman R, Alberts J, Anderson D, Carner K, Heard C, Norton F, Raab R, Reff M, Shuey S, Hanna N. "Primatization" of recombinant antibodies for immunotherapy of human diseases: a macaque/human chimeric antibody against human CD4. Biotechnology (N Y). 1992;10:1455-60.

Newman R, Hariharan K, Reff M, Anderson DR, Braslawsky G, Santoro D, Hanna N, Bugelski PJ, Brigham-Burke M, Crysler C, Gagnon RC, Dal Monte P, Doyle ML, Hensley PC, Reddy MP, Sweet RW, Truneh A. Modification of the Fc region of a primatized IgG antibody to human CD4 retains its ability to modulate CD4 receptors but does not deplete CD4(+) T cells in chimpanzees. Clin Immunol. 2001;98:164-74.

Niederer HA, Willcocks LC, Rayner TF, Yang W, Lau YL, Williams TN, Scott JA, Urban BC, Peshu N, Dunstan SJ, Hien TT, Phu NH, Padyukov L, Gunnarsson I, Svenungsson E, Savage CO, Watts RA, Lyons PA, Clayton DG, Smith KG. Copy number, linkage disequilibrium and disease association in the FCGR locus. Hum Mol Genet. 2010;19:3282–94.

Nielsen LK, Norderhaug L, Sandlie I, Dziegiel MH. In vitro functional test of two subclasses of an anti-RhD antibody produced by transient expression in COS cells. APMIS 2006;114:345–51.

Nimmerjahn F, Ravetch JV. Fcgamma receptors as regulators of immune responses. Nat Rev Immunol. 2008;8:34–47.

Nguyen DC, Masseoud F, Lu X, Scinicariello F, Sambhara S, Attanasio R. 17β-Estradiol restores antibody responses to an influenza vaccine in a postmenopausal mouse model. Vaccine. 2011;29:2515-8.

Nguyen DC, Scinicariello F, Attanasio R. Characterization and allelic polymorphisms of rhesus macaque (Macaca mulatta) IgG Fc receptor genes. Immunogenetics. 2011;63:351-62.

Norderhaug L, Olafsen T, Michaelsen TE, Sandlie I. Versatile vectors for transient and stable expression of recombinant antibody molecules in mammalian cells. J Immunol Methods. 1997;204:77-87.

Oi VT, Vuong TM, Hardy R, Reidler J, Dangle J, Herzenberg LA, Stryer L. Correlation between segmental flexibility and effector function of antibodies. Nature. 1984;307:136-40.

Oi VT, Morrison SL, Herzenberg LA, Berg P. Immunoglobulin gene expression in transformed lymphoid cells. Proc Natl Acad Sci U S A. 1983;80:825-9.

Papadea C, Reimer CB, Check IG. Human immunoglobulin G and immunoglobulin G subclasses: Biochemical, Genetic, and Clinical Aspects. Crit Rev Clin Lab Sci. 1989;27:27-58.

Parham P. The immune system. Garland Publishing/Elsevier Science Ltd. 2000;1-268.

Park JW, Smolen J. Monoclonal antibody therapy. Adv Protein Chem. 2001;56:369-421.

Parren PWHI, Burton DR. The anti-viral activity of antibodies in vitro and in vivo. Adv Immunol. 2001;77:195-262.

Perez LG, Costa MR, Todd CA, Haynes BF, Montefiori DC. Utilization of immunoglobulin G Fc receptors by human immunodeficiency virus type 1: a specific role for antibodies against the membrane-proximal external region of gp41. J Virol. 2009;83:7397-410.

Persic L, Roberts A, Wilton J, Cattaneo A, Bradbury A, Hoogenboom HR. An integrated vector system for the eukaryotic expression of antibodies or their fragments after selection from phage display libraries. Gene. 1997;187:9-18.

Pleass RJ, Woof JM. Fc receptors and immunity to parasites. Trends Parasitol. 2001;17:545-51.

Pont-Kingdon G. Creation of chimeric junctions, deletions, andinsertions by PCR. Methods Mol Biol. 1997;67:167-72.

Preston MJ, Gerceker AA, Reff ME, Pier GB. Production and characterization of a set of mouse-human chimeric immunoglobulin G (IgG) subclass and IgA monoclonal antibodies with identical

variable regions specific for Pseudomonas aeruginosa serogroup O lipopolysaccharide. Infect Immun. 1998;66:4137-42.

Radaev S, Sun P. Recognition of immunoglobulins by Fcgamma receptors. Mol Immunol. 2002;38:1073–83.

Radaev S, Motyka S, Fridman WH, Sautes-Fridman C, Sun PD. The structure of a human type III Fcgamma receptor in complex with Fc. J Biol Chem. 2001;276:16469–77.

Ravetch JV, Bolland S. IgG Fc receptors. Annu Rev Immunol. 2001;19:275–90.

Ravetch JV. Fc Receptors: Rubor Redux, Cell 1994;78:553-60.

Ravetch JV, Kinet JP. Fc receptors. Annu Rev Immunol. 1991;9:457–92.

Reddy MP, Kinney CA, Chaikin MA, Payne A, Fishman-Lobell J, Tsui P, Dal Monte PR, Doyle ML, Brigham-Burke MR, Anderson D, Reff M, Newman R, Hanna N, Sweet RW, Truneh A. Elimination of Fc receptor-dependent effector functions of a modified IgG4 monoclonal antibody to human CD4. J Immunol. 2000;164:1925-33.

Redpath S, Michaelsen TE, Sandlie I, Clark MR. The influence of the hinge region length in binding the human Fcgamma receptors. Hum Immunol. 1998;59:720-7.

Reichert JM. Which are the antibodies to watch in 2012? MAbs. 2012;4:1-3.

Reimann KA, Parker PA, Seaman MS, Beaudry K, Beddall M, Peterson L, Williams KC, Veazey RS, Montefiori DC, Mascola JR, Nabel GJ, Letvin NL. Pathogenicity of simian-human immunodeficiency virus SHIV-89.6P and SIVmac is attenuated in cynomolgus macaques and associated with early T-lymphocyte responses. J Virol. 2005;79:8878–85.

Rogers KA, Jayashankar L, Scinicariello F, Attanasio R. Nonhuman primate IgA: genetic heterogeneity and interactions with CD89. J Immunol. 2008;180:4816–24.

Rogers KA, Richardson JP, Scinicariello F, Attanasio R. Molecular characterization of immunoglobulin D in mammals: immunoglobulin heavy constant delta genes in dogs, chimpanzees and four old world monkey species. Immunology 2006a;118:88–100.

Rogers KA, Scinicariello F, Attanasio R. IgG Fc receptor III homologues in nonhuman primate species: genetic characterization and ligand interactions. J Immunol. 2006b;177:3848–56.

Rogers KA, Scinicariello F, Attanasio R. Identification and characterization of macaque CD89 (immunoglobulin A Fc receptor). Immunology 2004;113:178–86.

Roux KH, Strelets L, Michaelsen TE. Flexibility of human IgG subclasses. J Immunol. 1997;159:3372-82.

Rudich SM, Roux KH, Winchester RJ, Mongini PKA. Anti-IgM-mediated B cell signaling: molecular analysis of ligand binding requisites for human B cell clonal expansion. J Exp Med. 1988;168:247-66.

Sawyer LA. Antibodies for the prevention and treatment of viral diseases. Antiviral Res. 2000;47:57-77.

Scharf O, Golding H, King LR, Eller N, Frazier D, Golding B, et al. Immunoglobin G3 from polyclonal human immunodeficiency virus (HIV) immune globulin is more potent than other subclasses in neutralizing HIV type 1. J Virol 2001;75:6558-65.

Schmitz JE, Kuroda MJ, Santra S, Simon MA, Lifton MA, Lin W, Khunkhun R, Piatak M, Lifson JD, Grosschupff G, Gelman RS, Racz P, Tenner-Racz K, Mansfield KA, Letvin NL, Montefiori DC, Reimann KA. Effect of humoral immune responses on controlling viremia during primary infection of rhesus monkeys with simian immunodeficiency virus. J Virol. 2003;77:2165-73.

Schopf RE. IDEC-114 (IDEC). Curr Opin Investig Drugs. 2001;2:635-8.

Schroeder HW Jr, Cavacini L. Structure and function of immunoglobulins. J Allergy Clin Immunol. 2010;125:S41-52.

Schulze-Koops H, Lipsky PE. Anti-CD4 monoclonal antibody therapy in human autoimmune diseases. Curr Dir Autoimmun. 2000;2:24-49.

Scinicariello F, Masseoud F, Jayashankar L, Attanasio R. Sooty mangabey (Cercocebus torquatus atys) IGHG and IGHA genes. Immunogenetics. 2006;58:955-65.

Scinicariello F, Engleman CN, Jayashankar L, McClure HM, Attanasio R. Rhesus macaque antibody molecules: sequences and heterogeneity of alpha and gamma constant regions. Immunology 2004;111:66–74.

Scinicariello F, Attanasio R. Intraspecies heterogeneity of immunoglobulin alpha-chain constant region genes in rhesus macaques. Immunology 2001;103:441–8.

Shearer MH, Dark RD, Chodosh J, Kennedy RC. Comparison and characterization of immunoglobulin G subclasses among primate species. Clin Diagn Lab Immunol. 1999;6:953-8.

Shedlock DJ, Silvestri G, Weiner DB. Monkeying around with HIV vaccines: using rhesus macaques to define 'gatekeepers' for clinical trials. Nat Rev Immunol. 2009;9:717-28.

Shevchuk NA, Bryksin AV, Nusinovich YA, Cabello FC, Sutherland M, Ladisch S. Construction of long DNA molecules using long PCR-based fusion of several fragments simultaneously. Nucleic Acids Res. 2004;32:e19.

Shields RL, Namenuk AK, Hong K, Meng YG, Rae J, Briggs J, Xie D, Lai J, Stadlen A, Li B, Fox JA, Presta LG. High resolution mapping of the binding site on human IgG1 for Fc gamma RI, Fc gamma RII, Fc gamma RIII, and FcRn and design of IgG1 variants with improved binding to the Fc gamma R. J Biol Chem. 2001;276:6591-604.

Sibal LR, Samson KJ. Nonhuman primates: a critical role in current disease research. ILAR J. 2001;42:74-84.

Simmons CP, Bernasconi NL, Suguitan AL, Mills K, Ward JM, Chau NV, Hien TT, Sallusto F, Ha do Q, Farrar J, de Jong MD, Lanzavecchia A, Subbarao K. Prophylactic and therapeutic efficacy of human monoclonal antibodies against H5N1 influenza. PLoS Med. 2007;4:e178.

Smith KG, Clatworthy MR. FcgammaRIIB in autoimmunity and infection: evolutionary and therapeutic implications. Nat Rev Immunol. 2010;10:328-43.

Smith KA, Nelson PN, Warren P, Astley SJ, Murray PG, Greenman J. Demystified… recombinant antibodies. J Clin Pathol. 2004;57:912-7.

Sondermann P, Oosthuizen V. The structure of Fc receptor/Ig complexes: considerations on stoichiometry and potential inhibitors. Immunol Lett. 2002;82:51–56.

Staprans SI, Feinberg MB, Shiver JW, Casimiro DR. Role of nonhuman primates in the evaluation of candidate AIDS vaccines: an industry perspective. Curr Opin HIVAIDS 2010;5:377–85.

Steinitz M. Three decades of human monoclonal antibodies: past, present and future developments. Hum Antibodies. 2009;18:1-10.

Sumiyama K, Saitou N, Ueda S. Adaptive evolution of the IgA hinge region in primates. Mol Biol Evol. 2002;19:1093-9.

Sutton BJ, Phillips DC. The three-dimensional structure of the carbohydrate within the Fc fragment of immunoglobulin G. Biochem Soc Trans. 1983;11 Pt 2:130-2.

Takai T. Fc receptors and their role in immune regulation and autoimmunity. J Clin Immunol. 2005;25:1–18.

Tan LK, Shopes RJ, Oi VT, Morrison SL. Influence of the hinge region on complement activation, C1q binding, and segmental flexibility in chimeric human immunoglobulins. Proc Natl Acad Sci U S A. 1990;87:162-6. Erratum in: Proc Natl Acad Sci U S A 1991;88:5066.

Thomas C. Roadblocks in HIV research: five questions. Nature Med. 2009;15:855–9.

Thommesen JE, Michaelsen TE, Løset GA, Sandlie I, Brekke OH. Lysine 322 in the human IgG3 C(H)2 domain is crucial for antibody dependent complement activation. Mol Immunol. 2000;37:995-1004.

Tiller T, Meffre E, Yurasov S, Tsuiji M, Nussenzweig MC, Wardemann H. Efficient generation of monoclonal antibodies from single human B cells by single cell RT-PCR and expression vector cloning. J Immunol Methods. 2008;329:112-24.

Tonegawa S. Somatic generation of antibody diversity. Nature. 1983;302:575-81.

Torres M, Casadevall A. The immunoglobulin constant region contributes to affinity and specificity. Trends Immunol. 2008;29:91-7.

van de Winkel JG, Capel PJ. Human IgG Fc receptor heterogeneity: molecular aspects and clinical implications. Immunol Today 1993;14:215–21.

van Meurs GJE, Jonker M. Production of primate monoclonalantibodies. J Immunol Methods 1986;95:123–8.

van Sorge NM, van der Pol WL, van de Winkel JG. FcgammaR polymorphisms: Implications for function, disease susceptibility and immunotherapy. Tissue Antigens 2003;61:189–202.

Verma A, Ngundi MM, Meade BD, De Pascalis R, Elkins KL, Burns DL. Analysis of the Fc gamma receptor-dependent component of neutralization measured by anthrax toxin neutralization assays. Clin Vaccine Immunol. 2009;16:1405-12.

Warmerdam PAM, Van de Winkel JGJ, Vlug A, Westerdaal NAC, Capel PJA. A single amino acid in the second Ig-like domain of the human Fcg receptor II is critical for human IgG2 binding. J Immunol. 1991;147:1338–43.

Warncke M, Calzascia T, Coulot M, Balke N, Touil R, Kolbinger F, Heusser C. Different adaptations of IgG effector function in human and nonhuman primates and implications for therapeutic antibody treatment. J Immunol. 2012 (doi:10.4049/jimmunol.1200090).

Weiner LM, Surana R, Wang S. Monoclonal antibodies: versatile platforms for cancer immunotherapy. Nat Rev Immunol. 2010;10:317-27.

Williams AF, Barclay AN. The immunoglobulin superfamily–domains for cell surface recognition. Annu Rev Immunol. 1988;6:381–405.

Wrammert J, Smith K, Miller J, Langley WA, Kokko K, Larsen C, Zheng NY, Mays I, Garman L, Helms C, James J, Air GM, Capra JD, Ahmed R, Wilson PC. Rapid cloning of high-affinity human monoclonal antibodies against influenza virus. Nature. 2008;453:667-71.

Xu Y, Oomen R, Klein MH. Residue at position 331 in the IgG1 and IgG4 CH2 domains contributes to their differential ability to bind and activate complement. J Biol Chem. 1994;269:3469-74.

Yolov AA, Shabarova ZA. Constructing DNA by polymerase recombination. Nucleic Acids Res. 1990;18:3983-6.

Yon J, Fried M. Precise gene fusion by PCR. Nucleic Acids Res. 1989;17:4895.

Zeitlin L, Cone RA, Moench TR, Whaley KJ. Preventing infectious disease with passive immunization. Microbes Infect. 2000;2:701-8.

Zhang Y, Boesen CC, Radaev S, Brooks AG, Fridman WH, Sautes-Fridman C, Sun PD. Crystal structure of the extracellular domain of a human Fc gamma RIII. Immunity. 2000;13:387-95.